Exhibit 97

Journal of
Biomedical Nanotechnology
Vol. 7, 112–113, 2011

Nano-Talc Stabilizes TNF-α m-RNA in Human Macrophages

Mohd Imran Khan[1], Amogh A. Sahasrabuddhe[2], Govil Patil[1], Mohd Javed Akhtar[1], Mohd Ashquin[1], and Iqbal Ahmad[1]

[1] *Nanomaterial Toxicology Group, Indian Institute of Toxicology Research (CSIR), P. O. Box 80, M. G. Marg, Lucknow 226001, India*
[2] *Molecular and Structural Biology Division, Central Drug Research Institute (CSIR), Chattar Manzil, Lucknow 226001, India*

Particle size reduction of talc from micro- to nanoscale gradually enhanced its cytotoxicity however its inflammatory potential is still not explored. In the current study we observed increased TNF-α, IL-1β and IL-6 mRNA levels in macrophages exposed to Nano-Talc (NT). Further, NT particles also showed constituent phosphorylation of both p38 and ERK1/2 pathway however JNK phosphorylation was transient. Pre-treatment of macrophages with p38 and ERK1/2 inhibitors either alone or in combination showed significant reduction in TNF-α mRNA stability, clearly suggesting their role in TNF-α mRNA stabilization and expression. Our observations clearly demonstrated the inflammatory potential of NT particles which might be at least partial and potential mechanism in talc mediated pathogenecity in the exposed population.

Keywords: Nano-Talc, Macrophages, Inflammation, TNF-α, MAPKs.

1. INTRODUCTION

In recent past, our group showed that particle size reduction of talc from micro- to nanoscale gradually enhanced its cytotoxicity.[1–2] Epidemiological evidences earlier suggested that exposure of talc leads to development of talcosis and cancer in lungs.[3–4] The molecular mechanisms of toxicity of talc particles particularly in nanoscale is not fully known. It is noteworthy that talc in nanopowder form has got enormous applications in several industrial products namely cosmetics, pharmaceuticals, paper, paints etc. An attempt was therefore made to study nanotalc mediated inflammatory effects investigating cytokine mRNA and protein levels along with there respective mRNA stability in human macrophage cell line THP-1. Nano-Talc (NT) particles significantly enhanced transcription and translation of TNF-α. It was observed with interest that stabilization of TNF-α mRNA mediated by both ERK1/2 and p38 was potentially responsible for enhanced TNF-α production.

2. MATERIALS AND METHODS

Nano-Talc, particle size 80–130 nm was purchased from M. K. Impex Canada, Catalpa Road, Mississauga, Canada. Hydrodynamic particle size in culture medium was also determined as 418 ± 136 nm (DLS-Malvern Instruments, USA). Differentiated THP-1 (human monocytic cell line), obtained from NCCS, Pune, India, was used as a model system for human macrophages. Cytotoxicity of NT particles in macrophages was studied by MTT reduction assay. Based on the cytotoxicity results, nonsignificant dose concentrations (i.e., 10–100 μg/ml) were used to identify the inflammatory potential of NT particles upto 24 hrs. Briefly, cells were exposed to NT particles and mRNA was isolated to reverse transcribe for the preparation of cDNA. RT-PCR (reverse transcriptase-PCR) was performed to quanatitate the mRNA levels of various proinflammatory cytokines (TNF-α, IL-1β and IL-6). ELISA was done to quanatitate the protein levels of these cytokines. Further, exposed cells were lysed and western blot done by utilizing specific antibodies for ERK1/2, p38 and JNK. Northern blot analysis helped in assessing the mRNA stability and the role of various mitogen activated protein kinases (MAPKs) using specific probes in the presence of actinomycin D. Statistical analysis was done by using GraphPad Prism 5 and $P < 0.05$ was considered significant.

3. RESULTS AND DISCUSSION

RT-PCR results showed that exposure NT particles increased the TNF-α, IL-1β and IL-6 mRNA levels in macrophages. At 6 hrs, mRNA levels of both TNF-α and

 1550-7033/2011/7/112/002 doi:10.1166/jbn.2011.1227

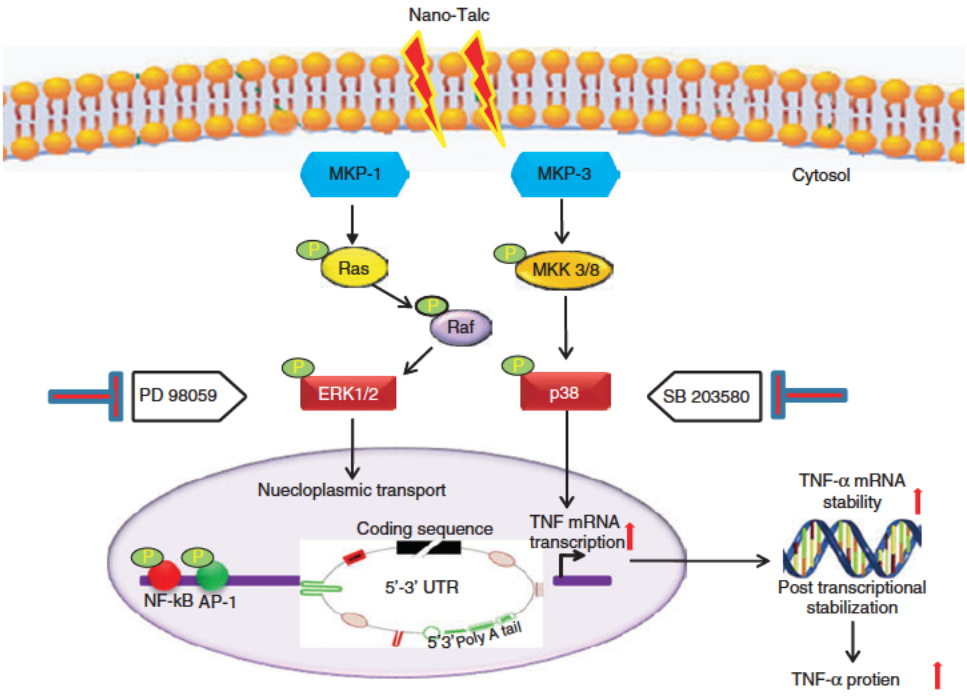

Fig. 1. Proposed hypothetical mechanism for induction of TNF-α in human macrophages.

IL-1β increased significantly in a concentration- dependent manner. Owing the impeccable role of TNF-α in lung fibrosis as well as cancer initiation and progression, special focus was TNF-α. Time course analysis of TNF-α m-RNA induction due to NT particles indicated that exposure period of 3–6 hr was optimum for maximal increase, however longer exposure periods lead to a diminished upregulation. ELISA results also corroborated well with the mRNA levels. NT particles showed constituent phosphorylation of p38 pathway upto 180 mins in THP-1 macrophages, which tends to decrease onwards i.e., 240 mins. Similarly ERK1/2 phosphorylation was peaked highest at 120 mins and decreased onwards. However JNK phosphorylation was transient (at 30 min) and was lost further with increase in time. In order to determine the role of ERK1/2 and p38 phosphorylation in NT particles mediated upregulation of TNF-α m-RNA level, the effects of MAPK inhibitors namely PD-98059 and SB-203580 on mRNA stability were investigated by using northern blot analysis. Inhibition of TNF-α m-RNA due to PD 98059 was significant in the presence of actinomycin D (a transcription inhibitor), which was insignificant in the case of SB-203580. Further we analyzed the combinatorial effect of both MAPK inhibitors in combination on TNF-α m-RNA stability; which showed nearly complete attenuation of TNF-α m-RNA level. Similar pattern was observed when protein levels were quantitated. Based on the study, a mechanism of TNF-α induction in hypothesized (Fig. 1).

4. CONCLUSION

Our observations clearly demonstrated the inflammatory potential of NT particles which might be at least partial and potential mechanism in talc mediated pathogenecity in the exposed population.

Acknowledgment: Authors wish to gratefully acknowledge the funding from CSIR, New Delhi under its network project (NWP-17) and ICMR (New Delhi) for funding to Mohd Imran Khan as Senior Research Fellow.

References and Notes

1. I. Ahmad, Nanotoxicity of talc: A comparative particle size dependent cytotoxicity study in isolated rat hepatocytes. *Nanotoxicology* 2, S37 (**2008**).
2. M. J. Akhtar, S. Kumar, R. C. Murthy, M. Ashquin, M. I. Khan, G. Patil, and I. Ahmad, The primary role of iron-mediated lipid peroxidation in the differential cytotoxicity caused by two varieties of talc nanoparticles on A549 cells and lipid peroxidation inhibitory effect exerted by ascorbic acid. *Toxicology In Vitro* 24, 1139 (**2010**).
3. P. Wild, Lung cancer risk and talc not containing asbestiform fibres: A review of the epidemiological evidence. *Occupational and Environmental Medicine* 63, 4 (**2006**).
4. M. A. Gates, S. S. Tworoger, K. L. Terry, L. Titus-Ernstoff, B. Rosner, I. D. Vivo, D. W. Cramer, and S. E. Hankinson, Talc use, variants of the GSTM1, GSTT1 and NAT2 genes, and risk of epithelial ovarian cancer. *Cancer Epidemiology Biomarkers and Prevention* 17, 2436 (**2008**).

Received: 10 December 2010. Accepted: 12 December 2010.

Exhibit 98

Disruption of Iron Homeostasis in Mesothelial Cells after Talc Pleurodesis

Andrew J. Ghio[1], Joleen M. Soukup[1], Lisa A. Dailey[1], Judy H. Richards[1], Jennifer L. Turi[2], Elizabeth N. Pavlisko[3], and Victor L. Roggli[3]

[1]National Health and Environmental Effects Research Laboratory, United States Environmental Protection Agency, Research Triangle Park, North Carolina; and [2]Department of Pediatrics, and [3]Department of Pathology, Duke University Medical Center, Durham, North Carolina

The mechanism for biological effects after exposure to particles is incompletely understood. One postulate proposed to explain biological effects after exposure to particles involves altered iron homeostasis in the host. The fibro-inflammatory properties of mineral oxide particles are exploited therapeutically with the instillation of massive quantities of talc into the pleural space, to provide sclerosis. We tested the postulates that (*1*) *in vitro* exposure to talc induces a disruption in iron homeostasis, oxidative stress, and a biological effect, and (*2*) talc pleurodesis in humans alters iron homeostasis. *In vitro* exposures of both mesothelial and airway epithelial cells to 100 μg/ml talc significantly increased iron importation and concentrations of the storage protein ferritin. Using dichlorodihydrofluorescein, exposure to talc was associated with a time-dependent and concentration-dependent generation of oxidants in both cell types. The expression of proinflammatory mediators was also increased after *in vitro* exposures of mesothelial and airway epithelial cells to talc. Relative to control lung tissue, lung tissue from patients treated with sclerodesis demonstrated an accumulation of iron and increased expression of iron-related proteins, including ferritin, the importer divalent metal transport–1 and the exporter ferroportin-1. Talc was also observed to translocate to the parenchyma, and changes in iron homeostasis were focally distributed to sites of retention. We conclude that exposure to talc disrupts iron homeostasis, is associated with oxidative stress, and results in a biological effect (i.e., a fibro-inflammatory response). Talc pleurodesis can function as a model of the human response to mineral oxide particle exposure, albeit a massive one.

Keywords: talc; iron; ferritin; pleurodesis; particulate matter

Humans are routinely exposed to the particulate matter (PM) included in air pollution, cigarette smoke, environmental tobacco smoke, forest fires, gas and wood stoves, and the burning of biomass other than wood, as well as those particles contacted during the mining and processing of coal and mineral oxides. Many of the major global causes of death reported by the World Health Organization (http://www.who.int/mediacentre/factsheets/fs310/en/index.html) are related to particle exposure, and contact with PM will increase human morbidity and mortality. This particle-related morbidity and mortality include lower respiratory infections, chronic obstructive pulmonary disease, respiratory cancers, coronary heart disease, stroke, and other cerebrovascular diseases (1–3).

CLINICAL RELEVANCE

This research concerns the disruption in iron homeostasis that occurs in the pleura and lungs of patients treated with talc pleurodesis. The accumulation of this metal, the accompanying oxidative stress, and inflammatory events after exposure to talc are comparable to those with other forms of particulate matter. Pleurodesis can function as a model of particle-related biological effect.

The production of reactive oxygen species (ROS) is fundamental to the biological effect of PM (4), but the specific mechanism of both the generation of oxidants and its relationship with the biological effect after exposure to particles is incompletely understood. One postulate to explain the biological effect after exposure to particles involves altered iron homeostasis in the host after exposure. Exposure to particles introduces a solid–liquid interface into cells. Oxygen-containing functional groups on the PM surface provide the capacity to complex cations, and as a result of its high affinity for oxygen-donor ligands, iron is frequently preferred. Such functional groups can include alcohols, aldehydes, and carboxylates on incompletely combusted carbon (e.g., cigarette smoke, diesel exhaust, and ambient air pollution particles), and silanol groups on silica and silicates. Particles retained in the lung consistently demonstrate a capacity to disrupt iron homeostasis and accumulate host metal (5). Endpoints reflecting oxidative stress and a biological effect can be correlated with this accumulation of iron that follows *in vivo* exposure to particles (6).

Pathologic processes observed in lungs among individuals exposed to particles include both inflammation and fibrosis (4, 7). In patients with recurrent pleural effusions, the fibro-inflammatory properties of mineral oxide particles are exploited therapeutically with the instillation of massive quantities (i.e., grams) of talc into the pleural space to provide sclerosis (8). This therapeutic use affords an opportunity to examine human tissue for evidence of a disruption in iron homeostasis after an extreme exposure to mineral oxide particles. We accordingly tested the postulates that (*1*) *in vitro* exposure to talc induces a disruption of iron homeostasis, oxidative stress, and a biological effect, and (*2*) talc pleurodesis in humans is also associated with altered iron homeostasis and an accumulation of metal.

MATERIALS AND METHODS

Iron Uptake in an Acellular Environment

Talc (Sclerosol, Bryan Corp., Woburn, MA) was agitated in either H_2O or 1,000 μM ferric ammonium citrate for 1 hour, centrifuged, and washed with H_2O (designated talc and talc–Fe, respectively). Ionizable metal concentrations associated with talc and talc–Fe were measured

(*Received in original form May 27, 2011; accepted in final form August 5, 2011*)

Disclaimer: This report was reviewed by the National Health and Environmental Effects Research Laboratory of the United States Environmental Protection Agency and was approved for publication. Approval does not signify that the contents necessarily reflect the views and policies of the Agency, nor does mention of trade names or commercial products constitute endorsement or recommendation for use.

Correspondence and requests for reprints should be addressed to Andrew Ghio, Division of Environmental Public Health, Human Studies Facility, United States Environmental Protection Agency, Campus Box 7315, 104 Mason Farm Road, Chapel Hill, NC 27711. E-mail: ghio.andy@epa.gov

This article has an online supplement, which is accessible from this issue's table of contents at www.atsjournals.org

Am J Respir Cell Mol Biol Vol 46, Iss. 1, pp 80–86, Jan 2012
Originally Published in Press as DOI: 10.1165/rcmb.2011-0168OC on November 17, 2011
Internet address: www.atsjournals.org

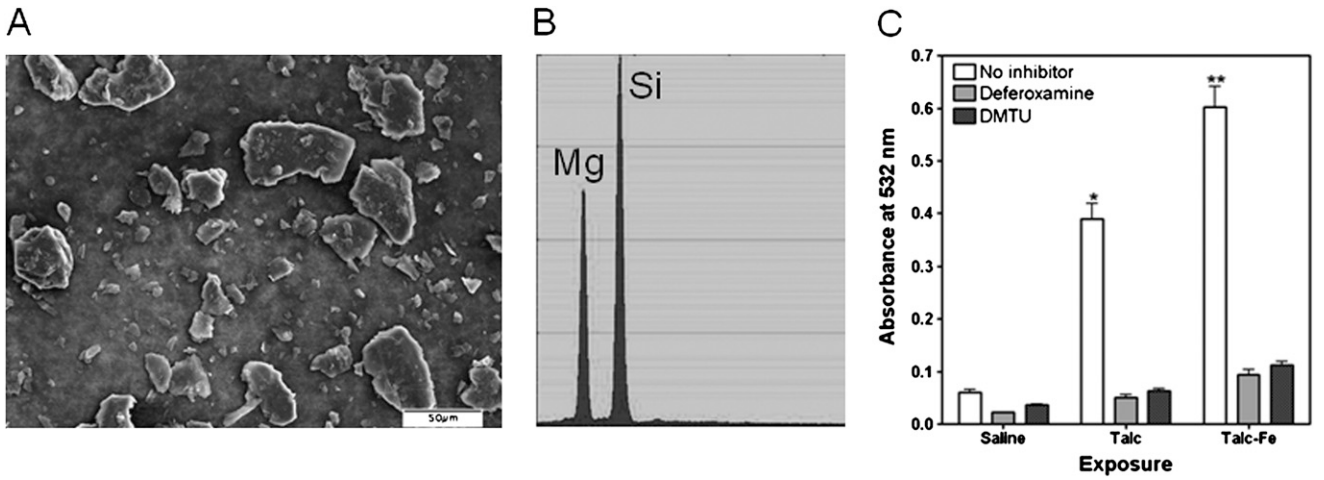

Figure 1. Particle size, composition, and capacity for generation of oxidants. (*A*) Talc was examined in a JEOL (Peabody, MA) scanning electron microscope at a screening magnification of approximately ×1,000 and a diameter ranging between 10 and 50 μm. (*B*) Energy-dispersive X-ray spectroscopy confirmed two peaks consistent with magnesium and silicon. (*C*). Talc demonstrated a capacity to generate hydroxyl radical in an acellular environment. This generation of oxidants was increased with a further complexation of surface iron by the talc, and was inhibited by inclusion of the metal chelator deferoxamine or the hydroxyl radical scavenger dimethylthiourea (DMTU) during incubation. *Significantly increased relative to saline. **Significantly increased relative to both saline and talc.

using inductively coupled plasma optical emission spectroscopy (ICPOES; Model Optima 4300DV; Perkin Elmer, Norwalk, CT).

Generation of Acellular Oxidants

The generation of acellular oxidants by talc and talc–Fe particles was measured with the thiobarbituric acid–reactive products of deoxyribose (9).

Cell Culture

Mesothelial cells (MeT-5A; American Type Culture Collection, Manassas, VA) were cultured in complete growth medium. In addition, BEAS-2B cells on uncoated, plastic 12-well plates in keratinocyte growth medium (Lonza, Walkersville, MD) were used.

RT-PCR

Mesothelial and BEAS-2B cells were exposed to either medium alone or 100 μg/ml talc. Quantitative PCR was performed using Taqman polymerase, with detection on an ABI Prism 7500 Sequence Detector (Applied Biosystems, Foster City, CA).

Cell Iron Homeostasis

Mesothelial and BEAS-2B cells were exposed for 4 hours to 200 μM ferric ammonium citrate (FAC), 100 μg/ml talc, and both FAC and talc. Cells were then scraped into 1.0 ml 3 N HCl/10% trichloroacetic acid. After hydrolysis, concentrations of iron and zinc were determined using ICPOES. Cell incubations were repeated for 24 hours, scraped into 0.5 ml PBS, and disrupted, and ferritin concentrations in the lysates were measured using an enzyme immunoassay (Microgenics Corp., Concord, CA).

Generation of Cellular Oxidants

Mesothelial and BEAS-2B cells were grown to confluence in 96-well, white-walled, tissue culture–treated plates (CoStar, Lowell, MA). We loaded 2′7′ dichlorodihydrofluorescein (DCF; 20 μM) diacetate (Sigma

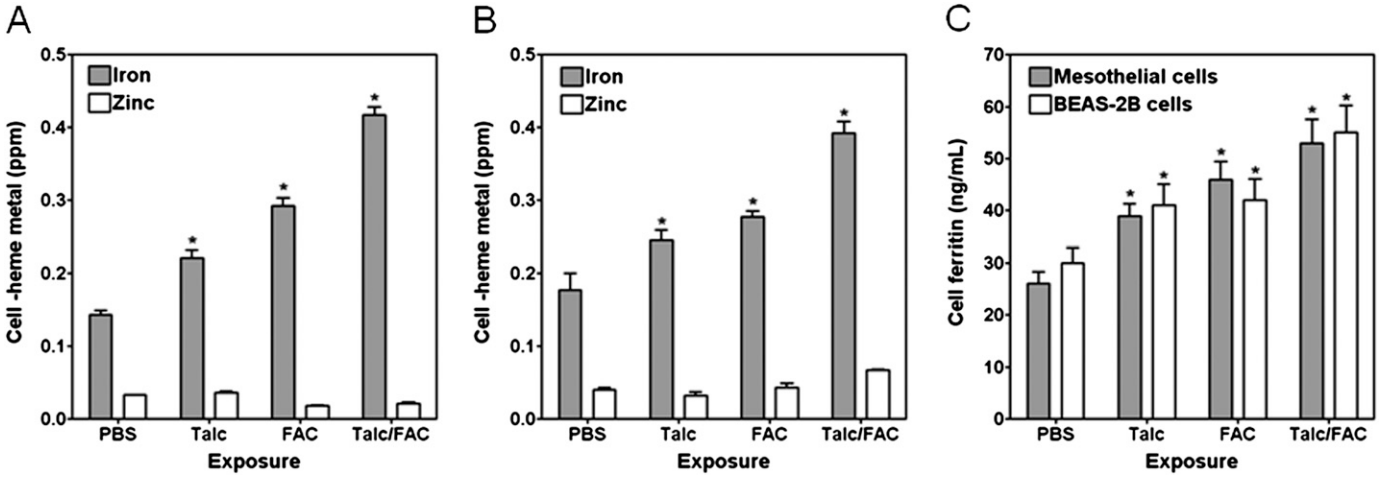

Figure 2. Cellular concentrations of nonheme metal and ferritin after *in vitro* exposure to talc. Mesothelial (*A*) and BEAS-2B cells (*B*) both increased cell nonheme iron after exposure to 100 μg/ml talc and 200 μM iron. The co-incubation of cells with both talc and iron further elevated nonheme iron. Cell zinc concentration showed no change after exposures to talc and iron. (*C*) Corresponding to concentrations of nonheme iron, concentrations of cell ferritin increased in both cell types after exposures to talc and iron. *Significantly increased, relative to PBS. FAC, ferric ammonium citrate.

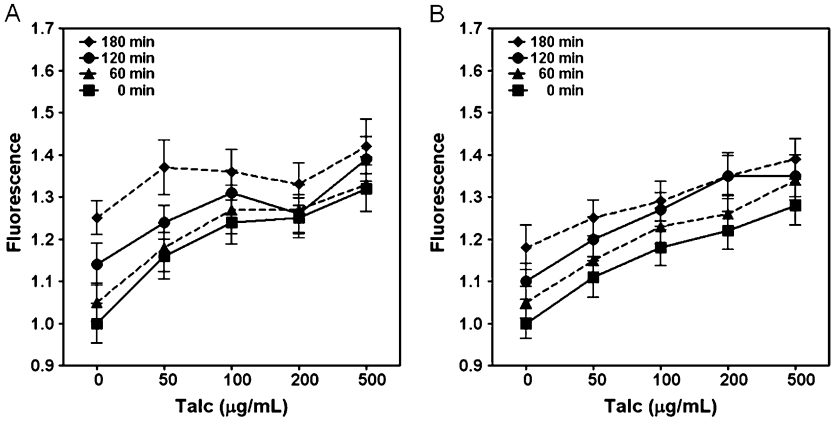

Figure 3. Cellular generation of oxidants after *in vitro* exposure to talc. Using 2′7′ dichlorodihydrofluorescein (DCF) diacetate fluorescence, mesothelial cells (*A*) and BEAS-2B cells (*B*) demonstrated a time-dependent and concentration-dependent generation of oxidants.

Chemical Co., St. Louis, MO), baseline readings were taken on a Perkin Elmer HTS 7000 fluorimeter using 485-nm excitation/535-nm emission filters, and PBS with and without talc was added. Fluorescence was measured at 0, 60, 120, and 180 minutes after addition.

Cellular Release of IL-8 and IL-6

Cells were exposed to either medium or 100 μg/ml talc in medium for 24 hours. Concentrations of IL-8 and IL-6 in the cell medium were measured using commercially available ELISA kits (R&D Systems, Minneapolis, MN).

Histochemistry and Immunohistochemisty

Our protocol was approved by the Institutional Review Board of the Duke University Health System. Staining was performed on six surgical specimens collected from patients who (*1*) had manifested talc pleurodesis 2–15 months previously (mean ± SD, 7 ± 6 months), followed by (*2*) an extrapleural pneumonectomy. Sections were stained for iron, using Perl's Prussian blue (Sigma). Immunohistochemistry for ferritin was performed using an human anti-ferritin antibody (Dako, Carpinteria, CA) at a dilution of 1:100 (10) and antibodies to divalent metal transport 1 (DMT1) and ferroportin 1 (FPN1) at a dilution of 1:200 (11, 12). Control lung tissue was obtained from (*1*) patients who had undergone a pneumonectomy for lung cancer, and (*2*) individuals diagnosed with idiopathic pulmonary fibrosis (IPF) and undergoing an autopsy.

Statistical Analysis

Data are expressed as mean values ± standard errors, unless specified otherwise. Differences between multiple groups were compared using ANOVA.

RESULTS

Scanning electron microscopy of the talc showed significant variability in PM size, with diameters of individual particles ranging from less than 10 μm to greater than 50 μm (Figure 1A). However, the majority of particles had diameters between 10 and 50 μm. No fibers were evident in the talc sample. Energy-dispersive X-ray spectroscopy revealed two peaks consistent with magnesium and silicon (Figure 1B). This finding is in agreement with the ideal molecular formula of talc ($Mg_3Si_4O_{10}(OH)_2$).

Comparable to numerous silicates (13), talc demonstrated a capacity for iron uptake in an acellular environment. Concentrations of ionizable iron were measured at 0.46 ± 0.11 ppm and 6.48 ± 1.08 ppm, respectively, for talc and talc–Fe, whereas concentrations of ionizable zinc were measured at 0.03 ± 0.01 and 0.01 ± 0.00 ppm, respectively. The capacity of particles to support the *in vitro* generation of oxidants in an acellular environment was significantly affected by the concentration of associated iron, with talc–Fe producing a significantly greater signal for malondialdehyde relative to talc (Figure 1C). This generation of oxidants was inhibited by the inclusion of either 1,000 μM deferoxamine, a metal chelator, or 1,000 μM dimethylthiourea, a hydroxyl radical scavenger (Figure 1C).

The *in vitro* exposure of mesothelial cells to talc for 4 hours resulted in an accumulation of nonheme iron. Cell zinc concentrations did not change (Figure 2A). The exposure to FAC alone confirmed the ability of mesothelial cells to import iron (Figure 2A). Co-incubation with both talc and FAC was associated with a greater accumulation of iron relative to FAC

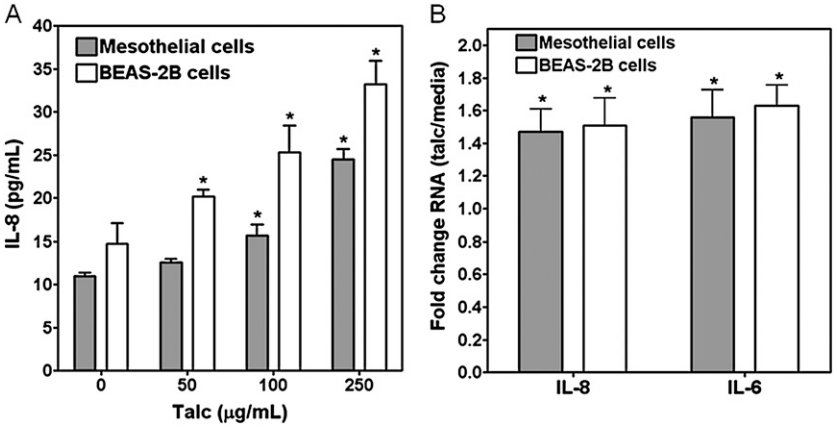

Figure 4. Release of IL-8 and changes in RNA for IL-8 and IL-6 after *in vitro* exposure to talc. (*A*) Concentrations of IL-8 were increased after exposure to 100 μg/ml talc in both cell types. (*B*) Changes in RNA for IL-8 and IL-6 were increased 4 hours after exposure to 100 μg/ml talc. * = significantly increased relative to PBS (*A*) and media (*B*).

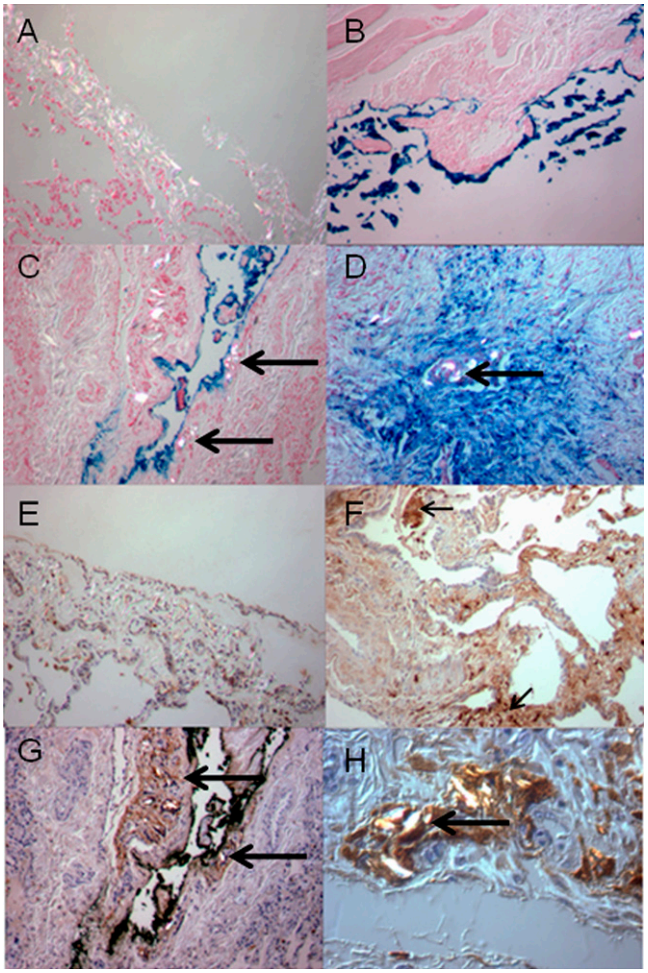

Figure 5. Stains for iron and ferritin in resected lung tissues. (*A*) Pleura from control lung tissue demonstrated no staining for iron by the pleura. Those tissue samples acquired after pleurodesis all showed positive iron staining. This staining included the parietal pleura (*B*) and visceral pleura (*C*). With translocation of the talc to both the subpleural region (*C*; *arrows* designate talc particles) and the parenchyma (*D*; *arrow* designates talc particle) of the lung, positive iron staining was evident in cells adjacent to the particle (*D*). (*E*) A small amount of uptake for the ferritin antibody by the pleura occurred in samples resected from patients treated with pneumonectomy. Specifically, this staining localized to the single cell layer of mesothelial cells and the loose fibrous tissue immediately beneath it. (*F*) Some expression of ferritin was also evident in chronic inflammatory cells resident in the lungs of patients with idiopathic pulmonary fibrosis (IPF; *arrows* designate areas of chronic inflammation distorting the alveolar and septal regions). (*G*) However, in patients with pleurodesis, talc was evident in the subpleural region, and uptake of the ferritin antibody by the pleura was very strong (*arrows* designate particles). (*H*) Talc was also detected in the lung parenchyma, and ferritin staining was similarly increased in cells adjacent to the particle (*arrow* designates particle). The expression of ferritin in the lungs of patients with pleurodesis was focally distributed to sites of talc retention. *Magnification*, approximately ×100.

exposure alone (Figure 2A). BEAS-2B cells exposed to talc and FAC revealed similar increases in cell nonheme metal. Again, co-incubations revealed an increased cell iron import relative to either talc or FAC alone (Figure 2B). These results demonstrate that the capacity of talc to complex iron in an acellular environment is retained during *in vitro* mesothelial and airway epithelial cell exposures. In addition, these data suggest that talc could deplete intracellular sources of iron, and resulting in the importation of greater quantities of metal. Comparable to cell nonheme iron concentration, an increase in cell ferritin occurred after exposures of mesothelial and airway epithelial cells to talc, and this increase was even greater after exposures to both FAC and talc (Figure 2C). RNA for ferritin, DMT1 (a major iron importer), and FPN1 (a major iron exporter) did not significantly change 4 hours after exposure of mesothelial cells to 100 μg/ml talc (Table E1 in the online supplement).

A fluorescence method using DCF diacetate demonstrated an increased generation of ROS by both mesothelial and BEAS-2B cells after exposure to talc (Figures 3A and 3B). This cellular generation of oxidants after exposure to particles was both time-dependent and concentration-dependent, supporting a capacity of cells to produce ROS after exposure to talc. RNA for heme oxygenase and cyclooxygenase, which are potential intracellular sources of oxidative stress, showed conflicting responses, with heme oxygenase significantly increasing in both mesothelial and airway epithelial cells 4 hours after exposure to 100 μg/ml talc, and the concentration of cyclooxygenase not changing (Table E1). Finally, mesothelial and BEAS-2B cells both increased the release of IL-8 after exposure to 100 μg/ml talc (Figure 4A). IL-6 demonstrated a trend toward increasing after exposure to talc, but significant differences were not evident. RNA for IL-8 and IL-6 similarly increased after a 4-hour exposure to talc in both mesothelial cells and BEAS-2B cells (Figure 4B). This increased release of proinflammatory mediators reflects a relevant *in vitro* biological response in both cell types after talc exposure.

All patients with pleurodesis were male. Their mean age (± SD) was 56 ± 18 years. All but one manifested malignant mesothelioma (the exception underwent surgical intervention for repeated pneumothoraces). Tissue specimens, used as control samples, were collected at the time of pneumonectomy for lung cancer ($n = 6$) and at autopsy of patients with IPF ($n = 6$). These individuals manifested no pleurodesis. The specimens obtained during pneumonectomy reflected tissue uninvolved by fibrosis, whereas specimens from patients diagnosed with IPF included fibrotic specimens unrelated to mineral oxide exposure. Control tissue collected during pneumonectomy and autopsy were from men with mean ages (± SD) of 70 ± 15 years and 68 ± 9 years, respectively. Control lungs demonstrated no staining for iron in the pleura or parenchyma (Figure 5A). Significant iron staining occurred in all specimens collected after pleurodesis. Iron was localized to both the parietal (Figure 5B) and visceral (Figure 5C) pleura. Some of the talc was observed to be subpleural (Figure 5C), and particles were also evident in the parenchyma of the lungs (Figure 5D). When particles moved subpleurally and into the parenchyma, they retained their capacity to accumulate the metal (Figure 5D). Some uptake of the ferritin antibody by pleura occurred in the control specimens collected from patients with lung cancer (Figure 5E) and IPF, but this uptake was minimal. Among patients with IPF, uptake for the ferritin body corresponded to areas of inflammation (Figure 5F). After exposure to talc, the staining for ferritin was so intense that the visceral pleura appeared black (Figure 5G). After transport to the lung parenchyma, talc continued to demonstrate an association with an increased expression of ferritin protein (Figure 5H). The expression of this storage protein was focally distributed to the talc, with increased staining immediately adjacent to the particle.

Little staining for DMT1 was evident in the pleura of lungs resected from control patients, and this staining was limited to respiratory epithelia (Figures 6A and 6B). The expression of this major iron importer in the pleura increased enormously after pleurodesis with talc (Figure 6C). Uptake for the iron

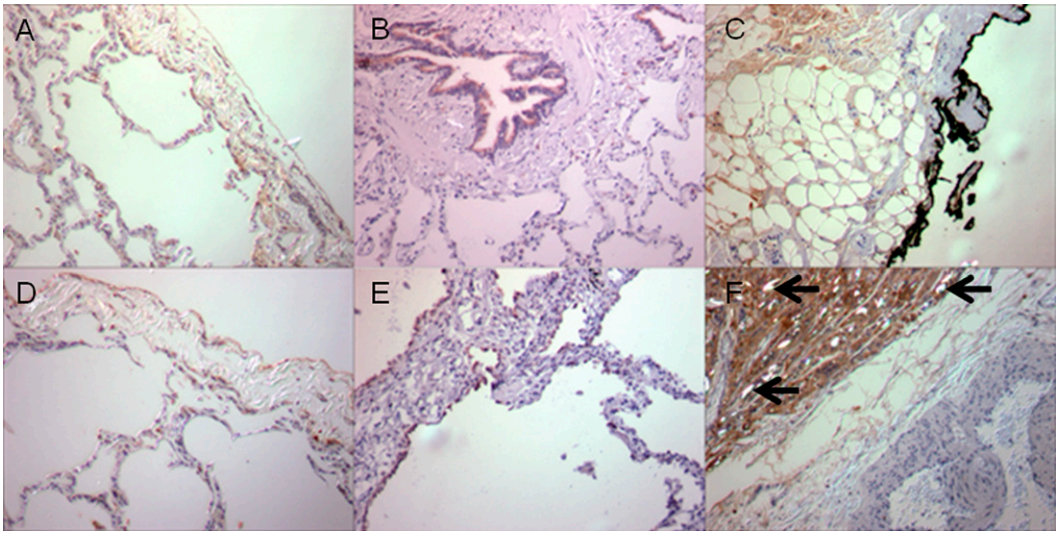

Figure 6. Divalent metal transport 1 (DMT1) and ferroportin 1 (FPN1) staining in resected lung tissue. Some binding of the antibody to both DMT1 and FPN1 was evident in lung tissue resected from patients unexposed to talc (*A* and *D*, respectively). Similarly, the uptake of antibodies for DMT1 and FPN1 in autopsy samples from patients with IPF was low (*B* and *E*, respectively). However, the expression of the iron importer DMT1 and iron exporter FPN1 both increased significantly among patients treated with pleurodesis (*C* and *F*, respectively). Comparable to the expression of ferritin, increased uptake for the antibodies to DMT1 and FPN1 occurred after translocation of the particle to the lung parenchyma (*F*; *arrows* designate particles). *Magnification*, approximately ×100.

exporter FPN1 was negligible among lungs resected from control patients (Figures 6D and 6E). Among those patients with talc pleurodesis, the expression of FPN1 was greatly increased at the pleura and in the lung cells immediately adjacent to translocated particles (Figure 6F). Finally, trichrome staining for collagen demonstrated minuscule, subpleural staining in the control specimens taken during pneumonectomy for lung cancer (Figure 7A). In contrast, sheets of collagen were verified by trichrome staining in lung tissue resected after talc pleurodesis (Figure 7B). In the lungs of patients with pleurodesis, the talc appeared at the periphery of the fibrosis (Figure 7B).

DISCUSSION

The surfaces of silica and silicate particles, including talc, contain some concentration of silanol groups (Si–OH). Si^{4+} has a high electron affinity, and the Si–O bond consequently has a significant ionic character and an acidic dissociation constant favoring dissociation at physiologic pH (14). The dissociation of silanol groups contributes to a net negative charge on the particle surface, which generates a capacity for the adsorption and exchange of cations (15). The open network of negatively charged silanol groups on a silica and silicate surface presents spaces large enough to accommodate adsorbed metal cations. As a result of its electropositivity, Fe^{3+} has a high affinity for oxygen-donor ligands (16, 17), and reacts with the silanol group to form a silicato–iron coordination complex (18):

$$Fe^{3+} + m(-SiOH) \rightarrow Fe(OSi)_m^{3-m+} + mH^+.$$

The dose-dependent adsorption of inorganic iron was demonstrated for surface silanol groups on crystalline silicates, with critical stability constants up to $1 \times 10^{17.15}$ (critical stability constant = 17.15) (19, 20). Our investigation confirmed the capacity of talc to complex iron from an acellular source comparable to other silica and silicate particles (13). The *in vitro* exposure to talc similarly affected an accumulation of nonheme iron in both mesothelial and airway epithelial cells. Although the source of this accumulated iron was not identified, the talc surface may complex host metal originally associated with ATP, ADP, GTP, citrate, DNA, free amino acids (21), and mitochondrial sources. However, the cell will recognize this loss of requisite iron, and subsequently increases metal import. After integration of the particle's capacity for complexation into the cell's requirement for iron, increased metal uptake and storage would occur. Reflecting these processes, concentrations of ferritin increased after *in vitro* exposure to talc. As a result of posttranscriptional control acting as a major contributor to expression (22–24), the

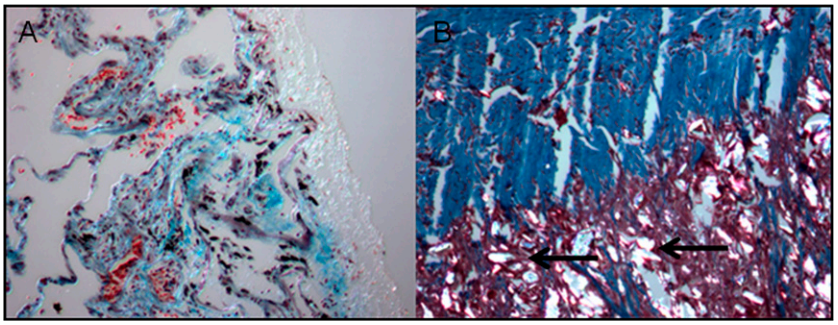

Figure 7. Masson's trichrome stain for collagen in resected lung tissue. (*A*) Control lungs demonstrated little trichrome staining (*blue*). (*B*) In contrast, tissue collected from patients with pleurodesis showed dense sheets of collagen. Talc was evident at the periphery of this collagen deposition, comparable to a silica nodule (*arrows* designate particles). *Magnification*, approximately ×100.

RNA for ferritin, DMT1, and FPN1 did not change in mesothelial and BEAS-2B cells.

Comparable to *in vitro* accumulation of iron after exposure to talc, significant metal accumulation occurred *in vivo* after pleurodesis. Perl's Prussian blue staining demonstrated metal in close proximity to retained talc particles in both the mesothelial cells of the pleura and the macrophages and airway epithelial cells of the parenchyma. Because the iron originally associated with the talc approximated normal cell and tissue concentrations, the accumulation of metal after pleurodesis had to originate from host sources of iron. Immunohistochemistry for ferritin showed elevations in expression by mesothelial cells at the pleura and in parenchymal cells after the introduction of talc. The stain for ferritin suggested a very focal response, with cells either directly contacting or immediately adjacent to the particle demonstrating uptake of the antibody to this storage protein. Similarly, the expression of the iron-importer DMT1 and the iron-exporter FPN1 both increased on staining in those patients treated with talc pleurodesis. In control tissue from patients with lung cancer and IPF, no positive staining for iron was evident. The uptake of the antibody to ferritin, DMT1, and FPN1 in these same tissues was minimal, but was evident in mesothelial cells of the visceral pleura, airway epithelial cells, and alveolar macrophages. In addition, ferritin was evident in the chronic inflammatory cells of autopsy samples from patients with IPF. The evidence for disrupted iron homeostasis in IPF was not compelling and this pathway is not proposed as a mechanism of biological effect in all fibrotic injuries.

Elevations in tissue concentrations of ferritin, DMT1, and FPN1 in tissues collected after pleurodesis challenge current understanding, because the controls of expression can be diametrically opposite to each other (22). The expression of these three proteins involves the same posttranscriptional mechanism, using the iron-responsive element (IRE). For ferritin and FPN1, a specific sequence at the 5′-untranslated end of ferritin mRNA (i.e., the IRE) binds a cubane iron–sulfur cluster, referred to as the iron-regulatory protein (IRP), when the IRP exists in the apoprotein form. Elevated concentrations of available iron react with IRP to alter its conformation, decrease affinity of the protein to the mRNA, and displace it from the mRNA, allowing translation to proceed. In contrast, DMT1 mRNA contains an IRE at the 3′-untranslated region that allows increased synthesis with iron depletion. The elevation in expression of all three of these proteins after pleurodesis supports an iron depletion that occurs after the complexation of essential cell metal by the surface of the endocytosed talc particle. This initiates an increase in intracellular iron as the cell elevates concentrations to meet the demands of a new equilibrium imposed by the talc. Subsequently, all three proteins can be elevated, but such expression may involve temporal and regional variability.

The disruption of cell iron homeostasis is frequently associated with oxidative stress (25, 26). In a similar manner, *in vitro* exposure to talc increased the generation of oxidants, measured as DCF diacetate fluorescence, by mesothelial and airway epithelial cells. The acellular assay for hydroxyl radical production suggests that surface functional groups on the talc complex a source of available iron in the cell, which then redox cycles, generating oxidant. An alternative proposal could involve talc sequestering cell iron and the host response involving superoxide generation as a ferrireductant to resecure the requisite metal. *In vitro* changes in heme oxygenase RNA after cellular exposures to talc also support oxidative stress.

The biological effect of talc was evaluated using indices of the fibro-inflammatory response. The *in vitro* cellular response to talc included the increased release of IL-8 and an elevation of RNA for both IL-8 and IL-6, comparable to those for many particles (27). Among patients treated with talc pleurodesis, the deposition of collagen was obvious on trichrome staining, again analogous to numerous particle exposures (6). The indices of both inflammation and fibrosis after exposure to mineral oxide particles were demonstrated to correlate with changes in iron homeostasis. The release of inflammatory mediators can directly correspond to the concentration of metal complexed to a particle surface (28). Regarding the relationship between iron and fibrotic injury, exposure to metal chelators such as bleomycin can increase the activity of prolyl hydroxylase, resulting in a deposition of collagen (29). *In vitro* and *in vivo* exposures both confirm that biological effects after talc include those proinflammatory and fibrotic events previously associated with mineral oxide particles.

We conclude that exposure to talc disrupts iron homeostasis in mesothelial and airway epithelial cells, and is associated with both oxidative stress and a biological effect, comparable to those of other particles. The resultant accumulation of iron and alterations in iron-related proteins are evident among patients with pleurodesis. Sclerosis after exposure to talc can be regarded as a model of therapeutic benefit after a massive and focal exposure to a mineral oxide particle.

Author Disclosure: A.J.G., J.M.S., L.A.D., J.H.R., J.L.T., and E.N.P. do not have a financial relationship with a commercial entity that has an interest in the subject of this manuscript. V.L.R. has testified in cases involving talc manufacturers in asbestos litigation.

References

1. Brook RD, Rajagopalan S, Pope CA III, Brook JR, Bhatnagar A, Diez-Roux AV, Holguin F, Hong Y, Luepker RV, Mittleman MA, *et al.* Particulate matter air pollution and cardiovascular disease: an update to the scientific statement from the American Heart Association. *Circulation* 2010;121:2331–2378.
2. Pelucchi C, Negri E, Gallus S, Boffetta P, Tramacere I, La Vecchia C. Long-term particulate matter exposure and mortality: a review of European epidemiological studies. *BMC Public Health* 2009;9:453.
3. Zhang JJ, Smith KR. Household air pollution from coal and biomass fuels in China: measurements, health impacts, and interventions. *Environ Health Perspect* 2007;115:848–855.
4. Mossman BT, Churg A. Mechanisms in the pathogenesis of asbestosis and silicosis. *Am J Respir Crit Care Med* 1998;157:1666–1680.
5. Ghio AJ, Churg A, Roggli VL. Ferruginous bodies: implications in the mechanism of fiber and particle toxicity. *Toxicol Pathol* 2004;32:643–649.
6. Ghio AJ, Jaskot RH, Hatch GE. Lung injury after silica instillation is associated with an accumulation of iron in rats. *Am J Physiol* 1994; 267:L686–L692.
7. Vallyathan V, Castranova V, Pack D, Leonard S, Shumaker J, Hubbs AF, Shoemaker DA, Ramsey DM, Pretty JR, McLaurin JL, *et al.* Freshly fractured quartz inhalation leads to enhanced lung injury and inflammation: potential role of free radicals. *Am J Respir Crit Care Med* 1995;152:1003–1009.
8. Rodriguez-Panadero F, Antony VB. Pleurodesis: state of the art. *Eur Respir J* 1997;10:1648–1654.
9. Ghio AJ, Kennedy TP, Stonehuerner JG, Crumbliss AL, Hoidal JR. DNA strand breaks following *in vitro* exposure to asbestos increase with surface-complexed (Fe^{3+}). *Arch Biochem Biophys* 1994;311:13–18.
10. Wang X, Ghio AJ, Yang F, Dolan KG, Garrick MD, Piantadosi CA. Iron uptake and NRAMP2/DMT1/DCT1 in human bronchial epithelial cells. *Am J Physiol Lung Cell Mol Physiol* 2002;282:L987–L995.
11. Ghio AJ, Wang X, Silbajoris R, Garrick MD, Piantadosi CA, Yang F. DMT1 expression is increased in the lungs of hypotransferrinemic mice. *Am J Physiol Lung Cell Mol Physiol* 2003;284:L938–L944.
12. Yang F, Liu XB, Quinones M, Melby PC, Ghio A, Haile DJ. Regulation of reticuloendothelial iron transporter MTP1 (SLC11A3) by inflammation. *J Biol Chem* 2002;277:39786–39791.
13. Ghio AJ, Kennedy TP, Whorton AR, Crumbliss AL, Hatch GE, Hoidal JR. Role of surface complexed iron in oxidant generation

and lung inflammation induced by silicates. *Am J Physiol* 1992;263: L511–L518.
14. Iler RK. The chemistry of silica. New York: John Wiley and Sons; 1979.
15. Grim RE. Clay mineralogy. New York: McGraw-Hill Book Co.; 1968.
16. Kragten J. Atlas of metal–ligand equilibria in aqueous solution. New York City: Halstead Press; 1978.
17. Crumbliss ALGJ. A comparison of some aspects of the coordination chemistry of aluminum (III) and iron (III). *Comm Inorg Chem* 1988;8: 1–26.
18. Dugger DLSJ, Irby BN, McConnell BL, Cummings WW, Mattman RW. The exchange of twenty metal ions with the weakly acidic silanol group of silica gel. *J Phys Chem* 1964;68:757–760.
19. Fordham AW. Sorption and precipitation of iron on kaolinite: factors involved in sorption equilibria. *Aust J Soil Res* 1969;7:185–197.
20. Herrara HRPM. Reaction of montmorillonite with iron (III). *Proc Soil Sci Soc Am* 1970;34:740–745.
21. Breuer W, Epsztejn S, Cabantchik ZI. Iron acquired from transferrin by K562 cells is delivered into a cytoplasmic pool of chelatable iron (II). *J Biol Chem* 1995;270:24209–24215.
22. Muckenthaler MU, Galy B, Hentze MW. Systemic iron homeostasis and the iron-responsive element/iron-regulatory protein (IRE/IRP) regulatory network. *Annu Rev Nutr* 2008;28:197–213.
23. Nunez MT. Regulatory mechanisms of intestinal iron absorption: uncovering of a fast-response mechanism based on DMT1 and ferroportin endocytosis. *Biofactors* 2010;36:88–97.
24. Thomson AM, Rogers JT, Leedman PJ. Iron-regulatory proteins, iron-responsive elements and ferritin mRNA translation. *Int J Biochem Cell Biol* 1999;31:1139–1152.
25. Caporossi D, Ciafre SA, Pittaluga M, Savini I, Farace MG. Cellular responses to H(2)O(2) and bleomycin-induced oxidative stress in l6C5 rat myoblasts. *Free Radic Biol Med* 2003;35:1355–1364.
26. Ghio AJ, Hilborn ED, Stonehuerner JG, Dailey LA, Carter JD, Richards JH, Crissman KM, Foronjy RF, Uyeminami DL, Pinkerton KE. Particulate matter in cigarette smoke alters iron homeostasis to produce a biological effect. *Am J Respir Crit Care Med* 2008;178:1130–1138.
27. Seagrave J. Mechanisms and implications of air pollution particle associations with chemokines. *Toxicol Appl Pharmacol* 2008;232:469–477.
28. Pritchard R, Ghio AJ, Lehmann J, Park P, Gilmour MI, Winsett DW, Dreher KL, Costa DL. Oxidant generation and lung injury after exposure to particulate air pollutants are associated with concentration of complexed iron. *Inhal Toxicol* 1996;8:457–477.
29. Giri SN, Misra HP, Chandler DB, Chen ZL. Increases in lung prolyl hydroxylase and superoxide dismutase activities during bleomycin-induced lung fibrosis in hamsters. *Exp Mol Pathol* 1983;39:317–326.

Exhibit 99

Cytotoxicity and Apoptosis Induction by Nanoscale Talc Particles from Two Different Geographical Regions in Human Lung Epithelial Cells

Mohd Javed Akhtar,[1,2] Maqusood Ahamed,[3] M. A. Majeed Khan,[3] Salman A. Alrokayan,[3] Iqbal Ahmad,[2] Sudhir Kumar[1]

[1]Fibre Toxicology Division, Indian Institute of Toxicology Research, Lucknow 226001, India

[2]Department of Zoology, University of Lucknow, Lucknow 226007, India

[3]King Abdullah Institute for Nanotechnology, King Saud University, Riyadh 11451, Saudi Arabia

Received 25 October 2012; revised 16 January 2012; accepted 21 January 2012

ABSTRACT: We have characterized the physicochemical properties of nanotalc particles from two different geographical regions and examined their toxicity mechanisms in human lung epithelial (A549) cells. Indigenous nanotalc (IN) of Indian origin and commercial nanotalc (CN) of American origin were used in this study. Physicochemical properties of nanotalc particles were characterized by X-ray diffraction (XRD), transmission electron microscopy (TEM), energy dispersive X-ray spectroscopy (EDS), Brunauer-Emmet-Teller (BET), and dynamic light scattering (DLS). Results showed that both IN and CN particles significantly induce cytotoxicity and alteration in cell cycle phases. Both IN and CN particles were found to induce oxidative stress indicated by induction of reactive oxygen species (ROS), lipid peroxidation, and depletion of antioxidant levels. DNA fragmentation and caspase-3 enzyme activation due to IN and CN particles exposure were also observed. We further showed that after iron chelation, IN and CN particles produce significantly less cytotoxicity, oxidative stress, and genotoxicity to A549 cells as compared with nonchelated particles. In conclusion, this study demonstrated that redox active iron plays significant role in the toxicity of IN and CN particles, which may be mediated through ROS generation and oxidative stress. © 2012 Wiley Periodicals, Inc. Environ Toxicol 29: 394 406, 2014.

Keywords: nanotalc particles; physicochemical characterization; iron chelation; toxicity; apoptosis

INTRODUCTION

Talc is a mineral compound [$Mg_3Si_4O_{10}$ $(OH)_2$] with unique attributes and significant commercial importance. Talc is widely used due to its intrinsic properties such as high thermal stability, low electrical conductivity, good absorption and adsorption properties, and high crystallinity (Pérez-Maqueda et al., 2005; Nkoumbou et al., 2008). Talc is utilized in various applications including paper, paint, cosmetic, plastic, ceramic, pesticide, and pharmaceuticals (Carretero, 2002; Bizi et al., 2003; Petit et al., 2004). Hence, occupational and consumer exposures to talc particles are wide and complex (Jaynes and Zartman, 2005). It has been reported that talc mine workers show higher rates of lung cancer and other respiratory diseases (National Toxicology Program, 1993). Epidemiologic evidence also suggests a possible association between genital use of talcum powder and risk of ovarian cancer (Wild,

Correspondence to: M. Ahamed; e mail: maqusood@gmail.com or mahamed@ksu.edu.sa

Contract grant sponsor: King Abdulaziz City for Science and Technology (KACST) under the National Plan for Science and Technology (NPST).

Contract grant number: 10 NAN1201 02

Contract grant sponsor: University Grants Commission (UGC), New Delhi, India (to M.J.A.)

Published online 13 February 2012 in Wiley Online Library (wileyonlinelibrary.com). DOI 10.1002/tox.21766

2006; Buz'Zard and Lau, 2007; Gates et al., 2008; Langseth et al., 2008). Talc also appears to induce reactive oxygen species (ROS) generation, oxidative stress, and inflammation (Harlow and Hartge, 1995; Buz'Zard and Lau, 2007).

Due to enhanced intrinsic properties, nanoscale talc particles are extensively utilized in many commercial and industrial products (Akhtar et al., 2008; Balamurugan and Maiti, 2010; Sakthivel and Pitchumani, 2011). Despite the wide-spread applications, there is a serious lack of information concerning the mechanisms of toxicity of nanotalc particles. Previously, we have observed that human cells exposed to nanotalc particles induce oxidative stress-mediated cytotoxicity (Akhtar et al., 2010a). However, physicochemical characterization of nanotalc particles and their association with the toxicological response in human cells is still remains unclear.

There are numerous reports suggesting that ROS is an important mediator of the toxicity of minerals such as asbestos and silica (Aung et al., 2007; Akhtar et al., 2010b). It has been known for years that the surface iron (II) or leachable iron (II) on mineral surfaces reduces molecular oxygen to superoxide anion, which is then dismutated to hydrogen peroxide (Shukla et al., 2003). In the presence of asbestos or silica, hydrogen peroxide and superoxide react via a Fenton reaction and/or Haber Weiss reaction driven by iron to form the potent hydroxyl radical in vitro leading to cellular oxidative damage (Persson et al., 2003).

The aim of this work was to characterize the physicochemical properties of nanotalc particles and to determine the role of iron in the toxicity mechanisms of nanotalc particles in human lung epithelial (A549) cells. We utilized two types of nanotalc particles from different geographical origins; indigenous nanotalc (IN) of Indian origin and commercial nanotalc (CN) of American origin. Cytotoxicity of IN and CN particles was examined by MTT and LDH assays. Oxidative stress response of IN and CN particles was assessed by measuring reactive oxygen species (ROS), lipid peroxidation (LPO), glutathione (GSH), superoxide dismutase (SOD), and catalase (CAT). Apoptotic response of IN and CN particles was evaluated by cell cycle analysis, DNA fragmentation, and caspase-3 enzyme activity. To explore the role of iron in the toxicity of IN and CN particles, we utilized deferoxamine mesylate (DFOM), a well-known iron chelator. The physicochemical properties of IN and CN particles were characterized by X-ray diffraction (XRD), transmission electron microscopy (TEM), energy dispersive X-ray spectroscopy (EDS), Brunauer-Emmet-Teller (BET), and dynamic light scattering (DLS). The A549 cells, derived from human lung carcinoma, have been widely utilized in toxicological studies (Zhang et al., 2010; Akhtar et al., 2010a,b; Ahamed et al., 2011a,b,c).

MATERIALS AND METHODS

Nanotalc Particles and Reagents

We have utilized the nanotalc particles from two different geographical regions. Indigenous nanotalc (IN) particles were collected from Rajasthan, India, as reported in our previous publication (Akhtar et al., 2010a). American origin commercial nanotalc (CN) particles (size 70 12 nm) were purchased from M.K. Impex (Mississauga, Canada).

Fetal bovine serum (FBS), penicillin-streptomycin, DMEM/F-12 medium, and HBSS were purchased from Invitrogen Co. (Carlsbad, CA). MTT [3-(4,5-dimethylthiazol-2-yl)-2,5 diphenyltetrazolium bromide], 2,7-dichlorofluorescin diacetate (DCFH-DA), deferoxamine mesylate (DFOM), glutathione (GSH), thiobarbituric acid (TBA), propidium iodide (PI), RNase A, diethylenetriaminepentaacetic acid (DETAPAC), *N*-acetyl-asp-glu-val-asp-7-amido-4-trifluoromethylcoumarin (Ac-DEVD-AFC), 7-amido-4-trifluoromethylcoumarin (AFC) standard, Bradford reagent, and bovine serum albumin (BSA) were obtained from Sigma-Aldrich (St. Louis, MO). Apoptotic DNA Ladder Kit was bought from Roche. All other chemicals used were of the highest purity available from commercial sources.

Characterization of Nanotalc Particles

Crystalline nature of both IN and CN particles were examined by taking X-ray diffraction (XRD) pattern at room temperature with the help of PANalytical X'Pert X-ray diffractometer equipped with a Ni filtered using Cu-K_α (λ = 1.54056 Å) radiations as X-ray source. Morphology and size of IN and CN particles were examined by field emission transmission electron microscopy (FETEM) (JEM-2100F, JEOL Inc., Tokyo, Japan) at an accelerating voltage of 200 kV. To check the purity of IN and CN particles, an energy dispersive X-ray spectroscopy (EDS) analysis was performed. Brunauer-Emmet-Teller (BET) surface area measurement of IN and CN particles was determined by multipoint nitrogen adsorption at 77 K using a Beckman Coulter SA3100 device.

Dynamic light scattering (DLS) and laser Doppler velocimetry (LDV) for the characterization of hydrodynamic size and zeta potential (ζ) of IN and CN particles in distilled water and cell culture media were performed on a Malvern Instruments Zetasizer Nano-ZS instrument as described by Murdock et al. (2008).

Treatment of Nanotalc Particles with Deferoxamine Mesylate

We treated both IN and CN particles with DFOM for iron chelation. In brief, IN and CN particles were incubated with 10 mM DFOM at a concentration of 1000 μg/mL for

20 h as described by Aung et al. (2007). Then particles were washed three times with cell culture medium by centrifuging at 4000 rpm for 10 min followed by resuspension.

Cell Culture and Exposure to Nanotalc Particles

Human lung epithelial (A549) cells were obtained from National Centre for Science (NCCS), Pune, India. Cells were used between passages 10 and 20. Cells were cultured in DMEM/F-12 medium supplemented with 10% FBS and 100 U/mL penicillin-streptomycin at 5% CO_2 and 37°C. At 85% confluence, cells were harvested using 0.25% trypsin and were subcultured into 75 cm^2 flasks, 6-well plates, or 96-well plates according to selection of experiments. Cells were allowed to attach the surface for 24 h before treatment. IN and CN particles were suspended in cell culture medium and diluted to a appropriate concentration (200 μg/mL). Suspension of nanotalc particles were then sonicated using a sonicator bath at room temperature for 10 min at 40 W to avoid particles agglomeration before administration to the cells. The selection of the 200 μg/mL concentration of nanotalc particles was based on our previous publication (Akhtar et al., 2010a). All the data presented in this study was that of 48 h exposure. Cells not exposed to nanotalc particles served as controls in each experiment.

Cell Viability Assay

Viability of A549 cells after exposure to nanotalc particles was assessed by MTT assay as described by Mossman (1983). The MTT assay assesses the mitochondrial function by measuring ability of viable cells to reduce MTT into blue formazon product. In brief, 10,000 cells per well were seeded in 96-well plate and exposed to IN and CN particles at the concentration of 200 μg/mL for 48 h. After the exposure completed, the medium was removed from each well to avoid interference of particles and replaced with new medium containing MTT solution in an amount equal to 10% of culture volume, and incubated for 3 h at 37°C until a purple colored formazan product developed. The resulting formazan product was dissolved in acidified isopropanol. Further, the 96-well plate was centrifuged at 2500 rpm for 5 min to settle down the remaining particles present in the solution. Then, a 100 μL supernatant was transferred to other fresh wells of 96-well plate and absorbance was measured at 570 by using a microplate reader (FLUOstar-Omega).

Lactate Dehydroganase Leakage Assay

Lactate dehydrogenase (LDH) is an enzyme widely present in cytosol that converts lactate to pyruvate. When plasma membrane integrity is disrupted, LDH leaks into culture media and its extracellular level is elevated. LDH assay was carried out with the method described earlier (Wroblewski and LaDue, 1955; Welder et al., 1991). In brief, 10,000 cells per well were seeded in 96-well plate and exposed to IN and CN particles at the concentration of 200 μg/mL for 48 h. After the exposure completed, the 96-well plate was centrifuged at 2500 rpm for 10 min to get the cell culture media. Then, a 100 μL of culture media transferred to new fresh tube containing 100 μL of sodium pyruvate (2.5 mg/mL phosphate buffer) and 100 μL of reduced nicotinamide adenine dinucleotide (NADH) (2.5 mg/mL phosphate buffer) in a total volume of 3.0 mL (0.1 M potassium phosphate buffer, pH 7.4). The rate of NADH oxidation was determined by following the decrease in absorbance at 340 nm for 3 min at 30-s interval using a spectrophotometer (Thermo-Spectronic).

Cell Cycle Analysis

Cell cycle distribution was assayed by determining DNA content. Cells were treated with IN and CN particles for 48 h. After exposure, cells were fixed in 3% (w/v) paraformaldehyde for 10 min, permeabilized on ice in phosphate buffer saline-0.5% Triton X-100 for 15 min, washed and resuspended in 0.5 ml of phosphate buffer saline containing 1% FBS, 1 mg/ml RNaseA, and 50 μg/ml propidium iodide. The samples were incubated for 30 min at 37°C. The data were acquired and analyzed on FACS-Calibur flow cytometer (Becton-Dickinson LSR II, San Jose, CA) using Cell Quest 3.3 software.

Measurement of Reactive Oxygen Species

For the measurement of ROS generation, cells were cultured in 12-well plate. The production of intracellular ROS was measured using 2,7-dichlorofluorescin diacetate (DCFH-DA) (Wang and Joseph, 1999). The DCFH-DA passively enters the cell where it reacts with ROS to form the highly fluorescent compound dichlorofluorescein (DCF). Briefly, 10 mM DCFH-DA stock solution (in methanol) was diluted in culture medium without serum or other additive to yield a 100 μM working solution. After exposure to IN and CN particles, cells were washed twice with HBSS and then incubated in 1 mL working solution of DCFH-DA at 37°C for 30 min. Cells were lysed in alkaline solution and centrifuged at 3000 rpm for 10 min. Then, a 200 μL supernatant (from 12-well plate) was transferred to the fresh well of black 96-well plates and fluorescence was measured using at 485 nm excitation and 520 nm emission using a microplate reader (FLUOstar-Omega). The values of ROS were expressed as percent of fluorescence intensity relative to controls.

Membrane Lipid Peroxidation Assay

The extent of membrane lipid peroxidation (LPO) was estimated by measuring the formation of thiobarbituric acid reactive species (TBARS) using the method of Ohkawa et al. (1979). Briefly, cells were cultured in 75 cm^2 culture flask and exposed to IN and CN particles at the concentration of 200 μg/mL for 48 h. After the treatment, a 200 μL of cell suspension was mixed with 800 μL of LPO assay cocktail containing TBA (0.4%, w/v), sodium dodecyl sulphate (0.5%, w/v), and acetic acid (5 %, v/v). Reaction mixture was then incubated at 95°C for 1 h. After cooling to room temperature the reaction mixture was centrifuged at 5000 rpm for 5 min. The absorbance of the supernatants was read at 532 nm against the standard. The amount of TBARS was expressed as nmol/mg protein.

Intracellular Glutathione Assay

Intracellular GSH was quantified using the method of Hissin and Hilf (1976). Briefly, cells were cultured in 75 cm^2 culture flask and exposed to IN and CN particles at the concentration of 200 μg/mL for 48 h. After the exposure completed, cells were lysed in 20 mM Tris (pH 7.0) and the centrifuged at 10,000 rpm for 10 min at 4°C. Further, protein of the supernatant was precipitated using 1% perchloric acid and again centrifuged at 10,000 rpm for 5 min at 4°C to get supernatant. Then 20 μL of supernatant was mixed with 160 μL of 0.1M potassium phosphate-5 mM EDTA buffer (pH 8.3) and 20 μL *O*-phthalaldehyde (1 mg/mL in methanol) in a black 96-well plate. After 2 h of incubation at room temperature in the dark, fluorescence was measured at emission wavelength of 460 nm and excitation wavelength of 350 nm. The amount of GSH was expressed as nmol GSH/mg protein.

Antioxidant Enzymes Activity Assay

Cells were cultured in 75 cm^2 culture flask and exposed to IN and CN particles at the concentration of 200 μg/mL for 48 h. After the exposure completed, cells were harvested in ice-cold phosphate buffer saline and washed twice with phosphate buffer saline at 4°C. The cell pellets were then lysed in cell lysis buffer. Following centrifugation (10,000 rpm for 10 min 4°C) the supernatant (i.e. cell lysate) was maintained on ice until assayed for activity of superoxide dismutase (SOD) and catalase (CAT) enzymes. The total SOD was determined using pyrogallol assay following the procedure described by Marklund and Marklund (1974), based on the competition between pyrogallol oxidation by superoxide radicals and superoxide dismutation by SOD, and spectrophotometrically read at 420 nm. The amount of SOD inhibiting the reaction rate by 50% in the given assay conditions was defined as one unit of SOD. The results were expressed as units/min/mg protein.

CAT activities were assayed by the method described by Claiborne (1985). One unit of CAT activity is defined as the amount of enzyme that decomposes 1 μmol H_2O_2/min. CAT activities were given as μmol H_2O_2 decomposed/min/mg protein.

DNA Ladder Assay

Cells were cultured in 6-well plate and exposed to IN and CN particles at the concentration of 200 μg/mL for 48 h. At the end of exposure DNA was extracted using an apoptotic DNA Ladder Kit (Roche, Cat# 11835246001). The extracted DNA was then evaluated on a 1% agarose gel using ethidium bromide. DNA fragmentation pattern was documented by a gel documentation system.

Assay of Caspase-3 Enzyme

Cells were cultured in 6-well plate and exposed to IN and CN particles at the concentration of 200 μg/mL for 48 h. Activity of caspase-3 enzyme was determined using a standard fluorometric microplate assay (Walsh et al., 2008) with some modifications. A reaction mixture containing 30 μL of cell lysate, 20 μL of Ac-DEVD-AFC (caspase-3 substrate), and 150 μL of protease reaction buffer (50 mM Hepes, 1 mM EDTA, and 1 mM DTT), pH 7.2, was incubated for 15 min. Fluorescence of reaction mixture was measured at 5 min interval for 15 min at excitation/emission wavelengths of 430/535 nm using a microplate reader (FLUOstar-Omega). A standard of 7-amido-4-trifluoromethylcoumarin (AFC) ranging from 5 to 15 μM was prepared and its fluorescence was recorded for calculation of caspase-3 activity in terms of pmol AFC released/min/mg protein.

Estimation of Protein

The protein content was measured by the method of Bradford (1976) using Bradford reagent (Sigma-Aldrich, St. Louis, MO), along with bovine serum albumin as standard.

Statistics

All the data represented in this study are means ± SD of three identical experiments made in three replicate. Statistical significance was determined by one-way analysis of variance (ANOVA) followed by Dunnett's multiple comparison test. Significance was ascribed at $p < 0.05$. All analyses were conducted using the Prism software package (GraphPad Software).

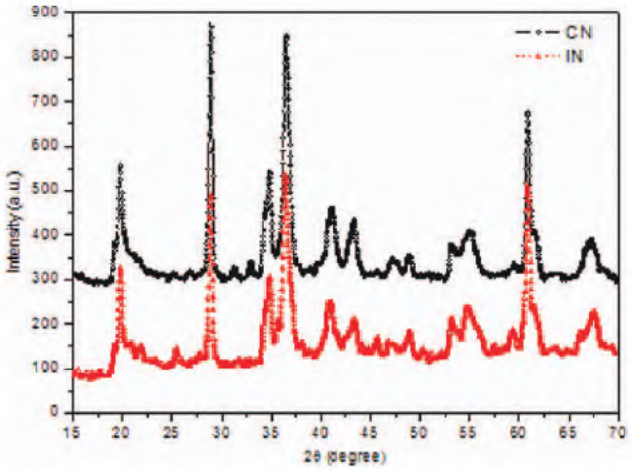

Fig. 1. XRD pattern of two types of nanotalc particles. IN; indigenous nanotalc particles, CN; commercial nanotalc particles. [Color figure can be viewed in the online issue, which is available at wileyonlinelibrary.com.]

RESULTS

Characterization of IN and CN Particles

Characterization of IN and CN particles was performed using a combination of XRD, TEM, DLS, zeta-potential, and BET in order to provide clear insight into crystalline nature, morphology, particle size, surface property, and chemical composition. These properties are necessary for a better understanding of nanotoxicology.

Figure 1 represents the XRD pattern of IN and CN particles. Image clearly exhibits that the crystalline nature of both IN and CN particles were same. The average size of nanocrystals calculated from the XRD results using Scherrer's equation (Patterson, 1939) was found to be 93 and 89 nm for IN and CN particles, respectively. Figure 2(A,B) show the typical TEM images of IN and CN particles, respectively. Images show that particles are aggregated. We never found small independent crystals in the TEM images.

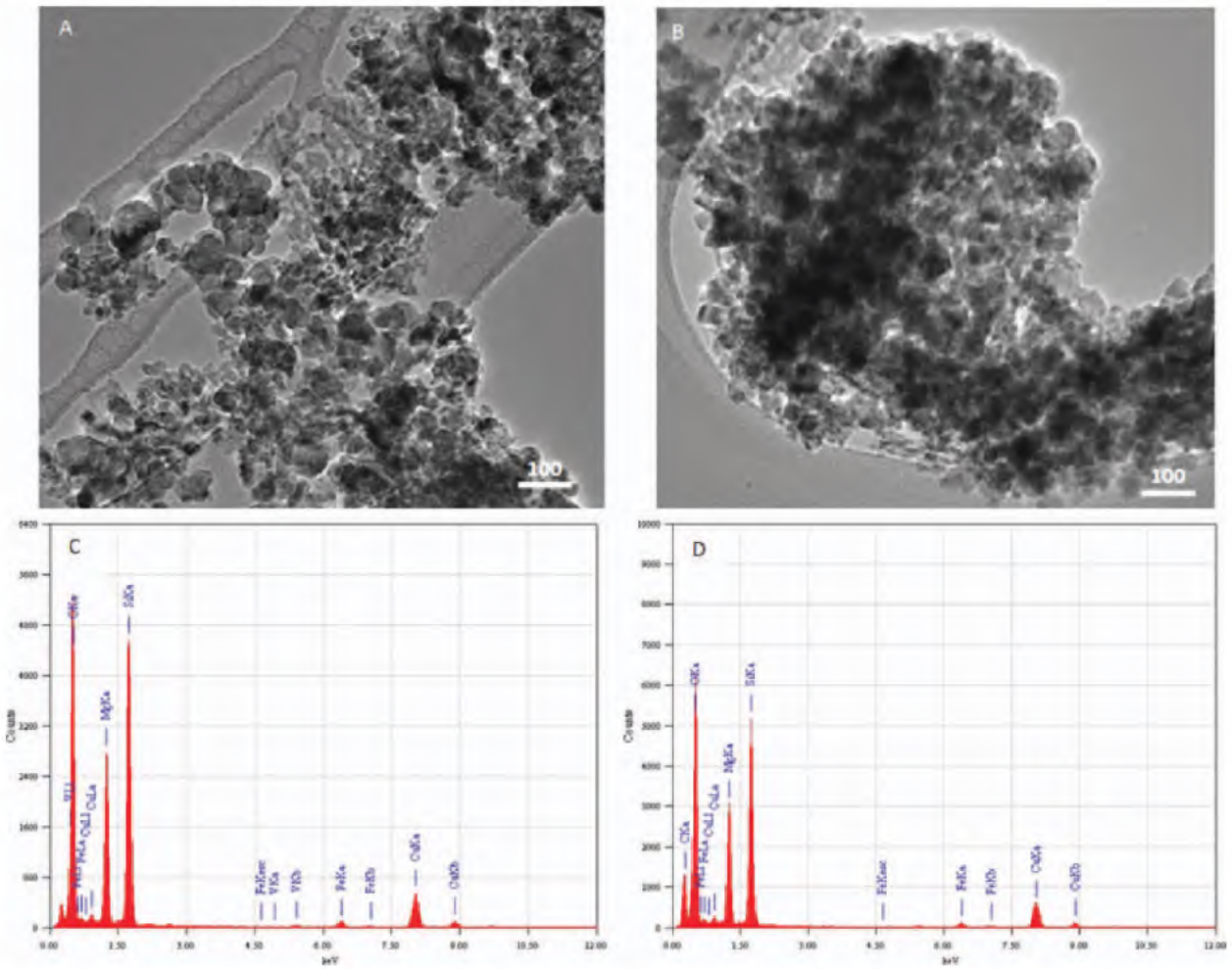

Fig. 2. TEM characterization of nanotalc particles. (A) FETEM of indigenous nanotalc particles, (B) FETEM of commercial nanotalc particles, (C) EDS spectrum of indigenous nanotalc particles, and (D) EDS spectrum of commercial nanotalc particles. [Color figure can be viewed in the online issue, which is available at wileyonlinelibrary.com.]

TABLE 1. Physicochemical properties of two types of nanotalc particles

	Indigenous Nanotalc (IN)	Commercial Nanotalc (CN)
Average XRD size (nm)	93	89
Average TEM size (nm)	94	91
Surface area (m^2/g)	15.4	15.7
Hydrodynamic size (nm)		
Distilled water	782	735
Cell culture medium	671	643
Zeta potential (mV)	20.3	20.8
Iron content (%)[a]	0.19	0.08

[a]This information is obtained from our previous publication (Akhtar et al., 2010a).

The average TEM size of IN and CN particles were 94 and 91 nm, respectively, which were consistent with the value observed by XRD. The EDS spectra of IN and CN particles are given in Figure 2(C,D), respectively. The presence of Cu and C signals was from the carbon-coated-copper TEM-grid. Presence of iron peaks in both IN and CN particles are in agreement with our previous reports where atomic absorption spectroscopy data showed that 0.19% and 0.08% of iron present in IN and CN particles, respectively (Akhtar et al., 2010 a). The specific surface area of IN and CN particles determined by BET was 15.4 and 15.7 m^2/g respectively.

The physicochemical properties of IN and CN particles are listed in Table 1. All the data from XRD, electron microscopy, and associated techniques was obtained under high vacuum and constitutes the size, morphology, and composition analysis characteristics of nanotalc particles. However, once the nanotalc particles were introduced aqueous media, the sizes changed to approximately 5 to 10 times of the primary size. The average hydrodynamic size of IN and CN particles in distilled water was 782 nm and 735 nm while in cell culture media was 671 and 643 nm, respectively. The higher size of IN and CN particles in aqueous state as compared to XRD and TEM results was due to the tendency of particles to aggregate in the aqueous state. This finding is supported by other investigators (Murdock et al., 2008) and has been briefly discussed in our previous publications (Ahamed et al., 2010a,b). The tendency of particles to form aggregates depends strongly on the surface charge. The particle charge, determined as zeta-potential by laser doppler velocimetry (LDV) was 20.3mV and 20.8 for IN and CN, respectively.

IN and CN Particles Induced Cytotoxicity

We examined the cell viability (MTT assay) and membrane damage (LDH leakage) as cytotoxicity end points. MTT results demonstrated that both IN and CN particles induced significant reduction in cell viability. The MTT reduction

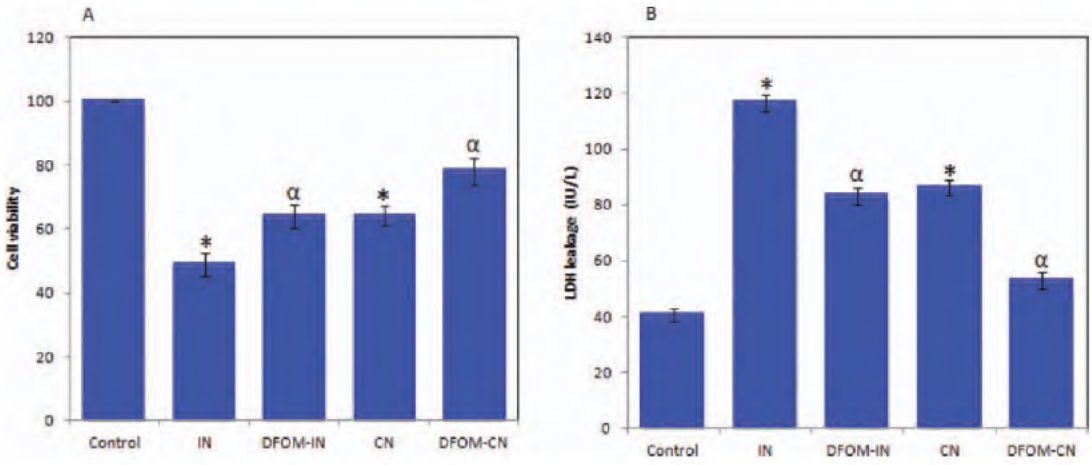

Fig. 3. Comparative effects of nanotalc particles and iron-chelated nanotalc particles on cell viability and LDH release in human lung epithelial A549 cells. Cells were treated with two types of nanotalc particles at the concentration of 200 μg/mL for 48 h. Iron chelator deferoxamine mesylate (DFOM) was co-exposed with nanotalc particles. At the end of treatment MTT and LDH assays were determined as described in materials and methods. (A) MTT assay and (B) LDH assay. Data represented are mean ± SD of three identical experiments made in three replicates. *Statistically significant difference in cell viability reduction and LDH release as compared with the controls ($p < 0.05$ for each). $^{\alpha}$Iron chelation by DFOM significantly reduces the cytotoxicity caused by nanotalc particles ($p < 0.05$ for each). IN; indigenous nanotalc particles, CN; commercial nanotalc particles, DFOM-IN; indigenous nanotalc particles treated with DFOM, DFOM-CN; commercial nanotalc particles treated with DFOM. [Color figure can be viewed in the online issue, which is available at wileyonlinelibrary.com.]

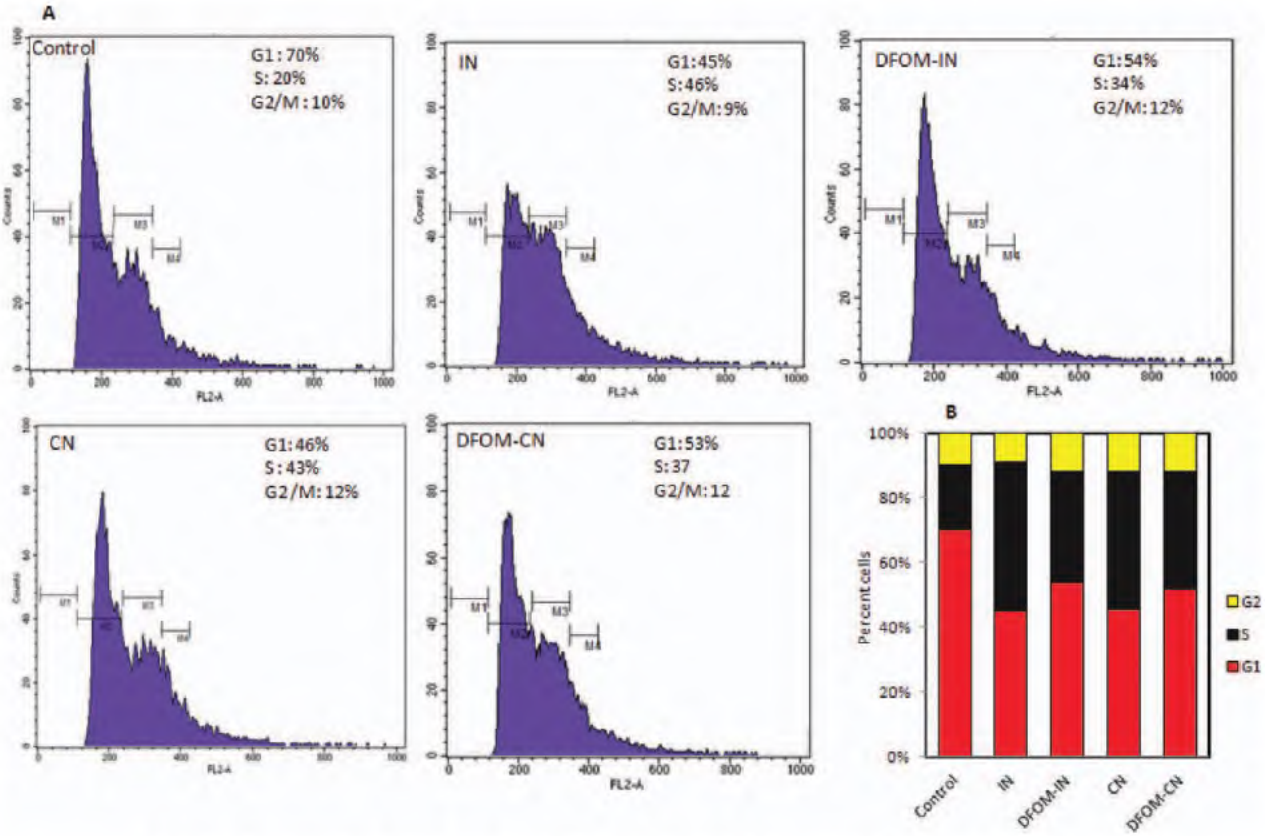

Fig. 4. Comparative effects of nanotalc particles and iron-chelated nanotalc particles on cell cycle in human lung epithelial A549 cells. Cells were treated with two types of nanotalc particles at the concentration of 200 μg/mL for 48 h. Iron chelator deferoxamine mesylate (DFOM) was coexposed with nanotalc particles. At the end of treatment cell cycle was analyzed as described in materials and methods. (A) Raw data generated by flow cytometric analysis of selected representative samples. The *y*-axis denotes cell count and the *x*-axis represents DNA content. M1, M2, M3, and M4 represent the SubG1, G1, S, and G2/M phase, respectively. (B) Percent of the distribution of cells in the G1, S, and G2/M phase of cell cycle. IN; indigenous nanotalc particles, CN; commercial nanotalc particles, DFOM-IN; indigenous nanotalc particles treated with DFOM, DFOM-CN; commercial nanotalc particles treated with DFOM. [Color figure can be viewed in the online issue, which is available at wileyonlinelibrary.com.]

observed after 48 h at the concentration of 200 μg/mL was 49% and 64% for IN and CN particles, respectively [Fig. 3(A)]. Both IN and CN particles were also found to induce LDH leakage in A549 cells [Fig. 3(B)]. To determine whether our observed cytotoxicity was due iron content, we treated both IN and CN particles with an iron chelator DFOM and tested the cytotoxic effect of chelated nanotalc particles in A549 cells. Results showed that iron chelated IN and CN particles induce less cytotoxicity than those of non-chelated one (Fig. 3).

IN and CN Particles Induced Cell Cycle Changes

Alteration in the cell cycle phases by IN and CN particles in A549 cells are shown in Figure 4. Both IN and CN particles induced significant S phase arrest. The S phase was 20% in the control. It was changed to 46% and 43% in the cells treated with IN and CN particles respectively. However, iron chelated IN and CN particles exert less effect on cell cycle arrest than those of nonchelated IN and CN particles.

IN and CN Particles Induced Oxidative Stress

ROS generation leads to oxidative damage, which has been reported to be one of the important mechanisms of nanoparticles toxicity (Ahamed et al., 2010c; Ahamed et al., 2011a,b). The potential of IN and CN particles to induce oxidative stress was examined by measuring the ROS, LPO, GSH, SOD, and CAT in A549 cells. Results showed that both IN and CN particles induced the

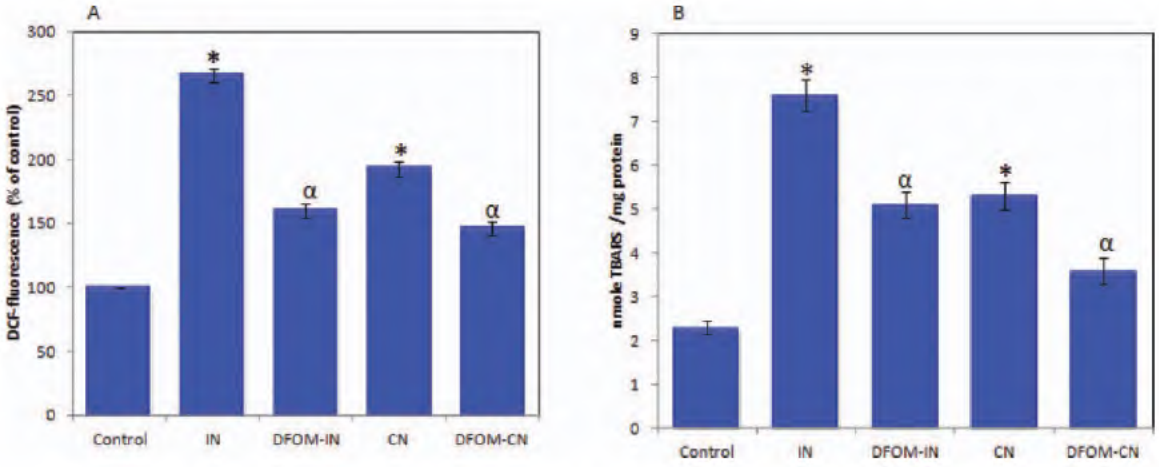

Fig. 5. Comparative effects of nanotalc particles and iron-chelated nanotalc particles on oxidant generations in human lung epithelial A549 cells. Cells were treated with two types of nanotalc particles at the concentration of 200 μg/mL for 48 h. Iron chelator deferoxamine mesylate (DFOM) was coexposed with nanotalc particles. At the end of treatment ROS and LPO levels were determined as described in materials and methods. (A) ROS and (B) LPO. Data represented are mean ± SD of three identical experiments made in three replicates. *Statistically significant difference in ROS and LPO induction as compared with the controls ($p < 0.05$ for each). $^{\alpha}$Iron chelation by DFOM significantly reduces the ROS and LPO induction caused by nanotalc particles ($p < 0.05$ for each). IN; indigenous nanotalc particles, CN; commercial nanotalc particles, DFOM-IN; indigenous nanotalc particles treated with DFOM, DFOM-CN; commercial nanotalc particles treated with DFOM. [Color figure can be viewed in the online issue, which is available at wileyonlinelibrary.com.]

intracellular ROS and LPO levels [Fig. 5(A,B)]. Nanotalc particles induced oxidative stress was further evidenced by depletion of GSH, SOD, and CAT [Fig. 6(A,B,C)]. Moreover, chelation of iron from IN and CN particles significantly reduced the oxidative stress due to these particles.

IN and CN Particles Induced Apoptosis

Apoptosis is executed by series of cysteine proteases known as caspases (Takadera and Ohyashiki, 2007; Tang et al., 2010). Caspase-9 activation is dependent on the release of cytochrome c from mitochondria to form the apoptosome which in turn activates caspase-3. In the present study, significant higher activity of caspase-3 enzyme was observed suggesting the involvement of caspase cascade in IN and CN particles induced apoptosis in A549 cells [Fig. 7(B)]. Figure 7(B) shows that in untreated cells, the DNA was intact whereas the cells treated with IN and CN particles had started apoptotic DNA fragmentation. Besides, iron chelation from IN and CN particles induced less DNA fragmentation as compared with the nonchelated particles.

Taken together, our data highlight the role of iron contaminant present in IN and CN particles in causing the cytotoxicity, oxidative stress, and apoptosis in human lung epithelial cells.

DISCUSSION

Characterization of physicochemical properties of nanoparticles has been suggested in the nanotoxicology research (Murdock et al., 2008; Li et al., 2011). Several parameters including shape, size, crystal structure, purity, hydrodynamic size, aggregation of particles, and aqueous stability have already been suggested (Nel et al., 2006; Yu et al., 2009). In this study, we employed XRD, TEM, EDS, BET, and DLS techniques to characterize the physicochemical properties of IN and CN particles. XRD and TEM results indicated that both IN and CN particles were crystalline, highly aggregated, and having the iron content as a contaminant. Aggregation and stability of nanoparticles in aqueous state are major concerns in nanotoxicity research. Both IN and CN particles were also aggregated in water and cell culture media as well. Zeta potential data also showed that the aqueous suspension of both IN and CN particles were not much stable in aqueous state. The hydrodynamic size of nanotalc particles was found to be approximately seven to eight times higher than those calculated from TEM and XRD. The higher size of nanoparticles in aqueous suspension as compared with XRD and TEM sizes might be due to the tendency of particles to aggregate in aqueous state. This finding is supported by other investigators (Bai et al., 2009) and has been briefly discussed in our previous publication (Ahamed et al., 2010b).

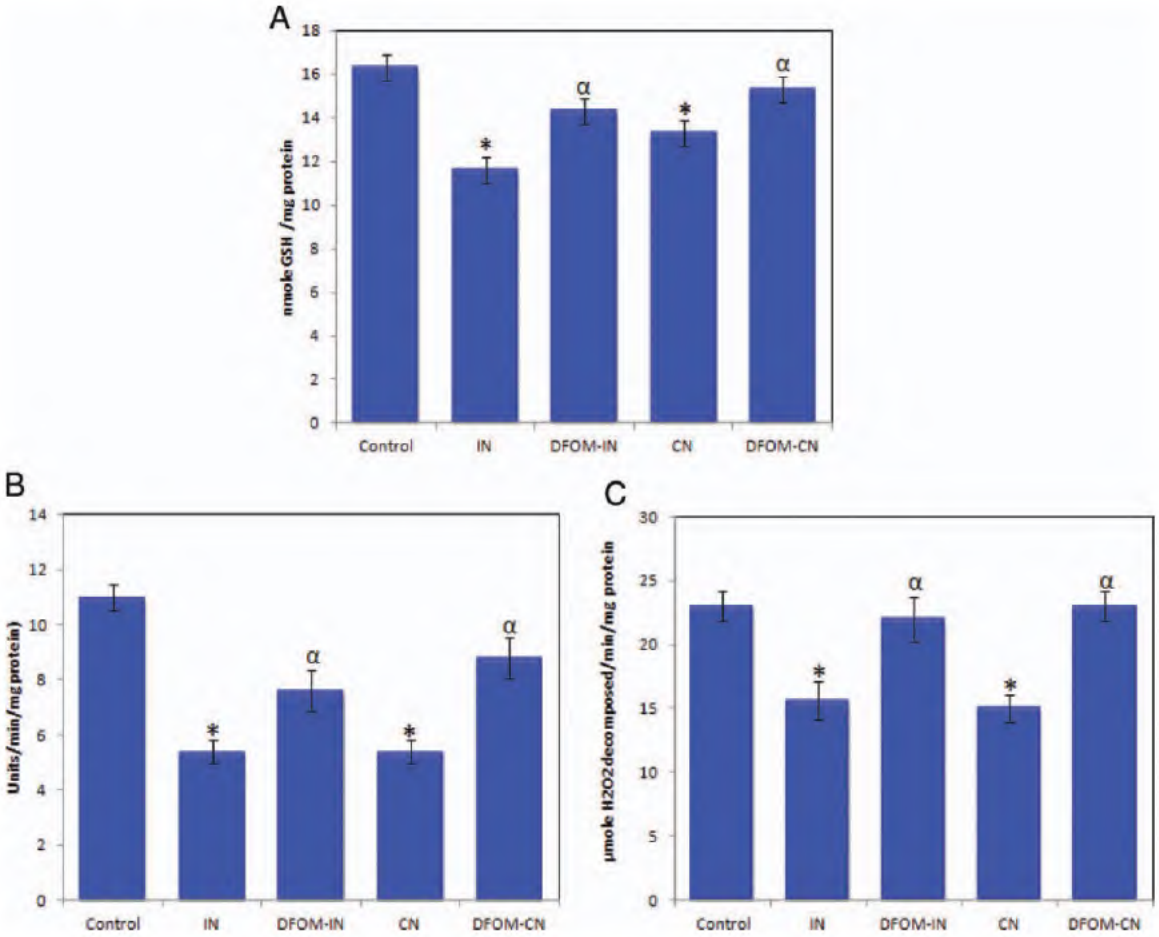

Fig. 6. Comparative effects of nanotalc particles and iron-chelated nanotalc particles on antoxidants reduction in human lung epithelial A549 cells. Cells were treated with two types of nanotalc particles at the concentration of 200 μg/mL for 48 h. Iron chelator deferoxamine mesylate (DFOM) was coexposed with nanotalc particles. At the end of treatment GSH, SOD, and CAT levels were determined as described in materials and methods. (A) GSH, (B) SOD, and (C) CAT. Data represented are mean ± SD of three identical experiments made in three replicates. *Statistically significant difference in GSH, SOD, and CAT reduction as compared to the controls ($p < 0.05$ for each). $^{\alpha}$Iron chelation by DFOM significantly induces the GSH, SOD, and CAT depletion caused by nanotalc particles ($p < 0.05$ for each). IN; indigenous nanotalc particles, CN; commercial nanotalc particles, DFOM-IN; indigenous nanotalc particles treated with DFOM, DFOM-CN; commercial nanotalc particles treated with DFOM. [Color figure can be viewed in the online issue, which is available at wileyonlinelibrary.com.]

In this study, we observed that IN and CN particles induced cell viability reduction and membrane damage in A549 cells. Both IN and CN particles also induced the cell cycle arrest in the S phase leading to apoptosis. In a previous study, S phase arrest was observed in mouse peritoneal macrophages (RAW264.7) exposed to silver nanoparticles (Park et al., 2010), and S phase arrest was also observed in human lung epithelial cells exposed to carbon black particles coated with benzo(a)pyrene (Mroz et al., 2007). Asharani et al. (2009) reported that starch-coated silver NPs induced G2/M phase arrest and DNA damage in human glioblastoma cells and fibroblasts. A perturbation of the cell cycle preceded by a reduction in cell viability associated with accumulation of cells in S phase leading to cell death is typical of compounds inhibiting DNA synthesis (Binkova et al., 2000; Park et al., 2010).

Cellular integrity is affected by oxidative stress when the production of ROS overwhelms antioxidant defense mechanism (Halliwell and Gutteridge, 1990). Our results showed that both IN and CN particles induce oxidant levels and deplete the antioxidant levels in human lung epithelial (A549) cells. LPO and ROS were significantly higher while the antioxidant GSH was significantly lower in cells treated with IN and CN particles. Antioxidant enzymes SOD and

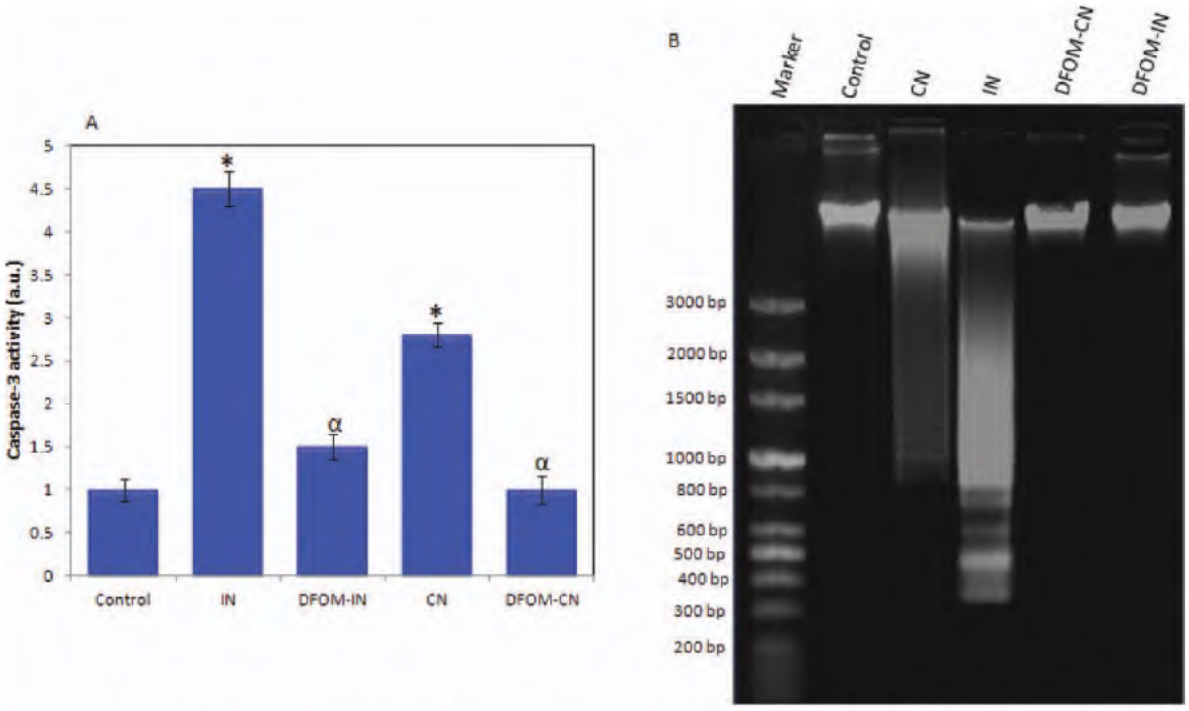

Fig. 7. Comparative effects of nanotalc particles and iron-chelated nanotalc particles on apoptotic markers in human lung epithelial A549 cells. Cells were treated with two types of nanotalc particles at the concentration of 200 μg/mL for 48 h. Iron chelator deferoxamine mesylate (DFOM) was coexposed with nanotalc particles. At the end of treatment DNA ladder and caspase-3 activity were determined as described in materials and methods. (A) Caspase-3 activity. Data represented are mean ± SD of three identical experiments made in three replicates. *Statistically significant difference in caspase-3 activation as compared with the controls ($p < 0.05$ for each). $^{\alpha}$Iron chelation by DFOM significantly reduces the activity of caspase-3 by nanotalc particles ($p < 0.05$ for each). (B) Representative image of DNA fragmentation. IN; indigenous nanotalc particles, CN; commercial nanotalc particles, DFOM-IN; indigenous nanotalc particles treated with DFOM, DFOM-CN; commercial nanotalc particles treated with DFOM. [Color figure can be viewed in the online issue, which is available at wileyonlinelibrary.com.]

CAT levels were also significantly lower in exposed cells. GSH constitutes the first line of the cellular defense mechanism against oxidative injury and is the major intracellular redox buffer in ubiquitous cell types (Meister, 1989). GSH acts as a cosubstrate in the GSH peroxidase-catalyzed reduction of hydrogen peroxide or lipid peroxides (Forman et al., 1997) leading to its depletion. Previous studies demonstrated that ROS generation following GSH depletion caused mitochondrial damage (Martensson et al., 1989), which has been implicated in apoptosis (Green and Reed, 1998). Enzymes such as SOD and CAT are meant for nullifying cellular oxidative stress. SOD catalyzes the dismutation of superoxide anion (O_2) to hydrogen peroxide (H_2O_2). CAT reduces hydrogen peroxide (H_2O_2) to water (H_2O) and oxygen (O_2) (Claiborne, 1985).

The activity of caspase-3 enzyme was significantly higher in cells treated with IN and CN particles. Apoptotic DNA fragmentation was observed in cells exposed to IN and CN particles. Caspases are activated in response to diverse cell death stimuli and ultimately dismantle the cell through restricted proteolysis of numerous cellular proteins that (Timmer and Salvesen, 2007). The activated caspase-3 is capable of autocatalysis as well as cleaving and activating other members of the caspase family, leading to rapid and irreversible apoptosis (Wang et al., 1996). Our previous studies also reported that different types of nanoparticles have potential to induce apoptosis in different kind of cells (Ahamed et al., 2010a; 2010b; 2010c; Ahamed et al., 2010b,c; 2011a).

In the toxicity mechanism of minerals, the iron content has been a key factor. In the present study, EDS analysis showed the presence of iron contamination in both IN and CN particles. These results are in agreement with our previous report where atomic absorption spectroscopy showed the presence of 0.19% and 0.08% of iron in IN and CN particles respectively (Akhtar et al., 2010a). Iron-dependent

ROS generation from fibers results in the generation of hydroxyl radicals through the Fenton reaction and the Haber-Weiss cycle. Iron-dependent ROS generation requires redox cycling of iron and does not necessarily require H_2O_2 or ROS (Halliwell and Gutteridge, 1990). The differential amount of iron present in the two types of nanotalc particles prompted us to investigate the role of iron by sequestering them with an iron chelator, deferoxamine mesylate (DFOM). Sequestering of redox active iron from IN and CN particles by DFOM caused significantly less cytotoxicity, oxidative stress, and genotoxicity than those of the nonchelated IN and CN particles. Similarly, incubation of crocidolite or chrysotile fibers overnight with deferoxamine (5 mM) to inactivate iron catalyzed oxygen radical production also significantly decreased asbestos-induced apoptosis (Broaddus et al., 1996). The role of iron in minerals such as asbestos or silica has been well reported in inflammation and carcinogenesis (Ghio et al., 1992; Hardy and Aust. 1995). Zastawny et al. (1995) have reported on DNA base modifications and membrane damage in cultured mammalian cells treated with iron itself. Similarly, intracellular iron was found to play a critical role in hydrogen peroxide-induced DNA damage (Barbouti et al., 2001). It is also worth to mention that IN particles caused higher toxicity to A549 cells than those of CN particles. This might be due to higher amount of iron present in IN particles (0.19%) as compared with the CN particles (0.08%).

In conclusion, both IN and CN particles significantly induced cytotoxicity, oxidative stress, and apoptosis in human lung epithelial cells. Further, chelation of iron from IN and CN particles by deferoxamine mesylate treatment caused significantly less toxicity as compared to non-chelated IN and CN particles. Therefore, iron content plays a significant role in the toxicity of IN and CN particles, which may be mediated through ROS generation and oxidative stress. This study suggests that one must be very careful regarding the metal impurities like iron present in nanotalc particles before commercial and industrial applications.

REFERENCES

Ahamed M, AlSalhi MS, Siddiqui MKJ. 2010a. Silver nanoparticle applications and human health. Clin Chim Acta 411:1841 1848.

Ahamed M, Posgai R, Gorey TJ, Nielsen M, Hussain S, Rowe J. 2010b. Silver nanoparticles induced heat shock protein 70, oxidative stress and apoptosis in *Drosophila melanogaster*. Toxicol Appl Pharmacol 242:263 269.

Ahamed M, Siddiqui MA, Akhtar MJ, Ahmad I, Pant AB, Alhadlaq HA. 2010c. Genotoxic potential of copper oxide nanoparticles in human lung epithelial cells. Biochem Biophys Res Commun 396:578 583.

Ahamed M. 2011a. Toxic response of nickel nanoparticles in human lung epithelial A549 cells. Toxicol In Vitro 25:930 936.

Ahamed M, Akhtar MJ, Raja M, Ahmad I, Siddiqui MKJ, AlSalhi MS, Alrokayan SA. 2011b. ZnO nanorod induced apoptosis via p53, survivin and bax/bcl 2 pathways mediated by oxidative stress in human alveolar adenocarcinoma cells. Nanomedcine:NBM 7:904 913.

Ahamed M, Akhtar MJ, Siddiqui MA, Ahmad J, Musarrat J, Al Khedhairy AA, AlSalhi MS, Alrokayan SA. 2011c. Oxidative stress mediated apoptosis induced by nickel ferrite nanoparticles in cultured A549 cells. Toxicology 283:101 108.

Akhtar S, Shukla D, Kumar V. 2008. Studies on effect of nano talc filler on nucleation, crystal morphology and crystallization behaviour of semi crystalline plastics. Solid State Phenomena 136:161 174.

Akhtar MJ, Kumar S, Murthy RC, Ashquin M, Khan MI, Patil G, Ahmad I. 2010a. The primary role of iron mediated lipid peroxidation in the differential cytotoxicity caused by two varieties of talc nanoparticles on A549 cells and lipid peroxidation inhibitory effect exerted by ascorbic acid. Toxicol In Vitro 24:1139 1147.

Akhtar MJ, Ahamed M, Kumar S, Siddiqui H, Patil G, Ashquin M, Ahmad I. 2010b. Nanotoxicity of pure silica mediated through oxidant generation rather than glutathione depletion in human lung epithelial cells. Toxicology 276:95 102.

AshaRani PV, Mun G, Hande MP, Valiyaveettil S. 2009. Cytotoxicity and genotoxicity of silver nanoparticles in human cells. ACS Nano 3:279 290.

Aung W, Hasegawa S, Furukawa T, Saga T. 2007. Potential role of ferritin heavy chain in oxidative stress and apoptosis in human mesothelial and mesothelioma cells: Implications for asbestos induced oncogenesis. Carcinogenesis 28:2047 2052.

Balamurugan GP, Maiti SN. 2010. Effects of nanotalc inclusion on mechanical, microstructural, melt shear rheological, and crystallization behavior of polyamide 6 based binary and ternary nanocomposites. Polym Eng Sci 50:1978 1993.

Bai W, Zhang Z, Tian W, He X, Ma Y, Zhao Y, Chai Z. 2009. Toxicity of zinc oxide nanoparticles to zebrafish embryo: A physicochemical study of toxicity mechanism. J Nanopart Res 12:1645 1654.

Barbouti A, Doulias PT, Zhu BZ, Frei B, Galaris D. 2001. Intracellular iron, but not copper, plays a critical role in hydrogen peroxide induced DNA damage. Free Radical Biol Med 31: 490 498.

Binkova B, Giguère Y, Rossner Jr P, Dost M, Srm RJ. 2000. The effect of dibenzo[a, 1]pyrene and benzo[a]pyrene on human diploid lung fibroblasts: The induction of DNA adducts, expression of p53 and p21(WAF1) proteins and cell cycle distribution. Mutat Res 471:57 70.

Bizi M, Flament MP, Leterne P, Baudet G, Gayot A. 2003. Relation between structural characteristics of talc and its properties as an antisticking agent in the production of tablets. Eur J Pharm Sci 19:373 379.

Bradford MM. 1976. A rapid and sensitive method for the quantitation of microgram quantities of protein utilizing the principle of protein dye binding. Anal Biochem 72:248 254.

Broaddus VC, Yang L, Scavo LM, Ernst JD, Boylan AM. 1996. Asbestos induces apoptosis of human and rabbit pleural mesothelial cells via reactive oxygen species. J Clin Invest 98: 2050 2059.

Buz'Zard AR, Lau BH. 2007. Pycnogenol reduces talc induced neoplastic transformation in human ovarian cell cultures. Phyt other Res 21:579 286.

Carretero MI. 2002. Clay minerals and their beneficial effects upon human health. Appl Clay Sci 21:155 163.

Claiborne A. 1985. Catalase activity. In: Greenwald RA, editor. Handbook of Methods for Oxygen Radical Research. CRC Press Inc. pp283 284.

Forman HJ, Liu R, Tian L. 1997. Glutathione cycling in oxidative stress. In: Clerch LB, Massaro DJ, editors.Oxygen, Gene Expression, and Cellular Function: Lung Biology in Health and Disease, Vol. 105. New York: Marcel Dekker. pp99 112.

Gates MA, Tworoger SS, Terry KL, Titus Ernstoff L, Rosner B, De Vivo I, Cramer DW, Hankinson SE. 2008. Talc use, var iants of the GSTM1, GSTT1, and NAT2 genes, and risk of epi thelial ovarian cancer. Cancer Epidemiol Biomar Prev 17: 2436 2444.

Green DG, Reed JC. 1998. Mitochodria and apoptosis. Science 281:1309 1312.

Halliwell B, Gutteridge JM. 1990. Role of free radicals and cata lytic metal ions in human disease: An overview. Methods Enzy mol 186:1 85.

Hardy JA, Aust AE. 1995. Iron in asbestos chemistry and carcino genicity. Chem Rev 95:97 118.

Harlow BL, Hartge PA. 1995. A review of perineal talc exposure and risk of ovarian cancer. Regul Toxicol Pharmacol 21: 254 260.

Hissin PJ, Hilf R. 1976. A fluorometric method for determination of oxidized and reduced glutathione in tissues. Anal Biochem 74:214 226.

Jaynes WF, Zartman RE. 2005. Origin of talc, iron phosphates, and other minerals in biosolids. Soil Sci Soc Am J 69: 1047 1056.

Langseth H, Hankinson SE, Siemiatycki J, Weiderpass E. 2008. Perineal use of talc and risk of ovarian cancer. J Epidemiol Community Health 62:358 360.

Li Y, Sun L, Jin M, Du Z, Liu X, Guo C, Li Y, Huang P, Sun Z. 2011. Size dependent cytotoxicity of amorphous silica nanopar ticles in human hepatoma HepG2 cells. Toxicol in Vitro 25:1343 1352.

Marklund S, Marklund G. 1974. Involvement of the superoxide anion radical in the autooxidation of pyrogallol and a convenient assay for superoxide dismutase. Euro J Biochem 47:469 474.

Martensson J, Jain A, Frayer ,W, Meister A. 1989. Glutathione metabolism in the lung: inhibition of its synthesis leads to lam mellar body and mitochondrial defects. Proc Natl Acad Sci USA 86:5296 5300.

Meister A. 1989. Taniguchi N, Higashi T, Sakamoto Y, Meister A, eds. In: *Glutathione Centennial: Molecular Properties and Clinical Applications*. New York, NY: Academic Press.

Mroz RM, Schins RP, Li H, Drost EM, Macnee W, Donaldson K. 2007. Nanoparticle carbon black driven DNA damage induces growth arrest and AP 1 and NFkappaB DNA binding in lung epi thelial A549 cell line. J Physiol Pharmacol 58(Suppl 5):461 470.

Mossman T. 1983. Rapid colorimetric assay for cellular growth and survival: Application to proliferation and cytotoxicity assays. J Immunol Methods 65:55 63.

Murdock RC, Braydich Stolle L, Schrand AM, Schlager JJ, Hus sain SM. 2008. Characterization of nanomaterial dispersion in solution prior to in vitro exposure using dynamic light scatter ing technique. Toxicol Sci 101:239 253.

National Toxicology Program. 1993. NTP Toxicology and Carci nogenesis Studies of Talc (Non Asbestiform) in Rats and Mice (Inhalation Studies), Vol. 421. pp1 287.

Nel A, Xia T, Madler L, Li N. 2006. Toxic potential of materials at the nanolevel. Science 311:622 627.

Nkoumbou C, Villieras F, Njopwouo D, Ngoune CY, Barres O, Pelletier M, Razafitianamaharavo A, Yvon J. 2008. Physico chemical properties of talc ore from three deposits of Lamal Pougue area (Yaounde Pan African Belt, Cameroon), in rela tion to industrial uses. Appl Clay Sci 41:113 132.

Ohkawa H, Ohisi N, Yagi Y. 1979. Assay for lipid peroxides in animal tissues by thiobarbituric acid reaction. Anal Biochem 95:351 358.

Park EJ, Yi J, Kim Y, Choi K, Park K. 2010. Silver nanoparticles induce cytotoxicity by a Trojan horse type mechanism. Toxicol In Vitro 24:872 878.

Patterson AL, 1939. The Scherrer formula for x ray particle size determination. Phys Rev 56:978 782.

Pérez Maqueda LA, Duran A, Pérez Rodriguez JL. 2005. Prepara tion of submicron talc particles by sonication. Appl Clay Sci 28:245 255.

Persson HL, Yu Z, Tirosh O, Eaton JW, Brunk UT. 2003. Preven tion of oxidant induced cell death by lysosomotropic iron chela tors. Free Radic Biol Med 34:1295 1305.

Petit S, Martin F, Wiewora A, De Parseval P, Decarreau A. 2004. Crystal chemistry of talc: A near infrared (NIR) spectroscopy study. Am Mineral 89:319 326.

Sakthivel S, Pitchumani B. 2011. Production of nano talc material and its applicability as filler in polymeric nanocomposites. Par ticle Sci Technol 29:441 449.

Takadera T, Ohyashiki T. 2007. Caspase dependent apoptosis induced by calcineurin inhibitors was prevented by glycogen synthase kinase 3 inhibitors in cultured rat cortical cells. Brain Res 1133:20 26.

Tang X, Guo Y, Nakamura K, Huang H, Hamblin M, Chang L, Villacorta L, Yin K, Ouyang ,H, Zhang J. 2010. Nitroalkenes induce rat aortic smooth muscle cell apoptosis via activation of caspase dependent pathways. Biochem Biophys Res Commun 397:239 244.

Timmer JC, Salvesen GS. 2007. Caspase substrates. Cell Death Differ 14:66 72.

Wang H, Joseph JA. 1999. Quantifying cellular oxidative stress by dichlorofluorescein assay using microplate reader. Free Radic Biol Med 27:612 616.

Wang X, Zelenski NG, Yang J, Sakai J, Brown MS, Goldstein JL. 1996. Cleavage of sterol regulatory element binding proteins (SREBPs) by cpp32 during apoptosis. EMBO J 15:1012 1020.

Welder AA, Grant R, Bradlaw J, Acosta D. 1991. A primary cul ture system of adult rat heart cells for the study of toxicologic agent. In Vitro Cell Dev Biol 27:921 926.

Wild P. 2006. Lung cancer risk and talc not containing asbesti form fibres: A review of the epidemiological evidence. Occup Environ Med 63:4 9.

Wroblewski F, LaDue JS. 1955. Lactate dehydrogenase activity in blood. Proc Soc Exp Biol Med 90:210 213.

Yu KO, Grabinski CM, Schrand AM, Murdock RC, Wang W, Gu B, Schlager JJ, Hussain SM. 2009. Toxicity of amorphous silica nanoparticles in mouse keratinocytes. J Nanopart Res 11:15 24.

Zastawny TH, Altman SA, Randers Eichhorn L, Madurawe R, Lumpkin JA, Dizdaroglu M, Rao G. 1995. DNA base modifications and membrane damage in cultured mammalian cells treated with iron ions. Free Radic Biol Med 18: 1013 1022.

Zhang J, Zhang T, Ti X, Shi J, Wu C, Ren X, Yin X. 2010. Curcumin promotes apoptosis in A549/DDP multidrug resistant human lung adenocarcinoma cells through an miRNA signaling pathway. Biochem Biophys Res Commun 6:1 6.

Exhibit 100

Alterations in Gene Expression in Human Mesothelial Cells Correlate with Mineral Pathogenicity

Arti Shukla[1]*, Maximilian B. MacPherson[1]*, Jedd Hillegass[1], Maria E. Ramos-Nino[1], Vlada Alexeeva[1], Pamela M. Vacek[2], Jeffrey P. Bond[3], Harvey I. Pass[4], Chad Steele[5], and Brooke T. Mossman[1]

Departments of [1]Pathology, [2]Medical Biostatistics, and [3]Microbiology and Molecular Genetics, University of Vermont College of Medicine, Burlington, Vermont; [4]Department of Cardiothoracic Surgery, NYU Langone Medical Center, New York, New York; and [5]Department of Medicine, University of Alabama at Birmingham School of Medicine, Birmingham, Alabama

Human mesothelial cells (LP9/TERT-1) were exposed to low and high (15 and 75 $\mu m^2/cm^2$ dish) equal surface area concentrations of crocidolite asbestos, nonfibrous talc, fine titanium dioxide (TiO_2), or glass beads for 8 or 24 hours. RNA was then isolated for Affymetrix microarrays, GeneSifter analysis and QRT-PCR. Gene changes by asbestos were concentration- and time-dependent. At low nontoxic concentrations, asbestos caused significant changes in mRNA expression of 29 genes at 8 hours and of 205 genes at 24 hours, whereas changes in mRNA levels of 236 genes occurred in cells exposed to high concentrations of asbestos for 8 hours. Human primary pleural mesothelial cells also showed the same patterns of increased gene expression by asbestos. Nonfibrous talc at low concentrations in LP9/TERT-1 mesothelial cells caused increased expression of 1 gene Activating Transcription Factor 3 (*ATF3*) at 8 hours and no changes at 24 hours, whereas expression levels of 30 genes were elevated at 8 hours at high talc concentrations. Fine TiO_2 or glass beads caused no changes in gene expression. In human ovarian epithelial (IOSE) cells, asbestos at high concentrations elevated expression of two genes (*NR4A2, MIP2*) at 8 hours and 16 genes at 24 hours that were distinct from those elevated in mesothelial cells. Since *ATF3* was the most highly expressed gene by asbestos, its functional importance in cytokine production by LP9/TERT-1 cells was assessed using siRNA approaches. Results reveal that *ATF3* modulates production of inflammatory cytokines (IL-1β, IL-13, G-CSF) and growth factors (VEGF and PDGF-BB) in human mesothelial cells.

Keywords: mesothelioma; crocidolite asbestos; talc; titanium dioxide; gene profiling

A myriad of natural and synthetic fibers and particles, including nanomaterials, are being introduced into the workplace and environment, and *in vitro* screening tests on human cell types are needed to predict their toxicity and mechanisms of action, especially in target cells of disease. Asbestos is a group of well-characterized fibrous minerals that are associated with the development of nonmalignant (asbestosis) and malignant (lung cancers, pleural, and peritoneal mesotheliomas) diseases in occupational cohorts (1–3), yet the molecular mechanisms of asbestos-related diseases are poorly understood. Although it is widely acknowledged that fibrous geometry, surface and chemical composition, and durability are important features in the development of asbestos-associated diseases, how these contribute to cell toxicity and transformation are unclear. Moreover, the early molecular events leading to injury by asbestos fibers and other pathogenic or innocuous particulates in human cells that may be targets for the development of disease remain enigmatic.

CLINICAL RELEVANCE

Results of work here suggest that transcriptional profiling can be used to reveal molecular events by mineral dusts that are predictive of their pathogenicity in mesothelioma.

The objective of work here was to compare acute toxicity and gene expression profiles of crocidolite asbestos, the type of asbestos most pathogenic in the causation of human mesothelioma (3, 4), to nonfibrous talc, fine titanium dioxide (TiO_2), and glass beads in a contact-inhibited, hTERT-immortalized human mesothelial cell line (5). In comparative studies, we also evaluated toxicity of particulates and gene expression changes in a contact-inhibited SV40 Tag-immortalized human ovarian epithelial cell line (IOSE) (6). This cell type is not implicated in asbestos-induced diseases, but is occasionally linked to inflammation and the development of ovarian cancer after use of talcum powder in the pelvic region, although such links are highly controversial (7).

Although most studies have evaluated the biological effects of particles and fibers on an equal mass or weight basis, the number, surface area, and reactivity of particulates at equal weight concentrations may be vastly different. Moreover, recent *in vitro* (8, 9) and *in vivo* (10–12), studies have confirmed that toxicity, oxidative stress, and inflammatory effects of ultrafine and other particles are related directly to surface area. For these reasons, and to avoid possible confounding alterations in gene expression or toxicity that might reflect or be masked in cells in different phases of the cell cycle, we introduced particulates at equal surface areas to confluent monolayers of human mesothelial (LP9/TERT-1) and human ovarian epithelial (IOSE) cells in a maintenance medium. Moreover, our studies included a nonfibrous talc sample and fine TiO_2 and glass particles, both traditionally used as nontoxic and nonpathogenic control particles in *in vitro* and animal experiments (reviewed in Refs. 13 and 14). Our studies provide novel insight into the early molecular events and responses occurring in human cells after exposure to asbestos and these materials.

MATERIALS AND METHODS

Human Mesothelial and Ovarian Epithelial Cell Cultures

Human mesothelial LP9/TERT-1 (LP9) cells, an hTERT-immortalized cell line phenotypically and functionally resembling normal human mesothelial cells (5), were obtained from Dr. James Rheinwald (Dana Farber Cancer Research Institute, Boston, MA). Human pleural mesothelial cells (NYU474) were isolated surgically from

(*Received in original form April 11, 2008 and in final form November 24, 2008*)

* These authors contributed equally to this research.

This work was supported by NIEHS training grant T32ES007122 to B.T.M., a contract from EUROTALC and the Industrial Minerals Association of North America, and NCI P01 CA 114,047 (H.I.P. and B.T.M.).

Correspondence and requests for reprints should be addressed to Arti Shukla, Ph.D., Department of Pathology, University of Vermont College of Medicine, 89 Beaumont Avenue, Burlington, VT 05405. E-mail: Arti.Shukla@uvm.edu

This article contains microarray data which can be found as a repository using the accession number GSE14034.

Am J Respir Cell Mol Biol Vol 41. pp 114–123, 2009 (1) Jul
Originally Published in Press as DOI: 10.1165/rcmb.2008-0146OC on December 18, 2008
Internet address: www.atsjournals.org

cancer-free patients by Dr. Harvey Pass (New York University, New York, NY). Briefly, tissue sample 2 × 2 cm^2 was harvested into saline solution and rinsed immediately with PBS (1×) and Dulbecco's modified Eagle's medium (DMEM) (1×). The tissue was then digested with 0.2% Collagenase type 1 (MP Biomedical Inc., Solon, OH) for 3 hours at 37°C. Finally, the digested tissue was scraped and cells collected were centrifuged for 5 minutes at 300 × *g*. The cell pellet thus obtained was resuspended in DMEM containing 10% fetal bovine serum (FBS) and 2% penicillin–streptomycin, transferred into 6-well plate, and allowed to grow at 5% CO_2 and 37°C. Mesothelial cells were characterized by staining with calretinin antibody. An SV40 Tag-immortalized, anchorage-dependent human ovarian epithelial cell line (IOSE 398) (6) was a kind gift from Dr. Nelly Auersperg (Canadian Ovarian Tissue Bank, University of British Columbia, Vancouver, BC, Canada). LP9/TERT-1 cells were maintained in 50:50 DMEM/F-12 medium containing 10% FBS, and supplemented with penicillin (50 units/ml), streptomycin (100 μg/ml), hydrocortisone (100 μg/ml), insulin (2.5 μg/ml), transferrin (2.5 μg/ml), and selenium (2.5 μg/ml). IOSE cells were maintained in 50:50 199/MCB105 medium containing 10% FBS and 50 μg/ml gentamicin. Cells at near confluence were switched to maintenance medium containing 0.5% FBS for 24 hours before particulate exposure. NYU474 cells were grown to near confluence in DMEM containing 10% FBS and supplemented with penicillin (50 units/ml) and streptomycin (100 μg/ml).

Characterization of Mineral Preparations

The physical and chemical characterization of the NIEHS reference sample of crocidolite asbestos has been reported previously (15). The surface area of asbestos fibers and particles was measured using nitrogen gas sorption analysis to allow computation of identical amounts of surface areas of particulates to be added to cells. Fiber and particle size dimensions were determined by scanning electron microscopy (SEM) as described previously (16). In addition, talc was examined using field emission scanning electron microscopy (FESEM) and transmission electron microscopy (TEM). The chemical composition, surface area, mean size, and source of each particulate preparation is presented in Table 1.

Introduction of Particulates to Cells

After sterilization under ultraviolet light overnight to avoid endotoxin and microbial contamination, particulates were suspended in HBSS at 1 mg/ml, sonicated for 15 minutes in a water bath sonicator, and triturated five times through a 22-gauge needle. This suspension was added to cells in medium.

SEM to Determine Particulate/Cell Interactions

Cells were grown on Thermonox plastic cover slips (Nalge Nunc International, Naperville, IL), exposed to particulates for 24 hours, and then processed for SEM as described previously (16). After samples were critical point-dried, they were mounted on aluminum specimen stubs and dried before being sputter-coated with gold and palladium in a Polaron sputter coater (Model 5100; Quorum Technologies, Guelph, ON, Canada) and examined on a JSM 6060 scanning electron microscope (JEOL USA, Inc., Peabody, MA).

Cell Viability Studies

After 24 hours, cells were collected with Accutase cell detachment reagent, and final cell suspensions in Accutase/complete medium/HBSS were mixed with 0.4% trypan blue stain, which is retained by dead cells. After 5 minutes, unstained cells were counted using a hemocytometer to determine the total number of viable cells per dish.

Based on the results of cell viability studies, asbestos and nonfibrous talc were evaluated in LP9 mesothelial cells for changes in gene expression at both low and high concentrations (15 and 75 $\mu m^2/cm^2$ dish) at 8 hours, and at low concentrations of minerals (15 $\mu m^2/cm^2$ dish) at 24 hours. These concentrations did not cause morphologic or toxic cellular changes at these time points. Negative control groups included cells exposed to fine TiO_2 (15 $\mu m^2/cm^2$ dish) at 8 and 24 hours and glass beads (75 $\mu m^2/cm^2$) at 24 hours. In IOSE cells, gene expression of all particulates was evaluated at 75 $\mu m^2/cm^2$ at 8 and 24 hours, as preliminary experiments revealed that no significant changes in mRNA levels were observed at 15 $\mu m^2/cm^2$ dish of asbestos. In NYU474 human mesothelial cells, QRT-PCR was used to validate a selected subset of gene expression changes identified by arrays in LP9/TERT-1 cells. Cells were exposed to 15 and 75 $\mu m^2/cm^2$ asbestos for 24 hours, and 8 genes highly expressed in LP9 cells were examined by QRT-PCR (*see below*).

RNA Preparation

Total RNA was prepared using an RNeasy Plus Mini Kit according to the manufacturers' protocol (Qiagen, Valencia, CA), as previously described (17).

Affymetrix Gene Profiling

Microarrays were performed on samples from three independent experiments. All cell types, time points, and mineral types and concenrations were included in all three experiments. For each experiment, $n = 3$ dishes were pooled into one sample per treatment group. Each of the pooled samples was analyzed on a separate array (i.e., $n = 3$ arrays per condition [3 independent biological replicates]). All procedures were performed by the Vermont Cancer Center DNA facility using standard Affymetrix protocol as previously described (14, 17). Each probe array, Human U133A 2.0 (Affymetrix, Santa Clara, CA) was scanned twice (Hewlett-Packard GeneArray Scanner, Palo Alto, CA), the images overlaid, and the average intensities of each probe cell compiled. Microarray data were analyzed using GeneSifter software (VizX Labs, Seattle, WA). This program used a "*t* test" for pairwise comparison and a Benjamini-Hochberg test for false discovery rate (FDR 5%) to adjust for multiple comparisons. A 2-fold cutoff limit was used for analysis.

Quantitative Real-Time PCR

Total RNA (1 μg) was reverse-transcribed with random primers using the Promega AMV Reverse Transcriptase kit (Promega, Madison, WI) according to the recommendations of the manufacturer, as described previously (17). In NYU474 mesothelial cells, eight genes (*ATF3*, *SOD2*, *PTGS2*, *FOSB*, *TFPI2*, *PDK4*, *NR4A2*, and *IL-8*) most highly expressed in LP9 cells were evaluated using the ΔΔCt method. Duplicate or triplicate assays were performed with RNA samples isolated from at least three independent experiments. The values obtained from cDNAs and hypoxanthine phosphoribosyl transferase (*hprt*) controls provided relative gene expression levels for the gene locus investigated. The primers and probes used to validate gene expression as observed in microarrays were purchased from Applied Biosystems (Foster City, CA).

TABLE 1. CHARACTERIZATION OF PARTICULATES

Name	Chemical Composition	Mean Surface Area ± SE (m^2/g)	Mean Size (μm)*	Source
Crocidolite Asbestos	$Na_2Fe_3^{2+}Fe_2^{3+}Si_8O_{22}(OH)_2$	14.97 ± 0.605	7.4 × 0.25	NIEHS Reference Sample
Talc (MP 10-52)†	$Mg_3Si_4O_{10}(OH)_2$	16.03 ± 0.654	1.1	Barrett's Minerals, Inc.
Titanium Dioxide	TiO_2	9.02 ± 0.185	0.69	Fisher Scientific
Glass Beads	SiO_2	2.78 ± 0.215	2.06	Polysciences Inc.

* Length X width for crocidolite asbestos, and diameter for nonfibrous talc, TiO_2, and glass beads.

† Although standard reference samples of asbestos and some particulates are available for use by the scientific community, reference samples of talc currently do not exist. For these reasons, the nonfibrous talc sample was also characterized for physical properties, particle size distribution (0.70 μm minimum to 1.20 μm maximum), and chemical/mineralogical (talc 95%, chlorite 4.5–5%, dolomite 0.3%) composition. For complete analysis or obtaining samples, please contact Brooke Mossman, Mark Ellis (markellis@ima-na.org), or Michelle Wyart at EUROTALC (mwyart@ima-europe.eu).

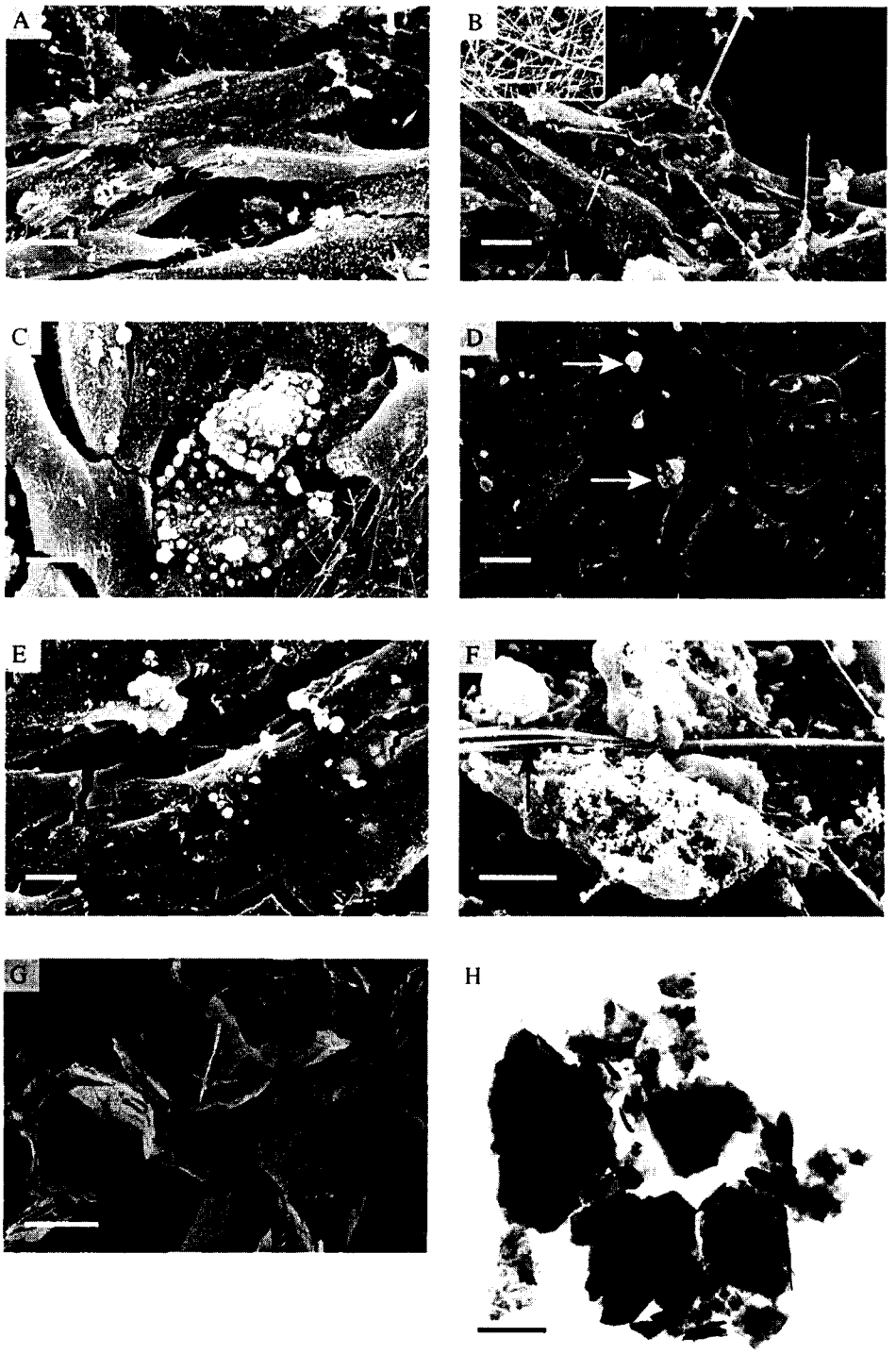

Figure 1. Interaction of fibers and particles with (*A–E*) LP9/TERT-1 human mesothelial cells and (*F*) IOSE ovarian epithelial cells after 24 hours of exposure to (*B, E, F*) high and (*C, D*) low concentrations of particulates. (*G*) Field emission scanning electron microscopy (FESEM) and (*H*) transmission electron microscopy (TEM) show structure of nonfibrous talc. (*A*) Morphology of unexposed near-confluent LP9/TERT-1 cells. (*B*) Membrane blebbing and piling up of cells in response to crocidolite asbestos (*arrows*). (*C*) Nonfibrous talc and (*D*) fine TiO_2 (*arrows*) on cell surface. (*E*) Single and small clumps of glass beads on plasma membrane. (*F*) Interaction of asbestos fibers (*arrows*) with IOSE cells that exhibit an exudate and membrane ruffling in response to fibers. *Bars* = 10 μm. (*G*) FESEM and (*H*) TEM showing morphology of platy talc bulk material. *Bars* = 2 μm.

Transfection of LP9 Cells with siRNA

On-Target plus Non-targeting siRNA #1 (scrambled control), and On-Target plus SMART pool human *ATF3* siRNA (100 nM; Dharmacon, Lafayette, CO) were transfected into LP9 cells at near confluence using Lipofectamine 2000 (Invitrogen, Carlsbad, CA), following the manufacturer's protocol. The efficiency of *ATF3* knockdown was determined by QRT-PCR after 48 and 72 hours.

Bio-Plex Analysis of Cytokine and Chemokine Concentrations in Medium of LP9/TERT-1 Cells

To quantify cytokine and chemokine levels in conditioned medium of cells transfected with siATF3 or scrambled control and exposed to asbestos for 24 hours, a multiplex suspension protein array was performed using the Bio-Plex protein array system as described previously (17) and a Human Cytokine 27-plex panel (Bio-Rad, Hercules, CA). Three biological replicates were used for each treatment group.

Statistical Analysis

Data from QRT-PCR and cell viability assays were evaluated by ANOVA using the Student Neuman-Keul's procedure for adjustment of multiple pairwise comparisons between treatment groups or using the nonparametric Kruskal-Wallis and Mann-Whitney tests. Differences with P values ≤ 0.05 were considered statistically significant.

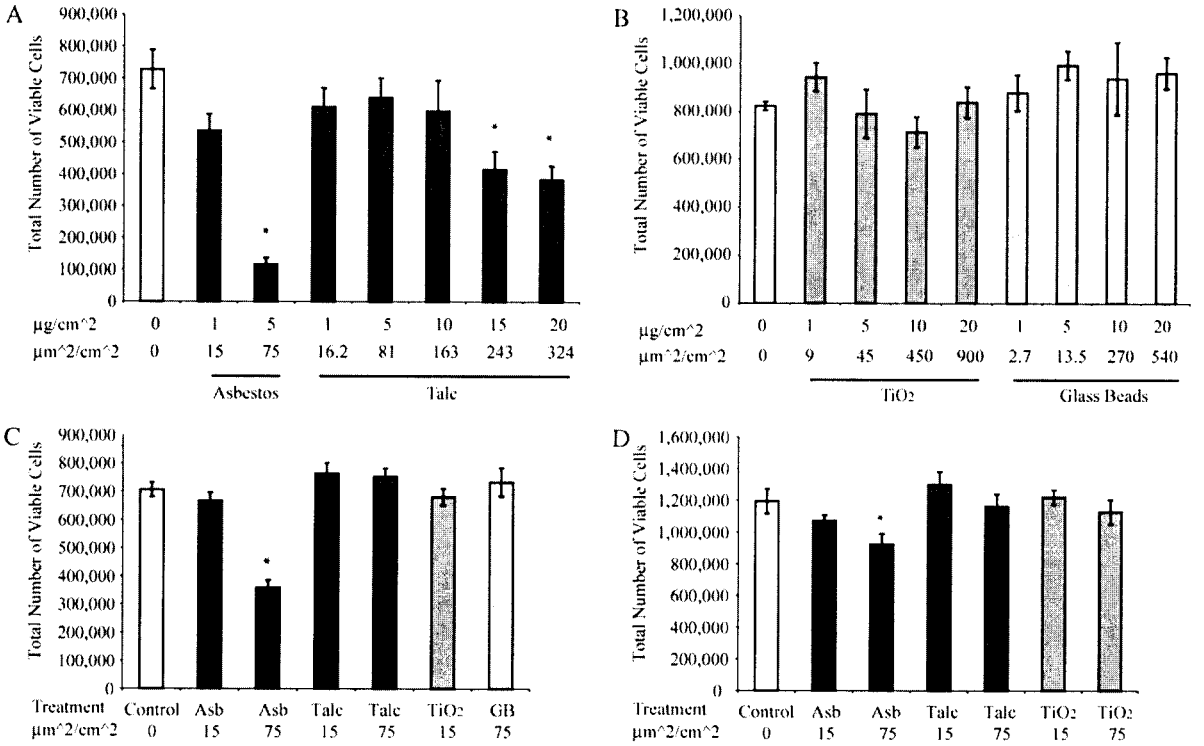

Figure 2. Cell viability after 24 hours of exposure to asbestos fibers and particles in (*A–C*) LP-9/TERT-1 and (*D*) IOSE (D). Mean +/− SE of 1 (A, B) or 3 (C, D) individual experiments where $n = 3$ per group per experiment. * $P \leq 0.05$ compared with untreated (0) groups.

RESULTS

Characterization of Particulate Preparations

Table 1 shows the major chemical formulas of crocidolite asbestos fibers (defined as having a greater than 3:1 length to width ratio) and particle samples used in experiments, although trace amounts of other elements occur in the NIEHS asbestos standards (15). In addition, we examined the morphology and cellular interactions of asbestos fibers, talc, and other particles using SEM (Figure 1). These studies revealed that only high (75 $\mu m^2/cm^2$) surface area concentrations of asbestos caused membrane blebbing and other toxic manifestations in cells (Figures 1B and 1F). In contrast, particles of nonfibrous talc (Figure 1C), fine TiO_2 (Figure 1D), and glass beads (Figure 1E) were nontoxic. Both asbestos fibers and particles were observed on the cell surface and were encompassed by cells. Nonfibrous talc occurred in platy particles that were uniform in appearance as viewed by FESEM (Figure 1G) and TEM (Figure 1H).

Asbestos Fibers at High Concentrations Are Toxic to LP9/TERT-1 Human Mesothelial Cells and Less So to Ovarian Epithelial Cells in Contrast to Particle Preparations

Figure 2 shows the results of trypan blue exclusion tests in LP9/TERT-1 and IOSE cells. In LP9/TERT-1 cells (Figures 2A–2C), asbestos at high surface area concentrations (75 $\mu m^2/cm^2$) caused significant decreases (50–80%) in cell viability that were more striking than those observed in IOSE cells (Figure 2D). Nonfibrous talc at 75 $\mu m^2/cm^2$ was nontoxic, and significant increases in toxicity were only achieved with addition of talc at ≥ 3-fold higher concentrations in LP9/TERT-1 cells (Figure 2A), but not in IOSE cells (data not shown). Neither TiO_2 nor glass beads were significantly toxic to either cell type over a range of concentrations (Figure 2B).

Asbestos Fibers, but Not Particle Preparations, Cause Dose- and Time-Related Changes in Gene Expression in Human LP9 Mesothelial Cells

Figure 3 shows a summary of significantly increased or decreased (> 2-fold compared with untreated controls) gene expression by asbestos (Figures 3A–3C) and nonfibrous talc (Figure 3D) in LP9/TERT-1 cells as well as the classification of genes by ontology. These studies revealed that gene expression changes by low concentrations of asbestos were less (29 increases) than at high concentrations (236 alterations including decreases) at 8 hours. Moreover, numbers of significant mRNA level alterations (205) at low concentrations of asbestos increased over time. In contrast, fewer numbers (30) of gene expression increases were observed at high concentrations of talc at 8 hours compared with identical surface areas of asbestos (236 changes), and no decreases in gene expression were observed. No significant alterations in gene expression were observed with low concentrations of talc at 24 hours or with TiO_2 or glass beads at either concentration or time point (data not shown). The major genes affected by asbestos or talc in LP9/TERT-1 cells are listed in Tables 2–4. This information reveals that the fold-increases in common genes expressed by asbestos-treated cells increase in a dose-related fashion at 8 hours. Although dose–responses were observed with talc at 8 hours, the numbers of significant gene increases as well as fold-increases were less than that observed with asbestos and decreased over time. Since mRNA expression of *ATF3* and *IL8* were increased by either asbestos or talc in LP9/TERT-1 cells, the increased expression of these genes was verified by QRT-PCR in mineral-exposed cells as compared with untreated control cells (Figure 4).

In NYU474 cells, QRT-PCR was used to validate that eight asbestos-induced genes in LP9 cells were up-regulated in

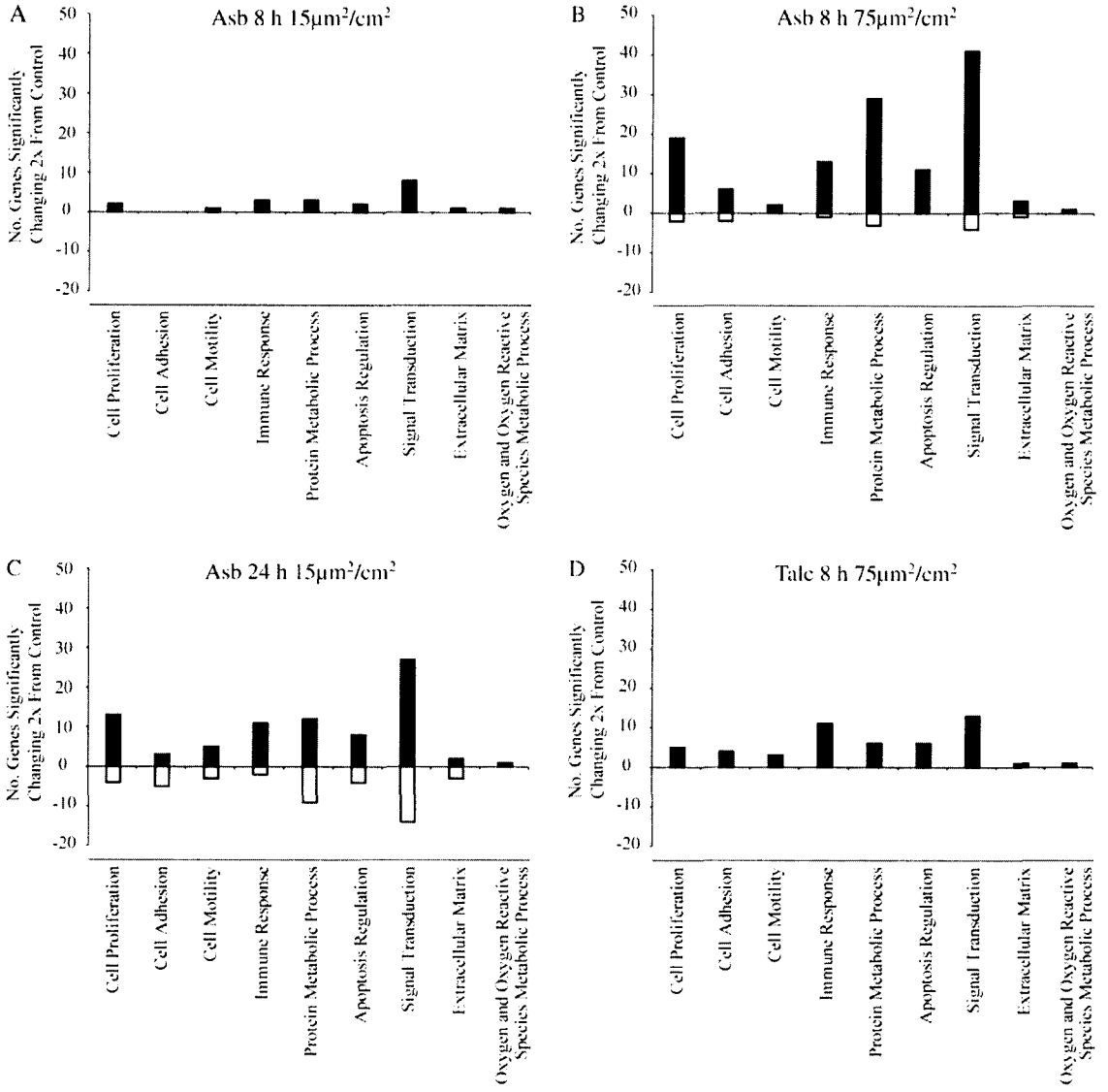

Figure 3. Numbers of changes ($P \leq 0.05$) in gene expression and classification by ontology in LP9/TERT-1 cells after exposure to (*A–C*) crocidolite asbestos or (*D*) nonfibrous talc.

normal human mesothelial cells (*ATF3*, *PTGS2* or *COX2*, *FOSB*, *IL8*, *NR4A2*, and *TFPI2*). Results showed that mRNA levels of six of the eight genes evaluated were increased in a dose-responsive fashion after exposure to asbestos for 24 hours (Figure 5).

IOSE Ovarian Epithelial Cells Exhibit Few Gene Expression Changes in Response to Asbestos

In contrast to LP9/TERT-1 and NYU474 mesothelial cells, IOSE cells showed no significant gene up-regulation or down-regulation in response to lower concentrations of asbestos at 8 or 24 hours (data not shown). At high concentrations of asbestos at 8 hours, mRNA levels of only two genes (*NR4A2* and *CXCL2* or *MIP2*) were increased in comparison to untreated IOSE cells (Table 4). At 24 hours, high concentrations of asbestos caused less than 4-fold increases in expression of only 16 genes, and decreased expression of 1 gene, *Profilin 1* (data not shown). No significant mRNA changes were observed with nonfibrous talc, fine TiO_2 or glass beads at either time point.

Inhibition of *ATF3* by siRNA Alters Asbestos-Induced Cytokines in LP9/TERT-1 Cells

Since *ATF3* was a common gene up-regulated by asbestos in mesothelial cells its functional role in cytokine production in LP9 cells was evaluated. As shown in Figure 6A, *ATF3* was successfully inhibited in LP9/TERT-1 cells using siATF3 as described in Materials and Methods. Cells transfected with control siRNA or siATF3 were then exposed to asbestos (75 $\mu m^2/cm^2$ $n = 3$) for 24 hours, and medium was collected and analyzed for cytokines and growth factors using Bio-Plex analyses. Inhibition of *ATF3* altered levels of asbestos-induced inflammatory cytokines (IL-1β, IL-13, G-CSF) and the growth factor (PGDF-BB) in LP9/TERT-1 cells (Figure 6B). Trends in diminishing levels of VEGF were also observed, although not statistically significant.

DISCUSSION

Gene expression analysis has been used for the classification of soluble toxicants in rodent and human cells *in vitro*. Models of

TABLE 2. TOP 10 GENES AFFECTED BY CROCIDOLITE ASBESTOS AT 8 AND 24 H IN LP9/TERT-1 HUMAN MESOTHELIAL CELLS

Concentration	Low ($15\ \mu m^2/cm^2$)		High ($75\ \mu m^2/cm^2$)
Time	8 h	24 h	8 h
	Fold Change		
Up-regulated			
Activating transcription factor 3 (*ATF3*)	9	9	27
Prostaglandin-endoperoxide synthase 2 (PTGS2)	7	8	16
Superoxide Dismutase 2 (SOD2)	6	6	2
Chemokine (C-X-C motif) ligand 3 (CXCL3)	4	NC	16
FBJ murine osteosarcoma viral oncogene homolog B (FOSB)	4	NC	NC
Tissue factor pathway inhibitor 2 (TFPI2)	4	14	11
Pyruvate dehydrogenase kinase, isozyme 4 (PDK4)	3	9	15
Chemokine (C-X-C motif) ligand 2 (CXCL2)	3	NC	NC
Angiopoietin-like 4 (ANGPLT4)	3	NC	NC
Kruppel-like factor 4 (gut) (KLF4)	3	NC	NC
Interleukin 8 C-terminal variant, 211506_s_t (IL8)	NC	8	12
Interleukin 1 receptor-like 1 (IL1R1)	NC	6	11
Nuclear receptor subfamily 4 (NR4A2)	NC	NC	11
Solute carrier family 7 (SLC7A2)	NC	6	10
Pleckstrin homology-like domain (PHLDA1)	NC	7	NC
Interleukin 8 (IL8)	NC	6	NC
Down-regulated			
Inhibitor of DNA binding 3 (ID3)	NC	NC	−5
Inhibitor of DNA binding 1 (ID1)	NC	NC	−3
Cytochrome P450, family 24 (CYP24A1)	NC	NC	−3
Basic helix-loop-helix domain (BHLHB3)	NC	NC	−3
SMAD family member 6 (SMAD6)	NC	NC	−3
S-phase kinase associated protein 2 (SKP2)	NC	NC	−3
Cadherin 10, type 2 (CDH10)	NC	NC	−3
START domain containing 5 (STARD5)	NC	NC	−3
211042_x_at	NC	NC	−2
Interferon-induced protein with tetratricopeptide (IFIT1)	NC	NC	−2
Oxytocin receptor (OXTR)	NC	−6	NC
Transcribed locus	NC	−5	NC
Chromosome 5 open reading frame (C5orf13)	NC	−5	NC
Cytochrome P450, family 24 (CYP24A1)	NC	−4	NC
Chromosome 21 open reading frame (C21orf7)	NC	−3	NC
KIAA1199	NC	−3	NC
Methyltransferase like 7A (METTL7A)	NC	−3	NC
PDZ domain containing RING finger 3 (PDZRN3)	NC	−3	NC
Periplakin (PPL)	NC	−3	NC
Phospholipase-C-like 1 (PLCL1)	NC	−3	NC

Definition of abbreviation: NC, no significant ($P \leq 0.05$) change > 2-fold from control.

transcript profiling for discrimination of toxic and nontoxic compounds in liver and other organs have also been developed in rodents (18), confirming the hypothesis that predictive modeling for classification of toxic agents and carcinogens is feasible. Here we used toxicogenomic approaches in human mesothelial cells, a cell type exquisitely sensitive to asbestos (19) and human contact-inhibited ovarian epithelial cells, a cell type not linked to carcinogenesis by asbestos, to determine whether the magnitude of altered gene expression by insoluble particulates correlated with their toxicity to cells and documented pathogenicity in humans. Although a recent study has examined gene expression profiles comparatively in crocidolite asbestos–exposed human lung adenocarcinoma (A549) and SV40-immortalized bronchial (BEAS-2B) or pleural mesothelial cell lines (MET5A) by cluster analysis (20), our studies are the first to examine gene expression changes by asbestos in comparison to other well-characterized particles in a human cell line that exhibits features of normal mesothelial cells (5). Although strict comparisons between cell types are not justified because SV40 Tag was used to immortalize the IOSE ovarian epithelial cell line (6), and SV40 infection is known to decrease sensitivity of human mesothelial cell lines to toxicity by asbestos (21), our studies suggest that the increased numbers of gene expression alterations observed in LP9/TERT-1 human mesothelial cells reflect elevated sensitivity of this cell type to asbestos. NYU474 human mesothelial cells were more resistant that LP9/TERT-1 cells to asbestos toxicity, permitting us to perform QRT-PCR studies at both concentrations of asbestos at 24 hours. These results confirmed common dose-related patterns of gene expression in mesothelial cells versus ovarian epithelial (IOSE) cells.

It is generally recognized that geometry and length and width (i.e., aspect ratio) of durable fibers such as amphibole asbestos types (crocidolite, amosite) are important properties determining toxicity, transforming potential, and carcinogeniciy in rodents and humans (13, 22, 23). Since talc can occur in various geometries (nonfibrous and fibrous) and can be contaminated with other minerals, including amphiboles, in some mining deposits (reviewed in Ref. 24), we used a well-characterized, nonfibrous talc sample here to allow evaluation of a particle not causing mesotheliomas or pleural sarcomas in rodents (23). Moreover, nonfibrous talc is regarded as noncarcinogenic in humans (25). Since talc is a magnesium silicate, and Mg^{2+} may interact with negatively charged molecules on the cell surface to

TABLE 3. GENES UP-REGULATED BY NONFIBROUS TALC IN LP9/TERT-1 HUMAN MESOTHELIAL CELLS

Gene	Fold Increase
8 h Low (15 $\mu m^2/cm^2$)	
Activating transcription factor 3 (*ATF3*)	3
8 h High (75 $\mu m^2/cm^2$)	
Activating transcription factor 3 (*ATF3*)	13
Inhibin, beta A (INHBA)	9
Chemokine (C-X-C motif) ligand 3 (CXCL3)	7
Superoxide dismutase 2 (SOD2)	7
Interleukin 8 C-terminal variant, 211506_s_t (IL8)	6
Prostaglandin-endoperoxide synthase 2 (PTGS2)	5
Interleukin 8 (IL8)	5
FBJ murine osteosarcoma viral oncogene homolog B (FOSB)	5
Tumor necrosis factor alpha-induced protein 6 (TNFAIP6)	4
Tissue factor pathway inhibitor 2 (TFPI2)	4
Chemokine (C-X-C motif) ligand 2 (CXCL2)	3
Intercellular adhesion molecule 4 (CICAM4)	3
ChaC, cation transport regulator homolog 1 (ChaC 1)	3
Nuclear receptor subfamily 4, group A, member 3 (NR4A3)	3
Pleckstrin homology-like domain, family A, member 1 (PHLDA1)	3
Interleukin 6 (IL-6)	3
Phorbol -12-myristate-13-acetate-induced protein 1 (PMA1P1)	3
Oxidized low density lipoprotein (lectin-like) receptor 1 (OLR1)	3
Chemokine (C-C motif) ligand 20 (CCL20)	3
v-maf musculoaponeurotic fibrosarcoma oncogene homolog F	3
Interleukin 1, alpha (IL-1α)	2
Tumor necrosis factor-α induced protein 3 (TNFA1P3)	2
Interleukin 1 receptor-like 1 (IL1RL1)	2
Angiopoieten-like 4 (ANGPLT4)	2
Kruppel-like factor 4 (KLF4)	2
GTP binding protein overexpressed in skeletal muscle (GEM)	2
Pentraxin-related gene, rapidly induced by IL-1 beta (PTX3)	2
Interleukin 1 beta (IL-1β)	2
HSPB (heat shock 27 kD) associated protein 1 (HSPBAP1)	2
Kynureninase (KYNU)	2

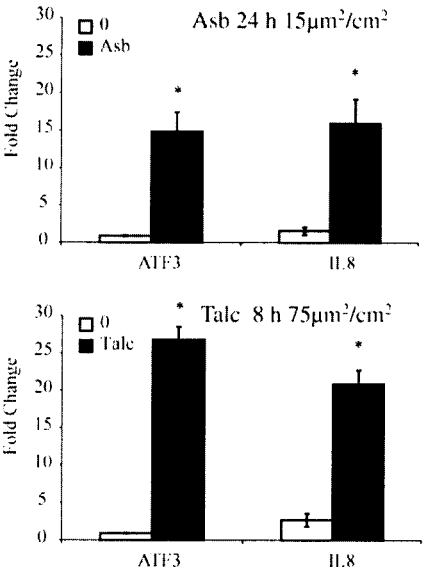

Figure 4. QRT-PCR confirms significant increases in *ATF3* and *IL8* expression by crocidolite asbestos at low concentrations and nonfibrous talc at high concentrations in LP9/TERT-1 mesothelial cells. *$P <$ 0.05 as compared to untreated (0) groups.

disturb cell homeostasis (reviewed in Ref. 26), this may explain the few mRNA expression increases that were observed initially with talc at 8 hours. However, these changes were not observed at 24 hours, suggesting that human mesothelial cells adapt to or undergo repair after exposure to this mineral.

Our gene profiling data here and in inhalation studies using chrysotile asbestos (14) also support the concept that fine TiO_2 is nontoxic and nonpathogenic to mesothelial or other cell types. Likewise, in the rat, inhalation of fine TiO_2 (defined as particles $>$ 0.1 μm in diameter), in contrast to ultrafine (particles $<$ 0.1 μm in diameter) does not give rise to predictive markers of toxicity, inflammation, pulmonary fibrosis, or oxidative stress, as indicated by elevated levels of Mn-containing superoxide dismutase (*SOD2*) in cells from bronchopulmonary lavage (27). The increased reactivity and toxicity of ultrafine particles as compared with larger fine or coarse particles have also been confirmed in a number of *in vitro* and *in vivo* experiments and is often attributed to their increased surface area and/or ability to penetrate lung cells.

TABLE 4: GENES UPREGULATED BY CROCIDOLITE ASBESTOS IN IOSE HUMAN OVARIAN CELLS

Gene	Fold increase
8 h High (75 $\mu m^2/cm^2$)	
Nuclear receptor subfamily 4 (NR4A2)	4
Chemokine (C-X-C motif) ligand 2 (MIP2)	2
24 h High (75 $\mu m^2/cm^2$)	
Nuclear receptor subfamily 4 (NR4A2)	4
DNA-damage-inducible transcript 3 (DDIT3)	3
Stromal cell-derived factor 2-like 1(SDF2L1)	3
Heat shock 70 kD protein 1A (HSPA1A)	3
DnaJ (Hsp40) homolog, subfamily C (DNAJC3)	2
Paraspeckle component 1	2
Heat shock 70 kD protein 1B (HSPA1B)	2
Homocysteine-inducible, endoplasmic reticulum stress-inducible, ubiquitin-like domain member (HERPUD1)	2
Serum/glucocorticoid regulated kinase family, member 3 (SKG3)	2
DnaJ (Hsp40) homolog, subfamily B, member 9 (DNAJB9)	2
Arginine-rich, mutated in early stage tumors (ARMET)	2
Syntaxin 1A (brain) (STX1A)	2
Heat shock 70 kD protein 5 (HSPA5)	2
ADAM metallopeptidase with thrombospondin type 1 motif	2
Heat shock protein 90kDa beta (Grp94), member 1 (HSP90B1)	2

Our studies reveal a number of novel genes induced by asbestos in LP9/TERT-1 cells. As previously described in a lung epithelial cell line (C10) or mouse lungs after inhalation of crocidolite asbestos (28), increases in expression of the early response gene, *FOSB*, that encodes a dimer of the activator protein-1 transcription factor, were seen. Increases in expression of several other genes linked to cell signaling proteins and transcription factor activation were observed in asbestos-exposed cells, including *NR4A2* and *PDK4*. A novel gene up-regulated at all time points and concentrations of asbestos or talc in human mesothelial cells was activating transcription factor 3 (*ATF3*), a member of the cAMP-responsive element–binding (CREB) transcription factor family that encodes two different isoforms leading to repression or activation of genes. Silencing of *ATF3* in the present study by siRNA significantly altered expression of a number of asbestos-induced inflammatory cytokines and growth factors documented in malignant mesotheliomas (29, 30). In support of our results here, other studies using *ATF3*-deficient mice and *in vitro* approaches have shown that *ATF3* is a negative regulator of pulmonary inflammation, eosinophilia, and airway responsiveness (31). Moreover, *ATF3* also negatively regulates IL-6 gene transcription in an NF-κB model of up-regulation using melanoma cells (32). In addition, trends in production of VEGF, a known important angiogenic peptide and independent prognostic factor in human mesotheliomas (33), were observed. We have recently shown that an extracellular signal–related

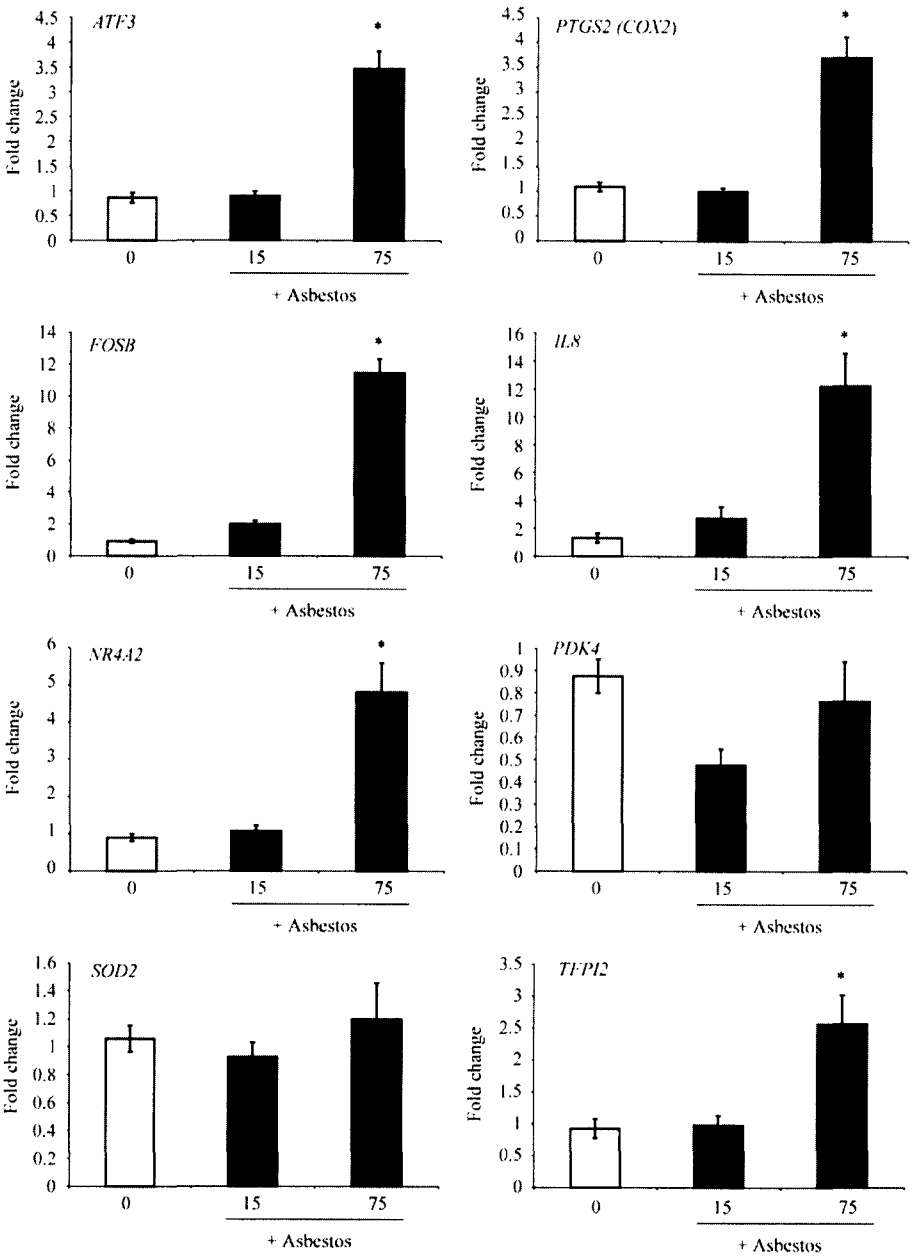

Figure 5. QRT-PCR confirms that human primary pleural mesothelial cells (NYU474) show similar patterns of asbestos-induced gene expression when compared with LP9/TERT-1 mesothelial cells. NYU474 cells were exposed to crocidolite asbestos (15 or 75 $\mu m^2/cm^2$) for 24 hours and cDNA was used for QRT-PCR. $*P \leq 0.05$ as compared with untreated cells (0).

CREB pathway in C10 lung epithelial cells modulates apoptosis after asbestos exposure (34), and recent studies are focusing on the effects of silencing *CREB* or *ATF3* on other functional and phenotypic changes in human mesothelial and mesothelioma cells (A. Shukla and colleagues, unpublished data).

Several other genes up-regulated by talc at 8 hours or affected by asbestos at both 8 and 24 hours may be important in repair from mineral-induced responses. For example, *SOD2*, (Mn-containing superoxide dismutase) is an antioxidant protein occurring in the mitochondria, a target cell organ of asbestos-induced apoptosis (35). *PTGS2* (prostaglandin-endoperoxide syntase or cyclooxygenase) is a key enzyme in prostenoid biosynthesis associated with modulation of mitogenesis and inflammation. More recently, this pathway has been explored after interaction of ultrafine particles with alveolar macrophages (9). *ANG PTL4* (angiopoietin-4) encodes a serum hormone directly involved in regulating glucose homeostasis and lipid metabolism and is an apoptosis survival factor for vascular endothelial cells. The up-regulation of angiopoietin-4 is also thought to play a role in inhibition of tumor cell motility and metastasis. *KLF4* (Kruppel-like factor 4) is a negative regulator of cell proliferation and can be a positive or negative modulator of DNA transcription.

Increased expression of genes encoding different cytokines/chemokines (i.e., *IL8*) and their receptors or ligands (e.g., IL-8 C-terminal variant, *IL1R1*, *CXCL2* or *MIP2*, *CXCL3*, and *TFPI2*) by asbestos or talc suggests that the mesothelial cell also may play a role in chemotaxis, inflammation, and blood coagulation. A number of gene expression changes by asbestos also support the hypothesis that this fibrous mineral affects calcium-dependent processes including related protein kinase cascades, cell adhesion, and protein/lipid metabolism (Table 2). Although numbers of changes were more modest in IOSE cells, with the exception of *NR4A2* and *CXCL2*, a unique subset of genes was induced by asbestos in this cell type (Table 4).

Results of work here suggest that transcriptional profiling can be used to reveal molecular events by mineral dusts that are

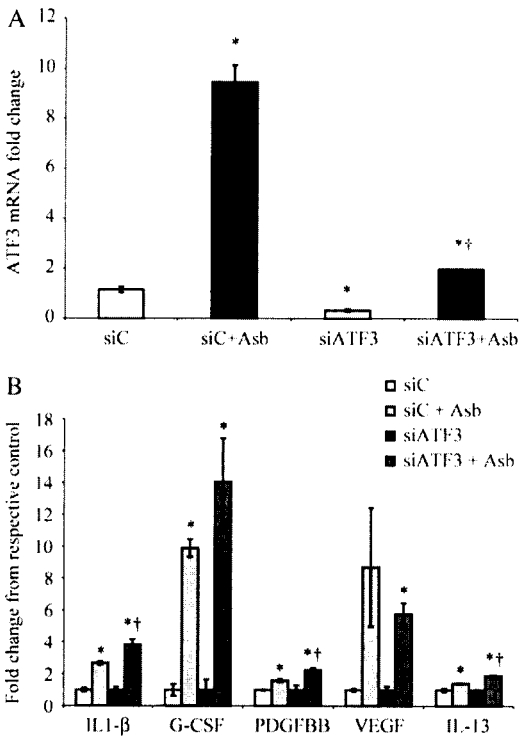

Figure 6. *ATF3* inhibition using siRNA approaches alters asbestos-induced production of inflammatory cytokines and growth factors. (*A*) LP9/TERT-1 cells transfected with siATF3 show significant inhibition of *ATF3* mRNA levels (untreated control [siC] versus siATF3 and asbestos-treated [siC Asb versus siATF3 Asb] groups). $^{*}P \leq 0.05$ as compared with siC; $^{\dagger}P \leq 0.05$ as compared with siC Asb group. (*B*) siATF3 altered asbestos-induced cytokine levels as detected in medium at 24 hours using Bio-Plex analyses. $^{*}P \leq 0.05$ as compared with control groups (siC and siATF3), respectively; $^{\dagger}P \leq 0.05$ as compared with asbestos-exposed scrambled control group (siC).

predictive of their pathogenicity in mesothelioma. Moreover, they reveal early and novel gene responses, including calcium-dependent transcription factors and antioxidant enzymes that may be pursued for their functional significance using RNA silencing or other approaches.

Conflict of Interest Statement: B.T.M. received support by EUROTALC and The Industrial Minerals Association (IMA) (11/1/05–10/31/06) for $90,000 for research. None of the other authors has a financial relationship with a commercial entity that has an interest in the subject of this manuscript.

Acknowledgments: The authors thank the Vermont Cancer Center DNA Analysis Facility for performing oligonucleotide microarray and real-time quantitative PCR, and Gary Tomiano (Minteg International, Inc./Specialty Minerals, Inc., Easton, PA) for talc characterization.

References

1. Mossman BT, Gee JB. Asbestos-related diseases. *N Engl J Med* 1989; 320:1721–1730.
2. Mossman BT, Churg A. Mechanisms in the pathogenesis of asbestosis and silicosis. *Am J Respir Crit Care Med* 1998;157:1666–1680.
3. Robinson BW, Lake RA. Advances in malignant mesothelioma. *N Engl J Med* 2005;353:1591–1603.
4. Mossman BT, Bignon J, Corn M, Seaton A, Gee JB. Asbestos: scientific developments and implications for public policy. *Science* 1990;247: 294–301.
5. Dickson MA, Hahn WC, Ino Y, Ronfard V, Wu JY, Weinberg RA, Louis DN, Li FP, Rheinwald JG. Human keratinocytes that express hTERT and also bypass a p16(INK4a)-enforced mechanism that limits life span become immortal yet retain normal growth and differentiation characteristics. *Mol Cell Biol* 2000;20:1436–1447.
6. Choi JH, Choi KC, Auersperg N, Leung PC. Overexpression of follicle-stimulating hormone receptor activates oncogenic pathways in pre-neoplastic ovarian surface epithelial cells. *J Clin Endocrinol Metab* 2004;89:5508–5516.
7. Merritt MA, Green AC, Nagle CM, Webb PM. Talcum powder, chronic pelvic inflammation and NSAIDs in relation to risk of epithelial ovarian cancer. *Int J Cancer* 2008;122:170–176.
8. Mossman BT, Shukla A, Fukagawa NK. Highlight Commentary on "Oxidative stress and lipid mediators induced in alveolar macrophages by ultrafine particles". *Free Radic Biol Med* 2007;43:504–505.
9. Beck-Speier I, Dayal N, Karg E, Maier KL, Schumann G, Schulz H, Semmler M, Takenaka S, Stettmaier K, Bors W, *et al.* Oxidative stress and lipid mediators induced in alveolar macrophages by ultrafine particles. *Free Radic Biol Med* 2005;38:1080–1092.
10. Oberdorster G, Ferin J, Gelein R, Soderholm SC, Finkelstein J. Role of the alveolar macrophage in lung injury: studies with ultrafine particles. *Environ Health Perspect* 1992;97:193–199.
11. Brown DM, Wilson MR, MacNee W, Stone V, Donaldson K. Size-dependent proinflammatory effects of ultrafine polystyrene particles: a role for surface area and oxidative stress in the enhanced activity of ultrafines. *Toxicol Appl Pharmacol* 2001;175:191–199.
12. Donaldson K, Tran CL. Inflammation caused by particles and fibers. *Inhal Toxicol* 2002;14:5–27.
13. Health Effects Institute - Asbestos Research. Asbestos in public and commercial buildings: a literature review and synthesis of current knowledge. Cambridge, MA: The Health Effects Institute; 1991.
14. Sabo-Attwood T, Ramos-Nino M, Bond J, Butnor KJ, Heintz N, Gruber AD, Steele C, Taatjes DJ, Vacek P, Mossman BT. Gene expression profiles reveal increased mClca3 (Gob5) expression and mucin production in a murine model of asbestos-induced fibrogenesis. *Am J Pathol* 2005;167:1243–1256.
15. Campbell WJ, Huggins CW, Wylie AG. Chemical and physical characterization of amosite, chrysotile, crocidolite, and nonfibrous tremolite for oral ingestion studies Washington, DC: National Institute of Environmental Health Sciences; 1980. No. 8542.
16. Blumen SR, Cheng K, Ramos-Nino ME, Taatjes DJ, Weiss DJ, Landry CC, Mossman BT. Unique uptake of acid-prepared mesoporous spheres by lung epithelial and mesothelioma cells. *Am J Respir Cell Mol Biol* 2007;36:333–342.
17. Shukla A, Lounsbury KM, Barrett TF, Gell J, Rincon M, Butnor KJ, Taatjes DJ, Davis GS, Vacek P, Nakayama KI, *et al.* Asbestos-induced peribronchiolar cell proliferation and cytokine production are attenuated in lungs of protein kinase C-delta knockout mice. *Am J Pathol* 2007;170:140–151.
18. Steiner G, Suter L, Boess F, Gasser R, de Vera MC, Albertini S, Ruepp S. Discriminating different classes of toxicants by transcript profiling. *Environ Health Perspect* 2004;112:1236–1248.
19. Lechner JF, Tokiwa T, LaVeck M, Benedict WF, Banks-Schlegel S, Yeager H Jr, Banerjee A, Harris CC. Asbestos-associated chromosomal changes in human mesothelial cells. *Proc Natl Acad Sci USA* 1985;82:3884–3888.
20. Nymark P, Lindholm PM, Korpela MV, Lahti L, Ruosaari S, Kaski S, Hollmen J, Anttila S, Kinnula VL, Knuutila S. Gene expression profiles in asbestos-exposed epithelial and mesothelial lung cell lines. *BMC Genomics* 2007;8:62.
21. Cacciotti P, Barbone D, Porta C, Altomare DA, Testa JR, Mutti L, Gaudino G. SV40-dependent AKT activity drives mesothelial cell transformation after asbestos exposure. *Cancer Res* 2005;65:5256–5262.
22. Davis JM, Addison J, Bolton RE, Donaldson K, Jones AD, Smith T. The pathogenicity of long versus short fibre samples of amosite asbestos administered to rats by inhalation and intraperitoneal injection. *Br J Exp Pathol* 1986;67:415–430.
23. Stanton MF, Layard M, Tegeris A, Miller E, May M, Morgan E, Smith A. Relation of particle dimension to carcinogenicity in amphibole asbestoses and other fibrous minerals. *J Natl Cancer Inst* 1981;67:965–975.
24. Guthrie GD Jr, Mossman BT. Health effects of mineral dusts. Washington, DC: Mineralogical Society of America; 1993.
25. IARC. Silica and some silicates. *IARC Monogr Eval Carcinog Risk Chem Hum* 1987;42:185.
26. Mossman B, Light W, Wei E. Asbestos: mechanisms of toxicity and carcinogenicity in the respiratory tract. *Annu Rev Pharmacol Toxicol* 1983;23:595–615.
27. Janssen YM, Heintz NH, Mossman BT. Induction of c-fos and c-jun proto-oncogene expression by asbestos is ameliorated by N-acetyl-L-cysteine in mesothelial cells. *Cancer Res* 1995;55:2085–2089.

28. Ramos-Nino ME, Heintz N, Scappoli L, Martinelli M, Land S, Nowak N, Haegens A, Manning B, Manning N, MacPherson M, *et al.* Gene profiling and kinase screening in asbestos-exposed epithelial cells and lungs. *Am J Respir Cell Mol Biol* 2003;29:S51–S58.
29. Yoshimoto A, Kasahara K, Saito K, Fujimura M, Nakao S. Granulocyte colony-stimulating factor-producing malignant pleural mesothelioma with the expression of other cytokines. *Int J Clin Oncol* 2005;10:58–62.
30. Vogelzang NJ, Herndon JE II, Miller A, Strauss G, Clamon G, Stewart FM, Aisner J, Lyss A, Cooper MR, Suzuki Y, *et al.* High-dose paclitaxel plus G-CSF for malignant mesothelioma: CALGB phase II study 9234. *Ann Oncol* 1999;10:597–600.
31. Gilchrist M, Henderson WR Jr, Clark AE, Simmons RM, Ye X, Smith KD, Aderem A. Activating transcription factor 3 is a negative regulator of allergic pulmonary inflammation. *J Exp Med* 2008;205:2349–2357.
32. Karst AM, Gao K, Nelson CC, Li G. Nuclear factor kappa B subunit p50 promotes melanoma angiogenesis by upregulating interleukin-6 expression. *Int J Cancer* 2009;124:494–501.
33. Demirag F, Unsal E, Yilmaz A, Caglar A. Prognostic significance of vascular endothelial growth factor, tumor necrosis, and mitotic activity index in malignant pleural mesothelioma. *Chest* 2005;128: 3382–3387.
34. Barlow CA, Barrett TF, Shukla A, Mossman BT, Lounsbury KM. Asbestos-mediated CREB phosphorylation is regulated by protein kinase A and extracellular signal-regulated kinases 1/2. *Am J Physiol Lung Cell Mol Physiol* 2007;292:L1361–L1369.
35. Shukla A, Stern M, Lounsbury KM, Flanders T, Mossman BT. Asbestos-induced apoptosis is protein kinase C delta-dependent. *Am J Respir Cell Mol Biol* 2003;29:198–205.

Exhibit 101

PHYTOTHERAPY RESEARCH
Phytother. Res. **21**, 579–586 (2007)
Published online 14 March 2007 in Wiley InterScience
(www.interscience.wiley.com) **DOI**: 10.1002/ptr.2117

Pycnogenol® reduces Talc-induced Neoplastic Transformation in Human Ovarian Cell Cultures

Amber R. Buz'Zard* and Benjamin H. S. Lau

Department of Biochemistry and Microbiology, School of Medicine, Loma Linda University, Loma Linda, CA 92350, USA

Talc and poor diet have been suggested to increase the risk of developing ovarian cancer; which can be reduced by a diet rich in fruit and vegetables. Talc is ubiquitous despite concern about its safety, role as a possible carcinogen and known ability to cause irritation and inflammation. It was recently shown that Pycnogenol® (Pyc; a proprietary mixture of water-soluble bioflavonoids extracted from French maritime pine bark) was selectively toxic to established malignant ovarian germ cells. This study investigated talc-induced carcinogenesis and Pyc-induced chemoprevention. Normal human epithelial and granulosa ovarian cell lines and polymorphonuclear neutrophils (PMN) were treated with talc, or pretreated with Pyc then talc. Cell viability, reactive oxygen species (ROS) generation and neoplastic transformation by soft agar assay were measured. Talc increased proliferation, induced neoplastic transformation and increased ROS generation time-dependently in the ovarian cells and dose-dependently in the PMN. Pretreatment with Pyc inhibited the talc-induced increase in proliferation, decreased the number of transformed colonies and decreased the ROS generation in the ovarian cells. The data suggest that talc may contribute to ovarian neoplastic transformation and Pyc reduced the talc-induced transformation. Taken together, Pyc may prove to be a potent chemopreventative agent against ovarian carcinogenesis. Copyright © 2007 John Wiley & Sons, Ltd.

Keywords: ovarian cancer; talc; Pycnogenol®; human neutrophils.

INTRODUCTION

Ovarian cancer is the sixth most commonly occurring cancer and ranks fifth in cancer deaths among women, accounting for more deaths than any other cancer of the female reproductive system. Epidemiological studies have suggested that diet, talc, industrial pollutants, smoking, asbestos and infectious agents may increase the risk of developing ovarian cancer (American Cancer Society, 2000) and may do so by causing localized inflammation (Ness and Cottreau, 1999). Specifically, talc exposure has been cited as a risk factor because of its similarity to asbestos (Cramer *et al.*, 1999).

Talc is a layered magnesium silicate [$Mg_3Si_4O_{10}(OH)_2$]. It is used in cosmetics (as the primary ingredient in talcum powder), pharmaceuticals (as an excipient in tablets) and in many other industrial applications (Bremmell and Addai-Mensah, 2005). Talc is used medically to induce pleurodesis because of its known ability to cause irritation and inflammation (Holthouse and Chleboun, 2001). Animal studies showed a systemic migration of talc particles to various organs despite route of entry (Henderson *et al.*, 1986; Werebe *et al.*, 1999). Exposure of rat ovaries to talc leads to cyst formation (Hamilton *et al.*, 1984). Talc was also shown to cause superoxide anion generation and release from murine macrophages (Van Dyke *et al.*, 2003). Thus controversy continues to surround the topic of talc, its safety (Janssen, 2004) and its role as a possible carcinogen (Cramer *et al.*, 1999; Wong *et al.*, 1999).

Lifestyle factors are important in the etiology of ovarian cancer and current evidence suggests the risk can be reduced by eating a diet rich in fruit and vegetables, among other lifestyle choices (Hanna and Adams, 2006). For the past 20 years, researchers have proposed that nutritional factors play one of the most important roles in the etiology of human cancer. It is estimated that 35% (range 10–70%) of all cancers are diet related and that consumption of certain fruits and vegetables is inversely associated with the incidence of specific forms of cancer. Past research has indicated that a large number of bioactive components, which proved to be protective on different stages of cancer formation, have been identified in nutrients that are of plant origin (Knasmuller and Verhagen, 2002).

Pycnogenol® (Pyc) is a proprietary mixture of water-soluble bioflavonoids extracted from the bark of French maritime pine (*Pinus maritima* Aiton; currently known as *Pinus pinaster* Aiton). The main constituents of Pyc are phenolic compounds, broadly divided into monomers (catechin, epicatechin and taxifolin) and condensed flavonoids (classified as procyanidins and proanthocyanidins). Pyc is known to possess potent antioxidant activity, it not only scavenges the free radicals but it also enhances the endogenous antioxidant systems (Nelson *et al.*, 1998; Wei *et al.*, 1997). Pyc has also been shown to selectively induce apoptosis in breast cancer cells (Huynh and Teel, 2000) and induce differentiation and apoptosis in human promyeloid leukemia cells (Huang *et al.*, 2005). It was previously

* Correspondence to: Dr Amber R. Buz'Zard, Department of Biochemistry and Microbiology, School of Medicine, Loma Linda University, Loma Linda, CA 92350, USA.
E-mail: abuzzard03b@llu.edu
Contract/grant sponsor: Horphag Research, Geneva, Switzerland.

Received 4 October 2006
Revised 1 January 2007
Accepted 8 January 2007

shown that Pyc selectively induced cell death in established malignant ovarian germ cells *in vitro* (Buz'Zard and Lau, 2004). This study now reports that Pyc prevents talc-induced neoplastic transformation of normal ovarian cells, *in vitro*.

MATERIALS AND METHODS

Reagents and chemicals. Pycnogenol® was supplied by Horphag Research (Geneva, Switzerland). Talc, crystal violet, Giemsa stain, RPMI-1640 medium and other miscellaneous chemicals were purchased from Sigma (St Louis, MO). Polymorphoprep™ was purchased from Greiner Bio-One, Inc. (Longwood, FL). Dulbecco's modification of Eagle's Medium (DMEM), Ham's F-12 medium and penicillin–streptomycin (P-S) were purchased from Cellgro (Herndon, VA). Fetal bovine serum (FBS) was purchased from HyClone (Logan, UT). The CellTiter 96® AQueous One Solution Cell Proliferation Assay was purchased from Promega (Madison, WI). High strength analytical grade agarose was purchased from Bio-Rad (Hercules, CA). Ionagar No. 2 was purchased from Oxoid (London, UK). 5-(and-6)-Carboxy-2′,7′-dichlorodihydrofluorescein diacetate (carboxy-H_2DCFDA) was purchased from Molecular Probes (Carlsbad, CA).

Water soluble extraction of Pycnogenol®. Pyc was incubated at 56 °C for 5 h in double distilled water, allowed to cool to room temperature and filtered using a Steriflip® Vacuum Filtration System (0.22 µm Durapore PVDF membrane; Millipore Corporation, Bedford, MA).

Cell culture and treatments. Two cell cultures of human origin were maintained at 37 °C in a humidified atmosphere containing 5% CO_2. OSE2a (immortalized normal ovarian epithelial) and GC1a (immortalized normal ovarian granulosa) cell cultures were donated by Dr Hitoshi Okamura at Kumamoto University, Japan (Okamura *et al.*, 2003). The cell lines were maintained in a 1:1 mixture of DMEM and Ham's F-12 medium supplemented with 10% FBS and 100 IU/mL P-S. In preparation for either talc or Pyc + talc treatments, each cell line was seeded (1×10^5 cells/ml) and grown to 80% confluence, unless otherwise specified. Cells were incubated with 0–500 µg/mL talc from 24 to 120 h; or 0–500 µg/mL Pyc for 24 h followed by 5 µg/mL talc for 24 or 72 h.

Neutrophil isolation and culture. Peripheral blood polymorphonuclear neutrophils (PMN) and monocytes were obtained from heparinized venous blood from healthy volunteers (protocol approved by Loma Linda University Institutional Review Board for Human Studies) and isolated by Polymorphoprep™ density gradient centrifugation followed by the hypotonic lysis of erythrocytes. The purity of PMNs was determined by Giemsa staining as greater than 95%. Purified cells were suspended at 5×10^5 cells/mL in RPMI-1640 containing 2 mM L-glutamine, 1 mM sodium pyruvate, supplemented with 10% FBS and 100 IU/mL P-S; and treated with varying concentrations of talc for 24 or 72 h. ROS generation was detected as detailed below.

Cell viability assay. The CellTiter 96® AQueous One Solution Cell Proliferation Assay was used to measure cell viability (Buz'Zard and Lau, 2004). The MTS [3-(4,5-dimethylthiazolyl-2-yl)-5-(3-carboxymethoxyphenyl)-2-(4-sulfophenyl)-2H-tetrazolium, inner salt] solution was used according to manufacturer's instructions. The absorbance was read at 490 nm using a model 3550 Microplate Reader (Bio-Rad). The percent cell viability was calculated as the absorbance of the treated cells divided by the absorbance of the untreated-control cells multiplied by 100.

Neoplastic transformation assay. A characteristic of cancer cells is their ability to grow and to divide when held in suspension without attachment or with minimal attachment to a rigid surface (Leung *et al.*, 2004). Thus, growth in soft agar demonstrates *in vitro* transformation of cells to their neoplastic counterparts (Morales *et al.*, 2003). After 72 h of incubation in the presence of talc; or in the presence of 0–500 µg/mL Pyc for 24 h followed by 5 µg/mL talc for 72 h, cells were collected, washed and suspended in 0.35% agarose at 5000 cells/well and layered on top of a base of 0.5% agar. The plates were incubated at 37 °C in a humidified incubator for 14 days. The cells were stained with 0.005% crystal violet and colonies were counted using an inverted microscope (Cory *et al.*, 1987).

Reactive oxygen species (ROS) detection. Carboxy-H_2DCFDA is a non-fluorescent dye that permeates the cells where it is deacetylated by viable cells to 2′,7′-dichlorofluorescin (DCFH), which is then oxidized to fluorescent 2′,7′-dichlorofluorescein (DCF) by endogenous hydrogen peroxide (H_2O_2) (Wan *et al.*, 1993). The cells were seeded in Optilux™ 96-well plates (BD Falcon, Bedford, MA) and treated with 0 to 500 µg/mL Pyc for 24 h. H_2O_2 (100 µM) was used as a positive control. Carboxy-H_2DCFDA (5 µM) was added and incubated for 1 h. The fluorescence intensity (excitation 485 nm/emission 530 nm) was measured as arbitrary fluorescent units (AFU) using a model 7600 Microplate Fluorometer (Cambridge Technology, Inc., Watertown, MA). The percent AFU (a.k.a. % ROS generation) was calculated as the 'treated cell-AFU' divided by the 'untreated cell-AFU' multiplied by 100. Immediately following the fluorescence detection, the fluorescence intensity was normalized by the cell viability assay.

Statistical analysis. Data were reported as mean ± SE. Statistical analysis was performed with the Student's paired *t*-test.

RESULTS

All experiments were performed a minimum of three times with reproducible results.

Effect of talc on cell viability of normal ovarian cells

Talc caused a bell-shaped curve response in OSE2a cells, with a statistically significant increase seen at 5 µg/mL (24 h) and a statistically significant decrease at 200 µg/mL (72 h) and 500 µg/mL (24 and 72 h) (Fig. 1).

DOI: 10.1002/ptr

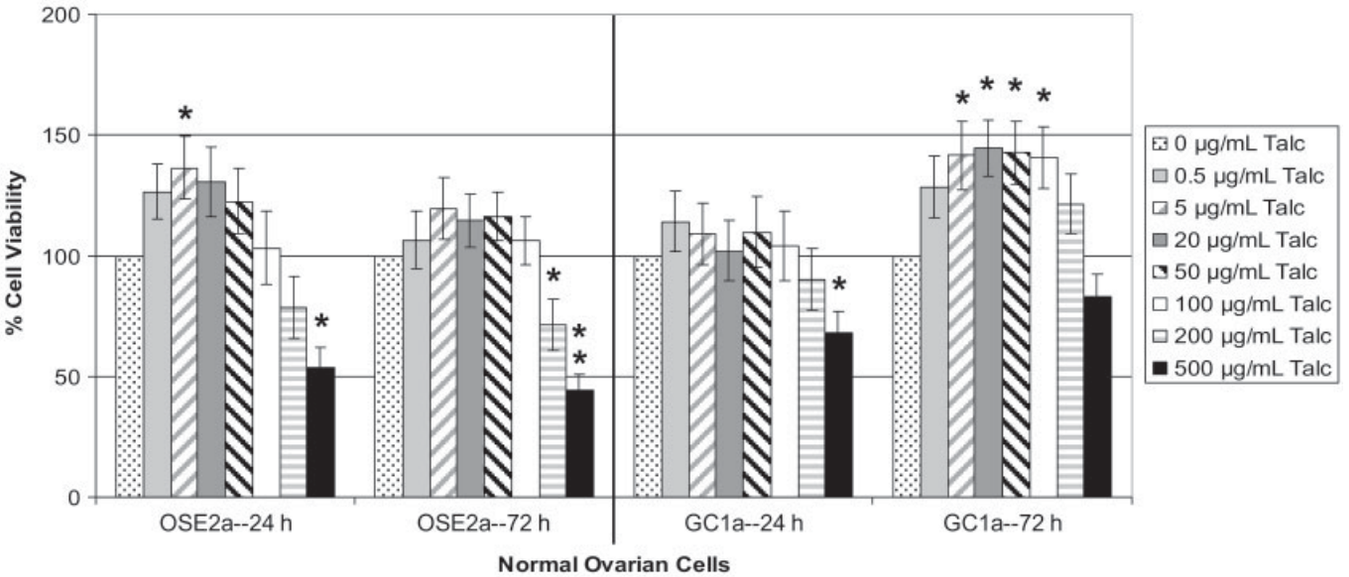

Figure 1. Effect of talc on the cell viability of ovarian cells. Normal ovarian epithelial (OSE2a) and normal ovarian stromal (GC1a) cells were treated with various concentrations of talc for 24 and 72 h. Cell viability was measured by the MTS assay and the percent cell viability was calculated as the absorbance of the treated cell divided by the absorbance of the untreated-control cells multiplied by 100. Each data point represents mean ± SE of five determinations. Statistical significance was determined by the Student's paired *t*-test. * $p < 0.05$, ** $p < 0.01$ comparing the treatment with the respective untreated control.

Also seen in Fig. 1, talc caused a bell-shaped curve response in GC1a cells, with a statistically significant increase seen at 5, 20, 50 and 100 µg/mL (72 h) and a statistically significant decrease at 500 µg/mL (24 h).

Effect of talc on neoplastic transformation of normal ovarian cells

Since the ability to grow suspended in soft agar is a characteristic of cells being transformed to their neoplastic counterparts (Leung *et al.*, 2004; Morales *et al.*, 2003), the study determined whether talc would be able to induce such a transformation. As shown in Fig. 2, talc caused a statistically significant increase in the number of transformed colonies in the OSE2a cells at 5 and 20 µg/mL talc and in the GC1a cells at 5, 20 and 100 µg/mL talc, compared with the untreated control. An exception was seen in the 100 µg/mL talc treatment in the OSE2a cells in which the number of transformed colonies was reduced significantly.

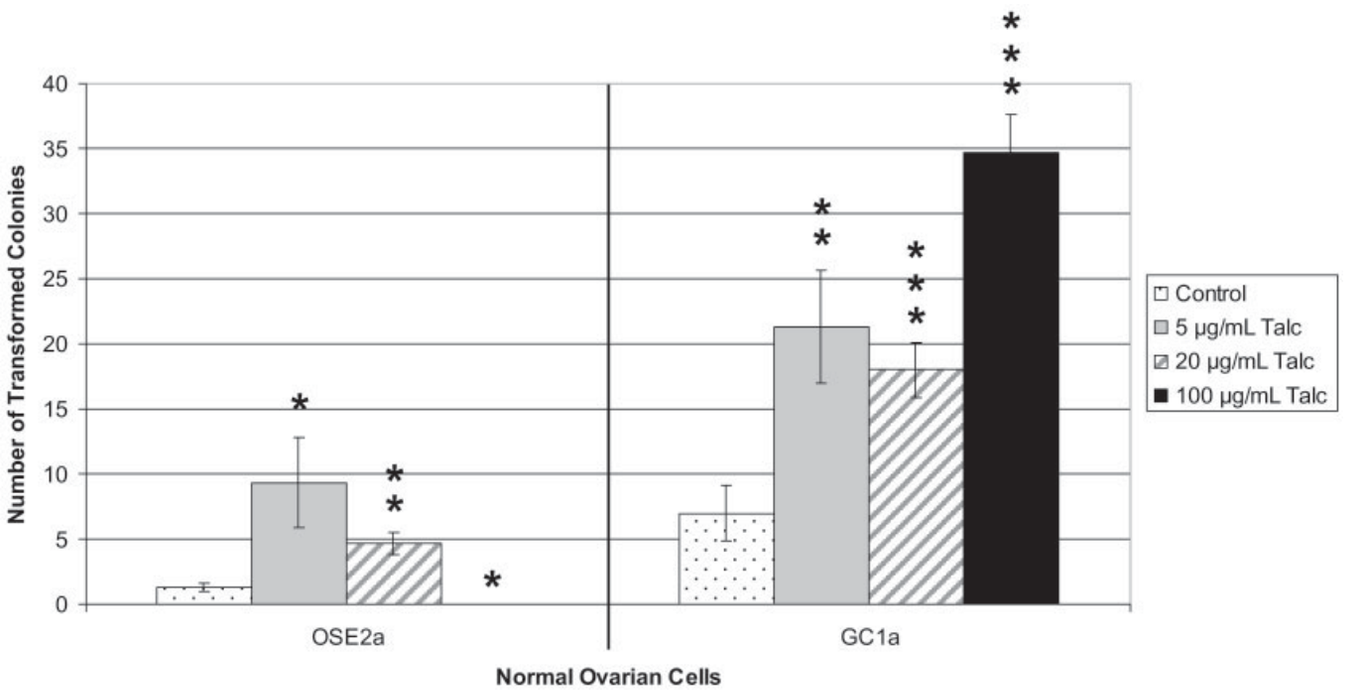

Figure 2. Neoplastic transformation of ovarian cells by talc. Normal ovarian epithelial (OSE2a) and normal ovarian stromal (GC1a) cells were incubated with various concentrations of talc for 72 h, collected, washed, seeded in soft agar suspension and grown for 14 days before colonies were counted. Each data point represents mean ± SE of three determinations. Statistical significance was determined by the Student's paired *t*-test. * $p < 0.05$, ** $p < 0.01$ and *** $p < 0.001$ comparing the treatment with the respective untreated control (0 µg/mL talc).

DOI: 10.1002/ptr

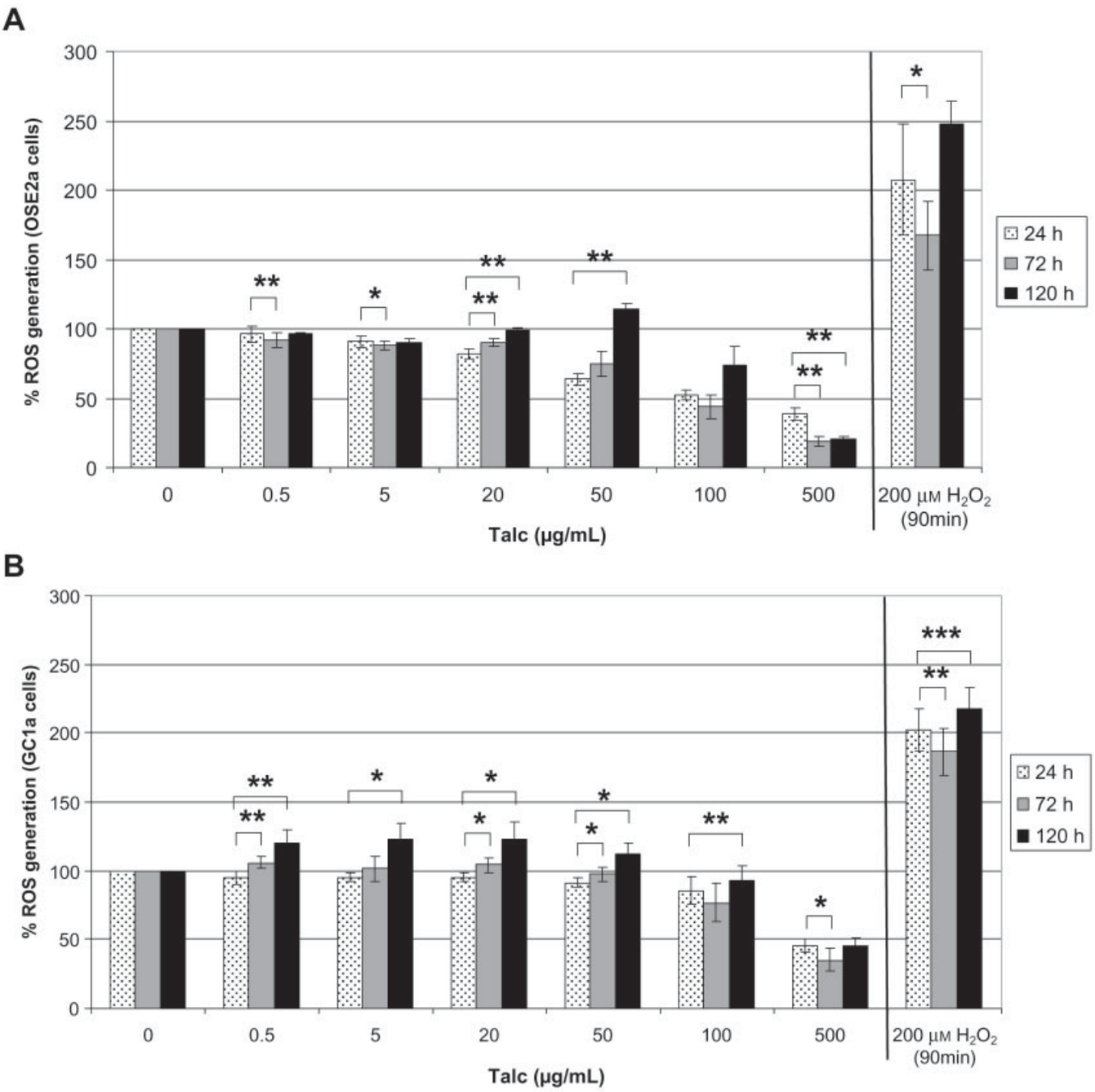

Figure 3. ROS generation of ovarian cells in response to talc treatments. Normal ovarian epithelial (OSE2a) and normal ovarian stromal (GC1a) cells were treated with various concentrations of talc for 24, 72 and 120 h and H_2O_2 during the last 90 min of each respective time point. H_2O_2 was used as a positive control for this assay. Fluorescence intensity were measured as arbitrary fluorescent units (AFU) at ex 485 nm/em 530 nm and normalized with the cell viability assay. Percent AFU (a.k.a. % ROS generation) was calculated as the average AFU of the treated cell divided by the average AFU of the untreated-control cells multiplied by 100. (A) ROS generation in OSE2a cells in response to talc treatments. (B) ROS generation in GC1a cells in response to talc treatments. Each data point represents mean ± SE of three determinations. Statistical significance was determined by the Student's paired *t*-test. * $p < 0.05$, ** $p < 0.01$ and *** $p < 0.001$ comparing the treatment with the respective untreated control (as demonstrated by the horizontal brackets).

Effect of talc on ROS generation in normal ovarian cells

Talc caused an initial dose-dependent decrease in ROS generation (24 h) which increased with time in OSE2a cells (Fig. 3A). However, as time increased, ROS generation rebounded and increased compared with the values at 24 h. A statistically significant increase was seen at 20 µg/mL (72 and 120 h) and 50 µg/mL (120 h). Talc also caused an initial dose-dependent decrease in ROS generation (24 h) in GC1a cells (Fig. 3B), but ROS generation increased with time in the talc treated cells. A statistically significant increase was seen with 0.5, 20 and 50 µg/mL (72 and 120 h), as well as 5 and 100 µg/mL (120 h) compared with the respective 24 h value.

Effect of talc on ROS generation in PMN

Since oxidative stress is often a component of the tumor microenvironment (Valko *et al.*, 2004), the study tested whether talc was capable of inducing ROS generation

DOI: 10.1002/ptr

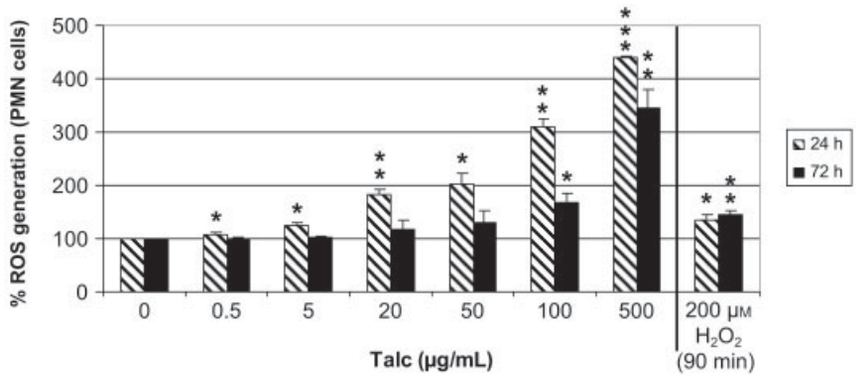

Figure 4. ROS generation of polymorphonuclear neutrophils (PMN) in response to talc treatments. PMNs were treated with various concentrations of talc for 24 and 72 h and H_2O_2 during the last 90 min of each respective time point. H_2O_2 was used as a positive control for this assay. Fluorescence intensity were measured as arbitrary fluorescent units (AFU) at ex 485 nm/em 530 nm and normalized with the cell viability assay. Percent AFU (a.k.a. % ROS generation) was calculated as the average AFU of the treated cell divided by the average AFU of the untreated-control cells multiplied by 100. ROS generation of PMNs in response to talc treatments. Each data point represents mean ± SE of three determinations. Statistical significance was determined by the Student's paired *t*-test. * $p < 0.05$, ** $p < 0.01$ and *** $p < 0.001$ comparing the treatment with the respective untreated control.

in human PMNs. Talc caused a dose-dependent increase in ROS generation at both time points (Fig. 4). The increase was statistically significant at 0.5, 5, 20, 50 µg/mL (24 h) and 100 and 500 µg/mL (24 and 72 h). The maximum ROS generation was seen at 500 µg/mL and was increased over 4-fold at 24 h and 3.5-fold at 72 h, compared with the respective untreated cells.

Effect of pretreatment with Pyc on talc-induced cell viability changes in normal ovarian cells

Pretreatment with Pyc did not cause a statistically different change in cell viability in the OSE2a cells (Fig. 5A). Pretreatment with Pyc caused a general decrease in cell viability in the GC1a cells (Fig. 5B) compared with the respective untreated GC1a cells. One exception is that of a slight, but statistically significant, increase in cell viability at 100 µg/mL Pyc + 5 µg/mL talc (72 h) compared with the respective untreated GC1a cells (Fig. 5B).

Effect of pretreatment with Pyc on talc-induced neoplastic transformation of normal ovarian cells

Pretreatment with Pyc decreased the number of neoplastically transformed colonies induced by talc in

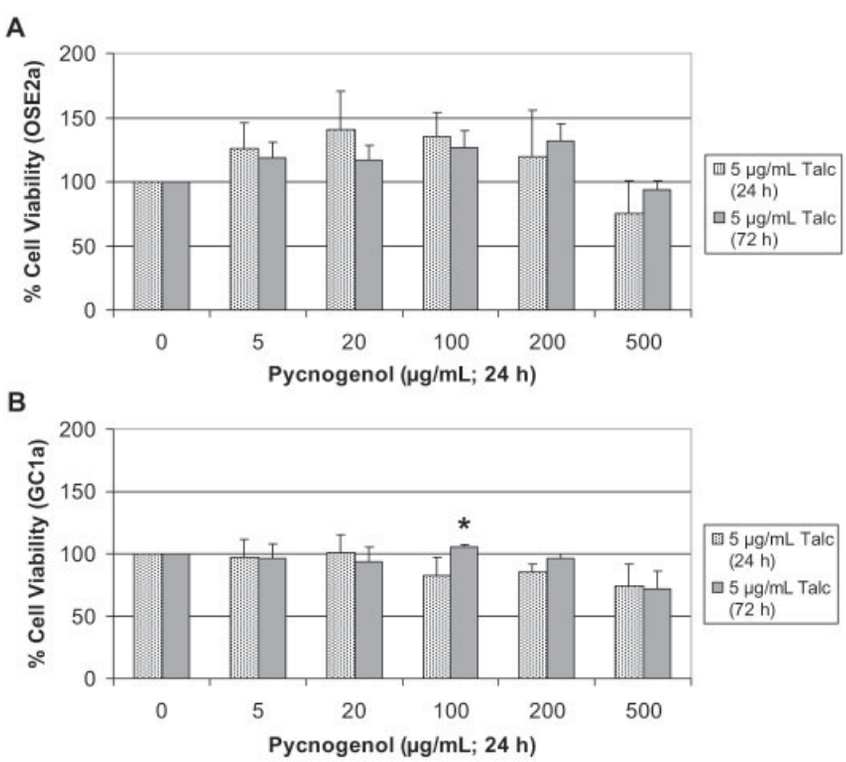

Figure 5. Effect of Pyc + talc treatments on the cell viability of ovarian cells. Normal ovarian epithelial (OSE2a) and stromal (GC1a) cells were treated with 0–500 µg/mL Pyc for 24 h followed by 5 µg/mL talc for 24 and 72 h. Cell viability was measured by the MTS assay and percent cell viability was calculated as the absorbance of the treated cell divided by the absorbance of the untreated-control cells multiplied by 100. (A) OSE2a cells. (B) GC1a cells. Each data represent mean ± SE of four determinations. Statistical significance was determined by the Student's paired *t*-test. * $p < 0.05$ comparing the treatment with the respective untreated control.

DOI: 10.1002/ptr

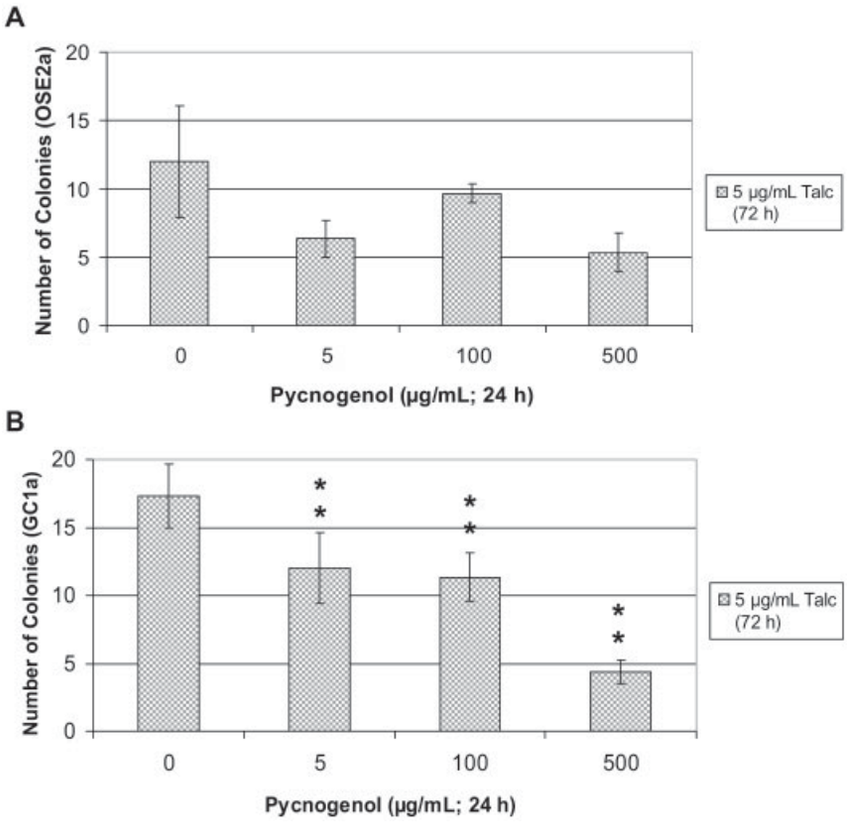

Figure 6. Pyc-induced protection against neoplastic transformation of ovarian cells by talc. Normal ovarian epithelial (OSE2a) and stromal (GC1a) cells were incubated with 0–500 µg/mL Pyc for 24 h followed by 5 µg/mL talc for 72 h, collected, washed, seeded in soft agar suspension and grown for 14 days before colonies were counted. (A) OSE2a cells. (B) GC1a cells. Each data represent mean ± SE of three determinations. Statistical significance was determined by the Student's paired *t*-test. ** $p < 0.01$ comparing the treatment with the respective control.

the OSE2a cells, but not in a statistically significant manner (Fig. 6A). Pretreatment with Pyc (5, 100 and 500 µg/mL; 24 h) caused a statistically significant decrease in the number of talc-induced neoplastically transformed colonies in the GC1a cells (Fig. 6B).

Effect of pretreatment with Pyc on talc-induced ROS generation in normal ovarian cells

Pretreatment with Pyc caused a statistically significant decrease in ROS generation at 5, 20, 50, 100 and 200 µg/mL Pyc + 5 µg/mL talc (24 h); and 500 µg/mL Pyc + 5 µg/mL talc (24 and 72 h) in the OSE2a cells (Fig. 7A). Pretreatment with Pyc caused a statistically significant decrease in ROS generation at 5, 20, 50, 200 and 500 µg/mL Pyc + 5 µg/mL talc (24 h) in the GC1a cells (Fig. 7B). Pretreatment with Pyc caused a statistically significant decrease in ROS generation at 5, 20, 50, 100, 200 and 500 µg/mL Pyc + 5 µg/mL talc (72 h) in the GC1a cells (Fig. 7B). The decrease seen at 100 µg/mL Pyc + 5 µg/mL talc (24 h) was not statistically significant (Fig. 7B).

DISCUSSION

Cancer development is a multi-step process comprising a series of cellular and molecular changes that are mediated by various endogenous and exogenous stimuli, such as aberrantly expressed ROS (Storz, 2005). Although ROS are a byproduct of endogenous biochemical processes, ROS (such as H_2O_2) at high concentrations or expressed in a chronic nature can damage cellular macromolecules and contribute to neoplastic transformation and tumor growth (Nicco *et al.*, 2005). A characteristic of neoplastically transformed cells is their ability to grow and to divide when held in suspension without attachment or with minimal attachment to a rigid surface (Leung *et al.*, 2004; Morales *et al.*, 2003). Our data show that talc not only increased cell viability (Fig. 1A), but also caused an increase in transformed cells in both the stromal and epithelial ovarian cells by their ability to grow, divide and form colonies while being suspended in soft agar (Fig. 2A).

It is known that substances that raise the intracellular level of H_2O_2 are able to trigger normal cell proliferation and abolish tumor cell proliferation (Ness and Cottreau, 1999; Nicco *et al.*, 2005). In normal cells, the basal level of H_2O_2 is low and its increase is initially associated with cell growth. H_2O_2 at high concentrations or expressed in a chronic nature in normal cells, can damage cellular macromolecules and contribute to neoplastic transformation and tumor growth (Nicco *et al.*, 2005). In this study, talc was shown to increase the ROS generation, after an initial suppression, in a time-dependent manner in the normal stromal cells (Fig. 3B) and less strongly in the normal epithelial cells (Fig. 3A).

Recent studies have expanded the concept that inflammation is a critical component of tumor progression. The neoplastic process (proliferation, survival and

DOI: 10.1002/ptr

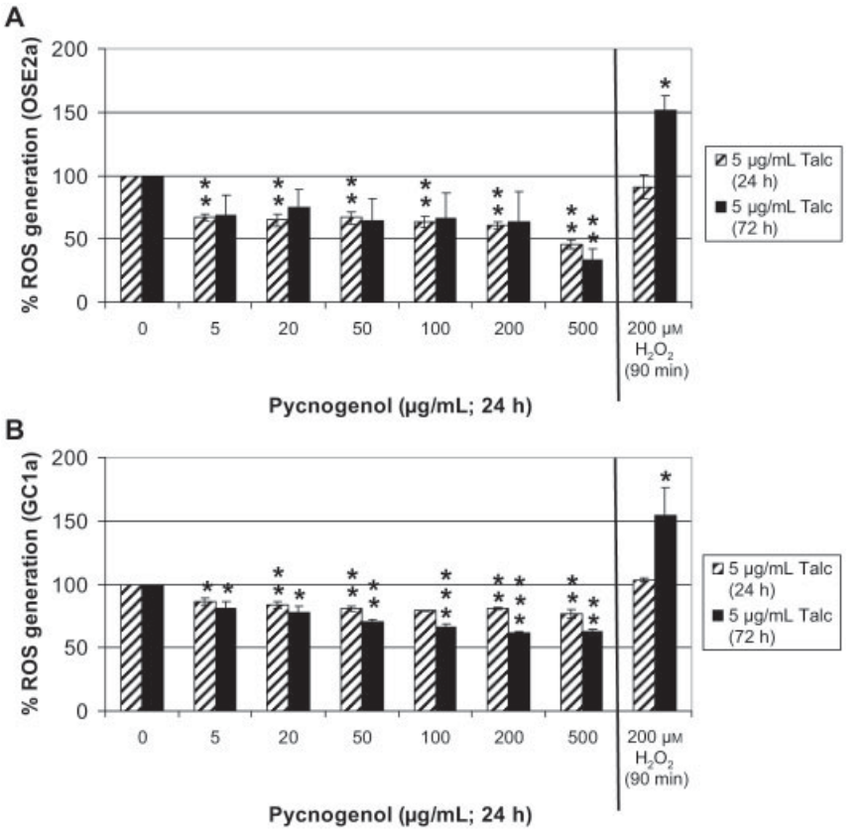

Figure 7. ROS generation of ovarian cells in response to Pyc + talc. Normal ovarian epithelial (OSE2a) and stromal (GC1a) cells were treated with 0–500 µg/mL Pyc for 24 h, followed by 5 µg/mL talc for 24 or 72 h and H_2O_2 (the last 90 min of each time point) as a positive control. Fluorescence intensity (AFU) was measured at ex 485 nm/em 530 nm and normalized by cell viability assay. The percent ROS generation was calculated as the average AFU of treated divided by AFU of untreated-control multiplied by 100. (A) OSE2a cells. (B) GC1a cells. Each data point represents mean ± SE of three determinations. Statistical significance was determined by the Student's paired *t*-test. * $p < 0.05$, ** $p < 0.01$ and *** $p < 0.001$ comparing the treatment with the respective untreated control.

migration) is linked with the tumor microenvironment and synchronized with inflammatory cells (Valko *et al.*, 2004). Polymorphonuclear neutrophils and macrophages are a main source of exogenous ROS in that they release large quantities of ROS in response to a variety of stimuli. This exogenously produced ROS is crucial in the innate immune system of the host for killing invading bacteria but may also be responsible for tissue injury, when expressed excessively or inappropriately (Lewis and Pollard, 2006). Inflammatory cells are prominent in the stromal compartment of virtually all types of malignancy. These highly versatile cells respond to the presence of stimuli in different parts of tumors (Balkwill and Mantovani, 2001). In an *in vitro* study of rat cells, both macrophages and neutrophils were found to be mutagenic in response to alpha-quartz dust, talc and diesel soot; however, neutrophils appeared to have a greater mutagenic effect (Driscoll *et al.*, 1997). This study found that talc not only increased the ROS generation in the ovarian cells (Fig. 3), but also increased the expression of ROS by the neutrophils (Fig. 4).

Talc has been shown to be ubiquitous in our modern environment (Bremmell and Addai-Mensah, 2005) despite concerns raised about its safety (Janssen, 2004), its role as a possible carcinogen (Cramer *et al.*, 1999; Wong *et al.*, 1999), and its known ability to cause irritation and inflammation (Holthouse and Chleboun, 2001). The data show that talc is capable of increasing cell proliferation, inducing neoplastic transformation of both the normal stromal and epithelial ovarian cells *in vitro*; and increasing ROS generation in these cells as well as the PMN cells.

Cancer chemoprevention is regarded as an efficient strategy to prevent cancer. The most useful cancer chemopreventive compounds will have minimal long-term toxicity, while significantly reducing tumor incidence, delaying tumor onset or preventing tumor progression (Kapadia *et al.*, 2003). It was hypothesized that Pyc, shown to induce apoptosis in various malignant cells (Huang *et al.*, 2005; Huynh and Teel, 2000), could prevent talc-induced neoplastic transformation of normal ovarian cells. It was recently shown that Pyc selectively induced cell death in established malignant ovarian germ cells *in vitro* (Buz'Zard and Lau, 2004). The present study showed that Pyc was capable of inhibiting the above mentioned talc-induced changes. Pretreatment with Pyc prevented the characteristic talc-induced increase in cell viability of GC1a cells (Fig. 5B). Pretreatment with Pyc was able to decrease the ROS generation compared with the respective controls both in a dose- and time-dependent manner (Fig. 7). The data show that pretreatment with Pyc reduced the number of talc-induced transformed colonies in both cell lines (Fig. 6). In the GC1a cells, the decrease in the number of transformed colonies was statistically significant at all concentrations of Pyc (Fig. 6B).

DOI: 10.1002/ptr

In conclusion, our *in vitro* data suggest that: (1) talc may contribute to ovarian carcinogenesis in humans by way of inducing aberrant ROS generation and (2) Pyc reduces talc-induced neoplastic transformation of ovarian cells. Taken together, Pyc may prove to be a chemopreventative agent against ovarian carcinogenesis.

Acknowledgements

This study was partially supported by a grant from Horphag Research, Geneva, Switzerland (Otherwise, there is no conflict of interest). We thank Dr Hitoshi Okamura for the cell lines. We thank El Chay for his guidance. We thank Vandana Shah, Marsha Yarnell and Christina Wright for their assistance.

REFERENCES

American Cancer Society. 2000. *Ovarian Cancer*, 1–29.

Balkwill F, Mantovani A. 2001. Inflammation and cancer: back to Virchow? *Lancet* **357**: 539–545.

Bremmell KE, Addai-Mensah J. 2005. Interfacial-chemistry mediated behavior of colloidal talc dispersions. *J Colloid Interface Sci* **283**: 385–391.

Buz'Zard AR, Lau BHS. 2004. Selective toxicity of Pycnogenol for malignant ovarian germ cells *in vitro*. *Int J Cancer Prev* **1**: 207–212.

Cory S, Bernard O, Bowtell D, Schrader S, Schrader JW. 1987. Murine c-myc retroviruses alter the growth requirements of myeloid cell lines. *Oncogene Res* **1**: 61–76.

Cramer DW, Liberman RF, Titus-Ernstoff L *et al.* 1999. Genital talc exposure and risk of ovarian cancer. *Int J Cancer* **81**: 351–356.

Driscoll KE, Deyo LC, Carter JM, Howard BW, Hassenbein DG, Bertram TA. 1997. Effects of particle exposure and particle-elicited inflammatory cells on mutation in rat alveolar epithelial cells. *Carcinogenesis* **18**: 423–430.

Hamilton TC, Fox H, Buckley CH, Henderson WJ, Griffiths K. 1984. Effects of talc on the rat ovary. *Br J Exp Pathol* **65**: 101–106.

Hanna L, Adams M. 2006. Prevention of ovarian cancer. *Best Pract Res Clin Obstet Gynaecol* **20**: 339–362.

Henderson WJ, Hamilton TC, Baylis MS, Pierrepoint CG, Griffiths K. 1986. The demonstration of the migration of talc from the vagina and posterior uterus to the ovary in the rat. *Environ Res* **40**: 247–250.

Holthouse DJ, Chleboun JO. 2001. Talc serodesis – report of four cases. *J R Coll Surg Edinb* **46**: 244–245.

Huang WW, Yang JS, Lin CF, Ho WJ, Lee MR. 2005. Pycnogenol induces differentiation and apoptosis in human promyeloid leukemia HL-60 cells. *Leukemia Res* **29**: 685–692.

Huynh HT, Teel RW. 2000. Selective induction of apoptosis in human mammary cancer cells (MCF-7) by pycnogenol. *Anticancer Res* **20**: 2417–2420.

Janssen JP. 2004. Is thoracoscopic talc pleurodesis really safe? *Monaldi Arch Chest Dis* **61**: 35–38.

Kapadia GJ, Azuine MA, Sridhar R *et al.* 2003. Chemoprevention of DMBA-induced UV-B promoted, NOR-1-induced TPA promoted skin carcinogenesis, and DEN-induced phenobarbital promoted liver tumors in mice by extract of beetroot. *Pharmacol Res* **47**: 141–148.

Knasmuller S, Verhagen H. 2002. Impact of dietary factors on cancer causes and DNA integrity: new trends and aspects. *Food Chem Toxicol* **40**: 1047–1050.

Leung DW, Tompkins C, Brewer J *et al.* 2004. Phospholipase C delta-4 overexpression upregulates ErbB1/2 expression, Erk signaling pathway, and proliferation in MCF-7 cells. *Mol Cancer* **3**: 15.

Lewis CE, Pollard JW. 2006. Distinct role of macrophages in different tumor microenvironments. *Cancer Res* **66**: 605–612.

Morales CP, Gandia KG, Ramirez RD, Wright WE, Shay JW, Spechler SJ. 2003. Characterisation of telomerase immortalised normal human oesophageal squamous cells. *Gut* **52**: 327–333.

Nelson AB, Lau BHS, Ide N, Rong Y. 1998. Pycnogenol inhibits macrophage oxidative burst, lipoprotein oxidation and hydroxyl radical-induced DNA damage. *Drug Dev Indust Pharm* **24**: 139–144.

Ness RB, Cottreau C. 1999. Possible role of ovarian epithelial inflammation in ovarian cancer. *J Natl Cancer Inst* **91**: 1459–1467.

Nicco C, Laurent A, Chereau C, Weill B, Batteux F. 2005. Differential modulation of normal and tumor cell proliferation by reactive oxygen species. *Biomed Pharmacother* **59**: 169–174.

Okamura H, Katabuchi H, Ohba T. 2003. What we have learned from isolated cells from human ovary? *Mol Cell Endocrinol* **202**: 37–45.

Storz P. 2005. Reactive oxygen species in tumor progression. *Front Biosci* **10**: 1881–1896.

Valko M, Izakovic M, Mazur M, Rhodes CJ, Telser J. 2004. Role of oxygen radicals in DNA damage and cancer incidence. *Mol Cell Biochem* **266**: 37–56.

Van Dyke K, Patel S, Vallyathan V. 2003. Lucigenin chemiluminescence assay as an adjunctive tool for assessment of various stages of inflammation: a study of quiescent inflammatory cells. *J Biosci* **28**: 115–119.

Wan CP, Myung E, Lau BH. 1993. An automated microfluorometric assay for monitoring oxidative burst activity of phagocytes. *J Immunol Methods* **159**: 131–138.

Wei ZH, Peng QL, Lau BHS. 1997. Pycnogenol enhances endothelial cell antioxidant defenses. *Redox Rep* **3**: 219–224.

Werebe EC, Pazetti R, Milanez DC, Jr *et al.* 1999. Systemic distribution of talc after intrapleural administration in rats. *Chest* **115**: 190–193.

Wong C, Hempling RE, Piver MS, Natarajan N, Mettlin CJ. 1999. Perineal talc exposure and subsequent epithelial ovarian cancer: a case-control study. *Obstet Gynecol* **93**: 372–376.

Exhibit 102

Toxicology in Vitro 24 (2010) 1139–1147

Contents lists available at ScienceDirect

Toxicology in Vitro

journal homepage: www.elsevier.com/locate/toxinvit

The primary role of iron-mediated lipid peroxidation in the differential cytotoxicity caused by two varieties of talc nanoparticles on A_{549} cells and lipid peroxidation inhibitory effect exerted by ascorbic acid

Mohd Javed Akhtar [a], Sudhir Kumar [b], Ramesh Chandra Murthy [c], Mohd Ashquin [a], Mohd Imran Khan [a], Govil Patil [a], Iqbal Ahmad [a,*]

[a] Fibre Toxicology Division, Indian Institute of Toxicology Research (CSIR), Lucknow 226 001, UP, India
[b] Department of Zoology, University of Lucknow, Lucknow 226 001, UP, India
[c] Analytical Chemistry Division, Indian Institute of Toxicology Research (CSIR), Lucknow 226 001, UP, India

ARTICLE INFO

Article history:
Received 8 October 2009
Accepted 3 March 2010
Available online 10 March 2010

Keywords:
Talc nanoparticles
Cytotoxicity
Lipid peroxidation
Reactive oxygen species
Glutathione
Oxidative stress
Iron contamination

ABSTRACT

Talc particles, the basic ingredient in different kinds of talc based cosmetic and pharmaceutical products, pose a health risk to pulmonary and ovarian systems due to domestic and occupational exposures. Two types of talc nanoparticles depending on the source of geographical origin indigenous and commercial talc nanoparticles were assessed for their potential *in vitro* toxicity on A_{549} cells; along with indigenous conventionally used microtalc particles. Cell viability, determined through live/dead staining and 3 (4,5 dimethyl thiazol 2 yl) 2,5 diphenyl tetrazolium bromide (MTT) assay, decreased as a function of concen tration, origin and size of particles. Both varieties of talc nanoparticles differentially induced lipid perox idation (LPO), which was correlated with the pattern of lactate dehydrogenase (LDH) leakage, reactive oxygen species (ROS) generation, and glutathione (GSH) depletion. Relatively higher cytotoxicity of indig enous nanotalc could be attributed to its higher content of iron as compared to commercial nanotalc. The known scavenger of ROS, L ascorbic acid significantly inhibited LPO induction due to talc particles. Data suggest that nanotalc toxicity on A_{549} cells was mediated through oxidative stress, wherein role of iron mediated LPO was much pronounced in differential cytotoxicity.

1. Introduction

Talc is a magnesium silicate mineral with chemical formula written as $3MgO\ 4SiO_2H_2O$ which corresponds to 4.8% H_2O, 31.7% MgO, and 63.5% SiO_2. It is chemically inert to acids and alkalis and can withstand temperatures up to 1300 °C. In pulverized form it is whiter in appearance. Talc is valued for its extreme softness, smoothness, high lubricating and hiding power and ability to ab sorb oil and grease. Talc is, therefore, used by organized sector of industries because of its valuable properties. Pulverized talc has wide industrial applications in cosmetics as body and face powder; filler in rubber, textile, plastic, asbestos products, polishes and soaps; as a loading agent for paper of all kinds; used in pharmaceu ticals as a carrier of insecticidal and pesticidal dusts.

Since, talc products are marketed in a multitude of grades which have physical or functional characteristics especially suited for particular applications and products, so occupational and con sumer exposures to talc are complex. Talc miners have shown higher rates of lung cancer and other respiratory illnesses from exposure to industrial grade talc, which contains dangerous silica and asbestos (Hollinger, 1990; National Toxicology Program, 1993). The common household hazard posed by talc is inhalation of baby powder by infants (Hollinger, 1990). Talc particles have been found to be translocated after intrapleural administration in rats (Werebe and Pazetti, 1999). Talc particles are able to move through the human reproductive system and become imbedded in the lining of the ovary. Researchers have found talc particles in ovarian tumors and have found that women with ovarian cancer have used talcum powder in their genital area more frequently than healthy women (Henderson et al., 1971; Harlow et al., 1992; Harlow and Hartge, 1995). Numerous studies have shown a strong link between frequent use of talc in the female genital area and ovarian cancer (Heller et al., 1996; Chang and Risch, 1997; Cook et al., 1997; Cramer et al., 1999; Mills et al., 2004; Wild, 2006). In an epidemiologic study aimed to analyze the interactions between talc use and genes involved in detoxification pathway, (viz; glutathione S transferase M1 (GSTM1), glutathione S trans ferase T1 (GSTT1), and N acetyltransferase 2 (NAT2), suggest that women with certain genetic variants may have a higher risk of

* Corresponding author. Address: Fibre Toxicology Division, Indian Institute of Toxicology Research, P.O. Box No. 80, Mahatma Gandhi Marg, Lucknow 226 001, UP, India. Tel.: +91 522 2620207/2227586; fax: +91 522 2628227.
E-mail addresses: iqbal@iitr.res.in, ahmadi@sify.com (I. Ahmad).

0887-2333/$ - see front matter © 2010 Elsevier Ltd. All rights reserved.
doi:10.1016/j.tiv.2010.03.002

ovarian cancer associated with genital use of talc (Gates et al., 2008).

Nanopowder of talc is a recent introduction and is used for improving quality of many industrial products. Nanopowder of talc is being used in plastics for higher strength and stiffness, better thermal and creep resistance; in papers for higher opacity, better gloss and printing quality; in cosmetics and paints for better gloss, smoother surface, resistance to water and cracking, etc. Owing to their unique nano size, nanoparticles are provided with many special physicochemical properties, and thereby may yield extraordinary hazards for human health (Donaldson et al., 2002; Kipen and Laskin, 2005; Holsapple et al., 2005; Nel et al., 2006; Borm et al., 2006). Since, talc with a multitude of physical and functional characteristics is used for particular applications, so occupational and consumer exposures to talc are likely to vary accordingly. Risk of occupational and environmental exposure to nanoparticles of talc has obviously increased.

Since, physical and functional characteristics of talc and other minerals depend, in part, from one geographical region/source to other, therefore, the first objective of the present study was to evaluate cytotoxicity of talc nanoparticles from the two sources indigenous nanotalc (Indian origin) and commercial nanotalc (American origin) using human bronchoalveolar carcinoma derived cells (A_{549}). Indigenous micro scale talc particle was used for comparative size dependent toxicity with the two types of nanotalc. The second objective was to study the mechanism of cytotoxicity induced by talc nano and micro particles. In the present study, different types of talc particles were dispersed in the cell culture medium at varying concentrations and then exposed to cells. Cytotoxicity was measured by determining cell viability using MTT assay and live dead staining method. To elucidate the possible mechanisms of cytotoxicity, biomarkers for cytotoxicity and oxidative stress, namely lactate dehydrogenase (LDH) leakage in cell culture medium, reactive oxygen species (ROS) generation, intracellular reduced glutathione (GSH) level, and malondialdehyde (MDA) as an indicator of lipid peroxidation and membrane damage, were measured. Antioxidant, ascorbic acid, was used to delineate further the potential mechanism of oxidative stress and as a potential preventive measure. In the toxicity of minerals, the iron content has been a key factor, acting through Fenton reaction and the Haber Weiss cycle. Some metals like Fe, Pb, and Cr was measured in the talc from two sources. A role of differential amount of iron present in indigenous and commercial talc, in the perspective of cytotoxicity and oxidative stress has, therefore, also been established.

2. Materials and methods

2.1. Nanoparticles

Indigenous cosmetic grade talc was collected from Udaipur, Rajasthan, India and prepared into micro and nanoparticles. As a standard reference, Nanopowder of talc (i.e. commercial nanotalc) was purchased from (M.K. Impex Canada, Catalpa Road, Mississauga, Canada). As per the information provided by the supplier, the powder size was 70 120 nm and the country of origin was USA. For indigenous nanotalc a stone of talc was crushed into fine particles and fed into a ball mill (PM 100, Retsch, Germany) and grinded for 5 days at an alternative cycles of grinding (10 min) and halt (30 min) at 350 rpm using a mixture of different sizes of balls. The sizes of nanoparticles were measured by transmission electron microscopy (TEM) and found to be 80 130 nm. Indian talc particles (i.e. indigenous micro talc) 50 65 μm served as negative control for a comparative study on nanotoxicity of indigenous and commercial varieties of nanotalc.

2.2. Chemicals

Fetal bovine serum, Penicillin streptomycin, DMEM F 12 medium, HBSS was purchased from Invitrogen Co. (Carlsbad, CA, USA). MTT [3 (4,5 dimethylthiazol 2 yl) 2,5 diphenyltetrazolium bromide], NADH, Pyruvic acid, L ascorbic acid, glutathione reduced (GSH), o phthalaldehyde (OPT), 2′,7′ dichlorofluorescin diacetate (DCFH DA), 1,1,3,3 tetraethoxypropane (TEP), 2 thiobarbituric acid (TBA), sodium dodecyl sulphate (SDS), Na_2HPO_4, NaH_2PO_4, were obtained from Sigma Aldrich. Ultrapure DI water was prepared using a Milli Q system (Millipore, Bedford, MA, USA). All other chemicals used were of reagent grade.

2.3. Estimation of heavy metals in indigenous and commercial talc

Talc samples were digested in digesting mixture (HNO_3 and perchloric acid in a ratio of 4:1) for 24 h on hot plate in a fume hood. The digested samples were dissolved in 1% HNO_3 and filtered. The filtrate was used for metal analysis by atomic absorption spectroscopy (AAS). Before analysis, AAS was calibrated every time by running at least three standard concentration (1, 3 and 5 mg/L) of each metal. Values have been expressed as% metal content in talc samples.

2.4. Measurement of hydrodynamic size of nanotalc

These particles were suspended in complete cell culture media, ultrasonicated at 30 W for 2 min (Sonics Vibra Cell, India) and a dynamic light scattering (DLS Malvern Instruments USA) performed for particle size distribution in culture media.

2.5. Cell culture and treatment with talc particles

The A_{549} cell line has been established in permanent culture from a human lung adenocarcinoma (Lieber et al., 1976). *In vitro*, these cells are largely differentiated as alveolar epithelial cells, type II (Croute et al., 1990). The A_{549} cells were obtained from National Centre For Cell Science (NCCS), Pune, India. Cells were maintained in DMEM F 12 medium supplemented with 10% fetal bovine serum, 100 U/ml penicillin, and 100 μg/ml streptomycin, and grown at 37 °C in a humidified, 5% CO_2 incubator. For the determination of GSH, MDA, and LDH levels, A_{549} cells were plated into 75 cm^2 flasks at a density of 2.0×10^6 cells per flask in 12 ml culture medium and allowed to attach for 24 h. Then, the freshly dispersed talc nanoparticles suspensions in cell culture medium were prepared and diluted to appropriate concentrations (50, 100, and 200 μg/ml) and immediately applied to the cells in 15 ml culture medium. Cells not exposed to particles served as controls in each experiment. The selection of the 50 200 μg/ml dosage range of talc nanoparticles was based on a preliminary dose response study (data not shown). A dosage level lower than 50 μg/ml did not result cytotoxicity significantly. The 48 h exposure time was chosen for investigation; the responses at 24 h exposure were not as pronounced as that at 48 h. Therefore, all the data presented here is that of 48 h exposure. Throughout the studies presented in this paper, we utilized a particle dose of 20 μg/cm^2 = 100 μg/ml.

2.6. Cell viability assay

Cytotoxicity was measured by determining cell viability using MTT assay and live dead staining method.

2.6.1. MTT assay

Cell proliferation/viability was assessed by the MTT assay as first described by Mossman (1983) and later modified by Hansen et al. (1989). This assay is based on the ability of viable cells, but

not of dead cells, to reduce soluble, yellow 3 (4,5 dimethyl thiazol 2 yl) 2,5 diphenyl tetrazolium bromide (MTT) into insoluble, blue formazon product. Briefly, around 10,000 A_{549} cells per well were plated in 96 well microtiter plates in a 100 μl of medium. The next day, the medium was changed and the cells were treated with talc nanoparticles at 50 , 100 , and 200 μg/ml for 48 h. After the expo sure time completed, the medium was aspirated off and 100 μl MTT laden media (0.5 mg MTT/ml of media without phenol red and serum, filtered through 0.22 μm filter) added and incubated for 2 h. The reaction was stopped and formazan crystal thus formed was solubilised by mixing an equal volume of stop mix solution containing 20% SDS in 50% *N,N* dimethylformamide and left overnight on a shaker. To minimize the interference in absor bance caused by previously dosed talc particles (at concentrations like 50 200 μg/ml obviously resulting in turbidity!), the plates were centrifuged at 3000 rpm for 5 min to settle down the particles and a clear 100 μl supernatant was transferred to other fresh wells of microtiter plate and then absorbance at 570 nm was taken by a microplate reader (Omega Fluostar). Following noncellular back ground (blank consisting of yellow MTT and stop mix solutions) subtraction, all data were normalized to the MTT conversion activ ity of media treated control cells. This value corresponds to 0% de crease in MTT conversion activity and represents 100% cell viability.

2.6.2. Live dead staining (trypan blue exclusion) assay

In addition to the MTT assay, the cell viability was also deter mined by the trypan blue exclusion method. The percentage of non stained live cells was evaluated using a haemocytometer. A total of 200 cells were counted for each measurement.

2.7. LDH leakage

The activity of cytoplasmic LDH released into the culture media was determined with the method described elsewhere (Wroblew ski and LaDue, 1955; Welder et al., 1991). A 100 μl sample from the centrifuged culture media was collected after the cells were treated for 48 h. The LDH activity was assayed in 3.0 ml of reaction mixture with 100 μl of pyruvic acid (2.5 mg/ml phosphate buffer) and 100 μl of NADH (2.5 mg/ml phosphate buffer) and the rest of the volume adjusted with phosphate buffer (0.1 M, pH 7.4). The rate of NADH oxidation was determined by following the decrease in absorbance at 340 nm for 3 min at 30 s interval at 25 °C using a spectrophotometer (Thermo Spectronic). The amount of LDH re leased is represented as LDH activity (IU/L) in culture media.

2.8. Intracellular ROS measurement

The generation of intracellular ROS was measured using 2′,7′ dichlorofluorescin diacetate (DCFH DA) probe (Wang and Joseph, 1999). DCFH DA passively enters the cell where it is broken down into cell impermeable, non fluorescent reduced dichlorofluorescin (DCFH) and diacetate by cellular esterases. Now DCFH becomes oxidized with intracellular ROS to form the highly fluorescent com pound dichlorofluorescin (DCF) that may be cell permeable. Briefly, 10 mM DCFH DA stock solution made in dimethyl sulfoxide (DMSO) was diluted in culture medium without serum or other additive to yield a 100 μM working solution. After 48 h of exposure to talc nanoparticles, the cells in the 12 well plate were washed twice with HBSS and then incubated in 1 ml working solution of DCFH DA at 37 °C for 30 min. The cells were lysed in alkaline solu tion and centrifuged at 3000 rpm. A 200 μl supernatant was trans ferred to black 96 well plate and fluorescence was then read at 480 nm excitation and 520 nm emission using a microplate reader (Omega Fluostar). The intensity of untreated control well was as sumed to be 100% and data is represented in percent of control.

2.9. Determination of intracellular GSH

The cellular content of GSH was quantified by the fluorometric assay of Hissin and Hilf (1976). After exposure, cells were lysed in 20 mM Tris (pH 7.0) by repeated cycles of freeze thaw and centri fuged at 10,000 rpm for 10 min at 4 °C. The supernatant was trans ferred to another tube and protein content was measured. For the determination of intracellular GSH, protein in this supernatant was precipitated at 1% perchloric acid and again centrifuged at 10,000 rpm for 5 min at 4 °C. Now 20 μl sample was mixed with 160 μl of 0.1 M phosphate 5 mM EDTA buffer, pH 8.3 and 20 μl *o* phthalaldehyde (OPT, 1 mg/ml in methanol) in a black 96 well plate. After 2 h incubation at room temperature in the dark, fluo rescence was measured at an emission wavelength of 460 nm and an excitation wavelength of 355 nm, along with similarly pre pared standards of GSH in 1% perchloric acid. Results are expressed as nmol GSH/mg of cellular protein.

2.10. Determination of thiobarbituric acid reactive substances (TBARS)

LPO was assessed by the TBARS assay, which detects mainly malondialdehyde (MDA), an end product of the peroxidation of polyunsaturated fatty acids and related esters. TBARS was mea sured by slight modification of the method of Ohkawa et al. (1979). Subconfluent cells were scraped in 75 cm^2 flasks, washed two times by isotonic trace element free Tris HCl buffer (400 mM, pH 7.3). A 200 μl aliquot of cell suspension was subse quently mixed with 800 μl of LPO assay cocktail containing (0.4% (w/v) thiobarbituric acid, 0.5% (w/v) SDS, 5% (v/v) acetic acid, pH 3.5 and incubated for 60 min at 95 °C. The sample was cooled using tap water and centrifuged at 5000 rpm for 5 min. The absorbance of the supernatants was read at 532 nm against a standard curve prepared using the MDA standard (10 mM 1,1,3,3 tetramethoxy propane in 20 mM Tris HCl, pH 7.4). Results were calculated as nmol of MDA/mg of cellular protein.

2.11. Addition of L ascorbic acid

To test the potential antioxidant effects afforded by ascorbic acid, 1.5 mM was applied to cell culture 30 min before exposure with particles. A dosage of 200 μg/ml of the two varieties of talc was then exposed for 48 h and MDA level was measured as illus trated above.

2.12. Estimation of protein

The total protein concentration was measured by the Bradford method (Bradford, 1976) using a ready to use Bradford reagent (Sigma Aldrich, USA) and bovine serum albumin as the standard.

2.13. Statistics

Data were expressed as the mean ± SD from three independent experiments. One way ANOVA and Dunnett's Multiple Comparison Test was applied using Graph Pad prism (Version 5.0) software for significance testing, using a p value $\leqslant 0.05$.

3. Results

3.1. Iron contamination in talc samples

Indigenous and commercial talc samples were analyzed for con tamination of heavy metals (Fe, Pb, and Cr). The results are given in Table 1. Indigenous talc contained almost 2.3 times higher iron level in comparison to commercial talc. Pb was not in detectable

Table 1
Metal contamination in talc samples.

Name of metal	% Metal content	
	Indigenous talc	Commercial talc
Fe	0.19	0.08
Cr	Not detectable	0.0046
Pd	Not detectable	Not detectable

limit in both the samples. However Cr was present in trace amount in commercial nanotalc.

3.2. Hydrodynamic size of talc nanoparticles in culture media

The size measured by a dynamic light scattering method was the particles hydrodynamic size, which indicates the extent of aggregation of particles in suspension. The measurements have been given in Table 2. Results show that aggregation occurred and the aggregation was not uniform.

3.3. The concentration , size , and origin dependent cytotoxicity of talc particles

The A_{549} cells were exposed with indigenous microtalc (50 65 μm) particles, indigenous talc nanoparticles (80 130 nm) and commercial talc nanoparticles (70 120 nm) for 48 h exposure, and the cell viability was assessed by MTT assay. Cell viability de creased as a function of concentration, size and geographical origin of particles. Cell viability decreased to 93.0%, 91.6%, and 83.6% for indigenous microtalc and 81.6%, 67.0%, and 47.30% for indigenous nanotalc and 88.3%, 77.6%, and 64.0% for commercial nanotalc par ticles when exposed at 50 , 100 , and 200 μg/ml, respectively (Fig. 1). Fig. 2 shows the results on cell viability obtained by trypan blue exclusion test for similar experiment. Cell viability decreased to about 93.0%, 90.6%, and 83.6% for indigenous microtalc and 83.6%, 73.6%, and 57.30% for indigenous nanotalc and 88.6%, 78.6%, and 69.6% for commercial nanotalc particles exposed at 50 , 100 , and 200 μg/ml, respectively. The IC_{50}s evaluated by MTT and trypan blue assay is given in Table 3.

3.4. Cell membrane damage

LDH release, a marker of cell membrane damage, was measured at 50, 100, and 200 μg/ml for the 48 h exposure (Fig. 3). Following exposure to talc particles at concentrations mentioned above, the LDH activity in the culture media is increased in a concentration dependent manner and found to 18.1%, 32.9%, and 61.3%, respec tively for indigenous microtalc and 99.2%, 193.6%, and 275.6%, respectively for indigenous nanotalc and 46.2%, 103.7%, and 178.7%, respectively for commercial nanotalc. The indigenous nan otalc induced a significantly higher ($p < 0.05$) cell membrane dam age when compared with its micro scale size and commercial nanotalc for a particular concentration. For instance, 50 , 100 , and 200 μg/ml exposure of indigenous nanotalc induced 1.4 , 1.44 , and 1.3 fold higher membrane damage when compared with the same concentrations of commercial nanotalc induced mem brane damage. Similarly indigenous nanotalc induced membrane damage was 1.6 , 2.2 , and 2.3 times higher than that of indigenous microtalc.

Table 2
Actual and hydrodynamic sizes of Indigenous and Commercial nanotalc in culture media.

Type of nanoparticles	Actual size (nm)	Hydrodynamic size (nm)
Commercial nanotalc	70–120	800 ± 100
Indigenous nanotalc	80–130	750 ± 120

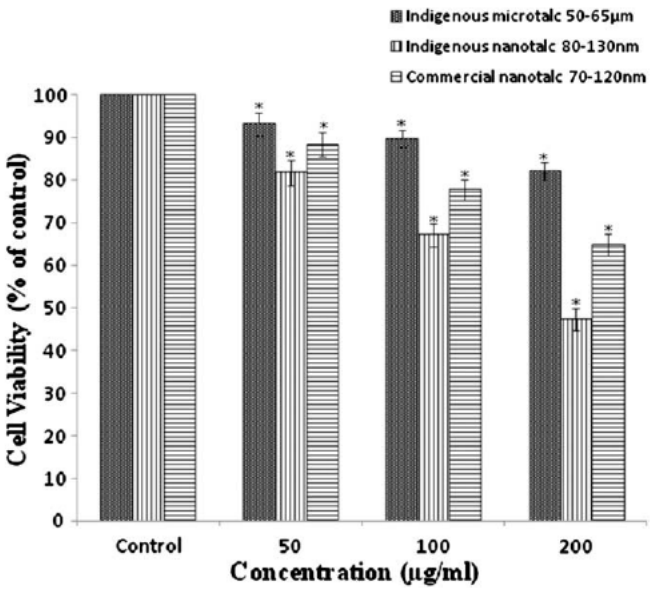

Fig. 1. Viability of A_{549} cells after 48-h exposure to indigenous microtalc, indigenous nanotalc and commercial nanotalc particles evaluated by MTT assay at indicated concentrations. Values are mean ± SD from three independent experiments. Triplicates of each treatment group were used in each independent experiment. *Denotes a significant difference from the control ($p < 0.05$).

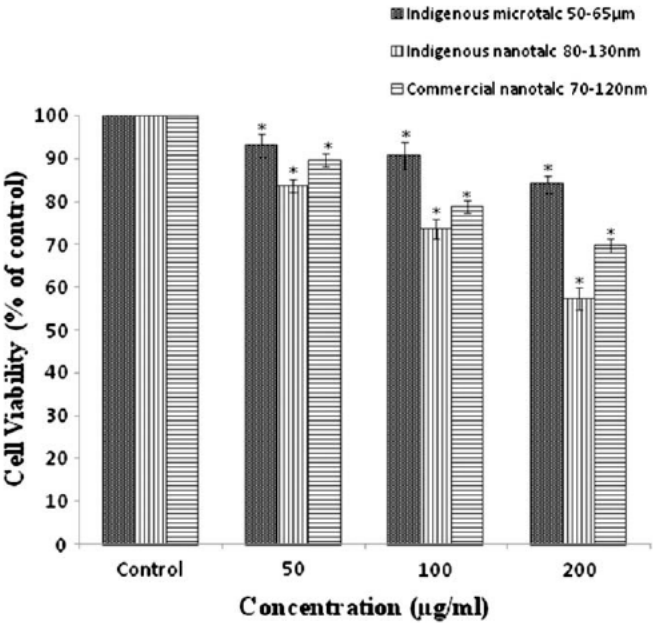

Fig. 2. Viability of A_{549} cells after 48-h exposure to indigenous microtalc, indigenous nanotalc and commercial nanotalc particles evaluated by trypan blue assay at indicated concentrations. Values are mean ± SD from three independent experiments. Triplicates of each treatment group were used in each independent experiment. *Denotes a significant difference from the control ($p < 0.05$).

3.5. ROS generation

The ability of talc micro and nanoparticles to induce intracellu lar oxidant production in A_{549} cells was assessed by measuring DCF fluorescence as a reporter of ROS generation. DCF fluorescence intensity significantly ($p < 0.05$) increased after 48 h exposure to all examined micro and nanoparticles at concentrations of 50 ,

Table 3
IC_{50} values of different talc particles measured by MTT and trypan blue.

Types of talc nanoparticles	IC_{50} by MTT assay (μg/ml)	IC_{50} by trypan blue assay (μg/ml)
Indigenous microtalc (50–65 μm)	600	630
Indigenous nanotalc (80–130 nm)	190	255
Commercial nanotalc (70–120 nm)	277.5	325

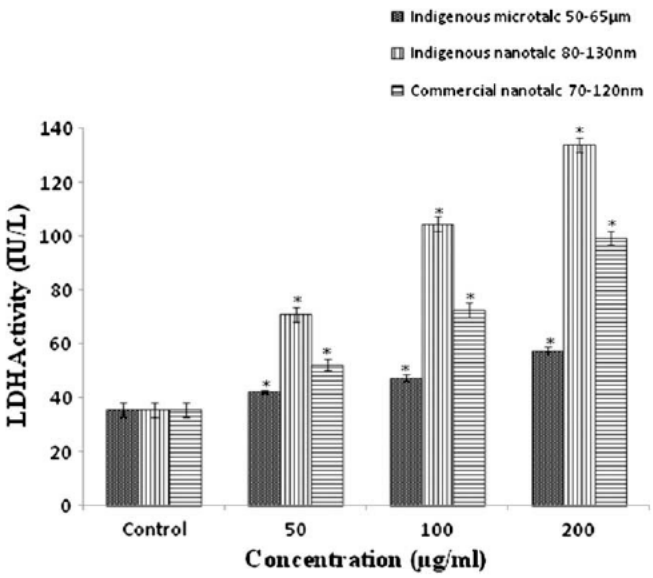

Fig. 3. The LDH activities in the cell culture medium after 48-h exposure to indigenous microtalc, indigenous nanotalc and commercial nanotalc particles at indicated concentrations. Values are mean ± SD from three independent experiments. *Denotes a significant difference from the control ($p < 0.05$).

100 , and 200 μg/ml, and evaluated to be 136%, 155%, and 175%, respectively for indigenous microtalc and 150%, 203%, and 265%, respectively for indigenous nanotalc and 136%, 175%, and 205%, respectively for commercial nanotalc (Fig. 4). The highest fluores cence obtained was that for indigenous nanotalc at 200 μg/ml.

3.6. Cellular GSH level and LPO induced by talc nanoparticles

Following exposure to talc particles at concentrations 50, 100, and 200 μg/ml for 48 h, the intracellular GSH level exhibited a con centration dependent decrease (Fig. 5). The GSH levels were re duced by 3%, 11.56%, and 18.8% for indigenous microtalc and 14.2%, 18.8%, and 25.4% for indigenous nanotalc and 6.6%, 11.5%, and 20.8%, respectively for commercial nanotalc.

In order to elucidate the lipid peroxidation induced by talc par ticles, the MDA concentration was measured. Each type of nano particles elevated the intracellular MDA concentration which was dependent on dosage and source of talc particle origins (Fig. 6). The MDA levels were elevated by 1.3 fold, 1.4 fold, and 1.9 fold, respectively for indigenous microtalc, and 1.6 fold, 2.3 fold, and 3.1 fold, respectively for indigenous nanotalc and 1.4 fold, 1.7 fold, and 2.1 fold, respectively for commercial nanotalc, compared to the control untreated groups.

3.7. Inhibitory effect afforded by ascorbic acid on LPO induced by talc nanoparticles

In an additional set of studies, L ascorbic acid was added to the cells during exposure to micro and nanotalc, each group ex

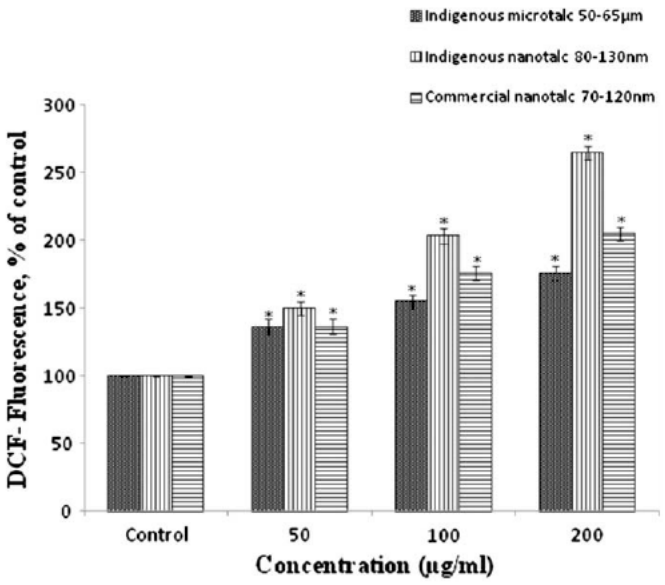

Fig. 4. DCF-fluorescence intensity after 48-h exposure to indigenous microtalc, indigenous nanotalc and commercial nanotalc particles at indicated concentrations. Values are mean ± SD from three independent experiments. *Denotes a significant difference from the control ($p < 0.05$).

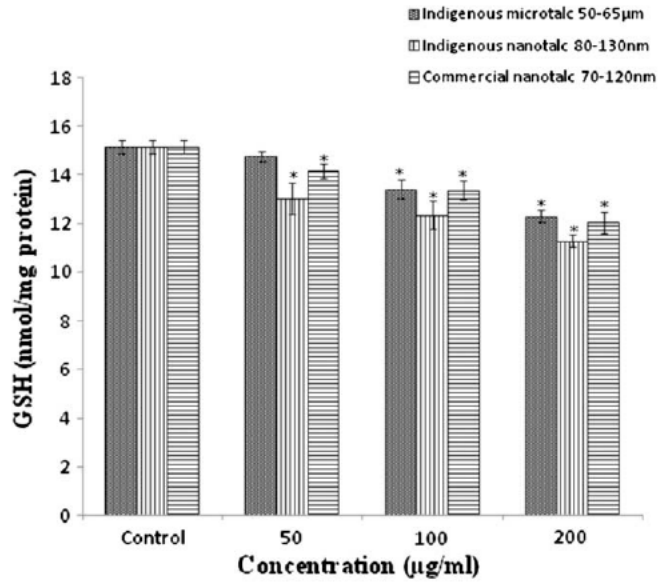

Fig. 5. Cellular GSH levels of A_{549} cells after 48-h exposure to indigenous microtalc, indigenous nanotalc and commercial nanotalc particles at indicated concentrations. Values are mean ± SD from three independent experiments. *Denotes a significant difference from the control ($p < 0.05$).

posed at 200 μg/ml, as a test to determine if the oxidative damage to A_{549} cells could be prevented. Results show that L ascorbic acid effectively prevented the generation of MDA level induced by talc particles (Fig. 7). MDA level was reduced up to control level for indigenous microtalc in the presence of ascorbic acid. When indigenous nanotalc induced MDA was 3.1 fold, in the presence of ascorbic acid it was reduced and found to be 2.1 fold of control. When commercial nanotalc induced MDA was 2.1 fold, in the presence of ascorbic acid it was 1.3 fold of control.

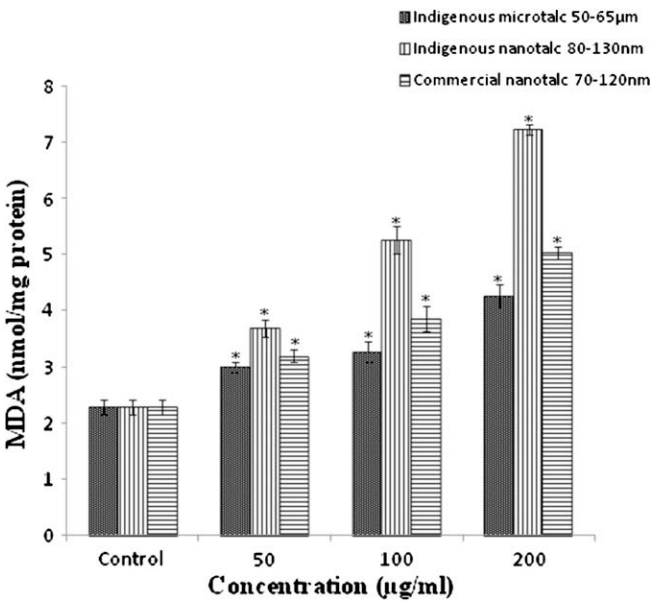

Fig. 6. Cellular MDA levels of A_{549} cells after 48-h exposure to indigenous microtalc, indigenous nanotalc and commercial nanotalc particles at indicated concentrations. Values are mean ± SD from three independent experiments. *Denotes a significant difference from the control ($p < 0.05$).

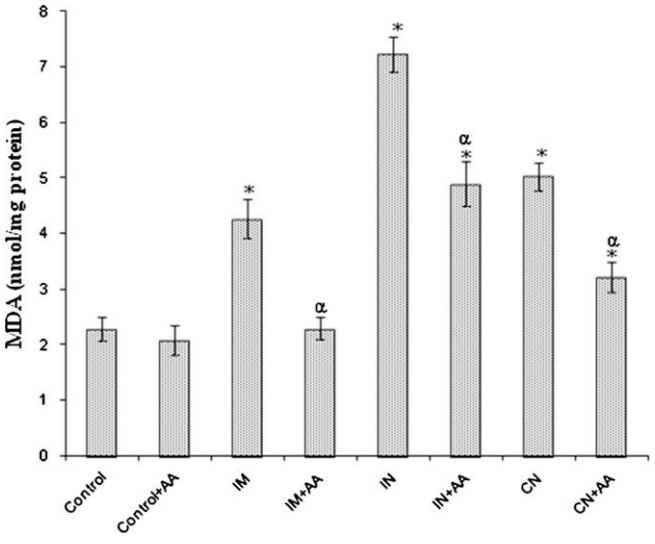

Fig. 7. Showing the inhibitory effect of ascorbic acid on cellular MDA levels of A_{549} cells under indicated conditions of 48-h exposure. #AA (1.5 mM L-ascorbic acid); IM (200 µg/ml indigenous microtalc); IN (200 µg/ml indigenous nanotalc); CN (200 µg/ml commercial nanotalc) Values are mean ± SD from three independent experiments. *Denotes a significant difference from the control ($p < 0.05$). α indicates the significant inhibitory effect of ascorbic acid (AA) on lipid peroxidation versus either, IM, IN or CN.

4. Discussion

At present, an *in vitro* toxicological study of talc nanoparticles is lacking. In this study, the cytotoxicity of two types of talc nanoparticles was investigated in cultured human bronchoalveolar carcinoma derived cells (A_{549}). This cell line has been widely used in *in vitro* cytotoxicity studies (Huang et al., 2004; Bakand et al., 2006). Present study showed that the two types of talc nanoparticles caused significant reduction in cell viability as a function of concentration and their iron content. The talc nanoparticles from two sources induced the enhanced generation of ROS and MDA production. Consequently, redundant free radicals would interact with biomolecules including proteins, enzymes, membrane lipids and even DNA which could be oxidized, modified, destructured and ultimately dysfunctioned (Marnett, 2000; Hensley and Floyd, 2002).

Oxidative stress has been suggested to play an important role in the mechanism of toxicity of a number of compounds whether by production of free radicals or by depleting cellular antioxidant capacity. Cellular integrity is affected by oxidative stress when the production of ROS overwhelms antioxidant defense mechanism (Halliwell et al., 1992; Chen and Yu, 1994). ROS are oxygen containing molecules, such as hydrogen peroxide (H_2O_2), superoxide anion ($O_2^{\cdot}$), and hydroxyl radical ($HO^{\cdot}$), that have a greater chemical activity than molecular oxygen. ROS are generated in many inflammatory conditions in the lung and have been associated with cell injury and apoptosis (Anderson et al., 1994; Meyer et al., 1993). Many other studies have shown that nanoparticles may produce toxicity by generating ROS. Recently, Buz'Zard and Lau (2007) have reported enhanced ROS generation in human ovarian cell culture and have found an increased cell proliferation and neoplastic transformation of human ovarian stromal and epithelial cells exposed with talc. In the present study too, talc micro and nanoparticles induced significantly higher ROS generation compared with untreated A_{549} cells when using the fluorescent dichlorofluorescin probe. Moreover, indigenous nanotalc resulted higher ROS generation than commercial nanotalc.

GSH is the most abundant nonproteinous tripeptide containing a sulfhydryl group in virtually all cells, and it plays a significant role in many biological processes. It also constitutes the first line of the cellular defense mechanism against oxidative injury and is the major intracellular redox buffer in ubiquitous cell types (Meister, 1989). GSH acts as a cosubstrate in the GSH peroxidase catalyzed reduction of hydrogen peroxide or lipid peroxides (Forman et al., 1997) leading to its depletion. Previous studies demonstrated that ROS generation following GSH depletion caused mitochondrial damage (Martensson et al., 1989; Meister, 1995), which has been implicated in apoptosis (Green and Reed, 1998). There was a significant depletion of GSH between the control and the treated groups except for indigenous microtalc at 50 µg/ml. In terms of GSH depletion, indigenous nanotalc was found to be the most toxic.

In the toxicity mechanism of minerals, the iron content has been a key factor. Iron dependent ROS generation from fibers results in the generation of hydroxyl radicals through the Fenton reaction and the Haber Weiss cycle. Iron dependent LPO could be important, since this process requires redox cycling of iron and does not necessarily require H_2O_2 or ROS (Halliwell and Gutteridge, 1990). Indeed, iron has a key role in both the initiation and propagation of LPO, leading to the generation of peroxyl and alkoxyl radicals as well as lipid peroxides (Halliwell and Gutteridge, 1990). It has been known for several years that the surface iron (II) or leachable iron (II) on mineral surfaces reduces molecular oxygen to superoxide anion, which then dismutates to hydrogen peroxide. In the presence of asbestos or silica, hydrogen peroxide and superoxide react via a Fenton like reaction driven by iron to form the potent hydroxyl radical *in vitro* leading to cellular LPO (Mossman et al., 1996). Since, LPO is a sensitive parameter for toxic effects of various environmental pollutants with oxidative properties (Krug and Culig, 1991; Beck Speier et al., 2001; Oberdorster, 2004; Sayes et al., 2005); the authors suspected that the relatively high iron content in both the nanotalc may play a key role to yield higher ROS and in turn caused higher LPO. There are other nanomaterials, such as C_{60}, which mediates cytotoxicity primarily through lipid peroxidation (Sayes et al., 2005; Isakovic et al., 2006) whereas carboxyfullerenes (made by certain surface modifications of C_{60}) have been shown to impart cytoprotective activity by eliminating reactive oxygen species (ROS) and antago

nizing the effects of the oxidative stress dependent cytotoxicity (Dugan et al., 1997, 2001; Bogdanovic et al., 2004; Isakovic et al., 2006). Recently Scarfì et al. (2009) has reported that plasma membrane contact with quartz, a kind of silica, is sufficient to trigger membrane LPO, TNF α release and cell death in mouse macrophage cell line RAW 264.7. The authors hypothesize that contact of particles with cell membranes initiate ROS generation and LPO in a ratio of amount of iron present in talc nanoparticles.

For a given mass compared with larger particles, the ratio of surface to total atoms or molecules increases exponentially with decreasing particle size. Particle size is thereby an essential determinant of the fraction of reactive groups on particle surface (Oberdorster et al., 2005; Nel et al., 2006). For example, several studies found that ultrafine particles of titania are more toxic than its larger counterparts having the same chemical composition (Donaldson et al., 1998; Gilmour et al., 1997; Oberdorster et al., 1992, 1995; Oberdorster, 1996, 2000). Similarly, surface area dependent induction of oxidative stress and consequently, proinflammatory effects have been found to correlate in case of polystyrene particles by Brown et al. (2001) and Lin et al. (2006) have reported higher toxicity of the two sizes (15 and 46 nm) of silica nanoparticles than micro silica (5 μm) on A_{549} cells. Here two sizes (15 and 46 nm) of silica nanoparticles induced no significant differences in the toxicity and similar was the case in a study done by Sayes et al. (2006), where smaller nanoparticles of titania had effects comparable to larger nanoparticles of titania but showed a phase dependent differential toxicity where anatase titania (photoactive phase), able to generate ROS more strongly, was 100 times more toxic than an equivalent sample of rutile titania. In the present study, both nanoparticles would have been resulted differential surface iron activity per given mass resulting in differential toxicity. When indigenous nanotalc induced toxicity is compared with indigenous microtalc, size dependent factor becomes apparent because all the compositional factors are constant. But when commercial nanotalc (having larger surface area but lower iron content) induced toxicity is compared with indigenous microtalc, the results show a complex function of size and impurities. Since, micro talc size is very large (50 65 μm), than commercial nanotalc (70 120 nm), perhaps size becomes the primary determinant of toxicity, resulting in higher toxicity of commercial nanotalc than indigenous micro talc.

Another pathway of free radical generation by asbestos, silica or particulates like these (e.g. talc particles) occurs via an oxidative burst when fibers and particles are phagocytised by AMs or other cell types, including alveolar epithelial cells and fibroblasts (Churg, 1996). Phagocytic cells can endocytose small particles, whereas bigger crystals and fibers are subject to so called "frustrated phagocytosis". Experimental studies suggest that in *in vivo* conditions "frustrated phagocytosis" appears to have a dramatic influence on the sustained generation of ROS (Hansen and Mossman, 1987; Vallyathan et al., 1992). Repeated "frustrated phagocytosis" would be expected to attract more phagocytes, resulting in chronic enhanced generation of ROS, which in turn contribute to inflammasome activation, resulting in the secretion of IL 1β leading to the initiation of pulmonary fibrosis (Dostert et al., 2008; Cassel et al., 2008). Since, talc and asbestos are physically and chemically similar, found together in nature and being particulate structure like silica and asbestos, talc particles may also generate ROS through activation of NADPH oxidase by frustrated phagocytosis, leading to the initiation of so called talcosis particularly in occupationally exposed workers.

Antioxidants, such as α tocopherol, uric acid and L ascorbic acid, typically prevent cellular damages caused by oxygen radicals by acting as ROS scavengers (Packer et al., 1979; Burton and Ingold, 1981). Ascorbic acid (or vitamin C) acts as a potent water soluble antioxidant in biological fluids (Frei et al., 1989, 1990) by scavenging physiologically relevant ROS and reactive nitrogen species (RNS) (Halliwell, 1996). However, it should be noted that antioxidative potential of ascorbic acid has not been validated in certain conditions (Bowry et al., 1992; Poulsen et al., 1998; Levine et al., 1998). Ascorbic acid contributes significantly to cellular antioxidation as a water soluble chain breaking radical scavenger (Asard, 2008) and to the recycling of plasma membrane α tocopherol (vitamin E) via the reduction of the α tocopheroxyl radical (Aguirre and May, 2008). The latter activity may assist ascorbic acid to protect against LPO in membranes (May et al., 1998). We, therefore, tested the LPO preventive potential of antioxidant L ascorbic acid, on nanotalc and microtalc challenged A_{549} cells. Results show that 1.5 mM L ascorbic acid effectively, but not completely, inhibited MDA level induced by talc nanoparticles. Determining the optimum concentration of ascorbic acid that might completely suppress LPO without causing any side effect is a matter of concern (Halliwell, 1999) and the evaluation of interrelationship between LPO and chelating effect of iron present on the surface of talc particles by deferoxamine mesylate on LPO is under investigation. Oxidative stress is known to elicit varying effects on the activity of antioxidant enzymes. The three primary scavenger enzymes involved in detoxifying ROS in mammalian systems are catalase, superoxide dismutase and glutathione peroxidase (MatÉs et al., 1999). For example the activity of GPx can provide important clue about the consumption rate of GSH in enzymatic detoxification of ROS. The activity of antioxidant enzymes can therefore provide further insight in understanding the mechanism of toxicity caused by talc particles and is currently under investigation.

5. Conclusion

We have presented a preliminary data on the toxicity response elicited by the two types of talc nanoparticles, depending on their different geological origin. Since, talc with a multitude of physical and functional characteristics due to different geological context and deposits, is used for particular applications, so occupational and consumer exposures to talc and its toxic effects are likely to vary accordingly, which is obvious in this study. The cytotoxicity seems to be due to primarily through induction of LPO, as a potential mechanism of toxicity discussed above. Addition of 1.5 mM of L ascorbic acid, a ROS scavenger, significantly, though not completely, reduced LPO. Data clearly suggest that exposure of talc, particularly nanopowder, should be protected in humans at risk of occupational as well as domestic exposure.

Acknowledgments

One of the authors (MJA) gratefully acknowledges the financial support provided by University Grants Commission (UGC), Govt. of India and CSIR networked project (NWP 17). The authors thank Dr. Alok Dhawan (*In Vitro* Toxicology Division, IITR, Lucknow, India) for providing DLS measurements. The IITR Communication no. of this article is 2782.

References

Aguirre, R., May, J.M., 2008. Inflammation in the vascular bed: importance of vitamin C. Pharmacology and Therapeutics 119, 96–103.

Anderson, M.T., Staal, F.J., Gitler, C., Herzenberg, L.A., 1994. Separation of oxidant-initiated and redox-regulated steps in the NF-κB signal transduction pathway. Proceedings of the National Academy of Sciences USA 91, 11527–11531.

Asard, H., 2008. Ascorbate. In: Banerjee, R. (Ed.), Redox Biochemistry. A John Wiley and Sons Inc., Hoboken, pp. 22–27.

Bakand, S., Winder, C., Khalil, C., Hayes, A., 2006. A novel in vitro exposure technique for toxicity testing of selected volatile organic compounds. Journal of Environmental Monitoring 8, 100–105.

Beck-Speier, I., Dayal, N., Karg, E., Maier, K.L., Roth, C., Ziesenis, A., Heyder, J., 2001. Agglomerates of ultrafine particles of elemental carbon and TiO_2 induce generation of lipid mediators in alveolar macrophages. Environmental Health Perspective 109, 613–618.

Bogdanovic, G., Kojic, V., Dordevic, A., Canadanovic-Brunet, J., Vojinovic-Miloradov, M., Baltic, V.V., 2004. Modulating activity of fullerol C-60 $(OH)_{(22)}$ on doxorubicin-induced cytotoxicity. Toxicology in Vitro 18, 629–637.

Borm, P.J., Robbins, D., Haubold, S., Kuhlbusch, T., Fissan, H., Donaldson, K., Schins, R., Stone, V., Kreyling, W., Lademann, J., 2006. The potential risks of nanomaterials: a review carried out for ECETOC. Particle and Fibre Toxicology 3, 11.

Bowry, V.W., Ingold, K.U., Stocker, R., 1992. Vitamin-E in human low density-lipoprotein—when and how this antioxidant becomes a prooxidant. Biochemical Journal 4, 288–341.

Bradford, M.M., 1976. A rapid and sensitive method for the quantitation of microgram quantities of protein utilizing the principle of protein-dye binding. Analytical Biochemistry 72, 248–254.

Brown, D.M., Wilson, M.R., MacNee, W., Stone, V., Donaldson, K., 2001. Size-dependent proinflammatory effects of ultrafine polystyrene particles: a role for surface area and oxidative stress in the enhanced activity of ultrafines. Toxicology and Applied Pharmacology 175, 191–199.

Burton, G.W., Ingold, K.U., 1981. Autoxidation of biological molecules. 1. The antioxidant activity of vitamin-E and related chain-breaking phenolic antioxidants in vitro. Journal of the American Chemical Society 103, 6472–6477.

Buz'Zard, A.R., Lau, B.H., 2007. Pycnogenol reduces talc-induced neoplastic transformation in human ovarian cell cultures. Phytotherapy Research 21, 579–586.

Cassel, S.L., Eisenbarth, S.C., Iyer, S.S., Sadler, J.J., Colegio, O.R., Tephly, L.A., Carter, A.B., Rothman, P.B., Flavell, R.A., Sutterwala, F.S., 2008. The Nalp3 inflammasome is essential for the development of silicosis. Proceedings of the National Academy of Sciences USA 105, 9035–9040.

Chang, S., Risch, H.A., 1997. Perineal talc exposure and risk of ovarian carcinoma. Cancer 79, 2396–2401.

Chen, J.J., Yu, B.P., 1994. Alteration in mitochondrial membrane fluidity by lipid peroxidation products. Free Radical Biology and Medicine 17, 411–418.

Churg, A., 1996. The uptake of mineral particles by pulmonary epithelial cells. American Journal of Respiratory and Critical Care Medicine 154, 1124–1140.

Cook, L.S., Kamb, M.L., Weiss, N.S., 1997. Perineal powder exposure and the risk of ovarian cancer. American Journal of Epidemiology 145, 459–465.

Cramer, D.W., Liberman, R.E., Titus-Ernstoff, L., Welch, W.R., Greenberg, E.R., Baron, J.A., Harlow, B.L., 1999. Genital talc exposure and risk of ovarian cancer. International Journal of Cancer 81, 351–356.

Croute, F., Gaubin, Y., Prevost, M.C., Beaupain, R., Pianezzi, B., Soleihavoup, J.P., 1990. Effects of hypergravity on lung carcinoma cells maintained in continuous organotypic culture. Aviation, Space, and Environmental Medicine, 1002–1006.

Donaldson, K., Li, X.Y., MacNee, W., 1998. Ultrafine (nanometre) particle mediated lung injury. Journal of Aerosol Science 29, 553–560.

Donaldson, K., Brown, D., Clouter, A., Duffin, R., MacNee, W., Renwick, L., Tran, L., Stone, V., 2002. The pulmonary toxicology of ultrafine particles. Journal of Aerosol Medicine 15, 213–220.

Dostert, C., Pétrilli, V., Bruggen, R.V., Steele, C., Mossman, B.T., Tschopp, J., 2008. Innate immune activation through Nalp3 inflammasome sensing of asbestos and silica. Science 320, 674–677.

Dugan, L.L., Lovett, E.G., Quick, K.L., Lotharius, J., Lin, T.T., O'Malley, K.L., 2001. Fullerene-based antioxidants and neurodegenerative disorders. Parkinsonism and Related Disorders 7, 243–246.

Dugan, L.L., Turetsky, D.M., Du, C., Lobner, D., Wheeler, M., Almli, C.R., Clifton, K.F., Shen, C.K.F., Luh, T.Y., Choi, D.W., Lin, T.S., 1997. Carboxyfullerenes as neuroprotective agents. Proceedings of the National Academy of Sciences USA 94, 9434–9439.

Forman, H.J., Liu, R., Tian, L., 1997. Glutathione cycling in oxidative stress. In: Clerch, L.B., Massaro, D.J. (Eds.), Oxygen, Gene Expression, and Cellular Function: Lung Biology in Health and Disease, vol. 105. Marcel Dekker, New York, pp. 99–112.

Frei, B., England, L., Ames, B.N., 1989. Ascorbate is an outstanding antioxidant in human blood plasma. Proceedings of the National Academy of Sciences USA 86, 6377–6381.

Frei, B., Stocker, R., England, L., Ames, B.N., 1990. Ascorbate: the most effective antioxidant in human blood plasma. Advances in Experimental Medicine and Biology 264, 155–163.

Gates, M.A., Tworoger, S.S., Terry, K.L., Titus-Ernstoff, L., Rosner, B., Vivo, I.D., Cramer, D.W., Hankinson, S.E., 2008. Talc use, variants of the *GSTM1*, *GSTT1*, and *NAT2* genes, and risk of epithelial ovarian cancer. Cancer Epidemiology, Biomarkers and Prevention 17, 2436–2444.

Gilmour, P., Brown, D.M., Beswick, P.H., Benton, E., MacNee, W., Donaldson, K., 1997. Surface free radical activity of PM10 and ultrafine titanium dioxide: A unifying factor in their toxicity? The Annals of Occupational Hygiene 41 (Suppl. 1), 32–38.

Green, D.G., Reed, J.C., 1998. Mitochondria and apoptosis. Science 281, 1309–1312.

Halliwell, B., Gutteridge, J.M., 1990. Role of free radicals and catalytic metal ions in human disease: an overview. Methods in Enzymology 186, 1–85.

Halliwell, B., 1996. Vitamin C: antioxidant or pro-oxidant in vivo? Free Radical Research 25, 439–454.

Halliwell, B., 1999. Establishing the significance and optimal intake of dietary antioxidants: the biomarker concept. Nutrition Reviews 57, 104–113.

Halliwell, B., Gutteridge, J.M., Cross, C.E., 1992. Free radicals, antioxidants, and human disease: where are we now? The Journal of Laboratory and Clinical Medicine 119, 598–620.

Hansen, K., Mossman, B.T., 1987. Generation of superoxide (O^2) from alveolar macrophages exposed to asbestiform and non-asbestiform particles. Cancer Research 47, 1681–1686.

Hansen, M.B., Nielsen, S.E., Berg, K., 1989. Re-examination and further development of a precise and rapid dye method for measuring cell growth/kill. Journal of Immunological Methods 119, 203–210.

Harlow, B.L., Cramer, D.W., Bell, D.A., Welch, W.R., 1992. Perineal exposure to talc and ovarian cancer risk. Obstetrics and Gynecology 80, 19–26.

Harlow, B.L., Hartge, P.A., 1995. A review of perineal talc exposure and risk of ovarian cancer. Regulatory Toxicology and Pharmacology 21, 254–260.

Heller, D.S., Westhoff, C., Gordon, R.E., Katz, N., 1996. The relationship between perineal cosmetic talc usage and ovarian talc particle burden. American Journal of Obstetrics and Gynecology 174, 1507–1510.

Henderson, W.J., Joslin, C.A., Turnbull, A.C., Griffiths, K., 1971. Talc and carcinoma of the ovary and cervix. The Journal of Obstetrics and Gynaecology of the British Commonwealth 78, 266–272.

Hensley, K., Floyd, R.A., 2002. Reactive oxygen species and protein oxidation in aging: a look back, a look ahead. Archives of Biochemistry and Biophysics 397, 377–383.

Hissin, P.J., Hilf, R., 1976. A fluorometric method for determination of oxidized and reduced glutathione in tissues. Analytical Biochemistry 74, 214–226.

Hollinger, M.A., 1990. Pulmonary toxicity of inhaled and intravenous talc. Toxicology Letters 52, 121–127.

Holsapple, M.P., Farland, W.H., Landry, T.D., Monteiro-Riviere, N.A., Carter, J.M., Walker, N.J., Thomas, K.V., 2005. Research strategies for safety evaluation of nanomaterials, part II: toxicological and safety evaluation of nanomaterials, current challenges and data needs. Toxicological Sciences 88, 12–17.

Huang, M., Khor, E., Lim, L.Y., 2004. Uptake and cytotoxicity of chitosan molecules and nanoparticles: effects of molecular weight and degree of deacetylation. Pharmaceutical Research 21, 344–353.

Isakovic, A., Markovic, Z., Todorovic-Markovic, B., Nikolic, N., Vranjes-Djuric, S., Mirkovic, M., Dramicanin, M., Harhaji, L., Raicevic, N., Nikolic, Z., Trajkovic, V., 2006. Distinct cytotoxic mechanisms of pristine versus hydroxylated fullerene. Toxicological Sciences 91, 173–183.

Kipen, H.M., Laskin, D.L., 2005. Smaller is not always better: nanotechnology yields nanotoxicology. American Journal of Physiology-Lung Cellular and Molecular Physiology 289, L696–L697.

Krug, H.F., Culig, H., 1991. Directed shift of fatty-acids from phospholipids to triacylglycerols in HL-60 cells induced by nanomolar concentrations of triethyl lead chloride – involvement of a pertussis toxin-sensitive pathway. Molecular Pharmacology 39, 511–516.

Levine, M.A., Daruwala, R.C., Park, J.B., Rumsey, S.C., Wang, Y., 1998. Does vitamin C have a pro-oxidant effect? Nature (London) 395, 231.

Lieber, M., Smith, B., Szakal, A., Nelson-Rees, W., Todoro, G., 1976. A continuous tumor cell line from a human lung carcinoma with properties of type II alveolar epithelial cells. International Journal of Cancer 17, 62–70.

Lin, W., Huang, Y.W., Zhou, X.D., Ma, Y., 2006. In vitro toxicity of silica nanoparticles in human lung cancer cells. Toxicology and Applied Pharmacology 217, 252–259.

Marnett, L.J., 2000. Oxyradicals and DNA damage. Carcinogenesis 21, 361–370.

Martensson, J., Jain, A., Frayer, W., Meister, A., 1989. Glutathione metabolism in the lung: inhibition of its synthesis leads to lamellar body and mitochondrial defects. Proceedings of the National Academy of Sciences USA 86, 5296–5300.

MatÉs, J.M., Pérez-Gómez, C., DeCastro, I.N., 1999. Antioxidant enzymes and human diseases. Clinical Biochemistry 32, 595–603.

May, J.M., Qu, Z.-C., Mendiratta, S., 1998. Protection and recycling of α-tocopherol in human erythrocytes by intracellular ascorbic acid. Archives of Biochemistry and Biophysics 349, 281–289.

Meister, A., 1989. Molecular properties and clinical applications. In: Glutathione Centennial. Academic Press, New York.

Meister, A., 1995. Mitochondrial changes associated with glutathione deficiency. Biochemica et Biophysica Acta 1271, 35–42.

Meyer, M., Schreck, R., Baeuerle, P.A., 1993. H_2O_2 and antioxidants have opposite effects on activation of NF-κB and AP-1 in intact cells: AP-1 as secondary antioxidant-responsive factor. The EMBO Journal 12, 2005–2015.

Mills, P.K., Riordan, D.G., Cress, R.D., Young, H.A., 2004. Perineal talc exposure and epithelial ovarian cancer risk in the Central Valley of California. International Journal of Cancer 112, 458–464.

Mossman, T., 1983. Rapid colorimetric assay for cellular growth and survival: application to proliferation and cytotoxicity assays. Journal of Immunological Methods 65, 55–63.

Mossman, B.T., Kamp, D.W., Weitzman, S.A., 1996. Mechanisms of carcinogenesis and clinical features of asbestos-associated cancers. Cancer Investigation 14, 466–480.

National Toxicology Program, 1993. NTP Toxicology and Carcinogenesis Studies of Talc (Non-asbestiform) in Rats and Mice (Inhalation Studies), vol. 421, pp. 1–287.

Nel, A., Xia, T., Madler, L., Li, N., 2006. Toxic potential of materials at the nanolevel. Science 311, 622–627.

Oberdorster, G., Ferin, J., Gelein, R., Soderholm, S., Finkelstein, J., 1992. Role of alveolar macrophage in lung injury: studies with ultrafine particles. Environmental Health Perspective 97, 193–199.

Oberdorster, G., Gelein, R., Ferin, J., Weiss, B., 1995. Association of particulate air pollution and acute mortality: involvement of ultrafine particles? Inhalation Toxicology 7, 111–124.

Oberdorster, G., 1996. Significance of particle parameters in the evaluation of exposure–dose–response relationships of inhaled particles. Inhalation Toxicology 8, 73–89.

Oberdorster, G., 2000. Toxicology of ultrafine particles: in vivo studies. Philosophical Transactions of the Royal Society 358, 2719–2740.

Oberdorster, E., 2004. Manufactured nanomaterials (fullerenes, C-60) induce oxidative stress in the brain of juvenile largemouth bass. Environmental Health Perspective 112, 1058–1062.

Oberdorster, G., Oberdorster, E., Oberdorster, J., 2005. Nanotoxicology: an emerging discipline evolving from studies of ultrafine particles. Environmental Health Perspective 113, 823–839.

Ohkawa, H., Ohisi, N., Yagi, Y., 1979. Assay for lipid peroxides in animal tissues by thiobarbituric acid reaction. Analytical Biochemistry 95, 351–358.

Packer, J.E., Slater, T.F., Willson, R.L., 1979. Direct observation of a free radical interaction between vitamin E and vitamin C. Nature (London) 278, 737–738.

Poulsen, H.E., Weimann, A., Salonen, J.T., Nyyssonen, K., Loft, S., Cadet, J., Douki, T., Ravanat, J., 1998. Does vitamin C have a pro-oxidant effect? Nature (London) 395, 231–232.

Sayes, C.M., Gobin, A.M., Ausman, K.D., Mendez, J., West, J.L., Colvin, V.L., 2005. Nano-C (60) cytotoxicity is due to lipid peroxidation. Biomaterials 26, 7587–7595.

Sayes, C.M., Wahi, R., Kurian, P.A., Liu, Y., West, J.L., Ausman, K.D., Warheit, D.B., Colvin, V.L., 2006. Correlating nanoscale titania structure with toxicity: a cytotoxicity and inflammatory response study with human dermal fibroblasts and human lung epithelial cells. Toxicological Sciences 92, 174–185.

Scarfì, S., Magnone, M., Ferraris, C., Pozzolini, M., Benvenuto, F., Benatti, U., Giovine, M., 2009. Ascorbic acid pre-treated quartz stimulates TNF-α release in RAW 264.7 murine macrophages through ROS production and membrane lipid peroxidation. Respiratory Research 10, 25.

Vallyathan, V., Mega, J.F., Shi, X., Dalal, N.S., 1992. Enhanced generation of free radicals from phagocytes induced by mineral dusts. American Journal of Respiratory Cell and Molecular Biology 6, 404–413.

Wang, H., Joseph, J.A., 1999. Quantifying cellular oxidative stress by dichlorofluorescin assay using microplate reader. Free Radical Biology and Medicine 27, 612–616.

Welder, A.A., Grant, R., Bradlaw, J., Acosta, D., 1991. A primary culture system of adult rat heart cells for the study of toxicologic agent. In Vitro Cellular and Developmental Biology 27A, 921–926.

Wild, P., 2006. Lung cancer risk and talc not containing asbestiform fibres: a review of the epidemiological evidence. Occupational and Environmental Medicine 63, 4–9.

Werebe, E.C., Pazetti, R., 1999. Systemic distribution of talc after intrapleural administration in rats. Chest 115, 190–193.

Wroblewski, F., LaDue, J.S., 1955. Lactate dehydrogenase activity in blood. Proceedings of the Society for Experimental Biology and Medicine 90, 210–213.

Exhibit 103

Original Article

Reproductive Sciences
1-10

DOI: 10.1177/1933719119831773
journals.sagepub.com/home/rsx
SAGE

Molecular Basis Supporting the Association of Talcum Powder Use With Increased Risk of Ovarian Cancer

Nicole M. Fletcher, PhD[1], Amy K. Harper, MD[2], Ira Memaj, BS[1], Rong Fan, MS[1], Robert T. Morris, MD[2], and Ghassan M. Saed, PhD[1,2]

Abstract

Genital use of talcum powder and its associated risk of ovarian cancer is an important controversial topic. Epithelial ovarian cancer (EOC) cells are known to manifest a persistent prooxidant state. Here we demonstrated that talc induces significant changes in key redox enzymes and enhances the prooxidant state in normal and EOC cells. Using real-time reverse transcription polymerase chain reaction and enzyme-linked immunosorbent assay, levels of CA-125, caspase-3, nitrate/nitrite, and selected key redox enzymes, including myeloperoxidase (MPO), inducible nitric oxide synthase (iNOS), superoxide dismutase (SOD), catalase (CAT), glutathione peroxidase (GPX), and glutathione reductase (GSR), were determined. TaqMan genotype analysis utilizing the QuantStudio 12K Flex was used to assess single-nucleotide polymorphisms in genes corresponding to target enzymes. Cell proliferation was determined by MTT proliferation assay. In all talc-treated cells, there was a significant dose-dependent increase in prooxidant iNOS, nitrate/nitrite, and MPO with a concomitant decrease in antioxidants CAT, SOD, GSR, and GPX ($P < .05$). Remarkably, talc exposure induced specific point mutations that are known to alter the activity in some of these key enzymes. Talc exposure also resulted in a significant increase in inflammation as determined by increased tumor marker CA-125 ($P < .05$). More importantly, talc exposure significantly induced cell proliferation and decreased apoptosis in cancer cells and to a greater degree in normal cells ($P < .05$). These findings are the first to confirm the cellular effect of talc and provide a molecular mechanism to previous reports linking genital use to increased ovarian cancer risk.

Keywords

talc, epithelial ovarian cancer, oxidative stress, single-nucleotide polymorphism, cell proliferation

Introduction

Ovarian cancer is the most lethal gynecologic malignancy and ranks fifth in cancer deaths among women diagnosed with cancer.[1] Epithelial ovarian cancer (EOC) has long been considered a heterogeneous disease with respect to histopathology, molecular biology, and clinical outcome.[1,2] Although surgical techniques and treatments have advanced over the years, the prognosis of EOC remains poor, with a 5-year survival rate of 50% in advanced stage.[2] This is largely due to the lack of early warning symptoms and screening methods and the development of chemoresistance.[1,2] Moreover, ovarian cancer is known to be associated with germline mutations in the *BRCA1* or *BRCA2* genes, but with a rate of only 20 % to 40%, suggesting the presence of other unknown mutations in other predisposition genes.[3] Additional genetic variations including single-nucleotide polymorphisms (SNPs) have been hypothesized to act as low to moderate penetrant alleles that contribute to ovarian cancer risk.[3,4]

The pathophysiology of EOC is not fully understood but has been strongly associated with inflammation and the resultant oxidative stress.[5] We have previously characterized EOC cells to manifest a persistent prooxidant state as evident by the upregulation of key oxidants and downregulation of key antioxidants, which is further enhanced in chemoresistant EOC cells.[6] The expression of key prooxidant/inflammatory enzymes such as inducible nitric oxide synthase (iNOS), nicotinamide adenine dinucleotide phosphate (NAD(P)H) oxidase, and myeloperoxidase (MPO), as well as an increase in nitric oxide (NO) levels, was increased in EOC tissues and cells.[6] Additionally, we have shown that EOC cells manifest lower apoptosis, which

[1] Department of Obstetrics and Gynecology, Wayne State University School of Medicine, Detroit, MI, USA
[2] Department of Gynecologic Oncology, Karmanos Cancer Institute, Detroit, MI, USA

Corresponding Author:
Ghassan M. Saed, Departments of Obstetrics and Gynecology and Oncology, Karmanos Cancer Institute, Wayne State University School of Medicine, Detroit, MI 48201, USA.
Email: gsaed@med.wayne.edu

was markedly induced by inhibiting iNOS, indicating a strong link between apoptosis and NO/iNOS pathways in these cells.[6]

The cellular redox balance is maintained by key antioxidants including catalase (CAT), superoxide dismutase (SOD), or by glutathione peroxidase (GPX) coupled with glutathione reductase (GSR).[5] Other important scavengers include thioredoxin coupled with thioredoxin reductase, and glutaredoxin, which utilizes glutathione (GSH) as a substrate.[7] We have previously reported that a genotype switch in key antioxidants is a potential mechanism leading to the acquisition of chemoresistance in EOC cells.[7] We have studied the effects of genetic polymorphisms in key redox genes on the acquisition of the oncogenic phenotype in EOC cells, including genes that control the levels of cellular reactive oxygen species and oxidative damage and SNPs for genes involved in carcinogen metabolism (detoxification and/or activation), antioxidants, and DNA repair pathways.[4,6] Several function-altering SNPs have been identified in key antioxidants, including CAT, GPX, GSR, and SOD.[4]

Several studies have suggested the possible association between genital use of talcum powder and risk of EOC.[7-12] Association between the use of cosmetic talc in genital hygiene and ovarian cancer was first described in 1982 by Cramer et al, and many subsequent studies supported this finding.[7-12] Talc and asbestos are both silicate minerals; the carcinogenic effects of asbestos have been extensively studied and documented in the medical literature.[7-12] Asbestos fibers in the lung initiate an inflammatory and scarring process, and it has been proposed that ground talc, as a foreign body, might initiate a similar inflammatory response.[7] The objective of this study was to determine the effects of talcum powder on the expression of key redox enzymes, CA-125 levels, and cell proliferation and apoptosis in normal and EOC cells.

Material and Methods

Cell Lines

Ovarian cancer cells SKOV-3 (ATCC), A2780 (Sigma Aldrich, St Louis, Missouri), and TOV112D (a kind gift from Gen Sheng Wu at Wayne State University, Detroit, Michigan) and normal cells human macrophages (EL-1; ATCC, Manassas, Virginia), human primary normal ovarian epithelial cells (Cell Biologics, Chicago, Illinois), human ovarian epithelial cells (HOSEpiC; ScienCell Research Laboratories, Inc, Carlsbad, California), and immortalized human fallopian tube secretory epithelial cells (FT33; Applied Biological Materials, Richmond, British Columbia, Canada) were used. All cells were grown in media and conditions following manufacturer's protocol. EL-1 cells were grown in IMDM media (ATCC) supplemented with 0.1 mM hypoxanthine and 0.1 mM thymidine solution (H-T, ATCC) and 0.05 mM β-mercaptoethanol. SKOV-3 EOC cells were grown in HyClone McCoy's 5A medium (Fisher Scientific, Waltham, Massachusetts), A2780 EOC cells were grown in HyClone RPMI-1640 (Fisher Scientific), and both TOV112D EOC cells were grown in MCDB105 (Cell Applications, San Diego, California) and Medium 199 (Fisher Scientific; 1:1). All media were supplemented with fetal bovine serum (Innovative Research, Novi, Michigan) and penicillin/streptomycin (Fisher Scientific), per their manufacturer specifications. Human primary normal ovarian epithelial cells were grown in complete human epithelial cell medium (Cell Biologics).

Treatment of Cells

Talcum baby powder (Johnson & Johnson, New Brunswick, NJ, #30027477, Lot#13717RA) was dissolved in dimethyl sulfoxide (DMSO; Sigma Aldrich) at a concentration of 500 mg in 10 mL and was filtered with a 0.2 µm syringe filter (Corning). Sterile DMSO was used as a control for all treatments. Cells were seeded in 100-mm cell culture dishes (3×10^6) and were treated 24 hours later with 5, 20, or 100 µg/mL of talc for 72 hours. Cell pellets were collected for RNA, DNA, and protein extraction. Cell culture media were collected for CA-125 analysis by enzyme-linked immunosorbent assay (ELISA).

Real-Time Reverse Transcription Polymerase Chain Reaction

Total RNA was extracted from all cells using the RNeasy mini kit (Qiagen, Valencia, California). Measurement of the amount of RNA in each sample was performed using a Nanodrop spectrophotometer (Thermo Fisher Scientific, Waltham, Massachusetts). A 20 µL complementary DNA reaction volume containing 0.5 µg RNA was prepared using the SuperScript VILO Master Mix Kit (Life Technologies, Carlsbad, California). Optimal oligonucleotide primer pairs were selected for each target using Beacon designer (Premier Biosoft, Inc; Table 1). Quantitative reverse transcription polymerase chain reaction (RT-PCR) was performed using the EXPRESS SYBR GreenER qPCR supermix kit (Life Technologies) and the Cepheid 1.2f detection system (Sunnyvale, CA) previously described.[6] Standards with known concentrations and lengths were designed specifically for β-*actin* (79 bp), *CAT* (105 bp), *NOS2* (89 bp), *GSR* (103 bp), *GPX1* (100 bp), *MPO* (79 bp), and *SOD3* (84 bp), allowing for construction of a standard curve using a 10-fold dilution series.[6] All samples were normalized to β-*actin*. A final melting curve analysis was performed to demonstrate specificity of the PCR product.

Protein Detection

Cell pellets were lysed utilizing cell lysis buffer (20 mM Tris–HCl [pH 7.5], 150 mM NaCl, 1 mM Na_2EDTA, 1 mM EGTA, 1% Triton, 2.5 sodium pyrophosphate, 1 mM β-glycerophosphate, 1 mM Na_3VO_4, 1 µg/mL leupeptin) containing a cocktail of protease inhibitors. Samples were centrifuged at 13 000 rpm for 10 minutes at 4°C. Total protein concentration of cell lysates from control and talc-treated cells was measured with the Pierce BCA protein assay kit (Thermo Scientific, Rockford, Illinois).

Table 1. Real-Time RT-PCR Oligionucleotide Primers.

Accession Number	Gene	Sense (5′-3′)	Antisense (3′-5′)	Amplicon (bp)	Annealing Time (seconds) and Temperature (°C)
NM_001101	β-*actin*	ATGACTTAGTTGCGTTACAC	AATAAAGCCATGCCAATCTC	79	10, 64
NM_001752	*CAT*	GGTTGAACAGATAGCCTTC	CGGTGAGTGTCAGGATAG	105	10, 63
NM_003102	*SOD3*	GTGTTCCTGCCTGCTCCT	TCCGCCGAGTCAGAGTTG	84	60, 64
NM_000637	*GSR*	TCACCAAGTCCCATATAGAAATC	TGTGGCGATCAGGATGTG	116	10, 63
NM_000581	*GPX1*	GGACTACACCCAGATGAAC	GAGCCCTTGCGAGGTGTAG	91	10, 66
NM_000625	*NOS2*	GAGGACCACATCTACCAAGGAGGAG	CCAGGCAGGCGGAATAGG	89	30, 59
NM_000250	*MPO*	CACTTGTATCCTCTGGTTCTTCAT	TCTATATGCTTCTCACGCCTAGTA	79	60, 63

Abbreviation: RT-PCR, reverse transcription polymerase chain reaction.

Detection of Protein/Activity by ELISA

The following ELISA kits were used (Cayman Chemical, Ann Arbor, Michigan): CAT, SOD, GSR, GPX, and MPO. Nitrite (NO_2^-)/nitrate (NO_3^-) were determined spectrophotometrically by Griess assay as previously reported.[6] CA-125 protein levels were measured in cell media by ELISA (Ray Biotech, Norcross, Georgia).

TaqMan SNP Genotyping Assay

DNA was isolated utilizing the EZ1 DNA tissue kit (Qiagen) for EOC cells. The TaqMan SNP genotyping assay set (Applied Biosystems, Carlsbad, California; NCBI dbSNP genome build 37, MAF source 1000 genomes) was used to genotype the SNPs (Table 1). The Applied Genomics Technology Center (AGTC, Wayne State University) performed these assays. Analysis was done utilizing the QuantStudio 12 K Flex real-time PCR system (Applied Biosystems).

Cell Proliferation and Apoptosis

Cell proliferation was assessed with the TACS MTT cell proliferation assay (Trevigen, Gaithersburg, Maryland) after treatment with talc (100 µg/mL) for 24 hours. The Caspase-3 Colorimetric Activity Assay Kit (Chemicon, Temecula, California) was used to determine levels of caspase-3 activity after treatment of normal and EOC cells with various doses of talc as previously described.[6] Equal concentrations of cell lysate were used. The assay is based on spectrophotometric detection of the chromophore p-nitroaniline (pNA) after cleavage from the labeled substrate DEVD-pNA. The free pNA can be quantified using a spectrophotometer or a microtiter plate reader at 405 nm. Comparison of the absorbance of pNA from an apoptotic sample with its control allows determination of the percentage increase in caspase-3 activity.

Statistical Analysis

Normality was examined using the Kolmogorov-Smirnov test and by visual inspection of quantile–quantile plots. Because most of the data were not normally distributed, differences in distributions were examined using the Kruskal-Wallis test. Generalized linear models were fit to examine pairwise differences in estimated least squares mean expression values by exposure to 0, 5, 20, or 100 µg/mL of talc. We used the Tukey-Kramer adjustment for multiple comparisons, and the regression models were fit using log2 transformed analyte expression values after adding a numeric constant "1" to meet model assumptions while avoiding negative transformed values. P values below .05 are statistically significant.

Results

Talc Treatment Decreased the Expression of Antioxidant Enzymes SOD and CAT in Normal and EOC Cells

Real-time RT-PCR and ELISA assays were utilized to determine the CAT and SOD messenger RNA (mRNA) and protein levels in cells before and after 72 hours talc treatment, respectively (Figure 1). The CAT (Figure 1A and C) and SOD (Figure 1B and D) mRNA and protein levels were significantly decreased in a dose-dependent manner in talc-treated cells compared to controls ($P < .05$).

Talc Treatment Increased the Expression of Prooxidants iNOS, NO_2^-/NO_3^-, and MPO in Normal and EOC Cells

Real-time RT-PCR and NO_2^-/NO_3^- assays were utilized to determine the iNOS mRNA and NO levels in cells before and after 72 hours talc treatment, respectively (Figure 2). The iNOS mRNA and NO levels were significantly increased in a dose-dependent manner in talc-treated cells as compared to their controls (Figure 2A and C, $P < .05$). As expected, there was no detectable MPO in normal ovarian and fallopian tube cells, and thus, talc treatment did not have any effect. However, MPO mRNA and protein levels were significantly increased in a dose-dependent manner in talc-treated ovarian cancer cells and macrophages compared to controls (Figure 2B and D, $P < .05$).

Talc Treatment Decreased the Expression of Antioxidant Enzymes, GPX and GSR, in Normal and EOC Cells

Real-time RT-PCR and ELISA assays were utilized to determine the GPX and GSR mRNA and protein levels in cells before and

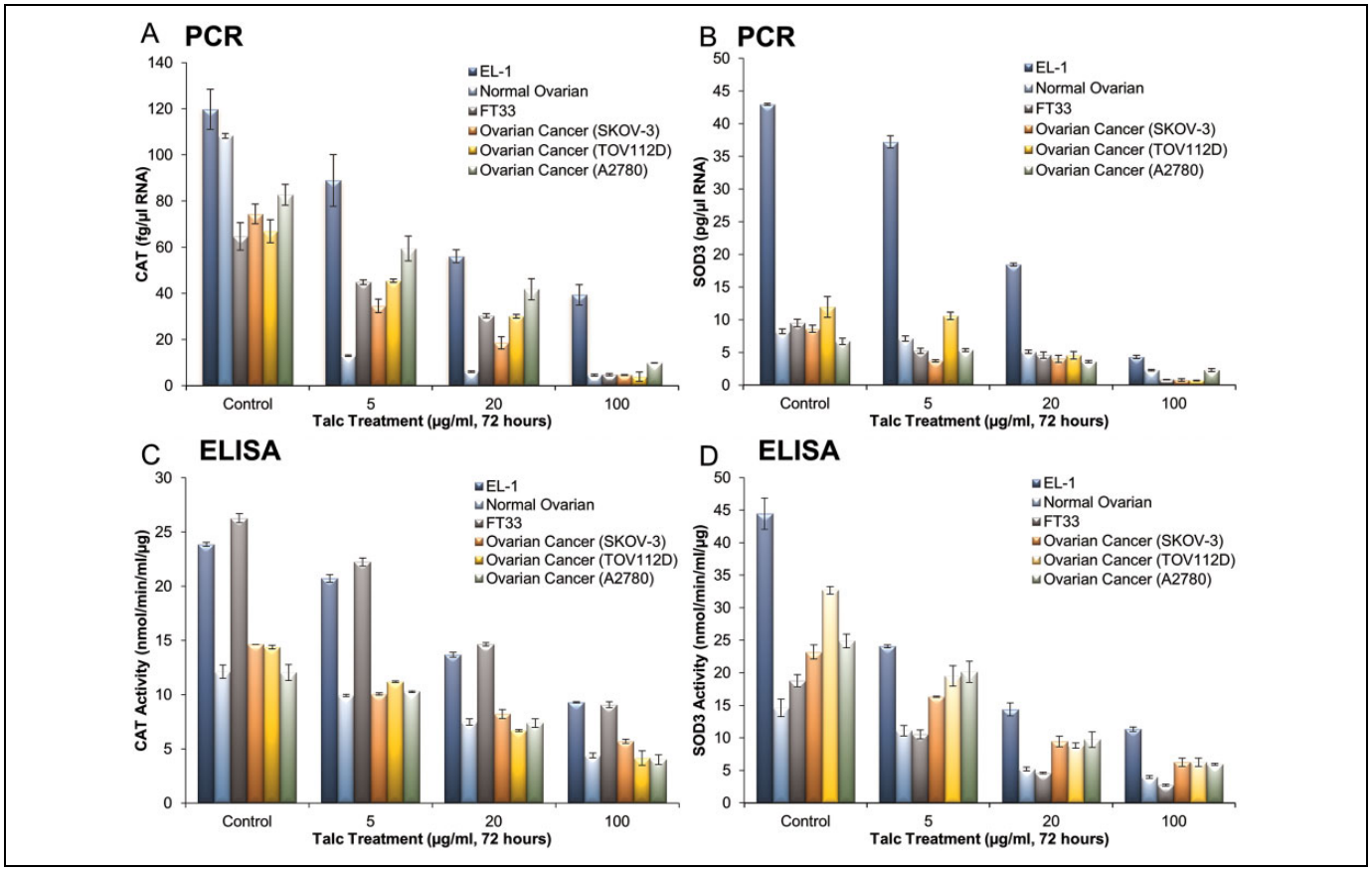

Figure 1. Decreased expression and activity of key antioxidant enzymes, CAT and SOD3. The mRNA (real-time RT-PCR) and protein/activity levels (ELISA) of CAT (A and C) and SOD3 (B and D) were determined in macrophages (EL-1), human primary ovarian epithelial cells (normal ovarian), fallopian tube (FT33), and ovarian cancer (SKOV-3, TOV112D, and A2780) cell lines before and after treatment with various doses of talc over 72 hours. Experiments were performed in triplicate. Expression is depicted as the mean, with error bars representing standard deviation. All changes in response to talc treatment were significant ($P < .05$) in all cells and in all doses as compared to controls. CAT indicates catalase; SOD3, superoxide dismutase 3; mRNA, messenger RNA; RT-PCR, reverse transcription polymerase chain reaction; ELISA, enzyme-linked immunosorbent assay.

after 72 hours of talc treatment, respectively (Figure 3). The GPX (Figure 3A and C) and GSR (Figure 3B and D) mRNA and protein levels were significantly decreased in a dose-dependent manner in talc-treated cells compared to controls ($P < .05$).

Talc Exposure Induced Known Genotype Switches in Key Oxidant and Antioxidant Enzymes

Talc treatment was associated with a genotype switch in *NOS2* from the common C/C genotype in untreated cells to T/T, the SNP genotype, in talc-treated cells, except in A2780 and TOV112D (Table 2). Additionally, the observed decrease in CAT expression and activity was associated with a genotype switch from common C/C genotype in CAT in untreated cells to C/T, the SNP genotype, in TOV112D and all normal talc-treated cells. However, there was no detectable genotype switch in CAT in A2780, SKOV3, and TOV112D (Table 2). Remarkably, there was no observed genotype switch in the selected SNP for SOD3 and GSR in all talc-treated cells. All cells, except for HOSEpiC cells, manifest the SNP genotype of *GPX1* (C/T). Intriguingly, talc treatment reversed this SNP genotype to the normal genotype (Table 2).

Talc Treatment Increased CA-125 Levels in Normal and EOC Cells

CA-125 ELISA assay was performed in protein isolated from cell media before and after talc treatment. CA-125 levels were significantly increased in a dose-dependent manner in all cells (Figure 4, $P < .05$). There was no detectable CA-125 protein in macrophages.

Talc Treatment Increased Cell Proliferation and Decreased Apoptosis

MTT cell proliferation assay was used to determine cell viability, and caspase-3 activity assay was utilized to determine apoptosis of all cell lines after 24 hours of talc treatment (Figure 5). Cell proliferation was significantly increased from the baseline in all talc-treated cells ($P < .05$), but to a greater degree in normal

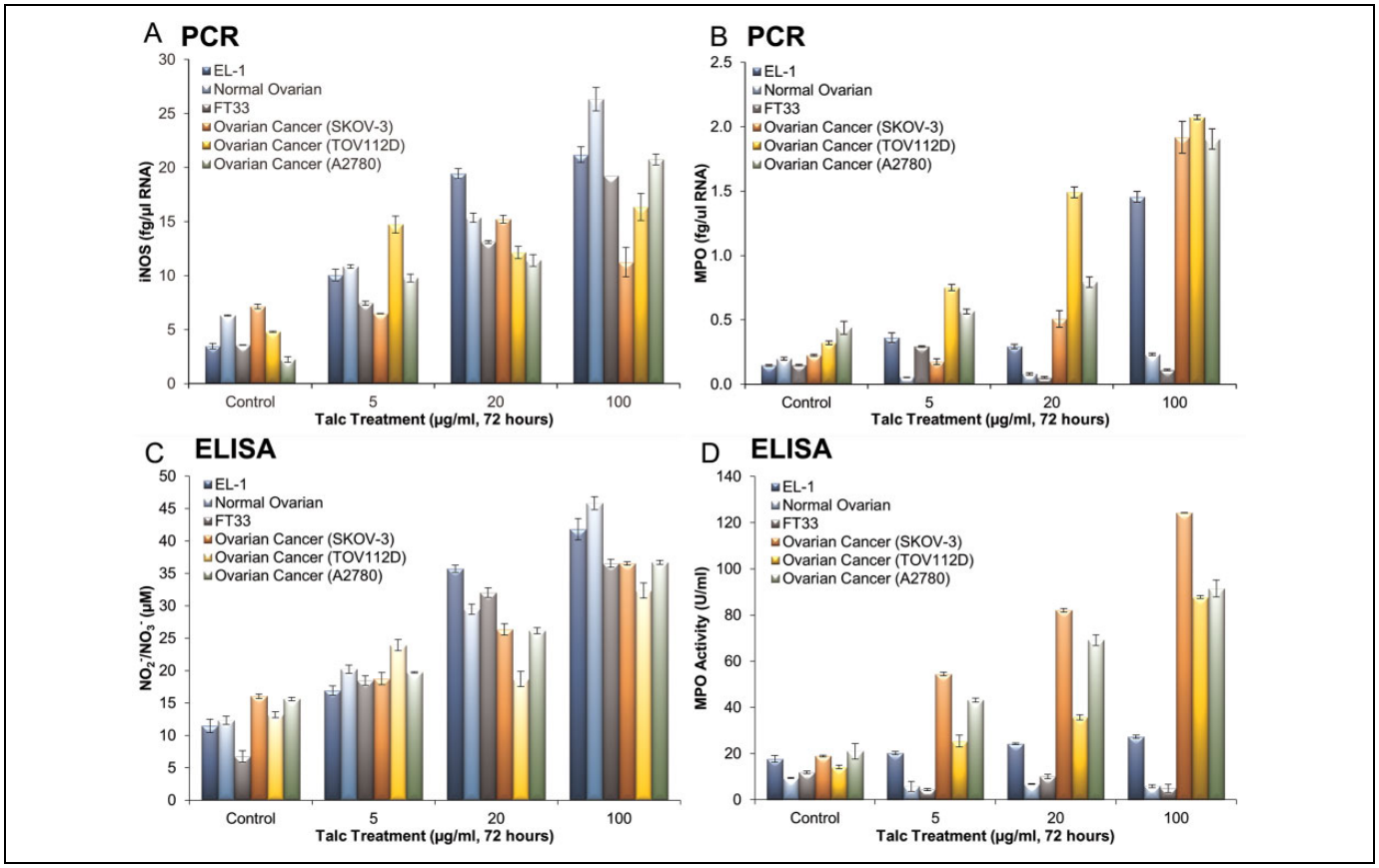

Figure 2. Increased expression and activity of key prooxidants, iNOS, NO_2^-/NO_3^-, and MPO. The mRNA (real-time RT-PCR) and protein/activity levels (ELISA) of iNOS (A and C) and MPO (B and D) were determined in macrophages (EL-1), human primary ovarian epithelial cells (normal ovarian), fallopian tube (FT33), and ovarian cancer (SKOV-3, TOV112D, and A2780) cell lines before and after treatment with various doses of talc over 72 hours. As expected, there was no detectable MPO in normal ovarian and fallopian tube cells, and thus, talc treatment did not have any effect. Experiments were performed in triplicate. Expression is depicted as the mean, with error bars representing standard deviation. All changes in response to talc treatment were significant ($P < .05$) in iNOS and MPO-positive cells and in all doses as compared to controls. iNOS indicates inducible nitric oxide synthase; MPO, myeloperoxidase; mRNA, messenger RNA; RT-PCR, reverse transcription polymerase chain reaction; ELISA, enzyme-linked immunosorbent assay.

as compared to cancer cells. As anticipated, caspase-3 was significantly reduced in cancer as compared to normal cells. Talc treatment resulted in decreased caspase-3 activity in all cells as compared to controls (Figure 6, $P < .05$), indicating a decrease in apoptosis.

Discussion

The claim that regular use of talcum powder for hygiene purpose is associated with an increased risk of ovarian cancer is based on several reports confirming the presence of talc particles in the ovaries and other parts of the female reproductive tract as well as in lymphatic vessels and tissues of the pelvis.[7-12] The ability of talc particles to migrate through the genital tract to the distal fallopian tube and ovaries is well accepted.[10] To date, the exact mechanism is not fully understood, though several studies have pointed toward the peristaltic pump feature of the uterus and fallopian tubes, which is known to enhance transport of sperm into the oviduct ipsilateral to the ovary bearing the dominant follicle.[8-12]

There are reports supporting the epidemiologic association of talc use and risk of ovarian cancer.[11,12] Recent studies have shown that risks for EOC from genital talc use vary by histologic subtype, menopausal status at diagnosis, hormone therapy use, weight, and smoking. These observations suggest that estrogen and/or prolactin may play a role via macrophage activity and inflammatory response to talc. There has been debate as to the significance of the epidemiologic studies based on the fact that the reported epidemiologic risk of talc use and risk of ovarian cancer, although consistent, are relatively modest (30%-40%), and there is inconsistent increase in risk with duration of use. This observation is due, in part, to the challenges in quantifying exposure as well as the failure of epidemiological studies to obtain necessary information about the frequency and duration of usage.[11-13]

In this study, we have shown beyond doubt that talc alters key redox and inflammatory markers, enhances cell proliferation, and inhibits apoptosis, which are hallmarks of ovarian cancer. More importantly, this effect is also manifested by talc in normal cells, including surface ovarian epithelium,

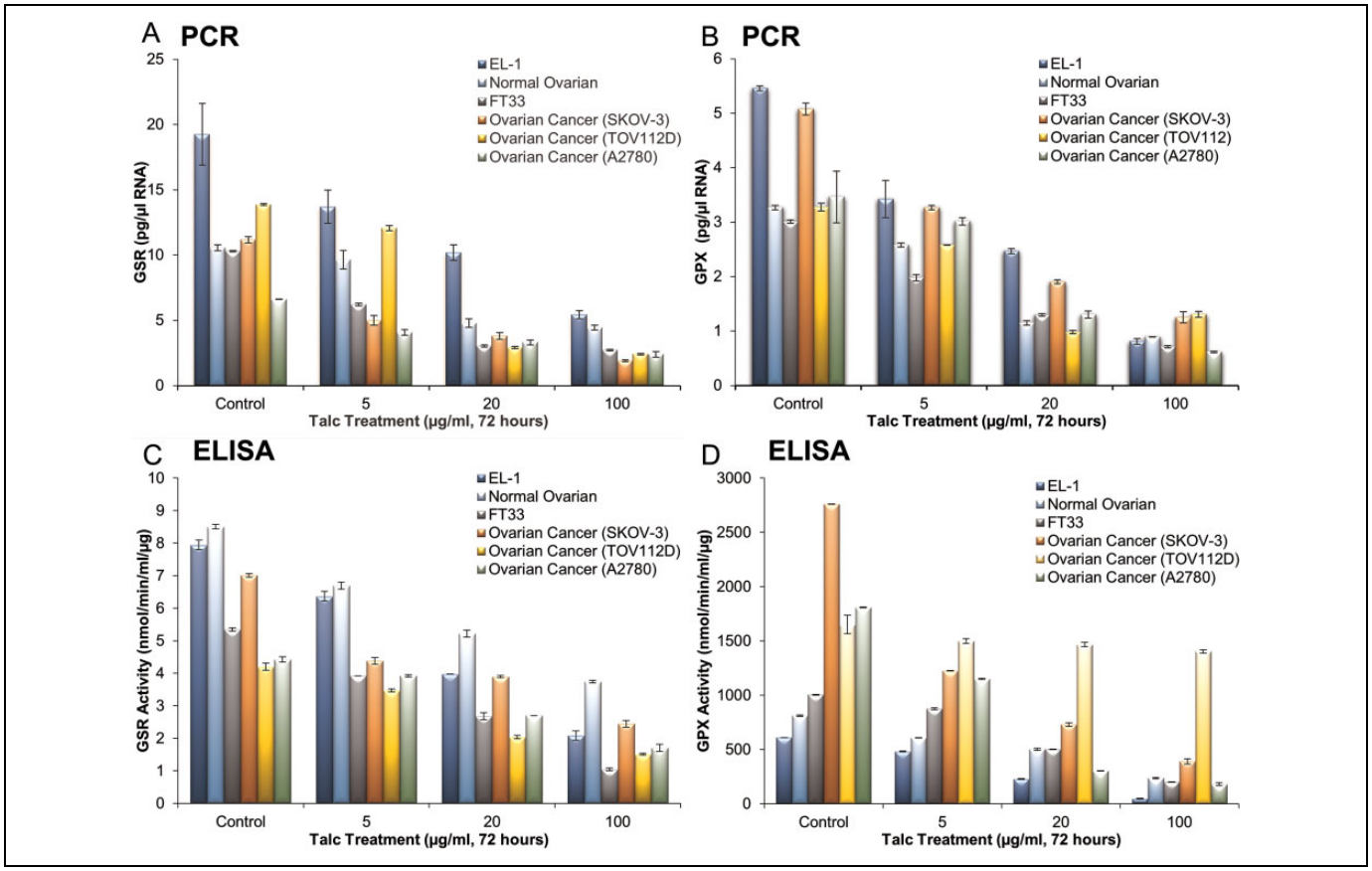

Figure 3. Decreased expression and activity of key antioxidant enzymes, GSR and GPX. The mRNA (real-time RT-PCR) and protein/activity levels (ELISA) of GSR (A and C) and GPX (B and D) were determined in macrophages (EL-1), human primary ovarian epithelial cells (normal ovarian), fallopian tube (FT33), and ovarian cancer (SKOV-3, TOV112D, and A2780) cell lines before and after treatment with various doses of talc over 72 hours. Experiments were performed in triplicate. Expression is depicted as the mean, with error bars representing standard deviation. All changes in response to talc treatment were significant ($P < .05$) in all cells and in all doses as compared to controls. GSR indicates glutathione reductase; GPX, glutathione peroxidase; mRNA, messenger RNA; RT-PCR, reverse transcription polymerase chain reaction; ELISA, enzyme-linked immunosorbent assay.

fallopian tube, and macrophages. Oxidative stress has been implicated in the pathogenesis of ovarian cancer, specifically by increased expression of several key prooxidant enzymes such as iNOS, MPO, and NAD(P)H oxidase in EOC tissues and cells as compared to normal cells indicating an enhanced redox state, as we have recently demonstrated (Figure 7).[6] This redox state is further enhanced in chemoresistant EOC cells as evident by a further increase in iNOS and NO_2^-/NO_3^- and a decrease in GSR levels, suggesting a shift toward a prooxidant state.[6] Antioxidant enzymes, key regulators of cellular redox balance, are differentially expressed in various cancers, including ovarian.[6,14] Specifically, GPX expression is reduced in prostate, bladder, kidney, and estrogen receptor negative breast cancer cell lines, though GPX is increased in other cancerous tissues from breast.[14] Glutathione reductase levels, on the other hand, are elevated in lung cancer, although differentially expressed in breast and kidney cancer.[5,15] Similarly, CAT was decreased in breast, bladder, and lung cancer while increased in brain cancer.[16-18] Superoxide dismutase is expressed in lung, colorectal, gastric ovarian, and breast cancer, while decreased activity and expression have been reported in colorectal carcinomas and pancreatic cancer cells.[18-21] Collectively, this differential expression of antioxidants demonstrates the unique and complex redox microenvironment in cancer. Glutathione reductase is a flavoprotein that catalyzes the NADPH-dependent reduction of oxidized glutathione (GSSG) to GSH. This enzyme is essential for the GSH redox cycle that maintains adequate levels of reduced cellular GSH. A high GSH to GSSG ratio is essential for protection against oxidative stress (Figure 5). Treatment with talc significantly reduced GSR in normal and cancer cells, altering the redox balance (Figure 3A and C). Likewise, GPX is an enzyme that detoxifies reactive electrophilic intermediates and thus plays an important role in protecting cells from cytotoxic and carcinogenic agents. Overexpression of GPX is triggered by exogenous chemical agents and reactive oxygen species and is thus thought to represent an adaptive response to stress.[15] Indeed, treatment of normal and cancer cells with talc significantly reduced GPX, which compromised the overall cell response to stress (Figure 3B and D).

Table 2. SNP Characteristics (A) and SNP Genotyping of Key Redox Enzymes in Untreated and Talc-Treated (100 μg/mL) Human Primary Ovarian Epithelial Cells (Normal Ovarian), Human Ovarian Surface Epithelial Cells (HOSEpiC), Fallopian Tube (FT33), and Ovarian Cancer (A2780, SKOV-3, TOV112D) Cell Lines (B).

	Gene (rs Number)				
	CAT (rs769217)	*NOS*$_2$ (rs2297518)	*GSR* (rs8190955)	*GPX1* (rs3448)	*SOD3* (rs2536512)
A					
MAF	0.123	0.173	0.191	0.176	0.476
SNP	C-262T	C2087T	G201T	C-1040T	A377T
Chromosome location	11p13	17q11.2	8p12	3q21.31	4p15.2
Amino acid switch	Isoleucine to Threonine	Serine to Leucine	Unknown	Unknown	Alanine to threonine
Effect on activity	Decrease	Increase	Unknown	Unknown	Decrease
B					
A2780: Control	C/C	C/C	G/G	C/T	A/A
A2780: Talc	C/C	C/C	G/G	C/C	A/A
SKOV-3: Control	C/C	C/C	G/G	C/T	A/A
SKOV-3: Talc	C/C	T/T	G/G	C/C	A/A
TOV112D: Control	C/C	C/C	G/G	C/T	A/A
TOV112D: Talc	C/T	C/C	G/G	C/C	A/A
HOSEpiC: Control	C/C	C/C	G/G	C/T	A/A
HOSEpiC: Talc	C/T	T/T	G/G	C/T	A/A
FT33: Control	C/C	C/C	G/G	C/T	A/A
FT33: Talc	C/T	T/T	G/G	C/C	A/A
Normal ovarian: Control	C/C	C/C	G/G	C/T	A/A
Normal ovarian: Talc	C/T	T/T	G/G	C/C	A/A

Abbreviation: SNP, single-nucleotide polymorphism.

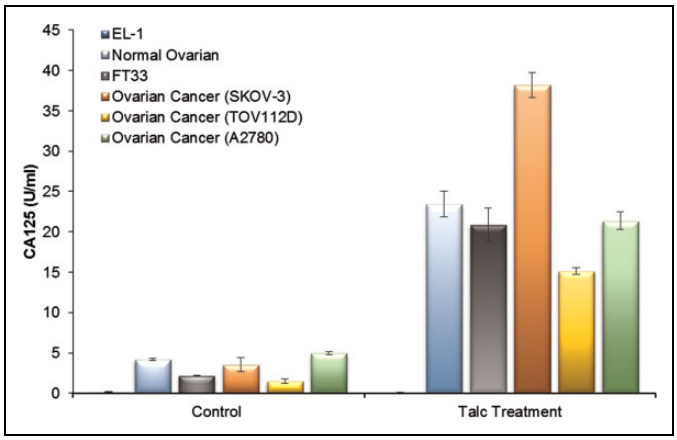

Figure 4. Increased CA-125 levels in response to talc treatment. The level of ovarian cancer biomarker CA-125 was determined by ELISA before and after 72 hours of talc treatment (100 μg/mL) in macrophages (EL-1), human primary ovarian epithelial cells (normal ovarian), fallopian tube (FT33), and ovarian cancer (SKOV-3, TOV112D, and A2780) cells. Experiments were performed in triplicate. Expression is depicted as the mean, with error bars representing standard deviation. All changes in response to talc treatment were significant ($P < .05$) in all cells as compared to controls. ELISA indicates enzyme-linked immunosorbent assay.

We have previously reported that EOC cells manifest increased cell proliferations and decreased apoptosis.[6] In this study, we have shown that talc enhances cell proliferation and induces an inhibition in apoptosis in EOC cells, but more importantly in normal cells, suggesting talc is a stimulus to the development of the oncogenic phenotype. We also previously reported a cross talk between iNOS and MPO in ovarian cancer, which contributed to the lower apoptosis observed in ovarian cancer cells.[6,22] Myeloperoxidase, an abundant hemoprotein, previously known to be present solely in neutrophils and monocytes, is a key oxidant enzyme that utilizes NO produced by iNOS as a 1-electron substrate generating NO^+, a labile nitrosylating species.[6,23,24] We were the first to report that MPO was expressed by EOC cells and tissues and that silencing MPO gene expression utilizing MPO-specific siRNA induced apoptosis in EOC cells through a mechanism that involved the S-nitrosylation of caspase-3 by MPO.[22] Additionally, we have compelling evidence that MPO serves as a source of free iron under oxidative stress, where both NO^+ and superoxide are elevated.[6] Iron reacts with hydrogen peroxide (H_2O_2) and catalyzes the generation of highly reactive hydroxy radical ($HO^\bullet$), thereby increasing oxidative stress, which in turn increases free iron concentrations by the Fenton and Haber-Weiss reaction.[6,24] We have previously highlighted the potential benefits of the combination of serum MPO and free iron as biomarkers for early detection and prognosis of ovarian cancer.[25] Collectively, we now have substantial evidence demonstrating that altered oxidative stress may play a role in maintaining the oncogenic phenotype of EOC cells. Treatment of normal or ovarian cancer cells with talc resulted in a significant increase in MPO and iNOS, supporting the role of talc in the enhancement of a prooxidant state that is a major cause in the development and maintenance of the oncogenic phenotype (Figure 2).

Furthermore, CA-125, which exists as a membrane-bound and secreted protein in EOC cells, has been established as a

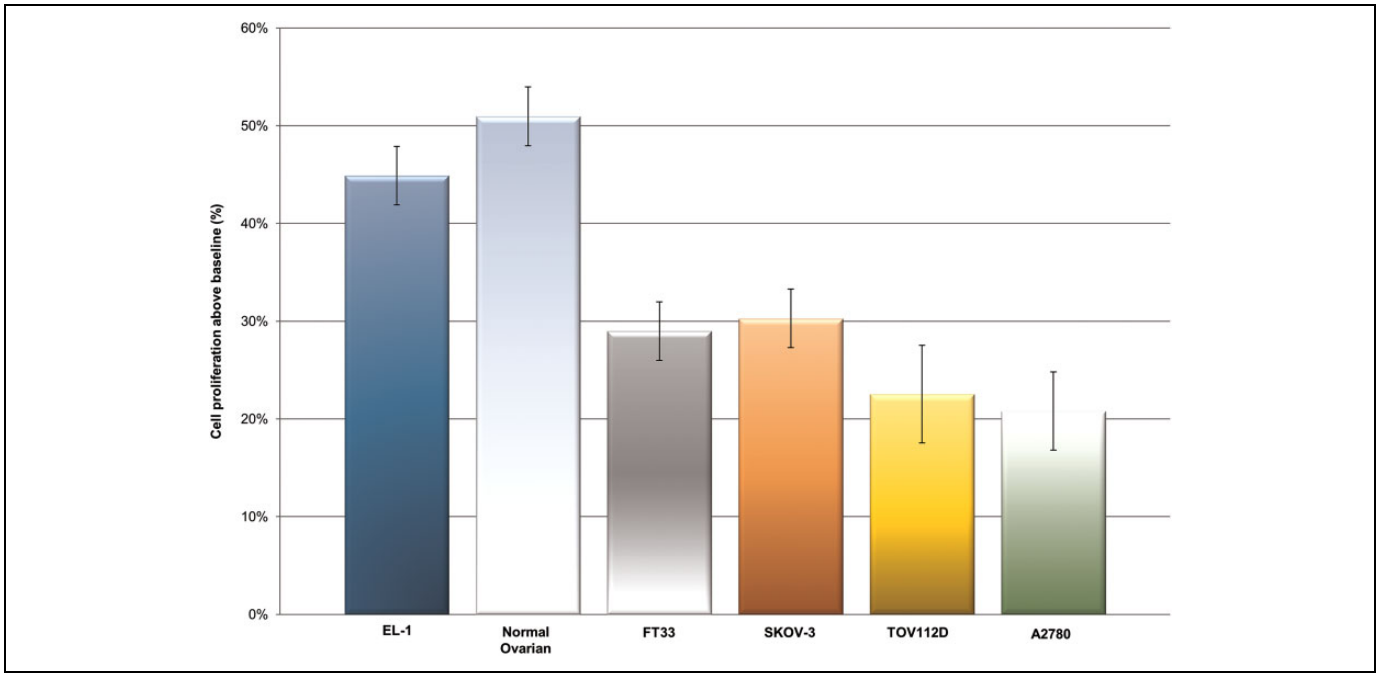

Figure 5. Increased cell proliferation in response to talc treatment. Cell proliferation was determined by MTT cell proliferation assay after 24 hours of talc treatment (100 μg/mL) in macrophages (EL-1), human primary ovarian epithelial cells (normal ovarian), fallopian tube (FT33), and ovarian cancer (SKOV-3, TOV112D, and A2780) cells. Experiments were performed in triplicate. Cell proliferation is depicted as the mean, with error bars representing standard deviation. All changes in response to talc treatment were significant ($P < .05$) in all cells as compared to controls.

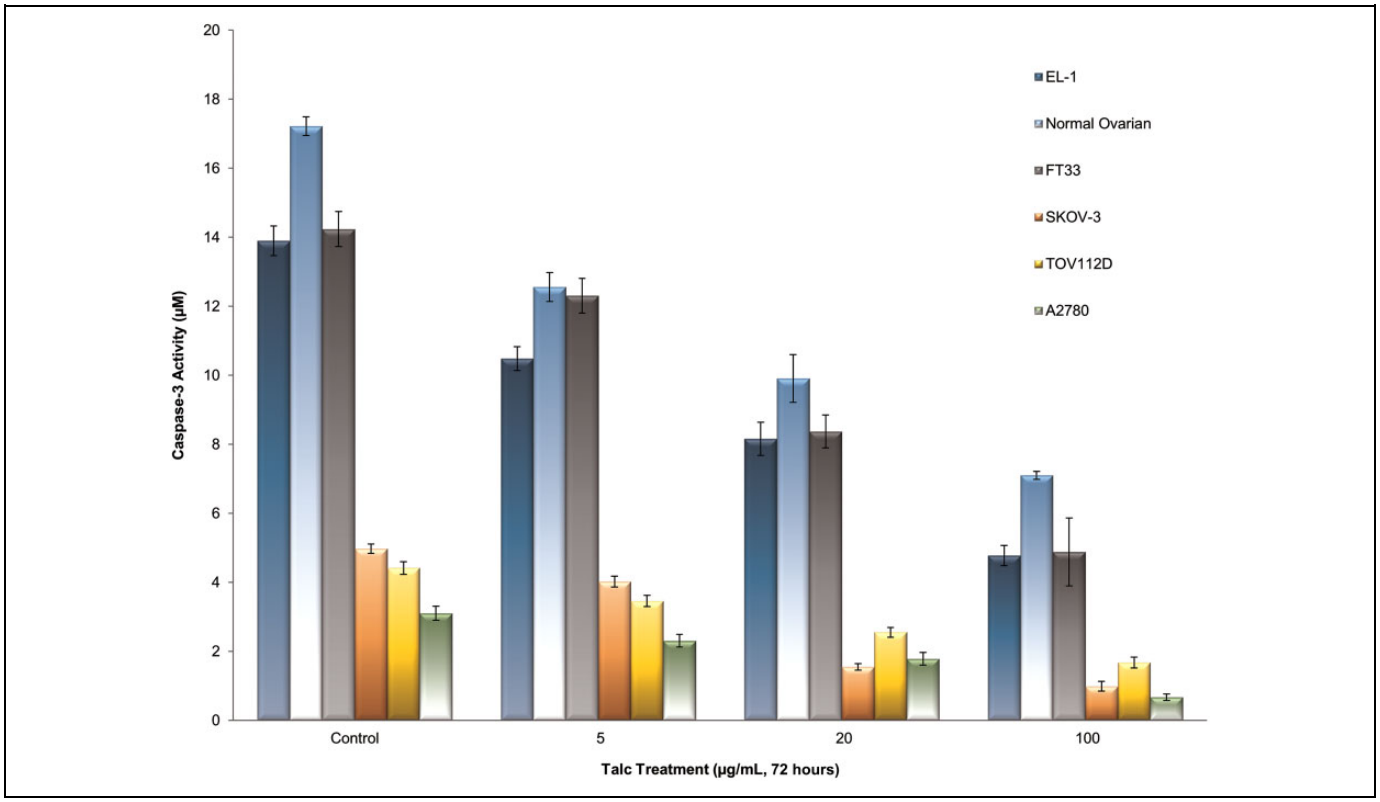

Figure 6. Decreased apoptosis in response to talc treatment. Caspase-3 activity was used to measure the degree of apoptosis in all cells. Caspase-3 activity assay was utilized to determine caspase-3 activity in macrophages (EL-1), human primary ovarian epithelial cells (normal ovarian), fallopian tube (FT33), and ovarian cancer (SKOV-3, TOV112D, and A2780) cell lines before and after treatment with various doses of talc over 72 hours. Experiments were performed in triplicate. Expression is depicted as the mean, with error bars representing standard error. All changes in response to talc treatment were significant ($P < .05$) in all cells and in all doses as compared to controls.

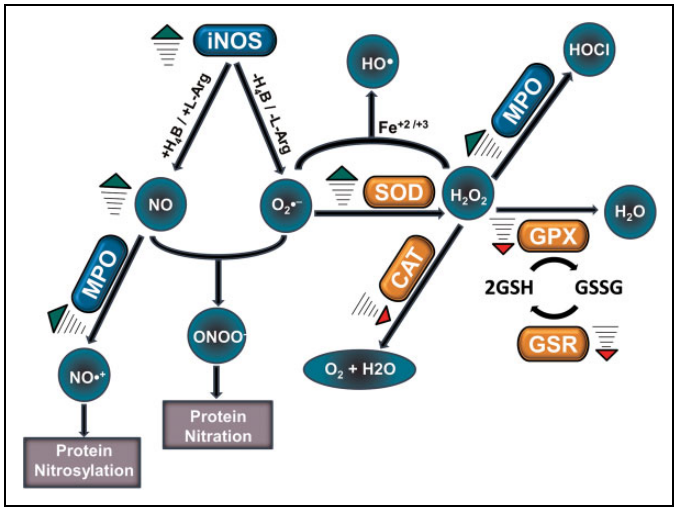

Figure 7. Epithelial ovarian cancer (EOC) cells have been reported to manifest a persistent prooxidant state as evident by the upregulation (green arrows) of key oxidants iNOS, NO, NO^+, $ONOO^-$, OH^-, O_2^+, and MPO (blue) and downregulation (red arrows) of key antioxidants SOD, CAT, GPX, and GSR (orange). This redox state was also shown to be further enhanced in chemoresistant EOC cells. In this study, talcum powder altered the redox state, as indicated by the arrows, of both normal and EOC cells to create an enhanced prooxidant state. iNOS indicates inducible nitric oxide synthase; MPO, myeloperoxidase; SOD, superoxide dismutase; CAT, catalase; GPX, glutathione peroxidase; GSR, glutathione reductase.

biomarker for disease progression and response to treatment.[2] CA-125 expression was significantly increased from nearly undetectable levels in controls to values approaching clinical significance (35 U/mL in postmenopausal women[26]) in talc-treated cells (Figure 4, $P < .05$) without the physiologic effects on the tumor microenvironment one would expect to be present in the human body, thus highlighting the implications of the prooxidant states caused by talc alone.

To elucidate the mechanism by which talc alters the redox balance to favor a prooxidant state not only in ovarian cancer cells, but more importantly in normal cells, we have examined selected known gene mutations corresponding to SNPs known to be associated with altered enzymatic activity and increased cancer risk.[6,27] Our results show that the *CAT* SNP (rs769217) resulting in decreased enzymatic activity was induced in all normal cell lines tested and in TOV112D EOC lines, but was not detected in A2780 or SKOV-3 cell lines (Table 2). Nevertheless, our results confirm a decrease in CAT expression and enzymatic activity in all talc-treated cells (Figure 1), indicating the existence of other *CAT* SNPs. The *SOD3* (rs2536512) and *GSR* (rs8190955) SNP genotypes were not detected in any cell line, yet SOD3 and GSR activity and expression were decreased in all talc-treated cells, again suggesting the presence of other SNPs. Our results have also shown that all cells, except for HOSEpiC cells, manifest the SNP genotype of *GPX1* (C/T) before talc treatment. Intriguingly, talc treatment reversed this SNP genotype to the normal genotype (Table 2). Consistent with this finding, we have previously reported that acquisition of chemoresistance by ovarian cancer cells is associated with a switch from the *GPX1* SNP genotype to the normal *GPX1* genotype.[6] It is not understood why a *GPX1* SNP genotype predominates in untreated normal and ovarian cancer cells. Our results showed that talc treatment was associated with a genotype switch from common C/C genotype in *NOS2* in untreated cells to T/T, the SNP genotype, in talc-treated cells, except in A2780 and TOV112D (Table 2). Nevertheless, our results confirm an increase in iNOS expression and enzymatic activity in all talc-treated cells (Figure 2), again suggesting the existence of other *NOS2* SNPs. Collectively, these findings support the notion that talc treatment induced gene point mutations that happen to correspond to SNPs in locations with functional effects, thus altering overall redox balance for the initiation and development of ovarian cancer. Future studies examining such SNPs are important to fully elucidate a genotype switch mechanism induced by talc exposure.

In summary, this is the first study to clearly demonstrate that talc induces inflammation and alters the redox balance favoring a prooxidant state in normal and EOC cells. We have shown a dose-dependent significant increase in key prooxidants, iNOS, NO_2^-/NO_3^-, and MPO, and a concomitant decrease in key antioxidant enzymes, CAT, SOD, GPX, and GSR, in all talc-treated cells (both normal and ovarian cancer) compared to their controls. Additionally, there was a significant increase in CA-125 levels in all the talc-treated cells compared to their controls, except in macrophages. The mechanism by which talc alters the cellular redox and inflammatory balance involves the induction of specific mutations in key oxidant and antioxidant enzymes that correlate with alterations in their activities. The fact that these mutations happen to correspond to known SNPs of these enzymes indicate a genetic predisposition to developing ovarian cancer with genital talcum powder use.

Authors' Note

Ghassan M. Saed is also affiliated with Department of Gynecologic Oncology, Karmanos Cancer Institute, Detroit, MI, USA.

Acknowledgment

Special thanks to Imaan Singh for her technical contributions in acquiring the data and in development of graphics.

Declaration of Conflicting Interests

The author(s) declared the following potential conflicts of interest with respect to the research, authorship, and/or publication of this article: Dr. Saed has served as a paid consultant and expert witness in the talcum powder litigation.

Funding

The author(s) received no financial support for the research, authorship, and/or publication of this article.

References

1. Berek JS, Bertelsen K, du Bois A, et al. Epithelial ovarian cancer (advanced stage): consensus conference (1998) [in French]. *Gynecol Obstet Fertil*. 2000;28(7-8):576-583.

2. Jelovac D, Armstrong DK. Recent progress in the diagnosis and treatment of ovarian cancer. *CA Cancer J Clin*. 2011;61(3):183-203.
3. Prat J, Ribe A, Gallardo A. Hereditary ovarian cancer. *Hum Pathol*. 2005;36(8):861-870.
4. Ramus SJ, Vierkant RA, Johnatty SE, et al. Consortium analysis of 7 candidate SNPs for ovarian cancer. *Int J Cancer*. 2008; 123(2):380-388.
5. Reuter S, Gupta SC, Chaturvedi MM, Aggarwal BB. Oxidative stress, inflammation, and cancer: how are they linked? *Free Radic Biol Med*. 2010;49(11):1603-1616.
6. Fletcher NM, Belotte J, Saed MG, et al. Specific point mutations in key redox enzymes are associated with chemoresistance in epithelial ovarian cancer. *Free Radic Biol Med*. 2016;102:122-132.
7. Cramer DW, Welch WR, Scully RE. Wojciechowski CA. Ovarian cancer and talc: a case-control study. *Cancer*. 1982;50:372-376.
8. Cramer DW, Liberman RF, Titus-Ernstoff L, et al. Genital talc exposure and risk of ovarian cancer. *Int J Cancer*. 1999;81: 351-356.
9. Ness RB, Grisso JA, Cottreau C, et al. Factors related to inflammation of the ovarian epithelium and risk of ovarian cancer. *Epidemiology*. 2000;11:111-117.
10. Henderson WJ, Joslin CA, Turnbull AC, Griffiths K. Talc and carcinoma of the ovary and cervix. *J Obstet Gynaecol Br Commonw*. 1971;78:266-272.
11. Terry KL, Karageorgi S, Shvetsov YB, et al. Genital powder use and risk of ovarian cancer: a pooled analysis of 8,525 cases and 9,859 controls. *Cancer Prev Res (Phila)*. 2013;6(8):811-821.
12. Penninkilampi R, Eslick GD. Perineal talc use and ovarian cancer: a systematic review and meta-analysis. *Epidemiology*. 2018; 29(1):41-49.
13. Reid BM, Permuth JB, Sellers TA. Epidemiology of ovarian cancer: a review. *Cancer Biol Med*. 2017;14(1):9-32.
14. Brigelius-Flohe R, Kipp A. Glutathione peroxidases in different stages of carcinogenesis. *Biochim Biophys Acta*. 2009;1790(11): 1555-1568.
15. Sun Y. Free radicals, antioxidant enzymes, and carcinogenesis. *Free Radic Biol Med*. 1990;8(6):583-599.
16. Popov B, Gadjeva V, Valkanov P, Popova S, Tolekova A. Lipid peroxidation, superoxide dismutase and catalase activities in brain tumor tissues. *Arch Physiol Biochem*. 2003;111(5):455-459.
17. Ray G, Batra S, Shukla NK, et al. Lipid peroxidation, free radical production and antioxidant status in breast cancer. *Breast Cancer Res Treat*. 2000;59(2):163-170.
18. Chung-man Ho J, Zheng S, Comhair SA, Farver C, Erzurum SC. Differential expression of manganese superoxide dismutase and catalase in lung cancer. *Cancer Res*. 2001;61(23):8578-8585.
19. Radenkovic S, Milosevic Z, Konjevic G, et al. Lactate dehydrogenase, catalase, and superoxide dismutase in tumor tissue of breast cancer patients in respect to mammographic findings. *Cell Biochem Biophys*. 2013;66(2):287-295.
20. Hu Y, Rosen DG, Zhou Y, et al. Mitochondrial manganese-superoxide dismutase expression in ovarian cancer: role in cell proliferation and response to oxidative stress. *J Biol Chem*. 2005; 280(47):39485-39492.
21. Svensk AM, Soini Y, Paakko P, Hiravikoski P, Kinnula VL. Differential expression of superoxide dismutases in lung cancer. *Am J Clin Pathol*. 2004;122(3):395-404.
22. Saed GM, Ali-Fehmi R, Jiang ZL, et al. Myeloperoxidase serves as a redox switch that regulates apoptosis in epithelial ovarian cancer. *Gynecol Oncol*. 2010;116(2):276-281.
23. Galijasevic S, Saed GM, Hazen SL, Abu-Soud HM. Myeloperoxidase metabolizes thiocyanate in a reaction driven by nitric oxide. *Biochemistry*. 2006;45(4):1255-1262.
24. Galijasevic S, Maitra D, Lu T, Sliskovic I, Abdulhamid I, Abu-Soud HM. Myeloperoxidase interaction with peroxynitrite: chloride deficiency and heme depletion. *Free Radic Biol Med*. 2009; 47(4):431-439.
25. Fletcher NM, Jiang Z, Ali-Fehmi R, et al. Myeloperoxidase and free iron levels: potential biomarkers for early detection and prognosis of ovarian cancer. *Cancer Biomark*. 2011;10(6):267-275.
26. Scholler N, Urban N. CA125 in ovarian cancer. *Biomark Med*. 2007;1(4):513-523.
27. Belotte J, Fletcher NM, Saed MG, et al. A single nucleotide polymorphism in catalase is strongly associated with ovarian cancer survival. *PLoS One*. 2015;10(8):e0135739.

Exhibit 104

Online version at https://www.minervamedica.it

Minerva Obstetrics and Gynecology 2023 April;75(2):150-7
DOI: 10.23736/S2724-606X.21.04989-7

ORIGINAL ARTICLE

Talcum powder induces malignant transformation in normal human primary ovarian epithelial cells

Amy K. HARPER [1, 2], Xin WANG [1], Rong FAN [1], Thea KIRSCH MANGU [1], Nicole M. FLETCHER [1], Robert T. MORRIS [2], Ghassan M. SAED [1, 2] *

[1]Department of Obstetrics and Gynecology, Karmanos Cancer Institute, Detroit, MI, USA; [2]Department of Gynecologic Oncology, Karmanos Cancer Institute, Detroit, MI, USA

*Corresponding author: Ghassan M. Saed, Departments of Obstetrics and Gynecology and Oncology, Karmanos Cancer Institute, Wayne State University School of Medicine, Detroit, MI 48201, USA. E-mail: gsaed@med.wayne.edu

ABSTRACT

BACKGROUND: Several studies have linked perineal use of talcum powder to increased risk of ovarian cancer (OC). Here, we determined that exposure to talcum powder induces malignant transformation in human normal ovarian cells.

METHODS: Human primary ovarian epithelial cells (HPOE), ovarian epithelial cells (HOSEpiC), and primary fibroblasts (NF) were treated with either 100 or 500 μg/mL of talcum powder or titanium dioxide (TiO_2) as a particulate control for 72 hours before assessment with a cell transformation assay and p53 and Ki-67 immunohistochemistry.

RESULTS: Treatment with talcum powder resulted in formation of colonies, indicating cell malignant transformation in a dose dependent manner in ovarian cell lines. No colonies formed in the untreated ovarian cells or control ovarian cells (TiO_2 treated) at either dose. There were no colonies formed in talc treated NF cells. Transformed ovarian cells were increased by 11% and 20% in HPOE and 24% and 40% in HOSEpic cells for talcum powder 100 and 500 μg/mL doses, respectively ($P<0.05$). There were no detectible transformed cells when cells were treated with TiO_2. Importantly, p53 mutant type as well as increased expression of Ki-67 were detected in HPOE and HOSEpic cells when exposed to talcum powder.

CONCLUSIONS: Exposure to talcum powder induces malignant transformation in ovarian epithelial cells but not in NF cells. These findings represent a direct effect of talcum powder exposure that is specific to normal ovarian cells and further supports previous studies demonstrating an association between the genital use of talcum powder and an increased risk of OC.

(*Cite this article as:* Harper AK, Wang X, Fan R, Kirsch Mangu T, Fletcher NM, Morris RT, *et al*. Talcum powder induces malignant transformation in normal human primary ovarian epithelial cells. Minerva Obstet Gynecol 2023;75:150-7. DOI: 10.23736/S2724-606X.21.04989-7)

KEY WORDS: Talc; Epithelial cells; Fibroblasts; Ovarian neoplasms; Cell proliferation.

Ovarian cancer is a gynecologic malignancy that ranks fifth in cancer deaths among women in USA.[1] Epithelial ovarian cancer (EOC) presents with various histopathology, molecular biology, and clinical outcome and is therefore considered a heterogeneous disease.[2] The pathogenesis of EOC is strongly associated with oxidative stress and inflammation.[3-5]

Epithelial ovarian cancer cells manifest a persistent pro-oxidant state that has been demonstrated *in vitro* and is also enhanced in chemoresistant EOC cells.[3, 4] Attenuation of the pro-oxidant state with antioxidants/scavengers has been shown in vitro to selectively induce apoptosis in EOC cells indicating a potential therapeutic value.[6, 7] Talcum Powder has been shown to induce oxidative stress and cell proliferation and to decrease apoptosis in normal ovarian cells and thus may play an important role in the pathogenesis of EOC.[8]

The association between genital use of talcum powder and risk of ovarian cancer have

been described in numerous studies.[8-11] Several meta-analyses have demonstrated a statistically significant increased risk of ovarian cancer with the genital use of talcum powder.[11-13] In addition, several animal studies have reported that talcum powder causes inflammation and oxidative stress.[14-16] Several *in-vitro* studies have demonstrated a biologic effect when cells in culture are exposed to talcum powder.[17-21]

In support of these previous findings, we have recently delineated the molecular basis of the association of talcum powder use with increased risk of ovarian cancer.[8] The specific mechanism by which talcum powder exposure causes ovarian cancer has not been definitively established. Here we clearly demonstrate that exposure to talcum powder induces malignant transformation in human primary normal ovarian epithelial cells and thus, providing a mechanism for the increased risk of ovarian cancer with the genital use of talcum powder.

Materials and methods

Normal human primary ovarian epithelial cells (HPOE)

Cells were received at passage 3 (Cell Biologics, Chicago, IL, USA) cryo-preserved in vials containing at least 0.5 $\times 10^6$ cells per mL. Cells were grown in gelatin pre-coated T25 flasks for 2 min and incubated in Cell Biologics Culture Complete Growth Medium. Cells were expanded for 2-4 passages at a split ratio of 1:2 under the cell culture conditions as specified by Cell Biologics. Human Epithelial Cell Medium is a complete medium designed for the culture of human epithelial cells. It was tested and optimized with epithelial cell growth and proliferation in vitro. Cells were incubated at 37 °C with 5% CO_2 and 95% air.

Normal human ovarian epithelial cells (HOSEpiC)

Cells were purchased from ScienCell Research Laboratories, Inc, Carlsbad, California. HOSEpiC cells were isolated from human ovary. HOSEpiC cells were received cryopreserved at passage one in frozen vials, each vial contains 5 $\times 10^5$ cells in 1 mL volume. Cells were further expanded for 2-3 passages in Ovarian Epithelial Cell Medium (OEpiCM, Cat. #7311). Cells were incubated at 37 °C with 5% CO_2 and 95% air.

Human normal primary peritoneal fibroblasts

This fibroblast cell line has been extensively characterized in previous studies.[22] Cells were grown in Dulbecco's Modified Eagle Medium (Invitrogen, Carlsbad, CA, USA), with 10% fetal bovine serum (FBS, Innovative Research, Novi, MI) and penicillin/streptomycin (Thermo Fisher Scientific, Waltham, MA, USA) as we have previously described.[22] Cells were incubated at 37 °C with 5% CO_2 and 95% air.

Talcum powder treatment

Talcum baby powder (Johnson & Johnson, New Brunswick, NJ, USA, #30027477, Lot#13717RA) or control particles, Titanium dioxide (TiO_2, Spectrum Chemical Corp, Lot No. 2EB0148) were used to treat cells. Talcum powder or TiO_2 were suspended in PBS (Stock solution of 50 mg/mL) and sonicated 3 times for 1 minute each with Sonic Dismembrator (Thermo Fisher Scientific, Model 100). Stock solutions were filtered through 30 µm nylon mesh filters. No visible loss of material has observed. Cells were seeded in 100 mm Petri cell culture dishes (1 $\times 10^6$) and were treated 24 hours later in duplicate in a fresh media with 100 or 500 µg/mL of talc or titanium dioxide (TiO_2) for 72 hours. Control: cells (30K) with media only and Negative control: cells (30K) with media and PBS. No cell death was observed after 72 hours in culture in control or treated cells. Titanium dioxide, a naturally occurring particle, has been classified in humans and animals as biologically inert.[19, 23] Titanium dioxide particles are produced and used as fine (~ 0.1-2.5 µm) and nanosize (<0.1 µm) particles.[23] In this study, we used TiO_2 as a particulate control to exclude the effect of material size. Culture plates were washed several times to remove residual particles and collected by trypsin in fresh media. Cells were counted and their concentration was adjusted with fresh media to 1.5 $\times 10^6$ cells/mL.

Cells were now ready to be assessed with cell transformation assay (colorimetric), according to the manufacturer protocol (Abcam-235698,

Cambridge, MA, USA). The 100 and 500 µg/mL doses were chosen based on our previous studies which showed talcum powder to induce changes in redox balance of cells at the molecular level.[8] The experiments were repeated 3 times with a fresh solution of talcum powder and TiO_2. This assay is more stable, faster and more sensitive than the traditional Soft-Agar Assay. Traditional assays require 3-4 weeks of incubation and inconsistent due to independent counting. An additional advantage of this assay is it's linear range from 10,000-400,000 cells.

A cell-dose curve was established as described in the manufacturer's protocol. Briefly, we used cells (5.34×10^5 cells/mL) were suspended in 1X DMEM/10% FBS medium. Cells were diluted into seven serial dilutions in a 1.5 mL centrifuge tubes. Serial dilution was performed using an 8-channel multi pipette by adding 150 µL of media to each well of a 96-well microplate. A 150 µL aliquot of the 5.34×10^5 cells/mL (80×10^3 cells) was added to the wells of the first duplicate row. A 150-µL aliquot from the first duplicate row was removed and added to the next well and mixed. The process was repeated until the seven serial dilutions were obtained. The final well was blank with media only and no cells. A 35-µL aliquot of 1X DMEM/10% FBS and 15 µL of WST working solution were then added into each well and incubate at 37 °C for 4 hours. The absorbance was measured by a microtiter plate reader at 450 nm (Figure 1).

Agarose and WST working solutions were prepared as described in the kit information sheet (Abcam-235698). The base agarose mix was added into the required wells in a 96-well plate and kept for 15 minutes at 4 °C to solidify the agarose. A top agarose layer stock solution was prepared by using talcum powder or TiO_2 treated stock cell solution of 1.5×10^6 cells/mL (30,000 cells per well, which is within the recommended range of the assay) in 1X DMEM/10% FBS medium. The agarose-cell mix was added into every well of a 96-well plate previously holding the solidified base agarose layer and placed at 4 °C for 10 minutes to solidify the layer. After placing the plate for 10 min at 37 °C, 1X DMEM/10% FBS medium was added to all the wells and incubated at 37 °C for 6-8 days. On the last day the upper medium on the top agarose layer was cautiously removed by pipetting. A 1X DMEM/10% FBS and WST working solution was added into each well, incubated for 4 hours at 37 °C. The absorbance was measured by a microtiter plate reader at 450 nm. Colonies of transformed cells were detected and photograph by a Zeiss Axiovert 40 C Inverted Phase Contrast Microscope with an Axio camera.

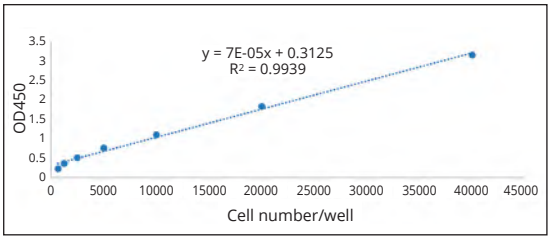

Figure 1.—Human primary normal ovarian epithelial cell-dose curve. The cell dose curve was established as described in methods using a serial dilution of cells.

Immunohistochemistry (IHC) staining and scoring

The IHC panel consisted of antibodies against p53 and Ki-67. The primary antibodies, suppliers, and staining conditions are listed in Table I.

Cytospin slides were prepared from cells and stained using immunoperoxidase labeling performed with the automated XT iVIEW DAB V.1 procedure on the Ultra BenchMark XT IHC/ISH Staining Module, Ventana with anti-p53 (clone DO-7 prediluted, Ventana). Antigen retrieval was carried out with CC1, pH 8.0 (Ventana). Sections were incubated with primary antibodies for 36 min at 37 °C. All slides were reviewed by two pathologists. Cases with discordant Ki-67 estimated results underwent a consensus review at a double-headed microscope. Diffuse "in-block" nuclear staining or complete negative staining with p53 was considered a positive reaction indicating mutated p53 status. Focal nuclear staining is consistent with "wild type" p53 and considered negative. The Proliferation

TABLE I.—*Primary antibodies, suppliers, and staining conditions.*

Antibody	Clone	Source	Detection System	Dilution
P53	DO-7	Ventana	Ventana ultraView DAB	1:500
Ki-67	Mib1	Ventana	Ventana ultraView DAB	1:2000

Index (PI) was assessed qualitatively using Ki-67-stained slides and classified as high PI (>50% positive cells) or low PI (<50% positive cell).

Statistical analysis

We performed ANOVAs with Tukey *post-hoc* tests to evaluate the difference between the three groups (no treatment control, talcum powder treatment and TiO_2 treatment). The values were expressed as mean and standard deviation. We used SPSS v. 24 for Windows (SPSS, Chicago, IL, USA); a $P<0.05$ defined significance.

Results

Treatment with talcum powder significantly increased the number of transformed normal epithelial ovarian cells by 11% and 20% in the 100 and 500 µg/mL talcum powder doses, respectively (Figure 2) ($P<0.05$). Likewise, but to a greater extent, treatment with talcum powder significantly increased the number of transformed HOSEpiC cells by 24% and 40% in the 100 and 500 µg/mL talcum powder doses, respectively (Figure 2) ($P<0.05$). Talcum powder had no detectable transformation effect on normal peritoneal fi-

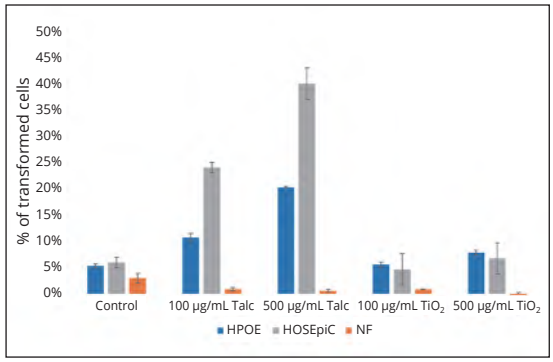

Figure 2.—Equal numbers (30K) of human primary normal ovarian epithelial cells (HPOE), human ovarian epithelial cells (HOSEpiC) and human normal peritoneal fibroblast cells (NF) were seeded for the cell transformation assay as described in methods. After 6 days, the cell number were measured. Standard and samples readings were taken 4 hours after adding WST working solution. Control: cells (30K) with media only.

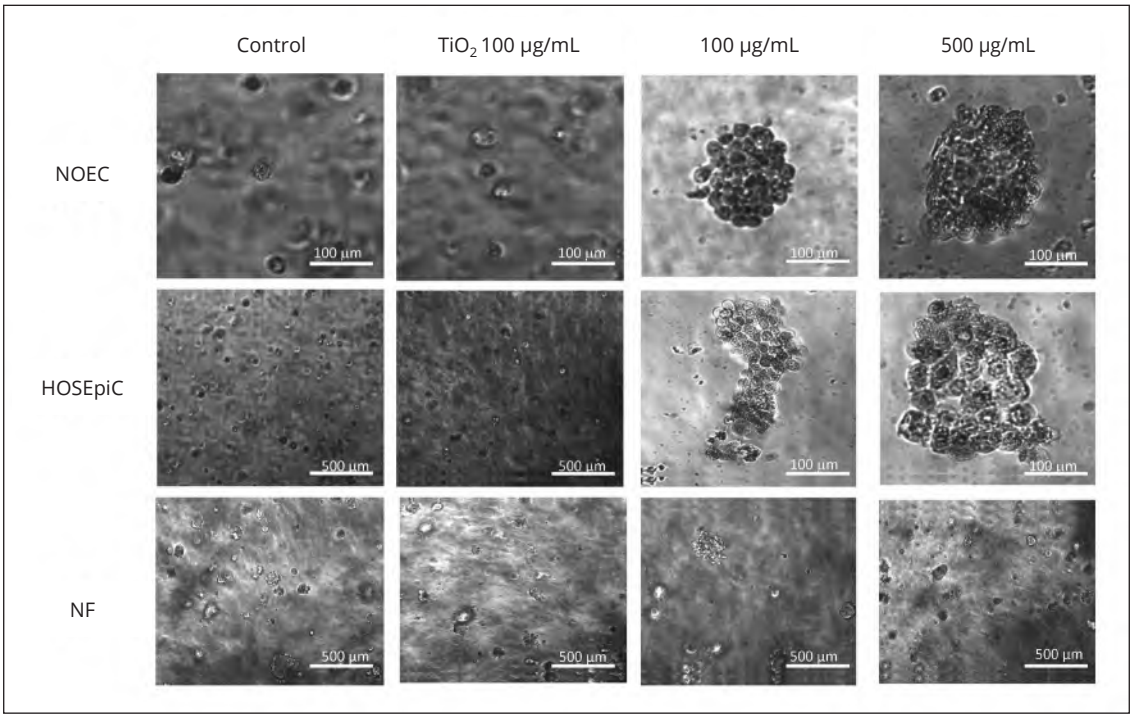

Figure 3.—Images of human primary normal ovarian epithelial cells (NOEC), human ovarian epithelial cells (HOSEpiC) and human normal peritoneal fibroblast cells (NF) treated with 100 and 500 µg/mL of talcum powder, after 6 days of culture. Colonies of transformed cells were detected and photograph by a Zeiss Axiovert 40 C Inverted Phase Contrast Microscope with an Axio camera.

broblasts at either dose (Figure 2). There was no significant difference between the no treatment control and the two doses of TiO_2 treatment control group (Figure 2) (P>0.05).

It is known that cancer cells are able to grow in culture without the need for matrix attachment. Treatment with talcum powder resulted in formation of colonies, indicating cell malignant transformation in normal epithelial ovarian cell lines in a dose dependent manner (Figure 3). There were no colonies formed in talcum powder treated normal fibroblasts (Figure 3). There were no colonies formed in either untreated ovarian cells or control ovarian cells at either dose. There were no detectible transformed cells when cells were treated with the particulate control, TiO_2.

To confirm malignant cell transformation observed with the cell transformation assay used in this study we performed IHC on the normal human primary ovarian epithelial (HPOE) and normal human ovarian epithelial cells (HOSEpiC) cells staining for p53 and Ki-67. Focal p53 nuclear staining indicating wild type p53 expression was observed in cells before treatment. After treatment of cells with talcum powder 100 µg/mL for 72 hours, diffused "in-block" nuclear staining was observed indicating p53 mutated form (Figure 4). Additionally, talcum powder treatment increased the proliferation index (PI) in both cell lines. The baseline PI for HPOE and HOSEpic cells was 50 and 70% respectively. The PI was significantly increased to 90% in both cell lines (Figure 4).

Discussion

This is the first study to directly show that exposure to talcum powder induces malignant transformation in ovarian epithelial cells. The ability of talcum powder exposure to induce transformation appears to be specific to ovarian cells as it did not induce transformation in peritoneal fibroblasts (Figure 3).

The link between talcum powder exposure and ovarian cancer have been supported by the harmful biological effects reported in various

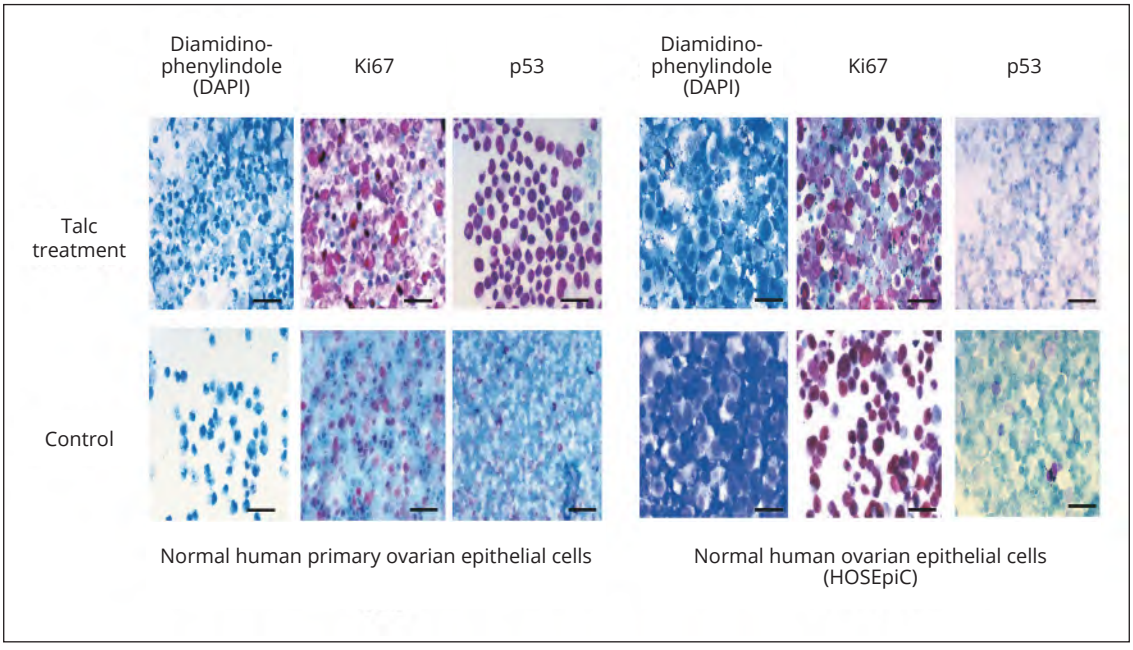

Figure 4.—Immunohistochemistry staining for p53 and Ki-67 in two normal human ovarian epithelial cells with and without Talcum powder (100 µg/mL) treatment for 72 hours. Slides were reviewed by two pathologists. Diffuse nuclear staining or complete negative staining with p53 is considered a positive reaction indicating mutated p53 status were observed in cells treated with talcum powder. Focal nuclear staining is consistent with wild type p53 and considered negative was observed in untreated cells (control). An increase in the proliferation index (Ki-67) was observes in talcum powder treated cells versus controls. Scale bar is 500 µm.

cell culture studies.[8, 14, 17-21, 24, 25] Macrophage activation and inflammatory response to talcum powder were suggested as a link to increased risk of ovarian cancer.[14, 18] Macrophages exposed to nano-talc manifested increased levels in inflammatory markers, TNF-alpha, IL-1beta and IL-6 as well as constituent phosphorylation of both p38 and ERK1/2 pathways.[18] p38 MAPK signaling pathway are known to be associated with cisplatin-resistant ovarian cancer.[26] Exposure of macrophages to talc and estradiol has led to increased production of reactive oxygen species and changes in expression of macrophage genes that play a role in cancer development and immunosurveillance.[24] These studies have also shown that ovarian cancer cells were present in larger numbers after co-culture with macrophages exposed to talc powder when in the presence of estradiol.[24]

Oxidative stress has been implicated in the pathogenesis of ovarian cancer, specifically, by increased expression of several key pro-oxidant enzymes in EOC tissues and cells as compared to normal cells.[3] Talcum powder exposure was shown to induce molecular changes in redox enzymes in normal ovarian cells similar to those known for ovarian cancer.[3, 8] In all talc-treated cells, there was a significant dose-dependent increase in key prooxidants with a concomitant decrease in key antioxidants enzymes. Remarkably, talcum powder exposure induced specific point mutations that are known to alter the activity in some of these key enzymes. The mechanism by which talcum powder alters the cellular redox and inflammatory balance involves the induction of specific mutations in key oxidant and antioxidant enzymes that correlate with alterations in their activities.[8]

We have previously identified a distinct oxidative stress/inflammation pattern for epithelial ovarian cancer and chemoresistant ovarian cancer.[3] We have utilized real time RT-PCR to measure levels of key redox and inflammation markers in response to talcum powder treatment and found that talcum powder altered specific markers to mimic the unique pattern characterized for ovarian cancer [8]. However, this effect was not observed in normal fibroblasts, hence, the effect is specific to epithelial ovarian cells.

Ovarian cancer cells were shown to manifest increased cell proliferation and decreased apoptosis, a hallmark of malignant cells, as compared to normal ovarian cells.[3] Indeed, talcum powder further enhanced cell proliferation and inhibited apoptosis in EOC cells, but more importantly in normal ovarian cells, suggesting talc is a stimulus to the development of the oncogenic phenotype.[8] Furthermore, CA-125, a membrane-bound and secreted protein, has been established as a biomarker for disease progression and response to ovarian cancer treatment.[27] CA-125 was significantly increased to values approaching clinical significance (35 U/mL in postmenopausal women) in talc treated normal ovarian cells.[8, 27] Thus, these findings confirmed the inflammatory/redox stress effects of talcum powder exposure to normal ovarian cells and indicated that this stress is a key mechanism in the malignant transformation of these cells.

The dose and time of talcum powder exposure in cell culture experiments used in this study was based on previous studies.[8] These doses are not intended to represent a typical dose when applied to the genital area in women over time. Despite this limitation, the development and use of in vitro models has been valuable in the advancement of research and knowledge on cancer pathogenesis.[28] The cellular transformation demonstrated in this study was significant and informative.

Anchorage-independent growth is one of the hallmarks of cell transformation and is accepted to be the most accurate and stringent in vitro assay for detecting malignant transformation of cells.[29, 30] The soft agar colony formation assay used in this study is widely accepted and used to evaluate cellular transformation.[29, 30] The Cell Transformation Assay Kit is faster, stable, more sensitive, and has a wide linear range (10,000-400,000) cells than the traditional Soft-Agar Assay. Therefore, in this study we used 30,000 of talcum powder and TiO_2 treated cells as well as control cells to stay within the recommended number of cells. The assay utilizes the conversion of tetrazolium salt to formazan by mitochondrial dehydrogenases which is directly proportional to the number of living transformed cells (Figure 2).

Tumor suppressor p53 gene mutations are frequently seen in ovarian cancers and can be used

as a biomarker to differentiate low from high grade serous ovarian carcinomas. The methods used for the assessment of p53 (mutant vs. wild type) and Ki-67 expression in this study is identical to the methods used in clinical pathology laboratories for the diagnosis of the different subtypes of ovarian cancer. The slides were scored and interpreted independently by two pathologists. Mutant p53 along with increased Ki-67 expression were detected in both HPOE and (HOSEpiC) ovarian cells treated with 100 μg/mL talcum powder for 72 hours (Figure 4). These findings supported the malignant transformation of normal ovarian cells seen in the agar transformation assay (Figure 3).

Conclusions

This study clearly demonstrate that talcum powder exposure induced malignant transformation of normal ovarian cells in culture which adds to the strong evidence of a causal relationship between the genital use of talcum powder and ovarian cancer. Therefore, we consider that future studies should aim to evaluate this finding utilizing animal models.

This study provides a step forward in understanding whether the distinct redox/inflammatory phenotype is the trigger of the oncogenic phenotype that leads to ovarian cancer. Indeed, we have shown that talcum powder in addition to altering the redox inflammatory status also alters p53 and Ki-67 genes, as in evidence of cell transformation. Cell transformation was also confirmed by the ability of talcum powder treated normal epithelial ovarian cells to form colonies using transformation assay. In conclusion, the ability of talcum powder exposure to induce malignant transformation appears to be specific to ovarian cells as it did not induce transformation in normal peritoneal fibroblasts. Further investigation to understand this specific effect of talcum powder on the ovaries is needed.

References

1. Torre LA, Trabert B, DeSantis CE, Miller KD, Samimi G, Runowicz CD, *et al.* Ovarian cancer statistics, 2018. CA Cancer J Clin 2018;68:284–96.

2. Lee JM, Minasian L, Kohn EC. New strategies in ovarian cancer treatment. Cancer 2019;125(Suppl 24):4623–9.

3. Saed GM, Diamond MP, Fletcher NM. Updates of the role of oxidative stress in the pathogenesis of ovarian cancer. Gynecol Oncol 2017;145:595–602.

4. Fletcher NM, Belotte J, Saed MG, Memaj I, Diamond MP, Morris RT, *et al.* Specific point mutations in key redox enzymes are associated with chemoresistance in epithelial ovarian cancer. Free Radic Biol Med 2017;102:122–32.

5. Savant SS, Sriramkumar S, O'Hagan HM. The Role of Inflammation and Inflammatory Mediators in the Development, Progression, Metastasis, and Chemoresistance of Epithelial Ovarian Cancer. Cancers (Basel) 2018;10.

6. Jiang Z, Fletcher NM, Ali-Fehmi R, Diamond MP, Abu-Soud HM, Munkarah AR, *et al.* Modulation of redox signaling promotes apoptosis in epithelial ovarian cancer cells. Gynecol Oncol 2011;122:418–23.

7. Saed GM, Fletcher NM, Jiang ZL, Abu-Soud HM, Diamond MP. Dichloroacetate induces apoptosis of epithelial ovarian cancer cells through a mechanism involving modulation of oxidative stress. Reprod Sci 2011;18:1253–61.

8. Fletcher NM, Harper AK, Memaj I, Fan R, Morris RT, Saed GM. Molecular Basis Supporting the Association of Talcum Powder Use With Increased Risk of Ovarian Cancer. Reprod Sci 2019;26:1603–12.

9. O'Brien KM, Tworoger SS, Harris HR, Anderson GL, Weinberg CR, Trabert B, *et al.* Association of Powder Use in the Genital Area With Risk of Ovarian Cancer. JAMA 2020;323:49–59.

10. Cramer DW, Vitonis AF, Terry KL, Welch WR, Titus LJ. The Association Between Talc Use and Ovarian Cancer: A Retrospective Case-Control Study in Two US States. Epidemiology 2016;27:334–46.

11. Berge W, Mundt K, Luu H, Boffetta P. Genital use of talc and risk of ovarian cancer: a meta-analysis. Eur J Cancer Prev 2018;27:248–57.

12. Kadry Taher M, Farhat N, Karyakina NA, Shilnikova N, Ramoju S, Gravel CA, *et al.* Critical review of the association between perineal use of talc powder and risk of ovarian cancer. Reprod Toxicol 2019;90:88–101.

13. Penninkilampi R, Eslick GD. Perineal Talc Use and Ovarian Cancer: A Systematic Review and Meta-Analysis. Epidemiology 2018;29:41–9.

14. Shim I, Kim HM, Yang S, Choi M, Seo GB, Lee BW, *et al.* Inhalation of Talc Induces Infiltration of Macrophages and Upregulation of Manganese Superoxide Dismutase in Rats. Int J Toxicol 2015;34:491–9.

15. National Toxicology Program. NTP Toxicology and Carcinogenesis Studies of Talc (CAS No. 14807-96-6)(Non-Asbestiform) in F344/N Rats and B6C3F1 Mice (Inhalation Studies). Natl Toxicol Program Tech Rep Ser 1993;421:1–287.

16. Keskin N, Teksen YA, Ongun EG, Ozay Y, Saygili H. Does long-term talc exposure have a carcinogenic effect on the female genital system of rats? An experimental pilot study. Arch Gynecol Obstet 2009;280:925–31.

17. Acencio MM, Silva BR, Teixeira LR, Alvarenga VA, Silva CS, da Silva AG, *et al.* Evaluation of cellular alterations and inflammatory profile of mesothelial cells and/or neoplastic cells exposed to talc used for pleurodesis. Oncotarget 2020;11:3730–6.

18. Khan MI, Sahasrabuddhe AA, Patil G, Akhtar MJ, Ashquin M, Ahmad I. Nano-talc stabilizes TNF-alpha m-RNA in human macrophages. J Biomed Nanotechnol 2011;7:112–3.

19. Shukla A, MacPherson MB, Hillegass J, Ramos-Nino

ME, Alexeeva V, Vacek PM, *et al.* Alterations in gene expression in human mesothelial cells correlate with mineral pathogenicity. Am J Respir Cell Mol Biol 2009;41:114–23.

20. Akhtar MJ, Ahamed M, Khan MA, Alrokayan SA, Ahmad I, Kumar S. Cytotoxicity and apoptosis induction by nanoscale talc particles from two different geographical regions in human lung epithelial cells. Environ Toxicol 2014;29:394–406.

21. Buz'Zard AR, Lau BH. Pycnogenol reduces talc-induced neoplastic transformation in human ovarian cell cultures. Phytother Res 2007;21:579–86.

22. Saed GM, Zhang W, Diamond MP. Molecular characterization of fibroblasts isolated from human peritoneum and adhesions. Fertil Steril 2001;75:763–8.

23. Skocaj M, Filipic M, Petkovic J, Novak S. Titanium dioxide in our everyday life; is it safe? Radiol Oncol 2011;45:227–47.

24. Mandarino A, Gregory DJ, McGuire CC, Leblanc BW, Witt H, Rivera LM, *et al.* The effect of talc particles on phagocytes in co-culture with ovarian cancer cells. Environ Res 2020;180:108676.

25. Akhtar MJ, Kumar S, Murthy RC, Ashquin M, Khan MI, Patil G, *et al.* The primary role of iron-mediated lipid peroxidation in the differential cytotoxicity caused by two varieties of talc nanoparticles on A549 cells and lipid peroxidation inhibitory effect exerted by ascorbic acid. Toxicol In Vitro 2010;24:1139–47.

26. Xie Y, Peng Z, Shi M, Ji M, Guo H, Shi H. Metformin combined with p38 MAPK inhibitor improves cisplatin sensitivity in cisplatin-resistant ovarian cancer. Mol Med Rep 2014;10:2346–50.

27. Karimi-Zarchi M, Dehshiri-Zadeh N, Sekhavat L, Nosouhi F. Correlation of CA-125 serum level and clinico-pathological characteristic of patients with endometriosis. Int J Reprod Biomed (Yazd) 2016;14:713–8.

28. Mossman BT. Mechanistic in vitro studies: what they have told us about carcinogenic properties of elongated mineral particles (EMPs). Toxicol Appl Pharmacol 2018;361:62–7.

29. Borowicz S, Van Scoyk M, Avasarala S, Karuppusamy Rathinam MK, Tauler J, Bikkavilli RK, *et al.* The soft agar colony formation assay. J Vis Exp 2014;e51998.

30. Kusakawa S, Yasuda S, Kuroda T, Kawamata S, Sato Y. Ultra-sensitive detection of tumorigenic cellular impurities in human cell-processed therapeutic products by digital analysis of soft agar colony formation. Sci Rep 2015;5:17892.

Conflicts of interest.—Ghassan M. Saed has served as a paid consultant and expert witness for the plaintiffs in the talcum powder litigation. The remaining authors have no potential conflicts of interest to report.

Funding.—A portion of Ghassan M. Saed's time conducting this research was paid for by the lawyers representing plaintiffs in the talcum powder litigation. Ghassan M. Saed received no financial support for the authorship or publication of this article.

Authors' contributions.—Amy K. Harper performed and designed experiments, and helped writing manuscript. Xin Wang and Rong Fan performed the experiments. Thea Kirsch Mangu helped writing and revised manuscript. Nicole M. Fletcher designed the experiment, and helped writing the manuscript. Robert T. Morris interpreted the data and revised the manuscript. Ghassan M. Saed designed the experiments, supervised all aspects of this work, and wrote the manuscript. All authors read and approved the final version of the manuscript.

Acknowledgements.—The authors acknowledge Dr. Ruba Ali-Fahmi and Dr. Ahmad Alrajjal from the Department of Pathology who helped with immunohistochemistry of p53 and Ki-67.

History.—Article first published online: November 26, 2021. - Manuscript accepted: November 8, 2021. - Manuscript revised: November 5, 2021. - Manuscript received: September 30, 2021.

Exhibit 105

Environmental Research 180 (2020) 108676

Contents lists available at ScienceDirect

Environmental Research

journal homepage: www.elsevier.com/locate/envres

The effect of talc particles on phagocytes in co-culture with ovarian cancer cells

Angelo Mandarino[a], David J. Gregory[b], Connor C. McGuire[c], Brian W. Leblanc[a], Hadley Witt[a], Loreilys Mejias Rivera[a], John J. Godleski[d,e,f], Alexey V. Fedulov[a,f,*]

[a] Alpert Medical School of Brown University, Department of Surgery, Division of Surgical Research, Rhode Island Hospital, Providence, RI, USA
[b] Harvard Medical School, Massachusetts General Hospital, Department of Pediatrics, Boston, MA, USA
[c] University of Rochester Medical Center, Department of Environmental Medicine, Rochester, NY, USA
[d] John J. Godleski, MD, PLLC, Milton, MA, USA
[e] Harvard Medical School, Department of Pathology (Emeritus), Boston, MA, USA
[f] Department of Environmental Health, Harvard TH Chan School of Public Health (Retired), Boston, MA, USA

ARTICLE INFO

Keywords:
"Talc"
"Titanium dioxide"
"Concentrated urban air particulates"
"Diesel exhaust particles"
"Ovarian cancer"
"Macrophages"
"Phagocytes"
"Immunosurveillance"
"Tumoricidal"

ABSTRACT

Talc and titanium dioxide are naturally occurring water-insoluble mined products usually available in the form of particulate matter. This study was prompted by epidemiological observations suggesting that perineal use of talc powder is associated with increased risk of ovarian cancer, particularly in a milieu with higher estrogen. We aimed to test the effects of talc vs. control particles on the ability of prototypical macrophage cell lines to curb the growth of ovarian cancer cells in culture in the presence of estrogen.

We found that murine ovarian surface epithelial cells (MOSEC), a prototype of certain forms of ovarian cancer, were present in larger numbers after co-culture with macrophages treated to a combination of talc and estradiol than to either agent alone or vehicle. Control particles (titanium dioxide, concentrated urban air particulates or diesel exhaust particles) did not have this effect. Co-exposure of macrophages to talc and estradiol has led to increased production of reactive oxygen species and changes in expression of macrophage genes pertinent in cancer development and immunosurveillance. These findings suggest that in vitro exposure to talc, particularly in a high-estrogen environment, may compromise immunosurveillance functions of macrophages and prompt further studies to elucidate this mechanism.

1. Introduction

Macrophages (MΦ) phagocytize foreign particles and destroy malignant cells (Dunn et al., 2004); however, it is not often that these two activities are analyzed in the same context. This study was prompted by the epidemiological observation that cosmetic talc powder may be contributing to the risk of ovarian cancer (OC) (Penninkilampi and Eslick, 2018): we tested the hypothesis that interaction with talc particles compromises the MΦs by reducing their anti-tumor abilities.

Talc (hydrous magnesium silicate) is a mined substance considered 'inert' and used in cosmetic products including baby powder. Until 1970's talcum powder may have been contaminated with asbestos, which prompted the International Agency for Research on Cancer (IARC) to declare it carcinogenic to humans (class 1). Since approximately this time talc has been thought to be asbestos-free; nevertheless the IARC concluded that even talc not containing asbestos is possibly carcinogenic to humans (class 2b) (Baan et al., 2006), however the mechanisms were not entirely clear. Dozens of epidemiologic studies (Booth et al., 1989; Chang and Risch, 1997; Chen et al., 1992; Cook et al., 1997; Cramer et al., 1999; Godard et al., 1998; Harlow et al., 1992; Harlow and Weiss, 1989; Mills et al., 2004; Ness et al., 2000a; Purdie et al., 1995; Rosenblatt et al., 1998; Tzonou et al., 1993; Whittemore et al., 1988; Wong et al., 1999; Gertig et al., 2000; Hankinson et al., 1993) have identified a 35% increase in ovarian cancer (OC) risk for women who used cosmetic talc powder in the genital area (Cramer et al., 2016; Langseth et al., 2008). While the association is being actively debated (Muscat and Huncharek, 2008), a recent epidemiologic study suggests the association is stronger for women who were premenopausal or were postmenopausal but taking estrogen replacement therapy (Cramer et al., 2016). It is estimated that

* Corresponding author. Alpert Medical School of Brown University, Department of Surgery, Division of Surgical Research, Rhode Island Hospital, NAB 210, 593 Eddy Street, Providence, RI, 02903, USA.
E-mail address: alexey@brown.edu (A.V. Fedulov).

https://doi.org/10.1016/j.envres.2019.108676
Received 6 July 2019; Received in revised form 15 July 2019; Accepted 15 August 2019
Available online 22 August 2019
0013-9351/

genital use of talc might account for 10–11% of OC cases in this country each year (Cramer et al., 1999); OC has a significant contribution to the quality of life and surgical burden of disease.

The mechanism behind this link is unknown; but there are some insights. First, there is clear evidence that particles the size of talc, if they are present in the vagina, easily traverse to the upper female genital tract (Henderson et al., 1971; Heller et al., 1996; Edelstam et al., 1997; Sjosten et al., 2004; Cramer et al., 2007; McDonald et al., 2019a, 2019b). Second, the talc association was more apparent in pre-menopausal women and those postmenopausal women who were taking estrogen replacement therapy (Cramer et al., 2016) suggesting higher estrogen may ignite the pathogenesis (Berge et al., 2018). Third, some but not all experimental data suggest that talc particles are not completely innocuous: (NTP, 1993; Hamilton et al., 1984; Frazier-Jessen et al., 1996).

The epidemiologic data are at odds with the perception of talcum powder as a relatively inert, insoluble cosmetic substance that appears to have been well-tested and safe - as a chemical. However it is possible that talc, while it may not be directly mutagenic as a chemical compound (Boorman and Seely, 1995; Pickrell et al., 1989), is a hazardous factor as a particle. The approach and assays we used here stem from our prior interest in particulate matter and how macrophages interact with particles (e.g. (Zhang et al., 2015; Fedulov et al., 2008)); here we focused not on the process of carcinogenesis but rather on the immunotoxic effect of talc. Our hypothesis is that, in a high-estrogen environment, exposure to talc particles alters MΦ functions to permit increased survival of malignant cells. We postulate this could occur via a release of tissue-damaging factors (e.g. reactive oxygen species, ROX) and/or by compromising immunosurveillance abilities of the MΦs and their tumoricidal effectiveness.

2. Materials and methods

We used phagocytic murine cells lines J774 and IC21 and in some experiments RAW264.7 (ATCC; Manassas, VA) as phagocytes. These lines have been historically used to test the effects of female hormones on MΦs with success (Benten et al., 2001a; Pisetsky and Spencer, 2011; Hayashi et al., 1998). The J774 cells are 'chromosomally female' and thus are a better 'prototypical macrophage' for testing of estrogen effects. The IC-21 cell line was obtained by transformation of normal C57BL/6 mouse peritoneal macrophages (Mauel and Defendi, 1971). This line shares many properties with normal mouse MΦ and displays MΦ-specific antigens. IC-21 cells have phagocytic and cytolytic properties, can lyse tumor targets in-vitro (Crawford et al., 1990) and appear to be a terminally differentiated macrophage line (Walker and Demus, 1975; Walker and Gandour, 1980). Hence they are more relevant to OC, however they are 'genetically male' and thus may be less responsive to estrogen although they also express estrogen receptors and respond to estrogen stimulation (Benten et al., 2001b).

These cells were maintained in 100-mm Petri dishes in DMEM (for J774) or RPMI-1640 (for IC21) free of phenol red, supplemented with 10% FBS, 2 mM L-glutamine, penicillin (100 U/mL), streptomycin (100 μg/mL) and 10 mM HEPES.

Tumoricidal efficiency of the MΦ was tested in a standard MΦ-tumor co-culture using the murine ovarian surface epithelial cell line (MOSEC) ID8 (Roby et al., 2000) provided by Dr. Katherine Roby (University of Kansas). ID8 cells most closely resemble human epithelial form of OC, which contributes to 90% of the cases (Roby et al., 2000; Greenaway et al., 2008). We have transduced these cells with an EF1α-GFP lentiviral construct (GenTarget, Inc.) containing Blasticidin-S deaminase and validated that fluorescence was at acceptably stable level in preliminary studies (Fig. 5). These cells were maintained in DMEM with stable L-Glutamine (10-101-CV, Corning) and supplemented with 10% FBS, penicillin (100 U/mL), streptomycin (100 μg/mL), Blasticidin S (10 μg/mL, Gibco) and 'ITS media supplement' containing 1.0 mg/mL recombinant human insulin, 0.55 mg/mL human transferrin (substantially iron-free), and 0.5 μg/mL sodium selenite (1:100) from Sigma-Aldrich.

Talc ($Mg_3Si_4O_{10}(OH)_2$, CAS Registry Number: 14807-96-6, USP grade, particle diameter < 10 μm, was obtained via JT Baker (Batch No: 0000184513) and is certified as asbestos-free. The particles were suspended in PBS and filtered through 30 μm nylon mesh filters (no visible loss of material has occurred). We did not use any commercial talc products.

Titanium dioxide (TiO_2), CAS Registry Number 13463-67-7, control particles (with mean particle size of ~1 μm) were a gift from Dr. L. Kobzik (Harvard School of Public Health, Boston, MA); these were used previously in our studies (Zhang et al., 2015; Fedulov et al., 2008).

Concentrated urban air particles (CAP) were obtained via Harvard School of Public Health particle concentrator (batch #816) and represent urban contaminants typically present in Boston air (Zhou and Kobzik, 2007; Imrich et al., 2000; Sigaud et al., 2007). They were suspended in PBS and used as is without filtering or sterilization.

Diesel exhaust particles (DEP) were generously provided by Dr. Ian Gilmour at the U.S. Environmental Protection Agency and used by us in earlier studies (Fedulov et al., 2008; Gregory et al., 2017). They were also suspended in PBS and used as is without filtering or sterilization.

All particles were of comparable "fine" size although not identical, see Fig. 1. All particles were sonicated on ice to break up clumps using Qsonica Q55 probe sonicator.

Prior to experiments the cells were serum-starved for 24 h in Macrophage-SFM (serum free medium) (Gibco/Life Sciences). Adherent cells (in black-walled 96-well tissue culture treated plates, Corning) were then treated to 17-β estradiol (E2) (cell culture grade, Sigma Aldrich) in a range of concentrations from 10 to 0.0001 μg/mL; ethanol served as vehicle control. Talc (or control particle) suspension was added at the same time as estradiol in doses from 0.1 to 20 μg/well in dose-response experiments and in dose 10 μg/well otherwise. Detection of reactive oxygen species (ROX) was performed after 4 h via Cell ROX Green Flow Cytometry Assay (Molecular Probes). Viability analysis and cell count verification were done after 24 h of incubation via staining with Annexin V and Sytox (Invitrogen). RNA isolation (via RNEasy kit, Qiagen) for gene expression testing was done after 24 h as well.

Co-cultures with MOSEC-GFP cells continued for 72 h; MOSEC-GFP cells were added at 5:1 (MΦ:MOSEC) ratio; particles were almost entirely phagocytized by MΦs by this time (Fig. 1 Panel 2) therefore we do not assume that MOSEC cells were exposed to particles. Medium with fresh estradiol (at the same concentration as the original) was replaced every 24 h to compensate for the estradiol decay. At 72 h the cells were detached (TrypLE, Lonza), washed once with phenol red – free RPMI containing 10% FBS and resuspended in flow cytometry (FACS) buffer (PBS + 0.5% bovine serum albumin, Gibco) for analysis.

Flow cytometry was performed using MACSQuant Analyzer cytometer (Miltenyi) running MACSQuantify Software V2.11. Samples were gated based on their forward and side scatter to exclude the smallest debris and large clumps. The analysis region (gate) distinguished GFP-bright MOSEC cells from mildly autofluorescent MΦ; we calculated percentage and mean fluorescence intensity (MFI) in the GFP channel for the GFP-bright MOSEC region. The integral fluorescence index was calculated as a product of 'percent positive' multiplied by 'MFI value' and reflects the ratio of surviving GFP-MOSEC cells normalized to the number of MΦs in combination with the extent of GFP transgene expression (Csepregi et al., 2018; Kamau et al., 2001). Talc particles did not contribute to the fluorescence signal (Fig. 5).

Microscopy. To visualize engulfment of talc particles the cells were treated with talc suspensions as described. After 24 h the cells were detached by trypsinization, and centrifuged onto standard microscopy slides (VWR) via Cytospin II (Shandon). The slides were fixed with methanol and stained by Diff-Quik, a version of Romanowski stain. The images were made on an Olympus BH-2 light microscope with attachments for polarized light microscopy and an Olympus Q-Color 5 camera. All pictures were taken with the same degree of partially

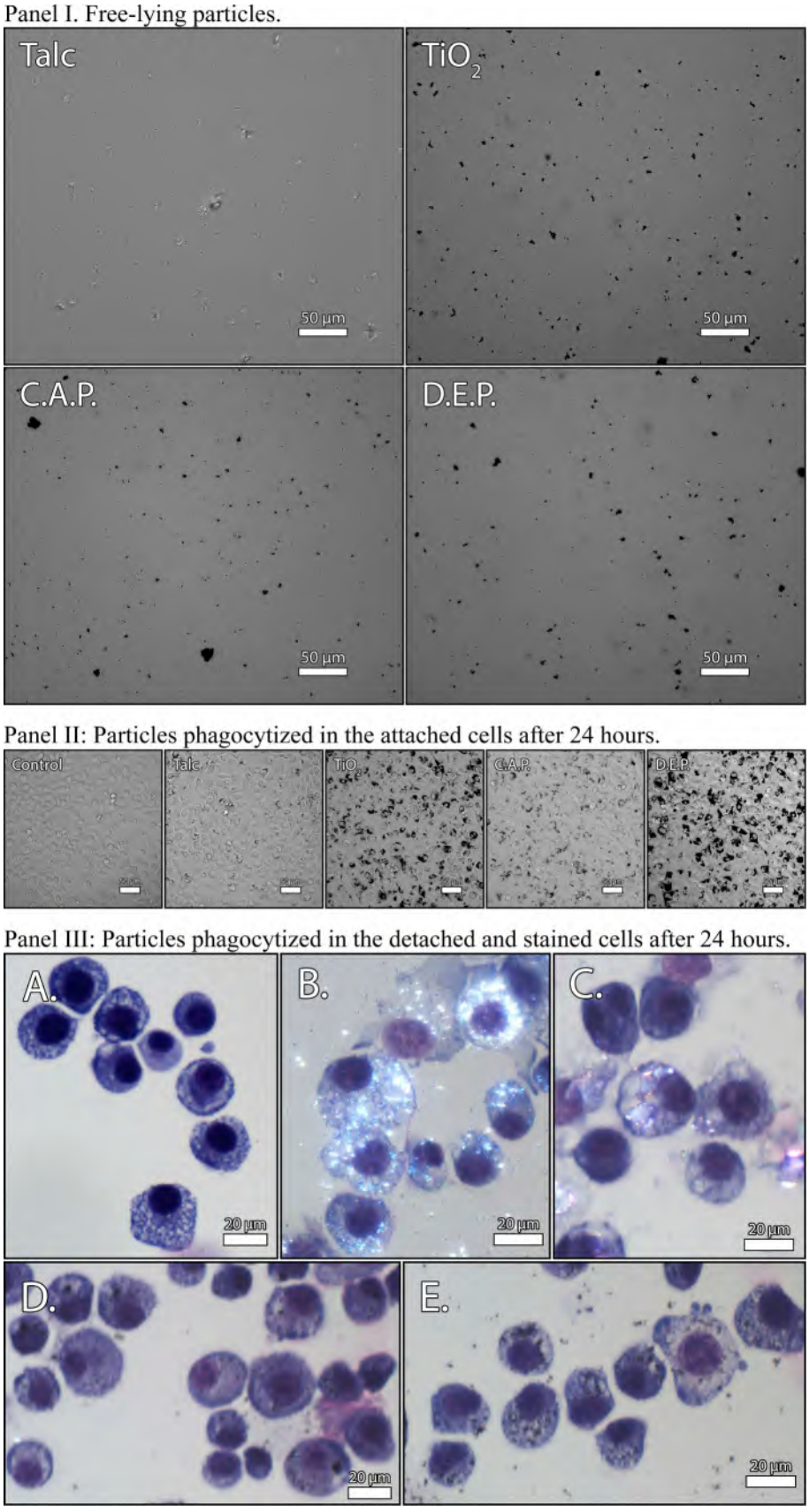

Fig. 1. Microscopic observation of particle phagocytosis.
Panel I: Free-lying particles. Particle suspensions were sonicated and plated freely in 300 μL of PBS, allowed to settle to the bottom for 1 hr and photographed using Nikon Eclipse Ti2 microscope. 400X.
Panel II: Particles phagocytized in the attached cells after 24 hours. Attached cells were treated to particle suspensions and allowed 24 hours to phagocytize. Nikon Eclipse Ti2; 400X.
Panel III: Particles phagocytized in the detached and stained cells after 24 hours. J774 cells without particles (A) and after 24 exposure to TiO_2 (B), talc (C), CAP (D) and DEP (E). Cytospin slides. Staining: Diff-Quik, original magnification for all images: 400X, on all images-bar: 20 μm. Olympus BH-2 light microscope with attachments for polarized light microscopy and an Olympus Q-Color 5 camera. All pictures were taken with the same degree of partially crossed polarizers so that black particles, birefringence of particles, and the cells could be seen. Note that talc and TiO_2 particles are birefringent, and single birefringent particles were seen in CAP and DEP preparations.

crossed polarizers so that black particles, birefringence of particles, and the cells could be observed.

To visualize the co-cultures with fluorescent MOSEC cells with and without talc and control particles we used Nikon Eclipse Ti2 microscope with associated camera and software.

Gene expression profiling was achieved via Cancer PathwayFinder

RT2 Profiler PCR Array (Qiagen) which interrogates 84 cancer-pertinent genes using the CFX96 real-time PCR system (Bio-Rad) and CFX Manager 2.0 software (Bio-Rad). Raw Cq values for all genes (GOI) were normalized to an average of 5 housekeeping genes (HKG): Actb, B2m, Gapdh, Gusb and HSP90ab1 (NormΔCq = (Cq(GOI) - Ave Cq (HKG)). Expression values were obtained using formula 2^(-NormΔCq)*1000. These values were assembled into a matrix to become an input file for statistical analysis via TIGR Mev 4.9 (Saeed et al., 2003). Data were analyzed via Pavlidis Template Matching (PTM) method (Pavlidis and Noble, 2001) using the threshold p-value 0.05. In the heatmaps, red color indicates higher expression, green – low expression; row-normalized color intensity is proportional to the value for each gene in each sample.

All co-culture experiments were repeated more than 3 times. Each measurement was done in duplicate or triplicate. Triplicate RNA samples were selected from one representative experiment for gene expression analysis. Data are presented as Mean ± SEM. Data plotting and statistical analysis (other than array data) was performed using Excel 2007 (Microsoft) and Prism 7.02 (GraphPad Software); statistical significance was accepted when $p < 0.05$. To estimate significance of differences between groups we used the non-parametric Mann-Whitney *U* test, one-way or two-way ANOVA with Tukey, Fisher or HolmeSidak tests, or Kruskal-Wallis ANOVA with Dunn's or Dunnett's test as dictated by the number of groups, data normality and experimental question.

3. Results

3.1. Effect of talc and estradiol on the phagocytes

MΦs were treated with vehicle alone (ethanol), talc alone, estradiol (E2) alone, or the combination of E2 and talc (Fig. 1). Costimulation of MΦs with estradiol (E2) and talc produced an additive effect on ROX production (Fig. 2). While control TiO_2 particles were also phagocytized, the production of ROX was only slightly increased in J774 cells and not increased in IC21 cells (not tested in RAW264.7).

Gene expression profiling was performed via PCR-array aimed at detection of genes relevant in cancer pathways (see Qiagen PAMM-033ZD for the full list). Fig. 3B demonstrates a cluster of genes significantly upregulated by talc in the two types of phagocytes: interestingly in J774 cells the effect of talc was prominent with or without E2, when in IC21 cells the co-effect of talc and E2 is better seen. When examining both cell types, we found patterns of similarity in the increased expression of this set of genes. Quite notably this cluster involves genes of extracellular, outer-membrane and releasable nature that are pertinent in carcinogenesis (see Discussion for details).

Fig. 3A demonstrates a cluster of genes co-inhibited by talc and E2, suggesting a strong co-effect of particles and the hormone, but also (more so for J774 cells) the effect of talc alone. Many of these genes encode intracellular factors pertinent to immunosurveillance, see Discussion for details. Many of the genes (but not all) were affected similarly in all three or in two out of the three cell types we tested.

In summary, talc alone and especially in combination with E2 produced changes in gene expression that may promote pro-tumorigenic environment and less efficient surveillance (tumoricidal) activity of the macrophages.

Exposure of MΦs to talc or E2 did not lead to significant increases in staining with Annexin V or Sytox (Fig. 4) or any noticeable changes in cell numbers in the 24 h period; the exceptionally high doses did occasionally decrease the viability of the MΦs (however slightly), hence we did not employ these concentrations in further experiments. Some variability in this staining is reported in Fig. S2.

3.2. Effect of phagocytes pre-treated with talc and estradiol on MOSEC ID8 cells

Wildtype MOSEC ID8 cells were transduced to express GFP under EF1a promoter. GFP^+ MOSEC ID8 cells were added for 72 h with addition of fresh E2 every 24 h of that period. Visualization of the co-culture was performed via an Eclipse Ti2 UV microscope (Nikon) with associated camera and software (Fig. 5). Detection of surviving GFP^+ MOSEC cells was performed via flow cytometry.

MΦs were treated with particles in the presence of estradiol (E2) or vehicle, as before; in control samples talc was replaced by TiO_2, CAP or DEP particles.

In dose-response experiments we observed that talc and E2 have potentiated the effect, the magnitude varied depending on the MΦ cell line but the findings (Fig. 6) reflect that both substances had dose-response kinetics. IC21 cells did not appear as sensitive to E2 as J774.

Fig. 7 demonstrates that neither particle had a statistically significant cytotoxic effect at 10 μg/well with or without E2 at 24 h (immediately before MOSEC cells were added). We report a microscopic observation that talc-treated cells appeared more fragile than any controls. Microscopically and via flow cytometry we also report that most particles were phagocytized at this timepoint, with only single particulates remaining outside the cells. MOSEC-GFP cells were then added and co-cultured for 72 h.

Our key finding is presented in Fig. 8. A combination of talc and E2 (but not of control particles and E2) has allowed significantly increased MOSEC-GFP readings compared to especially the vehicle-only control where most MOSEC cells were eliminated from the co-culture. Of note, talc alone tended to be effective (albeit not statistically significant in all experiments or pooled data), especially for IC-21 cells. The particles alone (when no MΦs were present) did not significantly affect the numbers of MOSEC cells after 72 h; there was a trend towards a slight decrease in cell numbers (Fig. 7G).

In a subset of experiments (with IC21 cells) we recorded the number

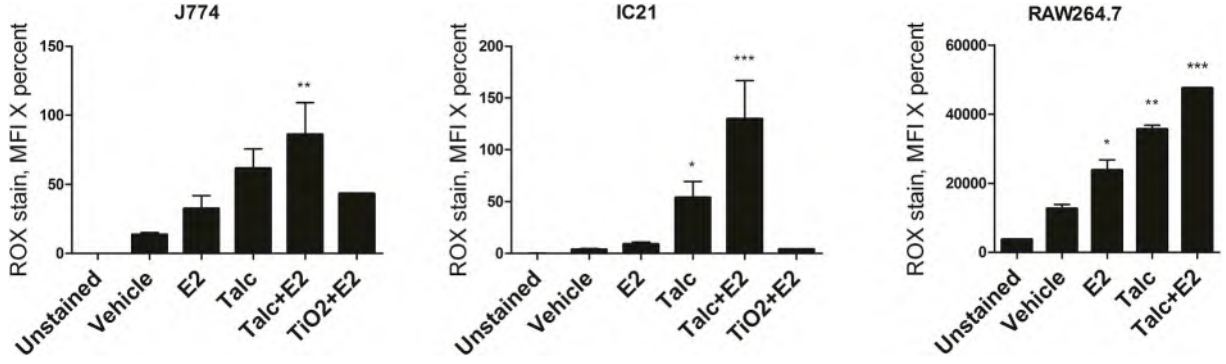

Fig. 2. Production of ROX at 4 h (flow cytometry) was enhanced by either E2 or talc alone, the effect was additive. n = 2/group. *P < 0.05, **P < 0.01, ***P < 0.05 (Tukey).

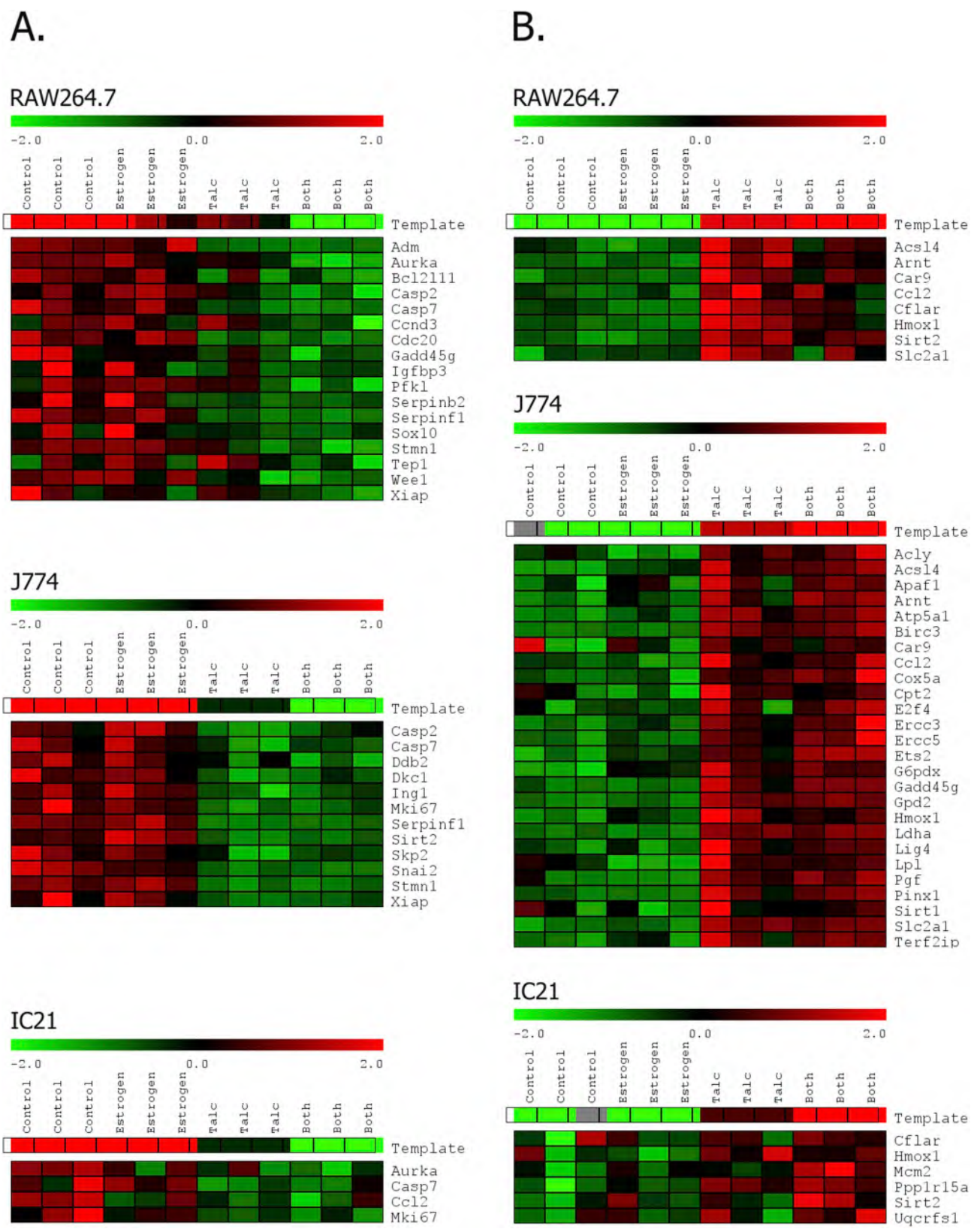

Fig. 3. PCR array profiling at 24 h exposure. Gene expression values were analyzed using Pavlidis Template Matching (PTM) with a threshold p-value of 0.05. Color is proportionate to gene expression (green = lowest, red = highest). A. Inhibitory effect: We aimed to identify genes most inhibited by the combination of estrogen and talc, but also affected by talc particles alone: the expression pattern of Aurka served as the template for RAW264.7 cell samples; matching template values (control: 0.9, estrogen: 0.9, talc: 0.4, both: 0) were used for J774 and IC21 cell samples. B. Stimulatory effect: Similarly, the template (control: 0, estrogen: 0, talc: 0.8, both: 1) aimed to identify targets most upregulated by the combination of estrogen and talc, but as well those increased by talc particles alone. Each sample tested is shown individually: N = 3 per group, total N = 36.

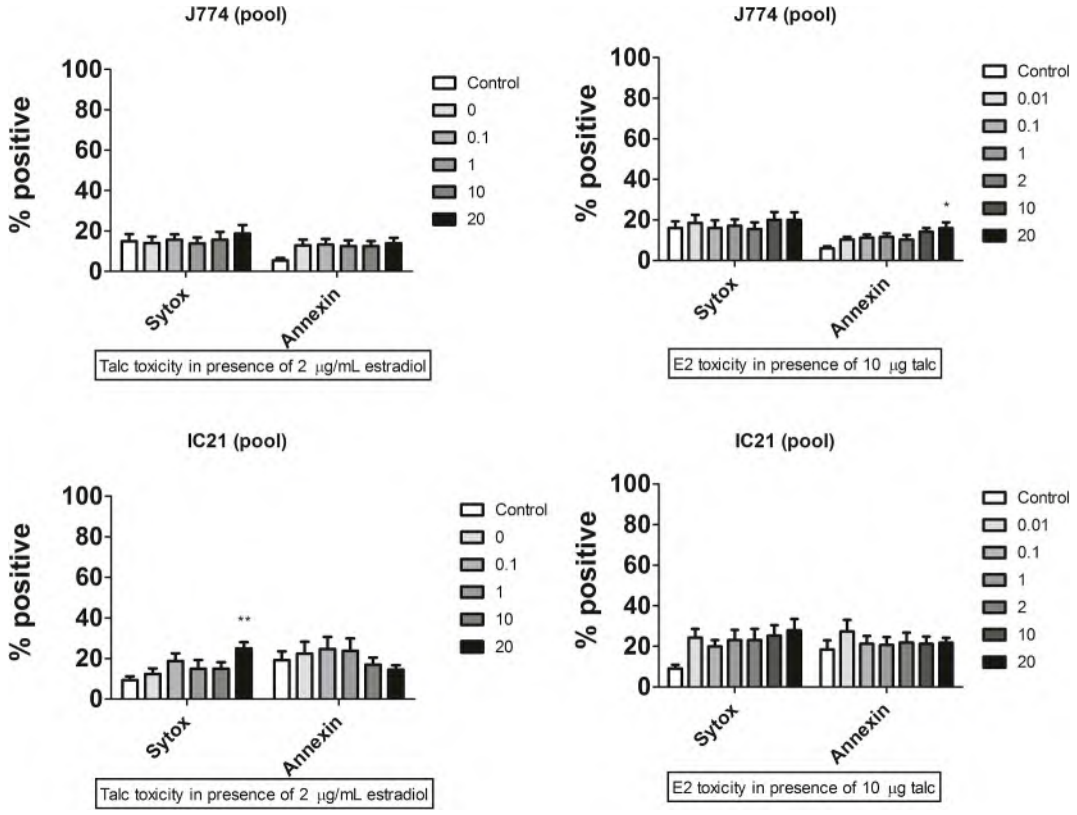

Fig. 4. Dose-response cytotoxicity analysis. Talc and E2 were not significantly toxic to macrophages alone or in combinations used. J774 cells or IC21 cells were exposed for 24 h to either increasing doses of estradiol in presence of 10 µg/well of talc, or to increasing doses of talc in presence of 2 µg/mL of estradiol. Cells were stained for apoptosis and necrosis via Annexin V and Sytox assay kit; flow cytometry determined the percentage of positive cells plotted here. Pooled data from three experiments are shown. n = 6 to 8 per group. *P < 0.05; **P < 0.01 (Dunn).

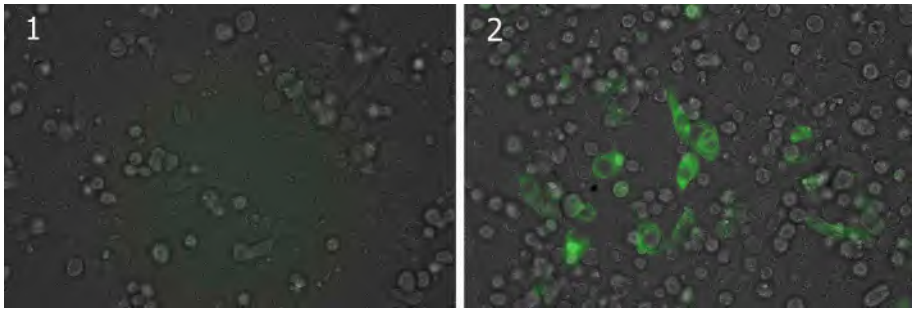

Fig. 5. Co-culture visualization: co-culture of IC21 macrophages with wildtype (1) or GFP$^+$ MOSEC cells (2) with talc photographed at the same setting in the FITC/GFP channel. Magnification X400; Nikon Eclipse Ti2.

of GFP$^+$ MOSEC (per microliter of cytometry buffer) and it was consistently (with fluorescence) higher in the wells where MΦs were treated with Talc + E2 but not with TiO_2 + E2 or E2 alone (Supplementary Fig. 1).

In a validation experiment we used an alternative approach which did not involve a GFP transgene. RAW 264.7 MΦs were treated to talc particles and E2 similarly and co-cultured with wildtype MOSEC cells. After a 72-h co-culture the MOSECs were labeled with Calcein AM whereas the MΦs were labeled with anti- Ly6-C and anti-CD45; a proliferation ratio calculation revealed that the combination of talc and E2 allowed a larger proportion of MOSEC cells than either agent alone (Fig. S3).

In summary, a combination of talc and E2 especially, and in some cases talc alone, affected the MΦs to permit higher MOSEC-GFP survival.

C, D: Cytotoxicity analysis. IC21 or J774 cells were treated to particles alone or in combination with E2 for 24 h and analyzed via Sytox Green and Annexin V PE staining. N = 3 per group.

4. Discussion

This is the first study linking the macrophage, talc particles and estrogen in a potential mechanism to explain the effect of talc behind the ovarian cancer statistics seen in epidemiology studies. Histology of surgically resected tissues shows that in the setting of known exposure, talc has been capable of migrating from the perineum to pelvic lymph nodes, ovary, fallopian tube, uterus and cervix (Cramer et al., 2007; McDonald et al., 2019a, 2019b); however carcinogenicity studies indicated that prolonged exposure to talc inhalation by some experimental animals does not induce cancer (Hamilton et al., 1984; Frazier-Jessen et al., 1996; Boorman and Seely, 1995; Pickrell et al., 1989) although some tumors, tumor-like morphological changes and

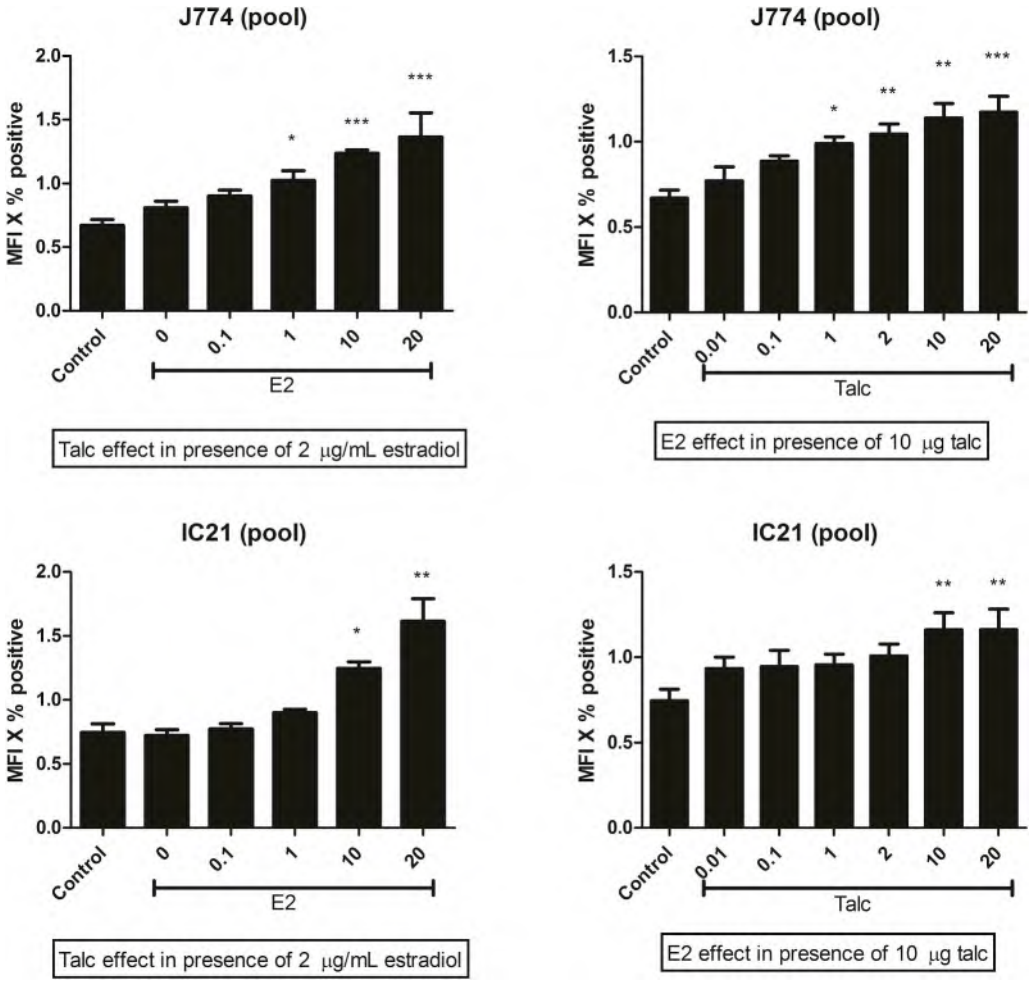

Fig. 6. Dose-response effect in the co-culture. J774 cells or IC21 cells were exposed for 24 h to either increasing doses of estradiol in presence of 10 μg/well of talc, or to increasing doses of talc in presence of 2 μg/mL of estradiol. After preincubation, fluorescent MOSEC ID8 GFP$^+$ cells were added for 72 h; medium and estradiol were replaced every 24 h. Flow cytometry at the end of co-culture recorded the percentage of GFP-positive cells and their MFI; the plots represent the product (MFI X percent). Data values from four experiments were normalized to average and pooled, n = 4/group. *P < 0.05; **P < 0.01; ***P < 0.005 (Dunn).

macrophage activation were reported (Shim et al., 2015; NTP, 1993; Hamilton et al., 1984).

Three particular lines of evidence argue that the estrogen milieu may determine the effects of talc: A) in humans, the talc association was more apparent in premenopausal women and those postmenopausal women who were taking estrogen replacement therapy (Cramer et al., 2016); B) in rodents, lung tumors developed in female, not male rats exposed to talc (NTP, 1993); and C) our own work indicating that estradiol (E2) affects MΦ uptake of particles (Zhang et al., 2015). Notably, there is no literature to suggest asbestos-free talcum powder causes any cancers in men.

Here we focused on the MΦ because A) MΦs are the first to encounter and engulf talc particles; once phagocytized, these particles persist inside the MΦ (Goldner and Adams, 1977); B) MΦs are part of innate immunity responsible for the removal of aberrant, malignant cells (Dunn et al., 2004); they are especially active when primed (Hagemann et al., 2008). C) MΦs produce aggressive molecules capable of driving persistent tissue damage; and D) in patients with ovarian tumors, talc is observed within MΦs (Cramer et al., 2007).

Of note, the literature does not suggest an association of chronic pelvic inflammatory diseases with perineal talc use (Merritt et al., 2008), indicating that typical cytokine pathways are unlikley to make a significant contribution (although inflammation can be a contributing factor in OC (Ness et al., 2000b)). Moreover, in a typical model, the MΦs are co-cultured over a large amount of tumor cells which leads to alternative activation (M2) phenotype, also called tumor-associated MΦs (Hagemann et al., 2006). These cells have distinct expression profiles and may be a suitable model to study processes in *established* tumors, whereas we are focused on the *onset* of the process. We emphasize that E2 pre-treatment does not affect this polarization *per se* (Wang et al., 2015); in our preliminary studies markers of M1 vs. M2 phenotype were unchanged (not shown). This is consistent with our hypothesis that combination of talc and E2 produces an effect in MΦs that is distinct from the heavily studied alterations.

Here we hypothesized that in a high-estrogen environment the talc particles alter MΦ function and decrease the killing of OC cells. We postulated this could occur via either a release of damaging factors that promote formation of aberrant (OC) cells, and/or via compromised immunologic surveillance (tumoricidal) ability of the MΦ, which could allow aberrant cells (that regularly appear in low numbers in the organism) to develop into clinical tumors. The latter premise was supported in part by a report that exposure of MΦs to talc can inhibit their phagocytic activity (Beck et al., 1987).

We found that talc and estradiol co-enhanced the production of ROX which participate in cell growth/proliferation, differentiation, protein synthesis, glucose metabolism and survival of malignant cells (Liou and Storz, 2010); ROX play important role in the pathogenesis of OC (Saed et al., 2017). This finding is consistent with in vivo data (Shim et al.,

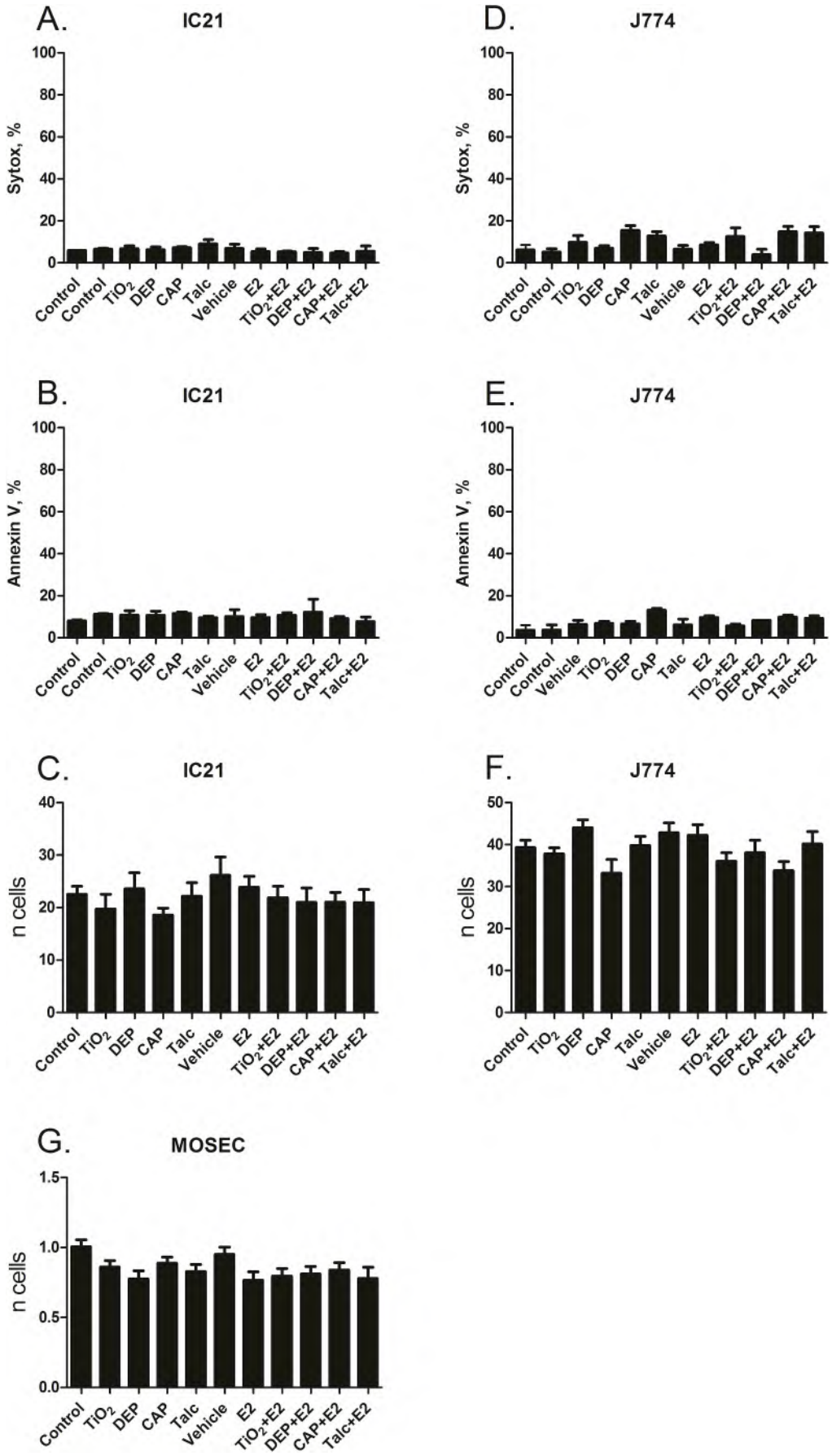

Fig. 7. Cytotoxicity analysis. IC21 cells (A, B) or J774 cells (D, E) were treated to particles alone or in combination with E2 for 24 hrs and analyzed via Sytox Green and Annexin V PE staining. n = 3 per group. Cell number: IC21 (C) or J774 cells (F) were visually counted in a haemocytometer after 24 hr incubation with particles and estrogen. Normalized average of 3 repeat experiments; N = 6 per group for IC21cells, n = 7 per group for J774 cells. G: The effect of particles on cell counts of MOSEC cells treated alone. MOSEC cells were visually counted in a haemocytometer after 72 hr incubation with particles and estrogen. Normalized average of 3 repeat experiments; n = 6 per group.

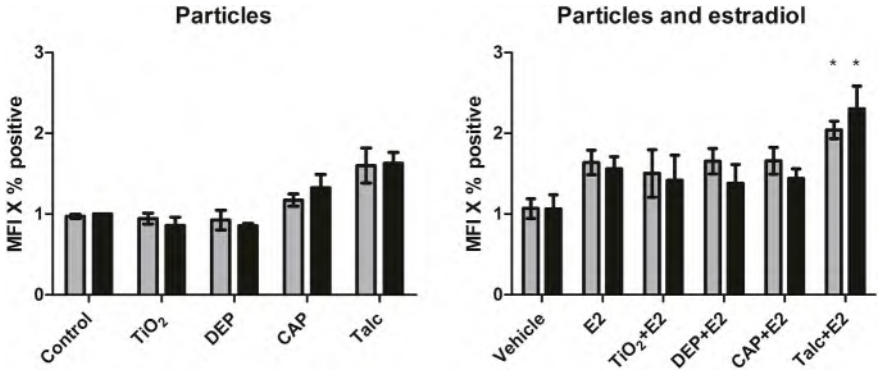

Fig. 8. The effect of talc and control particles in co-culture of MΦ and MOSEC cells. J774 cells or IC21 cells were exposed for 24 h to 2 μg/mL of E2 (or vehicle) and to 10 μg/well of talc, TiO_2, CAP or DEP particles, or combination. After 24-h pre-incubation, fluorescent MOSEC ID8 GFP^+ cells were added for 72 h; medium and estradiol were replaced every 24 h. Flow cytometry at the end of co-culture recorded the percentage of GFP positive cells and their MFI; the plots represent the product (MFI X percent). Data values from three experiments were normalized to control and pooled, n = 3/group. *P < 0.01 vs. Vehicle (two-way ANOVA with Tukey or Holm-Sidak).

2015).

Moreover, talc alone, and to some extent in concert with estradiol has upregulated a cluster of genes that encode factors of releasable, extracellular or outer-membrane nature whose increase alters the extracellular milieu and contributes to tumor growth and metastasis: 1) Carbonic anhydrase *Car9*: enhances extracellular acidity and promotes tumor growth (Swietach et al., 2007, 2009); 2) HMOX1: macrophageal heme oxygenase-1 in tumor microenvironment can dictate cancer growth and metastasis (Nemeth et al., 2015); 3) Solute carrier family 2 facilitated glucose transporter member 1 (SLC2A1), a membraneous protein which promotes tumor cell proliferation and metastasis (Yan et al., 2015); 4) CFLAR, a gene that encodes Cellular FLICE-inhibitory protein (CFLIP), remarkably associated with carcinogenesis including OC (Lozneanu et al., 2015); 5) Sirtuin 2 (SIRT2) – a known therapeutic target in cancer (Jing and Lin, 2016).

At the same time, and perhaps more importantly, we found that talc and estrogen co-inhibited expression of a cluster of genes responsible for intracellular, internal proteins playing a role in anti-tumor immunosurveillance. The cluster includes 1) *Aurka* - Aurora kinase A, an intracellular protein which regulates proliferation and ability to develop the 'anti-tumor' M1 phenotype by the MΦs (Ding et al., 2015; Sica and Mantovani, 2012). 2) *Gadd45g* - Growth arrest and DNA damage-inducible 45, an intracellular protein involved in MΦ maturation; its deficiency causes less efficient tumor immunosurveillance (Schmitz, 2013); although the expression change for this gene was cell-type dependent; 3) Casp7 (Caspase-7) – a protein playing role not only in apoptosis, but also important in MΦ phagocytosis: Casp7-deficient macrophages show impeded completion of phagocytosis (Akhter et al., 2009); 4) CDC20 (Cell division cycle 20) - a regulatory protein shown to be upregulated in MΦ recruited into the tumor and, comparatively, downregulated in those MΦ not engaging with the tumor (Poczobutt et al., 2016); 5) Mki67 – a known proliferation marker; 6) Stmn1 (Stathmin 1) is involved in cell cycle regulation and its inhibition leads to a decrease in proliferation as it is involved in microtubule stability inside the cell (Rubin and Atweh, 2004); Stmn1 affects how MΦs are activated (Xu and Harrison, 2015); interestingly, micro-RNA targeting Stmn1 can be transferred from MΦs to tumor cells (Aucher et al., 2013); 7) XIAP (X-linked inhibitor of apoptosis protein) is important in resistance to cell death in MΦs and is generally involved in MΦ innate immune functions (Rijal et al., 2018).

In combination, our gene expression data indicate both an "outward effect": induction of releasable extracellular deleterious factors, as well as an "internal effect": inhibition of important intracellular factors. Hence, this exploratory profiling has provided us with a hypothesis that together these effects can create preferential conditions for the survival of OC cells in co-culture. Our expression profiling was not comprehensive: a whole transcriptome analysis is needed to uncover full details of the deregulation in the MΦs. We also did not aim to determine whether the changes we found are unique to talc. The focus of our experiments was to demonstrate whether talc is inert when phagocytized in high-estrogen milieu, and we conclude that it is not inert.

In co-culture experiments, we determined that co-exposure of the MΦ to talc and E2 permits higher numbers of OC (MOSEC ID8) cells to survive. We first determined whether E2 and talc had any effect on the MΦ viability in monoculture. Talc or E2 had no toxic effect seen as either apoptosis or necrosis rate, aside of a slight change at 20 μg/mL E2; we have not used this excessive concentration further to assure that the viability of pre-exposed MΦs is the same in all samples. We noted that MΦs, which especially avidly phagocytized talc, had a slight morphological change in appearance, as seen in Fig. 1, which however did not lead to significant changes in counts (Fig. 7).

Hence, we treated the MΦ with a combination of 10 μg talc per well and 2 μg/mL E2, and in subsequent co-culture the fluorescence of GFP^+ MOSEC ID8 cells and their percentage were higher after 72 h (indicating their better survival) compared to controls where MΦ had been treated with vehicle alone or with either agent alone. When talc was replaced with control particles - TiO_2, CAP or DEP, the effect was also not seen (Fig. 8).

In dose-response experiments, the J774 cells, 'chromosomally female', appeared dose-responsively susceptible to the effect of E2 and talc, whereas the 'chromosomally male' IC21 were mostly susceptible to talc. In both cells, we note, even the lowest dose of E2 (1 ng/mL) has boosted (albeit not significantly) the effect of talc.

Because the survival of MOSEC cells is dependent on the number of macrophages in a well we mostly relied on the fluorescence parameters in the FITC/GFP channel, which takes into account the ratio of both cells types as well as the 'brightness' of the GFP transgene as a measure of viability (Csepregi et al., 2018; Kamau et al., 2001). However, in a subset of experiments we also physically counted the MOSEC-GFP^+ cells (see example from one experiment in Fig. S1) and used a transgene-independent method (Fig. S3) and these parameters gave consistent results.

We note that a bolus of 2 μg/mL of E2, although realistic, is likely at the higher end of concentration ranges. In normal mice and humans concentration of circulating E2 in serum is in the range of pg/mL to ng/mL (Wood et al., 2007; Zhang et al., 1999). However tissue levels of steroid hormones may exceed plasma by 20-30-fold (Batra, 1976; Akerlund et al., 1981; Straub, 2007) and ovarian tissue concentration of E2 is more than 100-fold higher than in serum (Lindgren et al., 2002). This may be an indication of why talc use is associated with ovarian cancer rather than at other sites. It is also worth noting that *in-vitro* bioavailability of the hormone from a single administration cannot be directly interpolated dose-wise to the sustained tissue exposure of the resident cells *in-vivo*. We also note that in modeling the effects of E2 sometimes even higher doses have been employed to make for a useful short-term model (Drew and Chavis, 2000).

Our report aims to establish the phenomenon of decreased anti-tumor (anti-MOSEC) activity of the phagocytes after talc and E2 combination pre-treatment; it also partly delineates what further studies are needed to elucidate the specific pathways involved into the inhibition of macrophageal activity. In our study we did not investigate carcinogenic properties of talc *per se*. Studies of other sources and batches of

talc as well as with other cell types are needed for a more comprehensive evaluation of the effect. Further research is needed to determine whether and to what extent the effect of talc on phagocytes exists in vivo, particularly in humans; these studies were beyond the scope of our project. We did not investigate whether the inhibited tumoricidal activity we discovered could entail an increased likelihood of tumor growth. However, we believe our findings can help reconcile the presumed innocuous nature of talc with epidemiological data on talc powder use and OC risk by suggesting that the effect can be mediated by the macrophages.

The findings of this study using phagocytic murine cell lines as prototypical macrophages and MOSECs as prototypical ovarian cancer cells suggest that in vitro exposure to talc particles, particularly in a high-estrogen environment, may compromise the macrophageal immunosurveillance functions. Control particles (titanium dioxide, concentrated urban air particulates or diesel exhaust particles) did not have this effect. Exposure of macrophages to talc and especially co-exposure to talc and estradiol has led to increased production of reactive oxygen species and changes in expression of macrophage genes pertinent in cancer development and immunosurveillance.

Acknowledgements

We thank Dr. Jonathan Reichner, Dr. Alfred Ayala and Dr. Chun-Shiang Chung for helpful discussions.

Abbreviations

MOSEC	murine ovarian surface epithelial cells
DEP	diesel exhaust particles
CAP	concentrated urban air particles
TiO_2	Titanium dioxide
E2	17-β estradiol
ROX	reactive oxygen species
MΦ	macrophage

Data statement

Data supporting the findings may be obtained for academic purposes from the corresponding author upon a reasonable request through the editorial office after disclosure of the conflict of interest.

Funding

The study was supported in part by a pilot project from the Harvard-NIEHS Center [ES-000002] to AVF and by the Particles Research Core of [ES-000002], by Rhode Island Hospital funds to AVF and BWL, by funds from National Institutes of Health NIGMS [P20GM121344] to BWL and by NHLBI T32 [HL134625] to HW. Funding for JJG in his role in this research was provided through John J. Godleski, MD, PLLC.

Declaration of interest

The authors: AM, DJG, CCM, BWL, HW, LMR and AVF have no competing interests. JJG has served as an independent expert and provided expert testimony in talc and other environmentally related litigation.

Appendix A. Supplementary data

Supplementary data to this article can be found online at https://doi.org/10.1016/j.envres.2019.108676.

References

Akerlund, M., Batra, S., Helm, G., 1981. Comparison of plasma and myometrial tissue concentrations of estradiol-17b and progesterone in non-pregnant women. Contraception 23, 447–455 PMID: 7273763.

Akhter, A., Gavrilin, M.A., Frantz, L., Washington, S., Ditty, C., Limoli, D., Day, C., Sarkar, A., Newland, C., Butchar, J., Marsh, C.B., Wewers, M.D., Tridandapani, S., Kanneganti, T.D., Amer, A.O., 2009 Apr. Caspase-7 activation by the Nlrc4/Ipaf inflammasome restricts Legionella pneumophila infection. PLoS Pathog. 5 (4), e1000361 PMID: 19343209.

Aucher, A., Rudnicka, D., Davis, D.M., 2013 Dec 15. MicroRNAs transfer from human macrophages to hepato-carcinoma cells and inhibit proliferation. J. Immunol. 191 (12), 6250–6260 PMID: 24227773.

Baan, R., Straif, K., Grosse, Y., Secretan, B., El Ghissassi, F., Cogliano, V., 2006 Apr. WHO international agency for research on cancer monograph working group. Carcinogenicity of carbon black, titanium dioxide, and talc. Lancet Oncol. 7 (4) 295–6. No abstract available. Erratum in: Lancet Oncol. 2006 May;7(5):365. PMID: 16598890.

Batra, S., 1976. Unconjugated estradiol in the myometrium of pregnancy. Endocrinology 99, 1178–1181 PMID: 991813.

Beck, B.D., Feldman, H.A., Brain, J.D., Smith, T.J., Hallock, M., Gerson, B., 1987 Feb. The pulmonary toxicity of talc and granite dust as estimated from an in vivo hamster bioassay. Toxicol. Appl. Pharmacol. 87 (2), 222–234 PMID: 3029896.

Benten, W.P., Stephan, C., Lieberherr, M., Wunderlich, F., 2001 Apra. Estradiol signaling via sequestrable surface receptors. Endocrinology 142 (4), 1669–1677 PMID: 11250949.

Benten, W.P., Stephan, C., Lieberherr, M., Wunderlich, F., 2001 Aprb. Estradiol signaling via sequestrable surface receptors. Endocrinology 142 (4), 1669–1677 PMID: 11250949.

Berge, W., Mundt, K., Luu, H., Boffetta, P., 2018 May. Genital use of talc and risk of ovarian cancer: a meta-analysis. Eur. J. Cancer Prev. 27 (3), 248–257 PMID: 28079603.

Boorman, G.A., Seely, J.C., 1995 Apr. The lack of an ovarian effect of lifetime talc exposure in F344/N rats and B6C3F1 mice. Regul. Toxicol. Pharmacol. 21 (2), 242–243 PMID: 7644712.

Booth, M., Beral, V., Smith, P., 1989. Risk factors for ovarian cancer: a case-control study. Br. J. Canc. 60, 592–598 PMC2247100.

Chang, S., Risch, H.A., 1997. Perineal talc exposure and risk of ovarian carcinoma. Cancer 79, 2396–2401 PMID: 9191529.

Chen, Y., Wu, P.C., Lang, J.H., Ge, W.J., Hartge, P., Brinton, L.A., 1992. Risk factors for epithelial ovarian cancer in Beijing, China. Int. J. Epidemiol. 21, 23–29 PMID: 1544753.

Cook, L.S., Kamb, M.L., Weiss, N.S., 1997. Perineal powder exposure and the risk of ovarian cancer. Am. J. Epidemiol. 145, 459–465 PMID: 9048520.

Cramer, D.W., Liberman, R.F., Titus-Ernstoff, L., Welch, W.R., Greenberg, E.R., Baron, J.A., Harlow, B.L., 1999. Genital talc exposure and risk of ovarian cancer. Int. J. Cancer 81, 351–356 PMID: 10209948.

Cramer, D.W., Welch, W.R., Berkowitz, R.S., Godleski, J.J., 2007 Aug. Presence of talc in pelvic lymph nodes of a woman with ovarian cancer and long-term genital exposure to cosmetic talc. Obstet. Gynecol. 110 (2 Pt 2), 498–501 PMID: 17666642.

Cramer, D.W., Vitonis, A.F., Terry, K.L., Welch, W.R., Titus, L.J., 2016 May. The association between talc use and ovarian cancer: a retrospective case-control study in two US states. Epidemiology 27 (3), 334–346 PMC4820665.

Crawford, E.K., Latham, P.S., Shah, E.M., Hasday, J.D., 1990. Characterization of tumor binding by the IC-21 macrophage cell line. Cancer Res. 50, 4578–4583 PMID: 2164442.

Csepregi, R., Temesfői, V., Poór, M., Faust, Z., Kőszegi, T., 2018 Jun 28. Green fluorescent protein-based viability assay in a multiparametric configuration. Molecules 23 (7) pii: E1575. PMC6100089.

Ding, L., Gu, H., Gao, X., Xiong, S., Zheng, B., 2015 Apr. Aurora kinase a regulates m1 macrophage polarization and plays a role in experimental autoimmune encephalomyelitis. Inflammation 38 (2), 800–811 PMID:25227280.

Drew, P.D., Chavis, J.A., 2000. Female sex steroids: effects upon microglial cell activation. J. Neuroimmunol. 111, 77–85 PMID: 11063824.

Dunn, G.P., Old, L.J., Schreiber, R.D., 2004. The three Es of cancer immunoediting. Annu. Rev. Immunol. 22, 329–360 PMID: 15032581.

Edelstam, G.A., Sjösten, A.C., Ellis, H., 1997. Retrograde migration of starch in the genital tract of rabbits. Inflammation 21, 489–499 PMID: 9343747.

Fedulov, A.V., Leme, A., Yang, Z., Dahl, M., Mariani, T.J., Kobzik, L., 2008. Pulmonary exposure to particles during pregnancy causes increased neonatal asthma susceptibility. Am. J. Respir. Cell Mol. Biol. 38 (1), 57–67 PMID: 17656681.

Frazier-Jessen, M.R., Mott, F.J., Witte, P.L., Kovacs, E.J., 1996 Apr 15. Estrogen suppression of connective tissue deposition in a murine model of peritoneal adhesion formation. J. Immunol. 156 (8), 3036–3042 PMID: 8609426.

Gertig, D.M., Hunter, D.J., Cramer, D.W., Colditz, G.A., Speizer, F.E., Willett, W.C., Hankinson, S.E., 2000. Prospective study of talc use and ovarian cancer. J. Natl. Cancer Inst. 92, 249–252 PMID: 10655442.

Godard, B., Foulkes, W.D., Provencher, D., Brunet, J.S., Tonin, P.N., Mes-Masson, A.M., Narod, S.A., Ghadirian, P., 1998. Risk factors for familial and sporadic ovarian cancer among French Canadians: a case-control study. Am. J. Obstet. Gynecol. 179, 403–410 PMID: 9731846.

Goldner, R.D., Adams, D.O., 1977. The structure of mononuclear phagocytes differentiating in vivo. III. The effect of particulate foreign substances. Am. J. Pathol. 89, 335–350 PMCID: PMC2032242.

Greenaway, J., Moorehead, R., Shaw, P., Petrik, J., 2008 Feb. Epithelial-stromal interaction increases cell proliferation, survival and tumorigenicity in a mouse model of human epithelial ovarian cancer. Gynecol. Oncol. 108 (2), 385–394 PMID: 18036641.

Gregory, D.J., Kobzik, L., Yang, Z., McGuire, C.C., Fedulov, A.V., 2017 Aug 1.

Transgenerational transmission of asthma risk after exposure to environmental particles during pregnancy. Am. J. Physiol. Lung Cell Mol. Physiol. 313 (2), L395–L405. https://doi.org/10.1152/ajplung.00035.2017. PMID: 28495853.

Hagemann, T., Wilson, J., Burke, F., Kulbe, H., Li, N.F., Plüddemann, A., Charles, K., Gordon, S., Balkwill, F.R., 2006 Apr 15. Ovarian cancer cells polarize macrophages toward a tumor-associated phenotype. J. Immunol. 176 (8), 5023–5032 PMID: 16585599.

Hagemann, T., Lawrence, T., McNeish, I., Charles, K.A., Kulbe, H., Thompson, R.G., Robinson, S.C., Balkwill, F.R., 2008 Jun 9. "Re-educating" tumor-associated macrophages by targeting NF-kappaB. J. Exp. Med. 205 (6), 1261–1268.

Hamilton, T.C., Fox, H., Buckley, C.H., Henderson, W.J., Griffiths, K., 1984 Feb. Effects of talc on the rat ovary. Br. J. Exp. Pathol. 65 (1), 101–106 PMCID: PMC2040939.

Hankinson, S.E., Hunter, D.J., Colditz, G.A., Willett, W.C., Stampfer, M.J., Rosner, B., Hennekens, C.H., Speizer, F.E., 1993. Tubal ligation, hysterectomy, and risk of ovarian cancer. A prospective study, vol. 270. pp. 2813–2818 PMID: 8133619.

Harlow, B.L., Weiss, N.S., 1989. A case-control study of borderline ovarian tumors: the influence of perineal exposure to talc. Am. J. Epidemiol. 130, 390–394 PMID: 2750733.

Harlow, B.L., Cramer, D.W., Bell, D.A., Welch, W.R., 1992. Perineal exposure to talc and ovarian cancer risk. Obstet. Gynecol. 80, 19–26 PMID: 1603491.

Hayashi, T., Yamada, K., Esaki, T., Muto, E., Chaudhuri, G., Iguchi, A., 1998 Feb. Physiological concentrations of 17beta-estradiol inhibit the synthesis of nitric oxide synthase in macrophages via a receptor-mediated system. J. Cardiovasc. Pharmacol. 31 (2), 292–298 PMID: 9475272.

Heller, D.S., Westhoff, C., Gordon, R.E., Katz, N., 1996. The relationship between perineal cosmetic talc usage and ovarian talc particle burden. Am. J. Obstet. Gynecol. 174, 1507–1510 PMID: 9065120.

Henderson, W.J., Joslin, C.A., Turnbull, A.C., Griffiths, K., 1971. Talc and carcinoma of the ovary and cervix. J. Obstet. Gynaecol. Br. Commonw. 78, 266–272 PMID: 5558843.

Imrich, A., Ning, Y., Kobzik, L., 2000 Sep 1. Insoluble components of concentrated air particles mediate alveolar macrophage responses in vitro. Toxicol. Appl. Pharmacol. 167 (2), 140–150 PMID: 10964765.

Jing, H., Lin, H., 2016 Apr 26. Lessons learned from a SIRT2-selective inhibitor. Oncotarget 7 (17), 22971–22972 PMC5029603.

Kamau, S.W., Grimm, F., Hehl, A.B., 2001 Dec. Expression of green fluorescent protein as a marker for effects of antileishmanial compounds in vitro. Antimicrob. Agents Chemother. 45 (12), 3654–3656 PMC90892.

Langseth, H., Hankinson, S.E., Siemiatycki, J., Weiderpass, E., 2008 Apr. Perineal use of talc and risk of ovarian cancer. J. Epidemiol. Community Health 62 (4), 358–360 PMID: 18339830.

Lindgren, P.R., Bäckström, T., Cajander, S., Damber, M.G., Mählck, C.G., Zhu, D., Olofsson, J.I., 2002 Sep. The pattern of estradiol and progesterone differs in serum and tissue of benign and malignant ovarian tumors. Int. J. Oncol. 21 (3), 583–589 PMID: 12168103.

Liou, G.Y., Storz, P., 2010 May. Reactive oxygen species in cancer. Free Radic. Res. 44 (5), 479–496 PMID: 20370557.

Lozneanu, L., Cojocaru, E., Giuşcă, S.E., Cărăuleanu, A., Căruntu, I.D., 2015. Lesser-known molecules in ovarian carcinogenesis. BioMed Res. Int. 2015, 321740 PMC4538335.

Mauel, J., Defendi, V., 1971. Infection and transformation of mouse peritoneal macrophages by simian virus 40. J. Exp. Med. 134, 335–350 PubMed: 4326994.

McDonald, S.A., Fan, Y., Welch, W.R., Cramer, D.W., Godleski, J.J., 2019b. Migration of talc from the perineum to multiple pelvic organ sites: five case studies with correlative light and scanning electron microscopy. Am. J. Clin. Pathol. https://doi.org/10.1093/AJCP/AQZ080.

McDonald, S.A., Fan, Y., Welch, W.R., Cramer, D.W., Stearns, R.C., Sheedy, L., Katler, M., Godleski, J.J., 2019a. Correlative polarizing light and scanning electron microscopy for the assessment of talc in pelvic lymph nodes. Ultrastruct. Pathol. 43, 13–27. https://doi.org/10.1080/01913123.2019.1593271.

Merritt, M.A., Green, A.C., Nagle, C.M., Webb, P.M., 2008 Jan 1. Australian Cancer Study (Ovarian Cancer); Australian Ovarian Cancer Study Group. Talcum powder, chronic pelvic inflammation and NSAIDs in relation to risk of epithelial ovarian cancer. Int. J. Cancer 122 (1), 170–176 PMID: 17721999.

Mills, P.K., Riordan, D.G., Cress, R.D., Young, H.A., 2004. Perineal talc exposure and epithelial ovarian cancer risk in the Central Valley of California. Int. J. Cancer 112, 458–464 PMID: 15382072.

Muscat, J.E., Huncharek, M.S., 2008 Apr. Eur. J. Cancer Prev. 17 (2), 139–146 Perineal talc use and ovarian cancer: a critical review. PMC3621109.

Nemeth, Z., Li, M., Csizmadia, E., Döme, B., Johansson, M., Persson, J.L., Seth, P., Otterbein, L., Wegiel, B., 2015 Oct 20. Heme oxygenase-1 in macrophages controls prostate cancer progression. Oncotarget 6 (32), 33675–33688 PMID:26418896.

Ness, R.B., Grisso, J.A., Cottreau, C., Klapper, J., Vergona, R., Wheeler, J.E., Morgan, M., Schlesselman, J.J., 2000a. Factors related to inflammation of the ovarian epithelium and risk of ovarian cancer. Epidemiology 11, 111–117 PMID: 11021606.

Ness, R.B.1, Grisso, J.A., Cottreau, C., Klapper, J., Vergona, R., Wheeler, J.E., Morgan, M., Schlesselman, J.J., 2000 Marb. Factors related to inflammation of the ovarian epithelium and risk of ovarian cancer. Epidemiology 11 (2), 111–117 PMID: 11021606.

NTP, 1993. Toxicology and Carcinogenesis Studies of Talc (CAS N° 14807-96-6) (Non-asbestiform) in F344/N Rats and B6C3F1 Mice (Inhalation Studies). National Toxicology Program TR-421 Research Triangle Park, NC.

Pavlidis, P., Noble, W.S., 2001. Analysis of strain and regional variation in gene expression in mouse brain. Genome Biol. 2 research0042.1-0042.15.

Penninkilampi, R., Eslick, G.D., 2018 Jan. Perineal talc use and ovarian cancer: a systematic review and meta-analysis. Epidemiology 29 (1), 41–49 PMID: 28863045.

Pickrell, J.A., Snipes, M.B., Benson, J.M., Hanson, R.L., Jones, R.K., Carpenter, R.L., Thompson, J.J., Hobbs, C.H., Brown, S.C., 1989 Aug. Talc deposition and effects after 20 days of repeated inhalation exposure of rats and mice to talc. Environ. Res. 49 (2), 233–245 PMID: 2753008.

Pisetsky, D.S., Spencer, D.M., 2011 Sep. Effects of progesterone and estradiol sex hormones on the release of microparticles by RAW 264.7 macrophages stimulated by Poly(I:C). Clin. Vaccine Immunol. 18 (9), 1420–1426 REF PMC3165218.

Poczobutt, J.M., De, S.1, Yadav, V.K.1, Nguyen, T.T.1, Li, H.2, Sippel, T.R.1, Weiser-Evans, M.C.3, Nemenoff, R.A.4, 2016 Mar 15. Expression profiling of macrophages reveals multiple populations with distinct biological roles in an immunocompetent orthotopic model of lung cancer. J. Immunol. 196 (6), 2847–2859 PMID: 26873985.

Purdie, D., Green, A., Bain, C., Siskind, V., Ward, B., Hacker, N., Quinn, M., Wright, G., Russell, P., Susil, B., 1995. Reproductive and other factors and risk of epithelial ovarian cancer: an Australian case-control study. Survey of Women's Health Study Group, vol. 62. pp. 678–684 PMID: 7558414.

Rijal, D., Ariana, A., Wight, A., Kim, K., Alturki, N.A., Aamir, Z., Ametepe, E.S., Korneluk, R.G., Tiedje, C., Menon, M.B., Gaestel, M., McComb, S., Sad, S., 2018 Jul 27. Differentiated macrophages acquire a pro-inflammatory and cell death-resistant phenotype due to increasing XIAP and p38-mediated inhibition of RipK1. J. Biol. Chem. 293 (30), 11913–11927 PMID: 29899110.

Roby, K.F., Taylor, C.C., Sweetwood, J.P., Cheng, Y., Pace, J.L., Tawfik, O., Persons, D.L., Smith, P.G., Terranova, P.F., 2000 Apr. Development of a syngeneic mouse model for events related to ovarian cancer. Carcinogenesis 21 (4), 585–591.

Rosenblatt, K.A., Mathews, W.A., Daling, J.R., Voigt, L.F., Malone, K., 1998. Characteristics of women who use perineal powders. Obstet. Gynecol. 92, 753–756 PMID: 9794663.

Rubin, C.I., Atweh, G.F., 2004 Oct 1. The role of stathmin in the regulation of the cell cycle. J. Cell. Biochem. 93 (2), 242–250 PMID: 15368352.

Saed, G.M., Diamond, M.P., Fletcher, N.M., 2017 Jun. Updates of the role of oxidative stress in the pathogenesis of ovarian cancer. Gynecol. Oncol. 145 (3), 595–602 PMID: 28237618.

Saeed, A.I., Sharov, V., White, J., Li, J., Liang, W., Bhagabati, N., Braisted, J., Klapa, M., Currier, T., Thiagarajan, M., Sturn, A., Snuffin, M., Rezantsev, A., Popov, D., Ryltsov, A., Kostukovich, E., Borisovsky, I., Liu, Z., Vinsavich, A., Trush, V., Quackenbush, J., 2003 Feb. TM4: a free, open-source system for microarray data management and analysis. Biotechniques 34 (2), 374–378.

Schmitz, I., 2013. Gadd45 proteins in immunity. Adv. Exp. Med. Biol. 793, 51–68 24104473.

Shim, I., Kim, H.M., Yang, S., Choi, M., Seo, G.B., Lee, B.W., Yoon, B.I., Kim, P., Choi, K., 2015 Nov-Dec. Inhalation of talc induces infiltration of macrophages and upregulation of manganese superoxide dismutase in rats. Int. J. Toxicol. 34 (6), 491–499 PMID: 26482432.

Sica, A., Mantovani, A., 2012 Mar. Macrophage plasticity and polarization: in vivo veritas. J. Clin. Investig. 122 (3), 787–795 PMC3287223.

Sigaud, S., Goldsmith, C.A., Zhou, H., Yang, Z., Fedulov, A., Imrich, A., Kobzik, L., 2007 Aug 15. Air pollution particles diminish bacterial clearance in the primed lungs of mice. Toxicol. Appl. Pharmacol. 223 (1), 1–9 PMID: 17561223.

Sjosten, A.C., Ellis, H., Edelstam, G.A., 2004. Retrograde migration of glove powder in the human female genital tract. Hum. Reprod. 19, 991–995 PMID: 15033954.

Straub, R.H., 2007. Complex role of estrogens in inflammation. Endocr. Rev. 28, 521–574 PMID: 17640948.

Swietach, P., Vaughan-Jones, R.D., Harris, A.L., 2007 Jun. Regulation of tumor pH and the role of carbonic anhydrase 9. Cancer Metastasis Rev. 26 (2), 299–310 PMID: 17415526.

Swietach, P., Patiar, S., Supuran, C.T., Harris, A.L., Vaughan-Jones, R.D., 2009 Jul 24. The role of carbonic anhydrase 9 in regulating extracellular and intracellular ph in three-dimensional tumor cell growths. J. Biol. Chem. 284 (30), 20299–20310 PMC2740455.

Tzonou, A., Polychronopoulou, A., Hsieh, C.C., Rebelakos, A., Karakatsani, A., Trichopoulos, D., 1993. Hair dyes, analgesics, tranquilizers and perineal talc application as risk factors for ovarian cancer. Int. J. Cancer 55, 408–410 PMID: 8375924.

Walker, W.S., Demus, A., 1975. Antibody-dependent cytolysis of chicken erythrocytes by an in vitro- established line of mouse peritoneal macrophages. J. Immunol. 114, 765–769 PMID: 1167563.

Walker, W.S., Gandour, D.M., 1980. Detection and functional assessment of complement receptors on two murine macrophage-like cell lines. Exp. Cell Res. 129, 15–21 PMID: 7428810.

Wang, Y., Chen, H., Wang, N., Guo, H., Fu, Y., Xue, S., Ai, A., Lyu, Q., Kuang, Y., 2015 May 7. Combined 17β-estradiol with TCDD promotes M2 polarization of macrophages in the endometriotic milieu with aid of the interaction between endometrial stromal cells and macrophages. PLoS One 10 (5), e0125559 PMCID: PMC4423913.

Whittemore, A.S., Wu, M.L., Paffenbarger Jr., R.S., Sarles, D.L., Kampert, J.B., Grosser, S., Jung, D.L., Ballon, S., Hendrickson, M., 1988. Personal and environmental characteristics related to epithelial ovarian cancer. II. Exposures to talcum powder, tobacco, alcohol, and coffee. Am. J. Epidemiol. 128, 1228–1240 PMID: 3195564.

Wong, C., Hempling, R.E., Piver, M.S., Natarajan, N., Mettlin, C.J., 1999. Perineal talc exposure and subsequent epithelial ovarian cancer: a case-control study. Obstet. Gynecol. 93, 372–376 PMID: 10074982.

Wood, G.A., Fata, J.E., Watson, K.L., Khokha, R., 2007. Circulating hormones and estrous stage predict cellular and stromal remodeling in murine uterus. Reproduction 133, 1035–1044 PMID: 17616732.

Xu, K., Harrison, R.E.2, 2015 Jul 31. Down-regulation of stathmin is required for the phenotypic changes and classical activation of macrophages. J. Biol. Chem. 290 (31), 19245–19260 PMID: 26082487.

Yan, S., Wang, Y., Chen, M., Li, G., Fan, J., 2015 Jul 16. Deregulated SLC2A1 promotes tumor cell proliferation and metastasis in gastric cancer. Int. J. Mol. Sci. 16 (7), 16144–16157 PMCID: PMC4519943.

Zhang, L., Fishman, M.C., Huang, P.L., 1999. Estrogen mediates the protective effects of pregnancy and chorionic gonadotropin in a mouse model of vascular injury. Arterioscler. Thromb. Vasc. Biol. 19, 2059–2065 PMID: 10479646.

Zhang, Y., Mikhaylova, L., Kobzik, L., Fedulov, A.V., 2015. Estrogen-mediated impairment of macrophageal uptake of environmental TiO2 particles to explain inflammatory effect of TiO2 on airways during pregnancy. J. Immunotoxicol. 12 (1), 81–91 PMID: 24825546.

Zhou, H., Kobzik, L., 2007 Apr. Effect of concentrated ambient particles on macrophage phagocytosis and killing of Streptococcus pneumoniae. Am. J. Respir. Cell Mol. Biol. 36 (4), 460–465 PMID: 17079778.

Exhibit 106

EPIGENETICS
2021, VOL. 16, NO. 10, 1053–1070
https://doi.org/10.1080/15592294.2020.1834925

Taylor & Francis
Taylor & Francis Group

RESEARCH PAPER

Transcriptomic and epigenomic effects of insoluble particles on J774 macrophages

T. Emi[a*], L. M. Rivera[a,b*], V. C. Tripathi [a], N. Yano[a], A. Ragavendran[c], J. Wallace [c], and Alexey V. Fedulov[a]

[a]Alpert Medical School of Brown University. Department of Surgery, Division of Surgical Research, Rhode Island Hospital. Providence, RI, USA; [b]Department of Biology, University of Puerto Rico, San Juan, Puerto Rico; [c]Computational Biology Core, COBRE Center for Computational Biology of Human Disease, Brown University, Providence, RI, USA

ABSTRACT

Here we report epigenomic and transcriptomic changes in a prototypical J774 macrophage after engulfing talc or titanium dioxide particles in presence of estrogen. Macrophages are the first immune cells to engage and clear particles of various nature. A novel paradigm is emerging, that exposure to so-called 'inert' particulates that are considered innocuous is not really free of consequences. We hypothesized that especially the insoluble, non-digestible particles that do not release a known hazardous chemical can be underappreciated agents acting to affect the regulation inside macrophages upon phagocytosis. We performed gene chip microarray profiling and found that talc alone, and especially with oestrogen, has induced a substantially more prominent gene expression change than titanium dioxide; the affected genes were involved in pathways of cell proliferation, immune response and regulation, and, unexpectedly, enzymes and proteins of epigenetic regulation. We therefore tested the DNA methylation profiles of these cells via epigenome-wide bisulphite sequencing and found vast epigenetic changes in hundreds of loci, remarkably after a very short exposure to particles; ELISA assay for methylcytosine levels determined the particles induced an overall decrease in DNA methylation. We found a few loci where both the transcriptional changes and epigenetic changes occurred in the pathways involving immune and inflammatory signalling. Some transcriptomic and epigenomic changes were shared between talc and titanium dioxide, however, it is especially interesting that each of the two particles of similar size and insoluble nature has also induced a specific pattern of gene expression and DNA methylation changes which we report here.

ARTICLE HISTORY
Received 17 July 2020
Revised 13 September 2020
Accepted 29 September 2020

KEYWORDS
DNA methylation; RRBS; macrophages; talc particles; titanium dioxide particles; epigenomic; transcriptomic; ovarian cancer; asthma

Introduction

Epigenetic regulation plays an important role in maturation and functioning of phagocytes [1]; however, short-term epigenetic changes that occur during phagocytosis have not been studied. The data that engulfment of certain bacteria lead to epigenetic changes in the macrophages (MΦ) [2] led us to hypothesize that phagocytosis of any particle can be associated with DNA methylation changes.

MΦs engulf particles quickly and to the extent that they can become overloaded; this especially occurs when particles are non-digestible [3–5]. Uptake and especially persistence of non-digested particles may contribute to disease by activating or inhibiting mechanisms in the MΦs. We sought to test this paradigm using two types of insoluble particles, generally considered 'immunologically inert' and vastly used in cosmetics and food products: talc (T) and titanium dioxide (TiO2); they are recently becoming recognized as not entirely innocuous. Previously we show that talc particles, especially in the context of increased oestrogen (E) levels, impair the tumoricidal function of MΦ allowing more ovarian cancer cells in a co-culture [6]; the study aims to provide a feasible mechanistic explanation to the intriguing epidemiological data linking talcum powder with ovarian cancer [7]. In another model, we linked the exposure to titanium dioxide (TiO2) particles and airway inflammation, again seen more so at high oestrogen levels [8,9]. While in both models the MΦ is a key and primary cell engaging the

CONTACT Alexey V. Fedulov alexey@brown.edu Alpert Medical School of Brown University. Division of Surgical Research, Rhode Island Hospital, Providence, RI 02903, USA

*These authors contributed equally to this work.

Supplemental data for this article can be accessed here.

particles, the mechanisms affected by T or TiO2 in the MΦ remained unknown.

Here we performed epigenomic and transcriptomic analysis of prototypical macrophages (J774) after incubation with talc or TiO2 particles with or without oestrogen to determine expression and methylation signatures resulting from these exposures and to detect potential biological pathways that could explain the pro-cancer and pro-inflammatory changes in the MΦs.

Materials and methods

We used phagocytic murine **cells line** J774 (ATCC; Manassas, VA): these 'chromosomally female' cells have been widely used as a macrophage/phagocyte model cell line [10,11] including studies of particle phagocytosis (e.g [12].), and of the effects of female hormones on macrophage responses [13] including our own prior studies [6,9]. The cells were maintained in 100-mm Petri dishes in DMEM (for J774) free of phenol red, supplemented with 10% FBS, 2 mM L-glutamine, penicillin (100 U/mL), streptomycin (100 µg/mL) and 10 mM HEPES. Prior to experiments, the cells were serum-starved for 48 hrs. in Macrophage-SFM (serum-free medium) (Gibco/Life Sciences). Adherent cells in tissue culture plates (Corning) were then treated to 2 µg/mL of 17-β oestradiol (E2) (cell culture grade, Sigma Aldrich) or ethanol used as vehicle control; the following day they were treated to talc and TiO2 particles as follows.

Talc ($Mg_3Si_4O_{10}(OH)_2$, CAS Registry Number: 14,807–96-6, USP grade, particle diameter < 10 µm, was obtained via JT Baker (Batch No: 0000184513); the specimen is certified by the manufacturer as asbestos-free and we have not tested the material for contamination. The particles were suspended in PBS and filtered through 30 µm nylon mesh filters (no visible loss of material has occurred). We did not use any commercial talc products.

Titanium dioxide (TiO2), CAS Registry Number 13,463–67-7, control particles (with mean particle size of 1 µm) were a gift from Dr. L. Kobzik (Harvard School of Public Health, Boston, MA); these were used previously in our studies [6,8,9].

Freshly sonicated (via Qsonica Q55 probe sonicator, setting of 10, 10 seconds with 10-s intervals, 3 times, on ice) particle suspensions were added at 10 µg/well with a fresh dose of oestradiol at the same time. 24 hours later the cells were processed for total RNA isolation via Qiagen RNEasy protocol with in situ lysis using the RLT buffer, or, in separate wells, for total DNA isolation via Qiagen DNEasy kit. Total RNA and DNA quality and quantity were assessed spectrophotometrically using NanoPhotometer N120 (Implen).

These protocols were tested previously and did not affect the viability of the cells [6].

Microarray. Gene chip microarray expression profiling was performed at Brown University Genomics Core using GeneChip™ Mouse Gene 2.0 ST Arrays (Affymetrix).

Global DNA methylation (5-mc) of DNA isolated from J774 cells cultured under the indicated conditions was evaluated using 5-mc ELISA Easy Kit (Epigentek, Farmingdale, NY) following the manufacturer's instruction. Briefly, 100 ng/well of sample DNA along with controls for a standard curve were bound to the assay plate, and then detection solution was added to the wells. Colorimetric analysis was done by measuring absorbance at 450 nm. The percentage of methylated DNA (5-mc) in total DNA was calculated using the following formula:

5-mc% = [(Sample OD – NC OD)/Slope x S] x 100%. NC; negative control, S is the amount of input sample DNA in ng.

Reduced-representation bisulphite sequencing (RRBS) [14,15] is the optimal method for genome-scale analysis of DNA methylation: it provides an efficient way to generate absolute quantification of methylation of more than 1 million CpG sites at single base-pair resolution with enrichment in loci more likely to be linked to transcriptional deregulation [16,17]. In brief, this method combines DNA digestion with a methylation-insensitive restriction enzyme and size selection to isolate a reproducible subset of the genome. This 'reduced representation' is sequenced using next-generation platforms, after an optimized bisulphite-treatment (to identify methylation marks) and Illumina library preparation. RRBS assay was performed by the Weill-Cornell Epigenomics Core.

Data analysis

Standard methods for data other than genomic and epigenomic profiling. Data are presented as Mean ± SEM. Data plotting and statistical analysis were performed using Excel 2007 (Microsoft) and Prism 7.02 (GraphPad Software); statistical significance was accepted when $p < 0.05$. To estimate significance of differences between groups we used the non-parametric Mann–Whitney U test, one-way or two-way ANOVA with Tukey, Fisher or Holme-Sidak tests, or Kruskal–Wallis ANOVA with Dunn's or Dunnett's test as dictated by the number of groups, data normality and experimental question.

Microarray data

Raw data were normalized with quantile background adjustment using RMA Express (v1.20) and extracted as natural scale values into a single tab-delimited data matrix. Statistical analyses were conducted using TIGR MeV 4.5.1 or 4.9.0. All datasets were filtered above the value of 20 to exclude the noise from unexpressed genes. We used Support Trees (ST) clustering analysis, Significance Analysis for Microarray (SAM), 2-factor Analysis of Variance (ANOVA) and Linear Models for Microarray Data (LIMMA) methods.

Parameters. ST: Bootstrapping over 100 iterations, Euclidean Distance metric, Average Linkage clustering. SAM: 2-class unpaired SAM was performed separately for talc+oestrogen vs. vehicle or for titanium+oestrogen vs. vehicle, ignoring other samples; using only unique permutations, S0 selected using Tusher et al. method, no q-values, imputation engine: K nearest neighbours; FDR ~1.3; average linkage clustering with Pearson l. ANOVA: 2- factor ANOVA was performed with p-values based on F distribution, critical p-value cut-offs 0.01 or 0.001, just alpha (no correction). LIMMA: Multi-class (6-class) analysis with p-value cut-offs $p < 0.05$, $p < 0.01$, $p < 0.01$. Default settings.

For heatmaps, green indicates lower expression and red – higher expression, colour brightness is proportionate to the value of each gene.

The raw data were deposited via NCBI Gene Expression Omnibus (GEO), accession no. GSE135238 [18].

Epigenome-wide methylation data

Initial QC of raw reads was run using 'FASTQC' [19]. Reads were trimmed using 'Trim Galore' [20] using the following settings: quality 20, adapter AGATCGGAAGAGC, stringency 1, length 50. 'Bismark' was used to prepare the reference genome (Ensembl Release 89 of GRCm38) and to align trimmed reads using the bowtie2 parameter [21]. Bismark methylation extractor was used to extract methylation information using the following parameters: bedGraph, comprehensive, ignore 3-s, merge_non_CpG.

The edgeR package was used to find differentially methylated loci [22]. The glMFit function was used to fit a negative binomial-generalized log-linear model. The experimental design matrix was constructed using modelMatrixMeth with a factorial experimental design (~hormone* treatment). The glmLRT function was used to find differentially methylated loci (DML) for comparisons of interest, which were made by constructing contrast vectors. Individual CpG sites were considered differentially methylated if the nominal p-value was < 0.02 and if the CpG was within 5 kilobases upstream or downstream of a transcription start site. Interaction term contrasts were only explored for loci where the inclusion of the interaction terms better fit the data (e.g., p-values were < 0.02 for glmLRT with both interaction coefficients).

The raw data were deposited via NCBI Gene Expression Omnibus (GEO), accession no. GSE150322 [23].

Results

Transcriptomics

Support trees

ST clustering analysis entails unsupervised clustering of samples to reflect the similarity between samples in the dataset. ST clustering (Figure 1) shows that all 3 talc+oestrogen (TE) samples were most dissimilar with vehicle (Veh, V) control samples. Talc alone (T) samples were clustering close to TE samples, and were second most dissimilar with Veh. This indicates that talc alone, and especially talc with oestrogen, has induced the most changes in the dataset compared to vehicle control.

Figure 1. ST clustering of microarray data (crop). Colour is proportional to gene value (green = low, red = high). Each row represents a separate probeset and each column represents a sample. (TE = Talc + Oestrogen, T = Talc, TiE = Titanium Dioxide + Oestrogen, Ti = Titanium Dioxide, E = Oestrogen and V = Vehicle Control).

SAM

Significance Analysis of Microarrays (SAM) is one of the more stringent statistical analyses that identifies highly significant genes in microarray data comparisons. Figure 2 shows that approximately 10 times more genes were significantly

different after talc and oestrogen exposure (A) vs. titanium dioxide and oestrogen (B) when either was compared to vehicle control. Figure 3 displays the specific input of talc (A) and oestrogen (B); the result indicates that talc had a substantially stronger influence than oestrogen.

2-factor ANOVA

To study further the effect of talc and oestrogen individually and combined we conducted a 2-factor Analysis of Variance (ANOVA). This analysis measures the interaction effect the two factors had on gene expression. Figure 4 demonstrates the amount of probesets significantly changed by two factors, talc and oestrogen, and their interaction. Talc-significant probesets were substantially greater than oestrogen significant. Their interaction shows slightly more significant probesets than oestrogen alone. In combination the results suggest that the input of talc was much more substantial than the effect of oestrogen, consistent with SAM results. ANOVA results also demonstrate the TiO2 induced substantially lesser effect than talc.

LIMMA

Grouped analysis using Linear Models for Microarray Data (LIMMA) enables the differential expression analysis of multiple groups and factors. Each experimental condition (e.g. talc alone, TiO2 alone, oestrogen alone, talc+oestrogen, TiO2+ oestrogen and vehicle) were compared to each other. The following trends can be observed in Figure 5: 1) Macrophages exposed to talc alone or in combination with oestrogen show significantly more differently expressed probesets than macrophages exposed to titanium dioxide alone or in combination with oestrogen when compared to vehicle control or oestrogen alone. 2) Comparisons between the two types of particles (with or without oestrogen) also show a great amount of significantly expressed probesets, suggesting the nature of the particle does affect the outcome.

Comparison to PCR array

We previously performed a PCR array testing of a small set of relevant genes using the same exposure, and identified a cluster of genes upregulated by talc or downregulated by talc [6]. We wanted to see whether the broader microarray approach reproduces the initial finding. Therefore, we hand-picked the values for probesets corresponding to the genes tested via PCR array in [6] and produced a heatmap seen in Figure 6. We conclude that the gene expression results were generally consistent between the two methods.

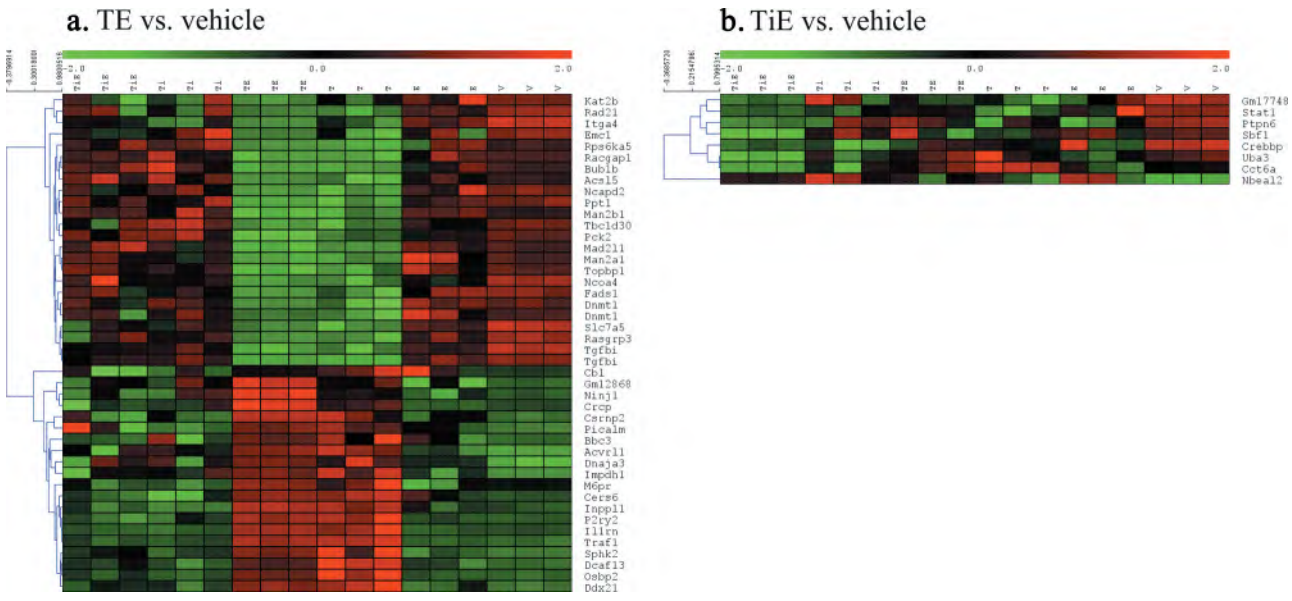

Figure 2. Heatmaps of hierarchical clusters after SAM analysis showing the number of significantly different probesets when comparing (a) TE vs. Vehicle, or (b) TiE vs. Vehicle. FDR: = 1.35. (n) = 3 per group. Colour is proportionate to expression (RMA) value (green = low, red = high). Rows have been normalized. TiE = Titanium Dioxide + Oestrogen, Ti = Titanium Dioxide; TE = Talc + Oestrogen, T = Talc, E = Oestrogen and V = Vehicle Control. (N) = 3).

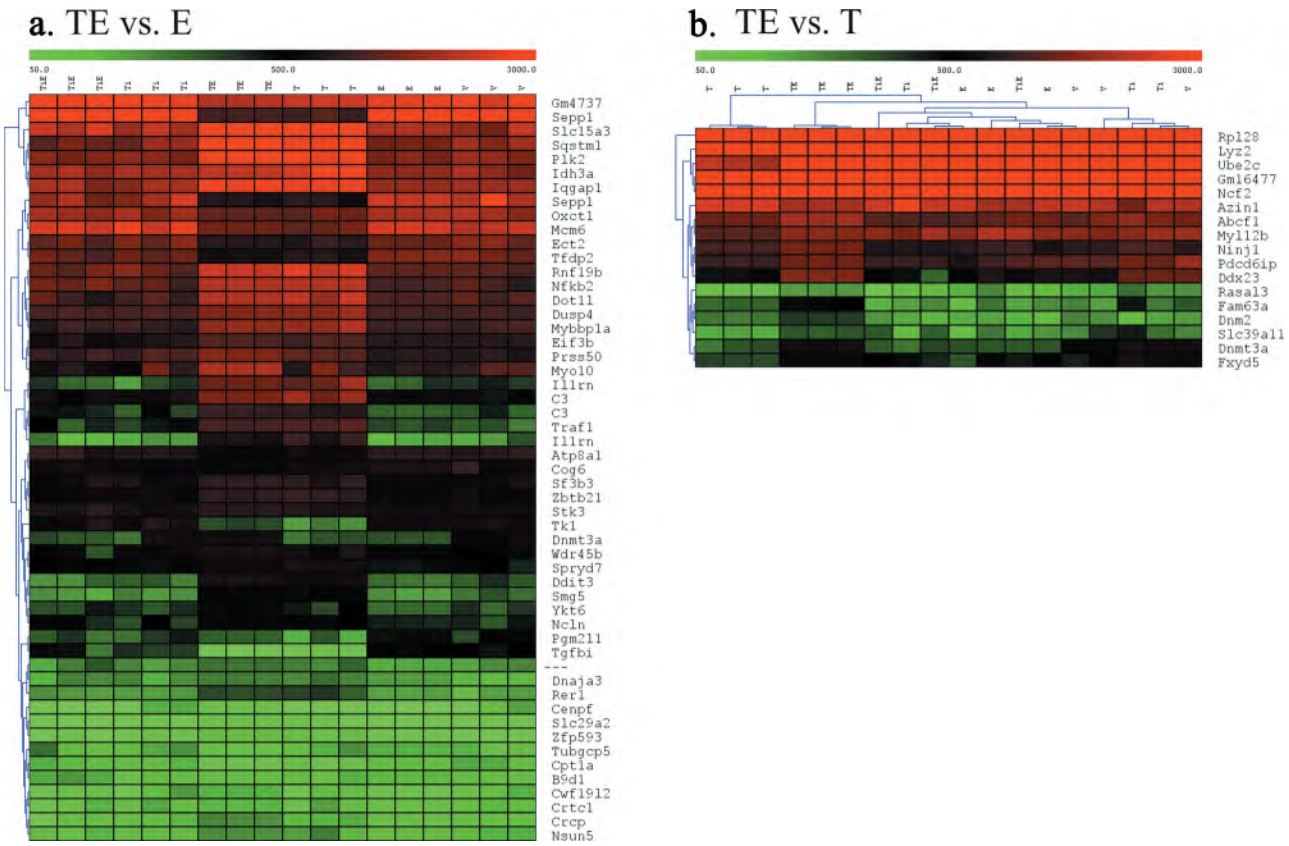

Figure 3. Heatmaps of hierarchical clusters after SAM analysis showing the number of significantly different probesets when comparing (a) TE vs. E, or (b) TE vs. T. FDR: = 0.8. (n) = 3 per group. Colour is proportionate to expression (RMA) value (green = low, red = high). (TiE = Titanium Dioxide + Oestrogen, Ti = Titanium Dioxide; TE = Talc + Oestrogen, T = Talc, E = Oestrogen and V = Vehicle Control. (N) = 3).

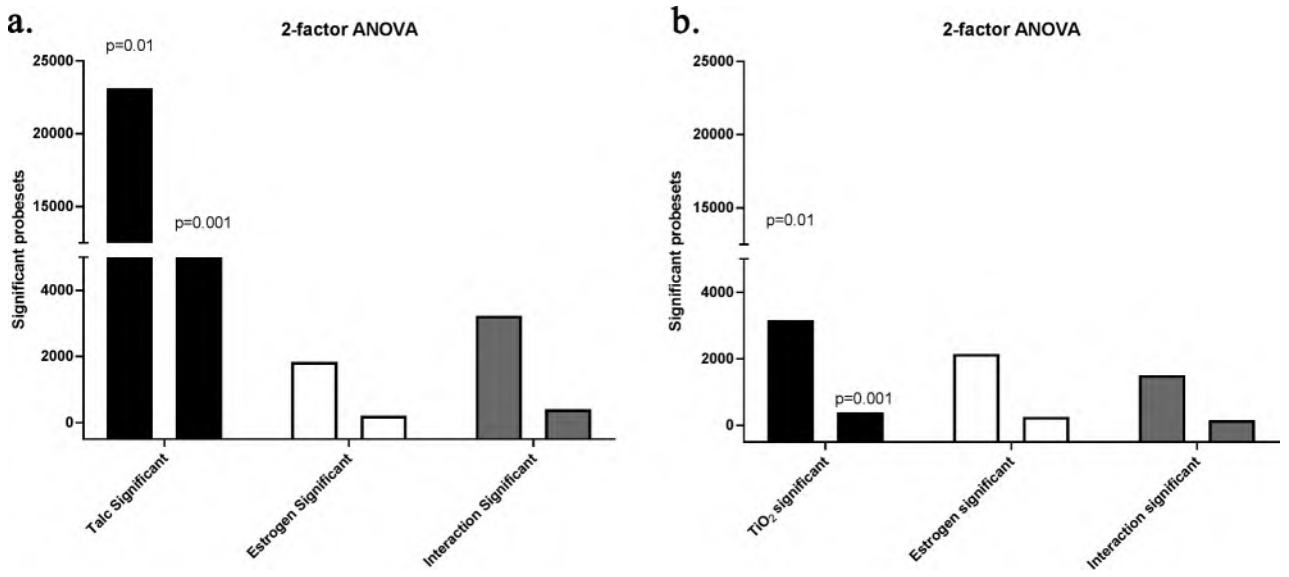

Figure 4. Two-factor ANOVA Analysis. (a). Number of significant probesets affected by talc alone, oestrogen alone and both (interaction). (b). Same, for TiO2. Cut-offs $p < 0.01$ (left bar) or $p < 0.001$ (right bar).

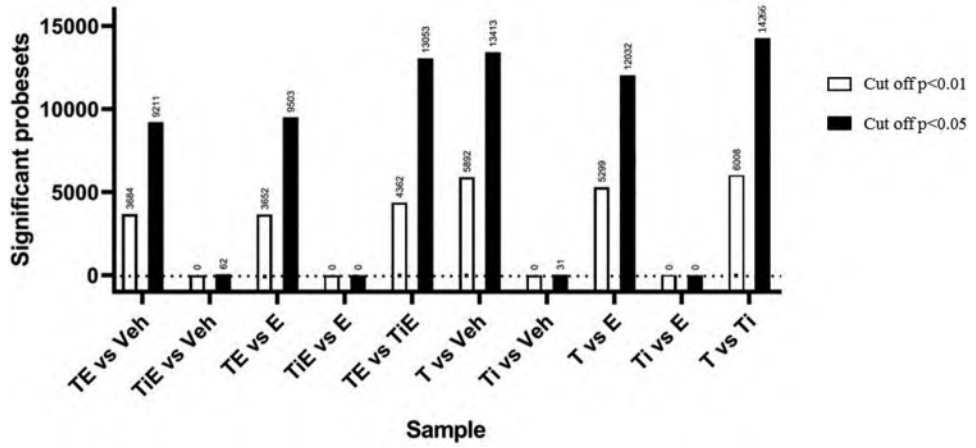

Figure 5. LIMMA Analysis. Group comparisons. Left blank bars have a $p < 0.01$ cut-off and right black bars have a $p < 0.05$ cut-off. (TE = Talc + Oestrogen, T = Talc, TiE = Titanium Dioxide + Oestrogen, Ti = Titanium Dioxide, E = Oestrogen and Veh = Vehicle Control).

Pathway analysis

We used the LIMMA $p < 0.01$ TE vs. V list of 3684 probesets to determine pathways where the genes with altered expression are involved. This list produced 1619 unique network objects in GeneGo Metacore pathway analysis tool. The analysis indicated that top 50 pathways could be grouped into the following processes: 1) Cell division/proliferation, 2) Macrophage phagocytosis/particle phagocytosis, 3) Immune response signalling pathways (OX40/OX40L, IL-1, IL-4, IL-6, IL-11, NF-kappaB, TNFR2, TLRs, TGFb and others), 4) MHC class 1 presentation, 5) Oxidative stress/ROS induced signalling, 6) Oestrogen/ESR1 signalling, 7) Apoptosis, 8) Epigenetic control of gene transcription. Figure 7 represents a Direct Interactions network, showing that the genes we identified as significantly affected were involved in interrelated pathways; the number of connections was substantially higher than in a control random list of gene names which indirectly confirms that the results are biologically meaningful.

Epigenetic involvement was a particularly interesting finding; as evident from Figure 8(a) number of epigenetically acting factors have changed expression, among them DNA methyltransferase 1 (DNMT1) was most substantially downregulated by both particles, but to a greater extent by talc (Figure 9).

mC ELISA

Because 'epigenetic control of gene transcription' was one of the involved pathways (Figure 8), we tested the levels of overall DNA methylation (percentage of methylated cytosines) after talc and TiO2. As shown in Figure 10, average 5-mc % in the control cells (3.27 ± 0.10%, Mean ±SEM, $n = 3$) was significantly higher than in talc (2.44 ± 0.25%, $n = 3$, $p < 0.05$) or in titanium (1.75 ± 0.10%, $n = 3$, $p < 0.01$) treated cells. Co-treatment with oestrogen significantly reduced the 5-mc % in the talc-treated cells (1.45 ± 0.22%, $n = 3$, $p < 0.05$), but neither in the control (2.94 ± 0.27%, $n = 3$) nor in the titanium-treated cells (1.91 ± 0.36%, $n = 3$).

We therefore performed a detailed analysis of DNA methylation changes via RRBS.

Epigenomics

Analysis of RRBS data indicates that both talc and TiO2 exposures were associated with vast changes in the DNA methylation profiles; this was true at a various stringencies and seen via different statistical methods (Figure 11), here we report a representative set of results via the model we selected as described in Methods and using $p < 0.02$ as a cut-off threshold. We selected only the loci 5000 bp up- or downstream of the transcription start site to identify the effects that most likely are associated with

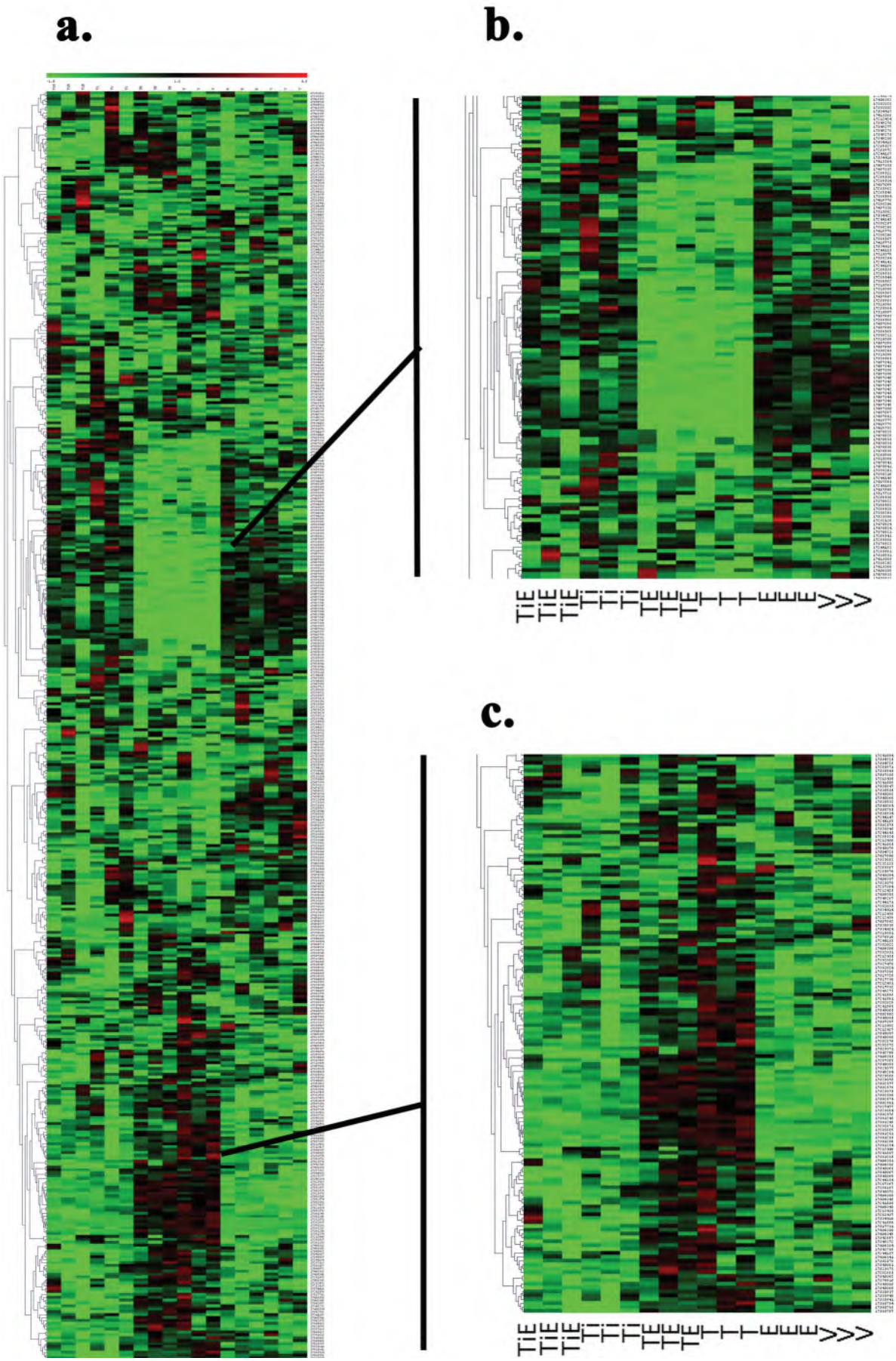

Figure 6. (a) Comparison of microarray data to previously published [6] Cancer PathwayFinder RT2 Profiler PCR array data. (b) Inhibitory Effect of talc alone and in combination with oestrogen on macrophages after 24 h exposure when compared to other samples. (c) Stimulatory effect of talc alone and in combination with oestrogen. (TiE = Titanium Dioxide + Oestrogen, Ti = Titanium Dioxide, TE = Talc + Oestrogen, T = Talc, E = Oestrogen and V = Vehicle Control). (n) = 3/group. Colour is proportional to gene value (green = low, red = high).

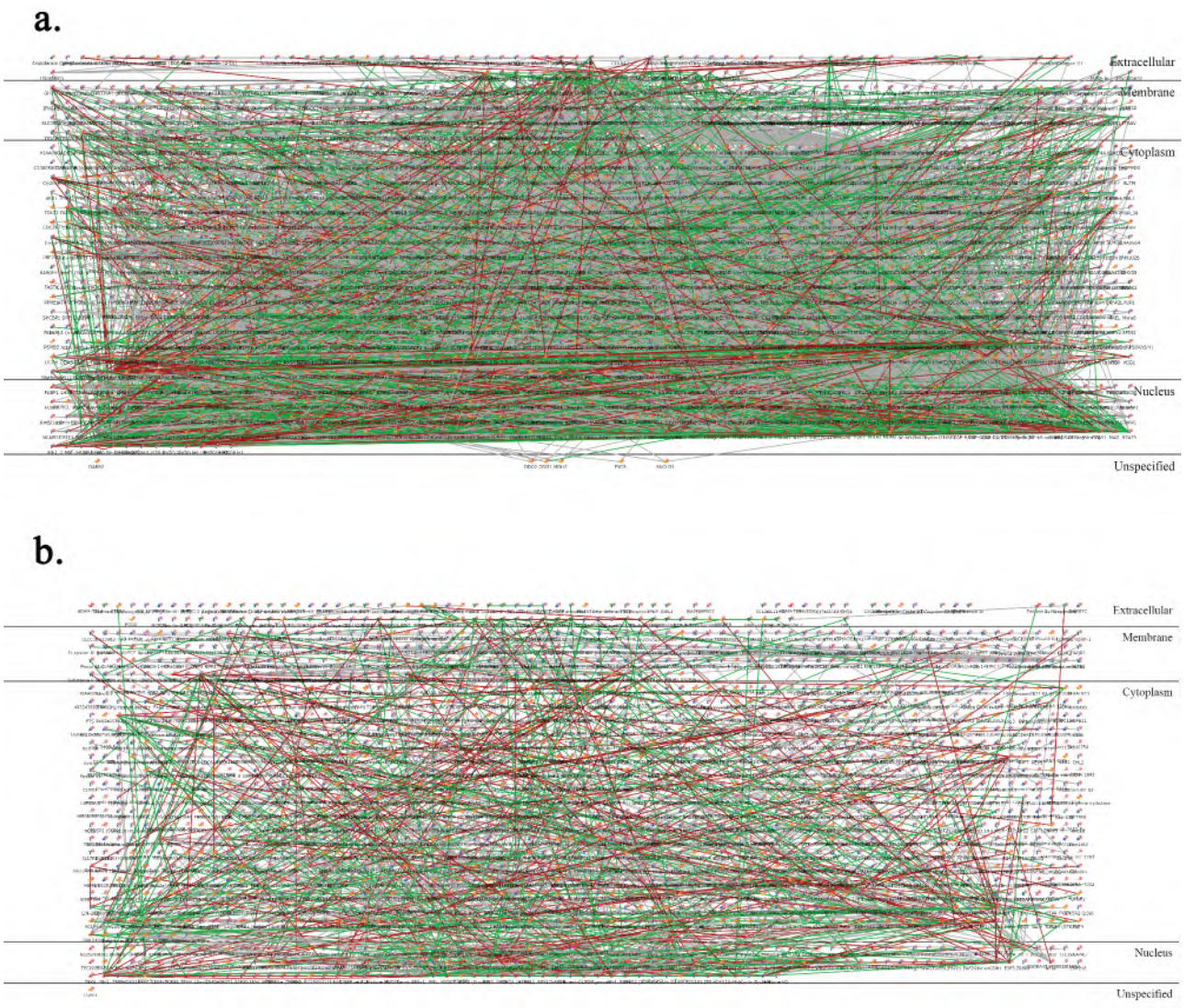

Figure 7. Metacore GeneGo Pathway analysis: Direct interactions network. (a). 1619 unique gene names from the list of significantly different probesets between TE and Vehicle via LIMMA at $p < 0.01$ stringency. (b) Control random list of 1620 gene names. Titanium dioxide particles did not induce enough changes to build a network.

transcriptional regulation. Raw data are available via NCBI GEO [GSE150322]; the analysis algorithm is available via Github.

First, we aimed to determine how many differentially methylated loci (DML) occur after exposure to either particle at stringency $p < 0.05$. We found 1243 DMLs for talc interaction and 883 DMLs for TiO2 interaction (Figure 11). Then we determined the DMLs occurred in presence of oestrogen vs. oestrogen alone using $p < 0.02$ stringency after filtering the data to include loci 5000 bp up- or downstream of the transcription start site. We found 402 DMLs in TE vs. E alone comparison, and 477 DMLs in TiE vs. E alone comparison (Figure 12). Among these, 91 loci were the same for both particles and the others were unique to each. We then compared a list of DMLs induced by talc in the oestrogen milieu (TE vs E) to the list of DMLs induced by talc in absence of oestrogen (T vs. Veh.) using a 'contrast' approach and found 447 DMLs; a similar comparison for TiO2 resulted in 533 DMLs.

Next, we looked for overlapping gene names in the list of TE vs E DMLs and the list of differentially expressed targets from the microarray results (output of LIMMA $p < 0.05$, $n = 9211$ probesets) and found only 50 overlapping gene names. Similarly, comparison of T vs Vehicle DMLs had only 39 overlapping gene names and they were

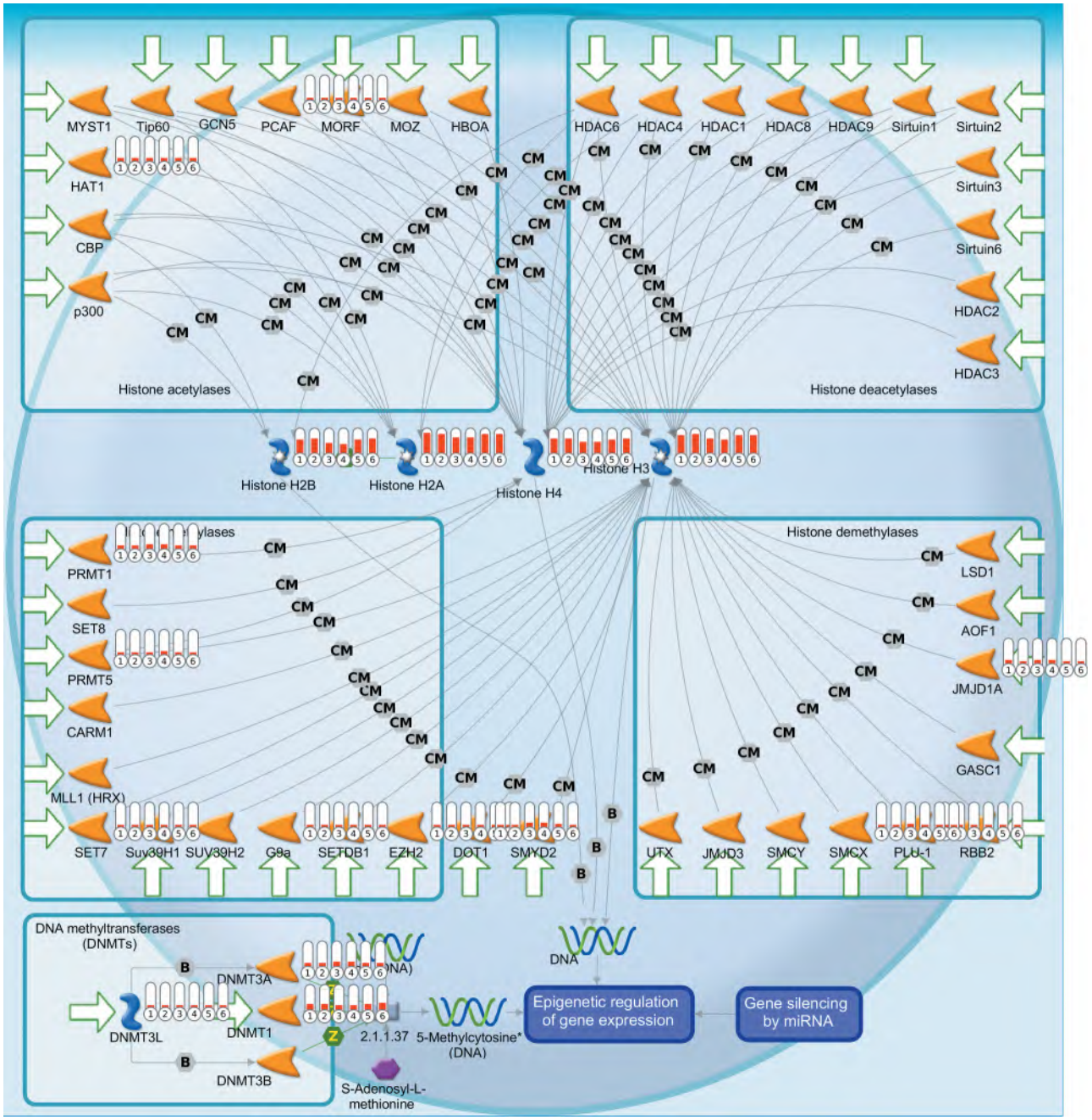

Figure 8. Pathway analysis. A predesigned map entitled 'Epigenetic control of transcription' in Metacore GeneGo with highlighted genes (depicted with red bar sets where bar height is proportionate to RMA expression value) determined to be significantly different between TE and Vehicle via LIMMA. (1 = TiE, 2 = Ti, 3 = TE, 4 = T, 5 = E, 6 = V; (n) = 3).

largely not the same as in the previous comparison. We conclude that the epigenome-wide DNA methylation changes we detected are largely not associated with a resultant transcription change.

Pathway analysis

Pathway analysis of TE vs. E comparison allowed 337 unique annotated gene names; in a 'direct interactions' network they have shown a good extent of interacting with 577 edges (Figure 13(a)) involving, among others: WNT/beta-catenin, NF-kappa B, and ETS1 transcription pathways and TAL1 protein interactions as well as SMAD3 pathway. In contrast, TiE vs. E comparison allowed 381 unique annotated gene names but resulted in a less involved 'direct interactions' network with only 493

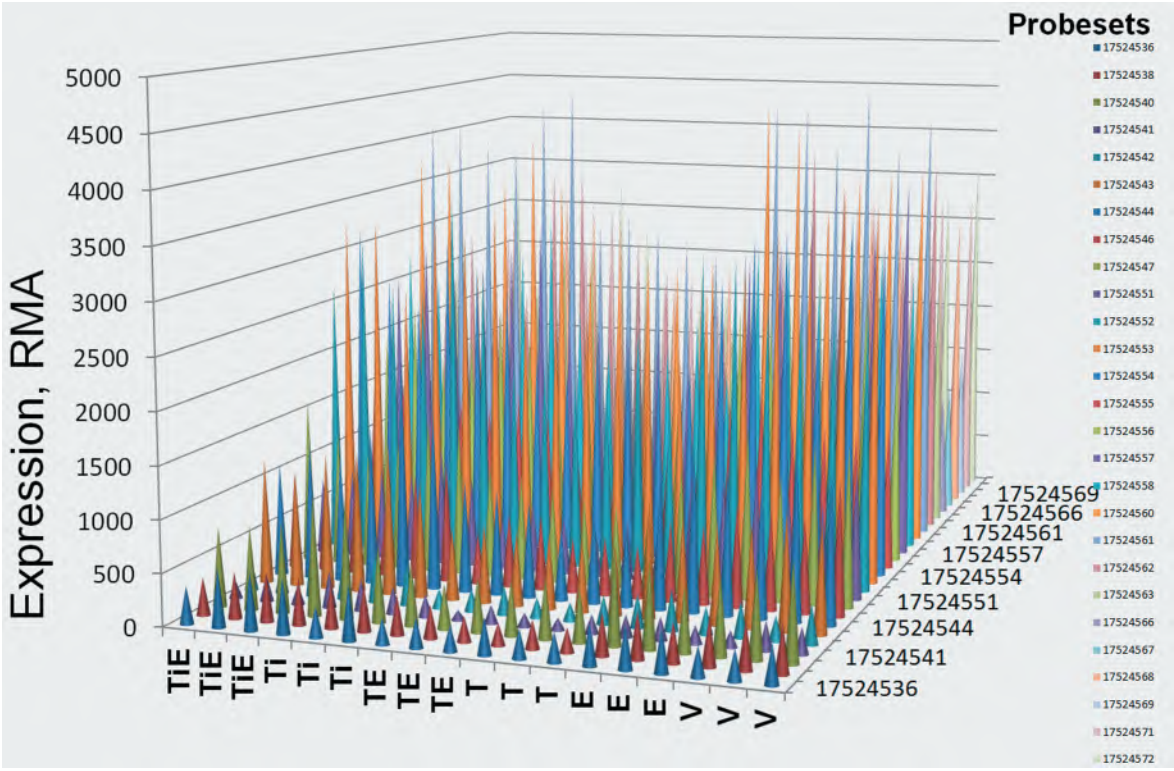

Figure 9. DNMT1 expression. Normalized and background adjusted RMA expression values for the 27 probesets interrogating DNMT1 gene shown across individual samples.

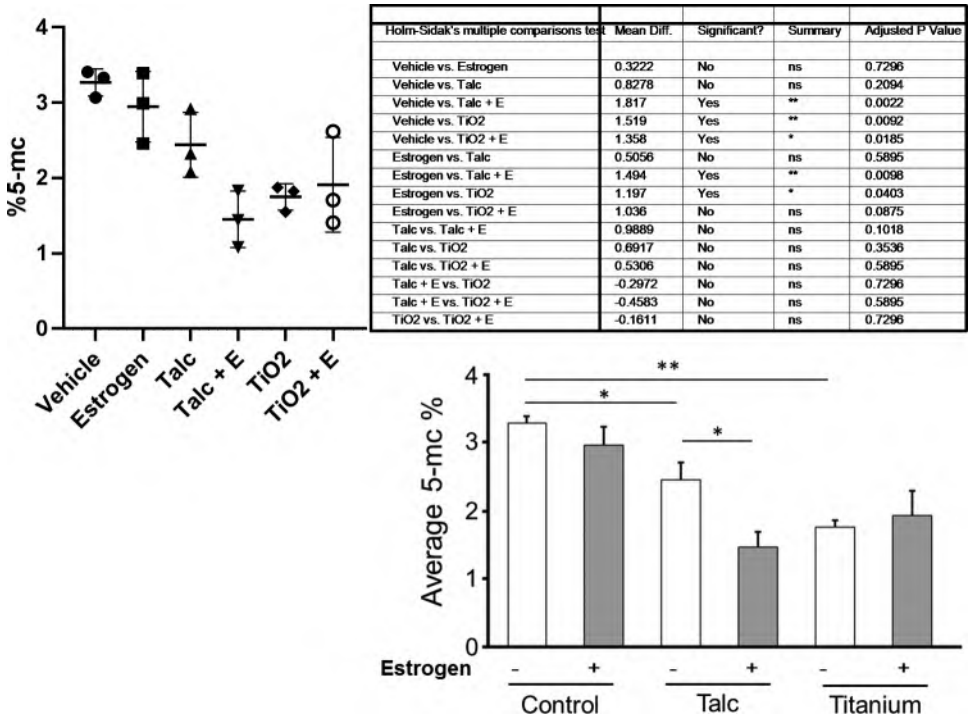

Holm-Sidak's multiple comparisons test	Mean Diff.	Significant?	Summary	Adjusted P Value
Vehicle vs. Estrogen	0.3222	No	ns	0.7296
Vehicle vs. Talc	0.8278	No	ns	0.2094
Vehicle vs. Talc + E	1.817	Yes	**	0.0022
Vehicle vs. TiO2	1.519	Yes	**	0.0092
Vehicle vs. TiO2 + E	1.358	Yes	*	0.0185
Estrogen vs. Talc	0.5056	No	ns	0.5895
Estrogen vs. Talc + E	1.494	Yes	**	0.0098
Estrogen vs. TiO2	1.197	Yes	*	0.0403
Estrogen vs. TiO2 + E	1.036	No	ns	0.0875
Talc vs. Talc + E	0.9889	No	ns	0.1018
Talc vs. TiO2	0.6917	No	ns	0.3536
Talc vs. TiO2 + E	0.5306	No	ns	0.5895
Talc + E vs. TiO2	-0.2972	No	ns	0.7296
Talc + E vs. TiO2 + E	-0.4583	No	ns	0.5895
TiO2 vs. TiO2 + E	-0.1611	No	ns	0.7296

Figure 10. 5-mC ELISA. DNA samples were evaluated for global DNA methylation (5-mC) by ELISA. Values represent mean ± SEM (N = 3) from duplicated samples for each treatment at varying conditions. *, $p < 0.05$, **, $p < 0.01$. (a) One representative experiment of 3 is shown. (b) Pooled data from 3 experiments.

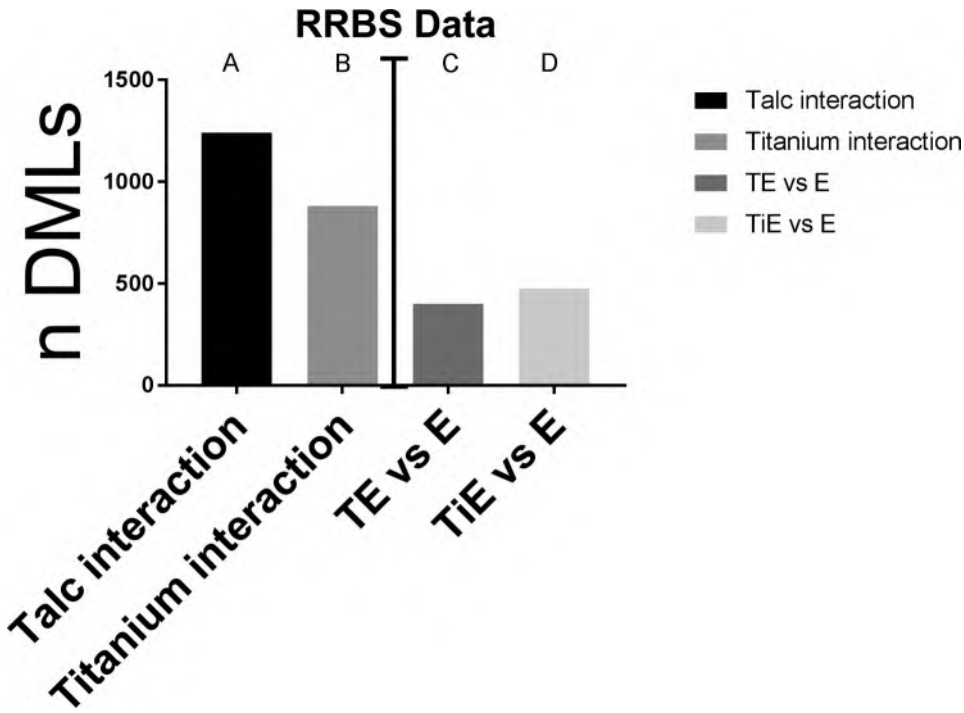

Figure 11. RRBS data analysis. Number of DMLs resultant from different comparisons. DMLs between (a) talc effect for oestrogen and no oestrogen, and (b) between TiO2 effect for oestrogen and no oestrogen: P value threshold <0.05. (c) TE vs. E at P value threshold <0.02 and (d) TiE vs. E: P value threshold <0.02 and filtered to only include loci <5000 bp from a nearest transcript. (n) = 3 each group.

edges (Figure 13(b)), the bigger hubs here also included ETS1 and NF-kappa B but, uniquely, SOX9 and HNF3-beta. Hence, we conclude that there were some shared and some unique loci of DNA methylation change induced by talc and titanium. The characteristic signatures of exposure can be found in Figure 13 and supplementary tables.

Figure 14 shows a 'direct interactions' network for the 50 (38 annotated) gene names seen in both the list of DMLs in a TE vs. E comparison and the list of differentially expressed genes in the same comparison, i.e., those where epigenetic change is accompanied by transcriptional change. It appears most genes in this list interact with each other, mainly because of their link to NF-kappa B and another transcription factor ETS. The other approaches to link epigenomic and transcriptomic effects were less informative.

In summary, we report that a 24 h *in vitro* exposure of J774 MΦs to talc particles alone, and especially to a combination of talc with oestrogen leads to substantial genome-wide gene expression changes that occur to a much lesser extent after exposure to TiO2 particles with or without oestrogen. Among the pathways affected, epigenetically acting enzymes were involved, especially striking was the inhibition of DNMT1 expression. We therefore sought, and found, substantial epigenome-wide DNA methylation changes after exposure to both talc and TiO2 (in the context of oestrogen or alone) seen as a decline of overall DNA methylation and as specific bidirectional changes in methylation in hundreds of loci. We found a few loci where both the transcriptional changes and epigenetic changes occurred at the same time in the pathways involving immune and inflammatory signalling. We note, that while some transcriptomic and epigenomic changes were shared between T and TiO2, it is especially interesting that each of the two particles of very similar size and insoluble, monocomponent, and non-digestible nature has also induced a specific pattern of gene expression and DNA methylation changes.

Discussion

Epigenetic regulation plays a very important and substantial role in macrophage functions [1]; aberrations

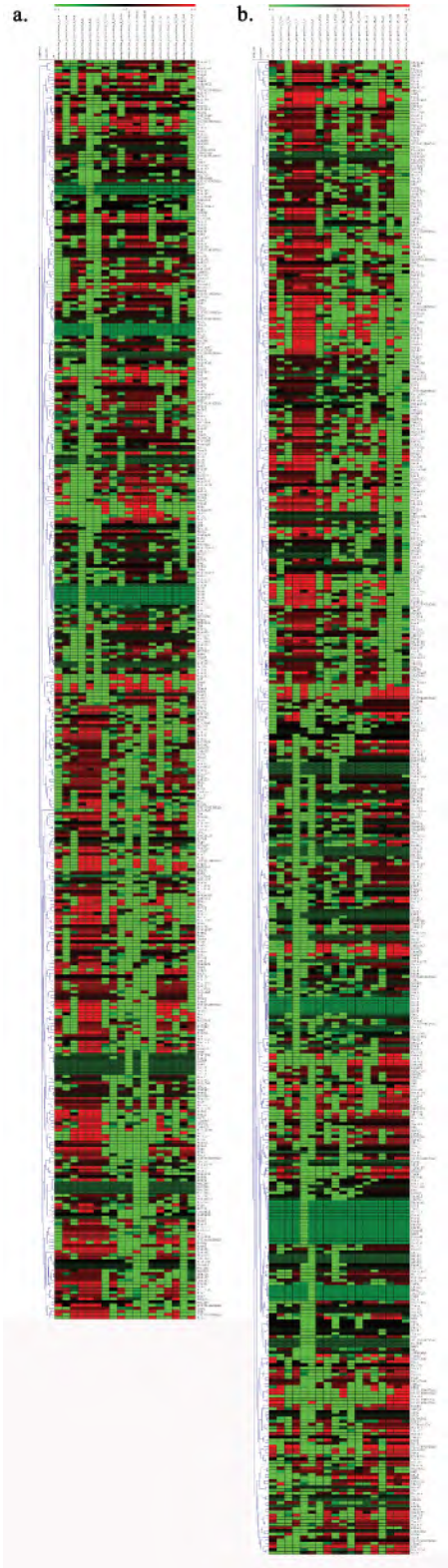

Figure 12. Hierarchical clustering of DML values. (a). TE vs E. (b) TiE vs E). Colour is proportionate to row-normalized CpG methylation values (green = low, red = high). Rows have been normalized. (Veh = Vehicle Control, E = Oestrogen, T = Talc, TE = Talc + Oestrogen, Ti = Titanium Dioxide, TiE = Titanium Dioxide + Oestrogen).

in the epigenome can lead to compromised immune responses [24]. Phagocytosis is a complex process involving activation of a broad spectrum of cellular mechanisms including gene expression changes [25]; these changes are linked to epigenetic mechanisms including DNA methylation. While some changes are ubiquitous to the various processes of phagocytosis, others can be characteristic to a phagocytized object.

Here, we used two types of insoluble particles, generally considered 'inert' and often used as control particulates in studies of other, more 'toxic' environmental particles. Talc and TiO2 are broadly used in cosmetics, medical and food products. However, these particulates are not entirely innocuous; hence, while one particle in this study serves as a control for the other, both represent biological phenomena that we hypothesized may involve epigenetic deregulation.

Talc (hydrous magnesium silicate) is a mined product considered 'inert' and used in cosmetics including 'baby powder'. The International Agency for Research on Cancer (IARC) has recently concluded that even talc not contaminated by asbestiform fibres (a carcinogenic contaminant seen in talc in the past) is possibly carcinogenic to humans (class 2b) [26]. Epidemiology data suggest an increase in ovarian cancer risk for women who used cosmetic talc powder in the genital area [27,28]. Particles the size of talc, if they are present in the vagina, can traverse to the upper female genital tract and have been detected in and around tumour-associated immune cells, particularly inside the cytoplasm of macrophages in specimens from ovarian cancer patients with the history of perineal talc use [29]. The talc association was more apparent in premenopausal women and those postmenopausal women who were taking oestrogen replacement therapy [27] suggesting higher oestrogen may fuel the pathogenesis. The most current meta-analysis confirms the association [7], however the potential mechanism has remained elusive. We recently show that J774 (or IC21) macrophages exposed to talc particles are less capable to curb the growth of OC cells in vitro [6], hence, we postulated the increased cancer risk may be mediated by inhibitory effect of talc on the MΦ.

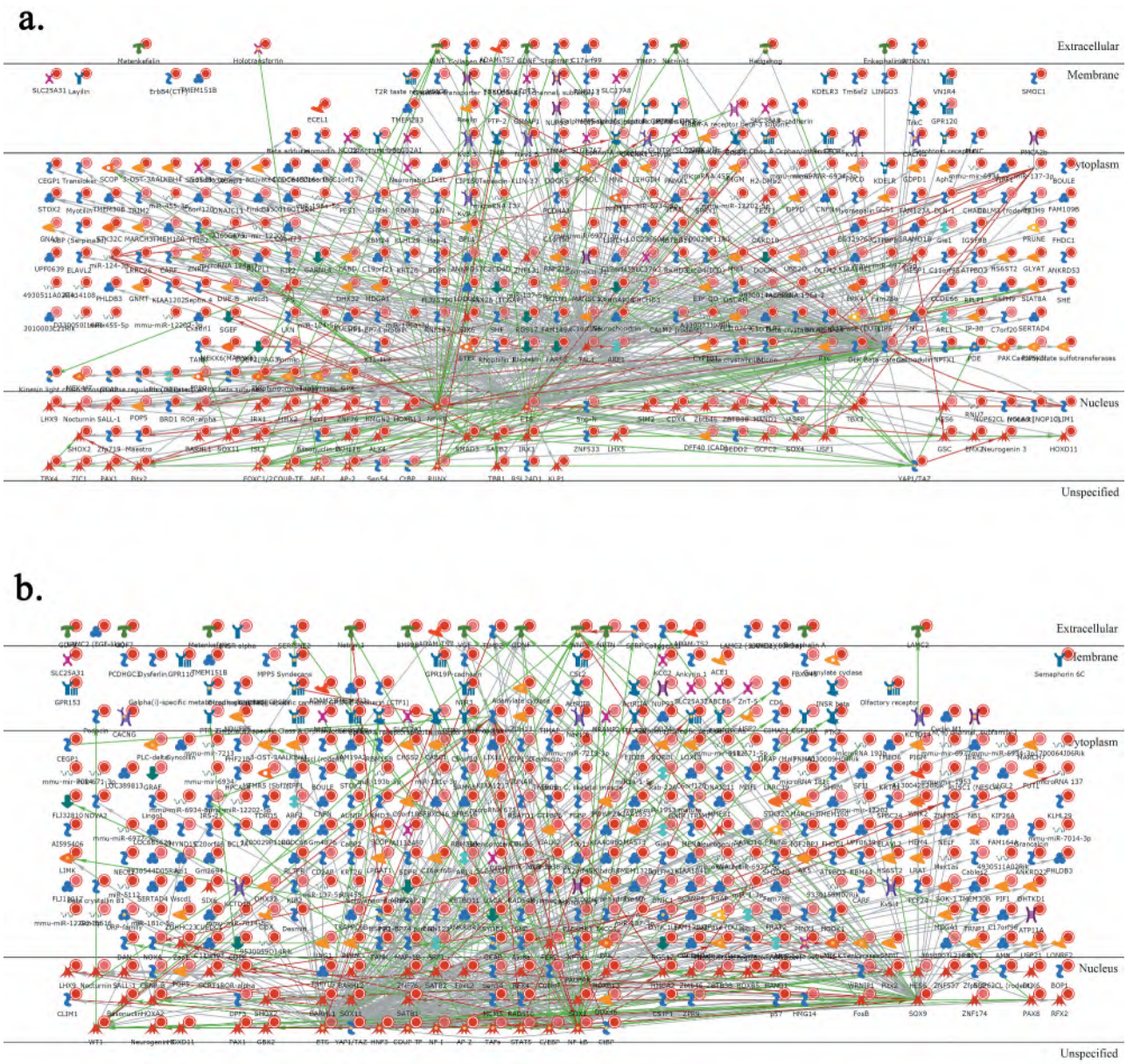

Figure 13. Pathway analysis. Metacore 'Direct interactions' networks for TE vs. E comparison (a) and TiE vs. E comparison (b).

Titanium dioxide is an insoluble particulate that is seen mostly as fine-size particles (but also is increasingly used in nano-size) as a component of white pigment broadly applicable from white paint to toothpaste and other cosmetic and food products [30,31] and while human exposure to it has become almost ubiquitous, it is also not as entirely innocuous as considered. TiO2 contributes to inflammation [8,9,32], cancer [33,34] and asthma [8,35], and as pointed out by IARC no biomarkers of exposure have been identified in spite of various health risks [34]. Similar to talc, TiO2 is not digestible and has also been shown to accumulate inside macrophages [36]. We previously show that TiO2 exposure during pregnancy is inflammatory to the airways of pregnant mice and is linked to increased asthma risk in their neonates [8] which led us to hypothesize that TiO2 may also have epigenetic effects. We have also previously linked oestrogen to how macrophages interact with TiO2 [9].

Besides the chemical composition, one potential difference worth noting is that it is impossible to guarantee that all particles are identical in size

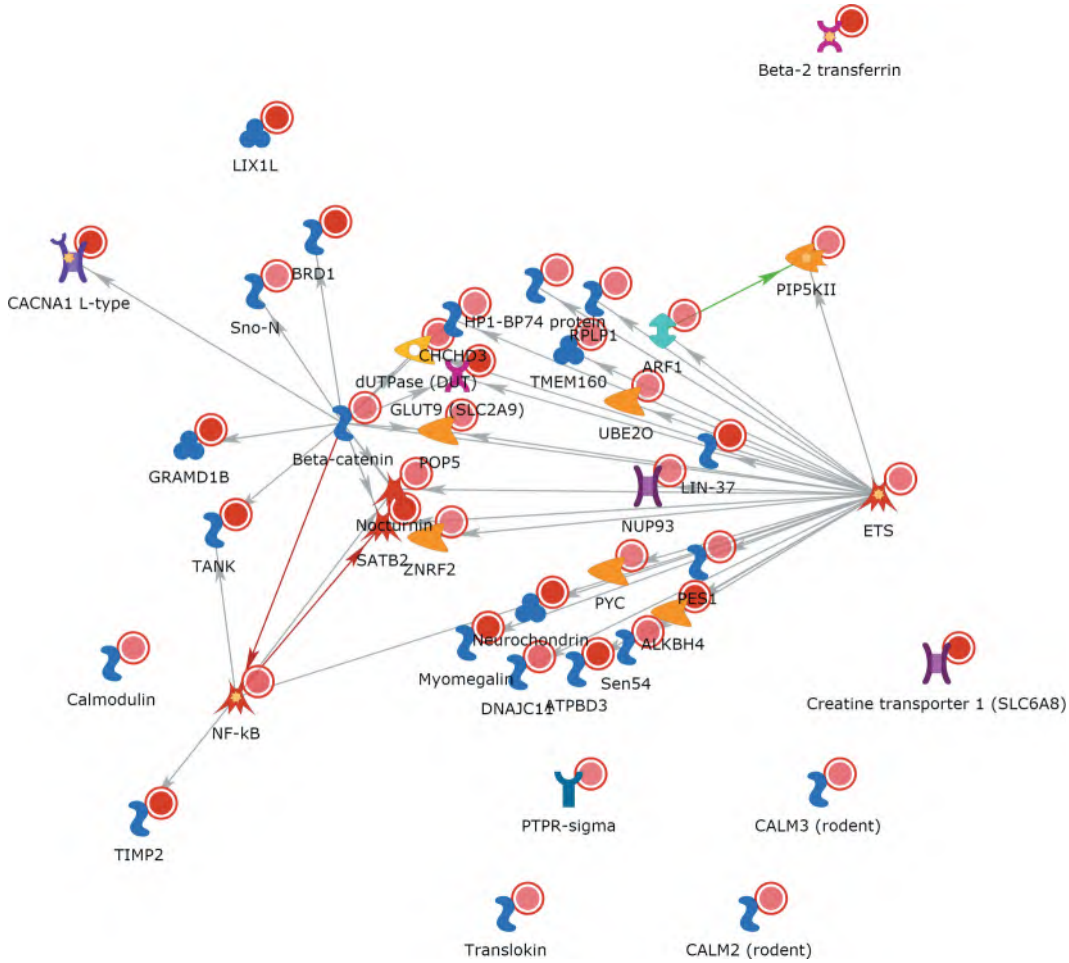

Figure 14. A Metacore 'direct interactions' network using the list of 50 gene names where both differential methylation and differential expression was induced by talc in the presence of oestrogen.

because particles derived from naturally mined products will have an especially broad size distribution differing from batch to batch and even in the same bottle (bottom layer vs. top). However, as evident from micrographs in [6] the average size of both particles is approximately the same ranging from 1 μm to 10 μm.

Of note, while oestrogen is considered to exert its action to promote tumour growth and progression directly through oestrogen receptors in cancer cells, our data show that oestrogen also has synergic effect with talc/TiO2 to induce genetic and epigenetic changes in the murine MΦ cell line J774. The finding helps explain our data [6] on compromised tumoricidal activity of the immunocompetent cells and consequently on how oestrogen helps promote progression of the cancer cells indirectly. Notably, the doses of particles and oestrogen used here were selected so that they do not interfere with cell viability, as determined previously [6].

Our transcriptional profiling builds on prior exploratory PCR array results that identified inhibition of 'useful' genes involved in anti-tumorigenic activity and upregulation of extraneous procarcinogenic factors by talc [6]. The ST2.0 array data reported here validate and expand the prior findings. Here we show that talc particles had substantially stronger transcriptomic effects than TiO2, a combination of talc + oestrogen had marginally more effect than talc alone, and that talc is more 'important' than oestrogen. With lower stringency however TiO2 exposure has also led to transcriptional responses, consistent with the expectation that the act of phagocytosis itself involves gene expression changes.

Pathway analysis has identified that the pathways affected by talc included cell proliferation, immune responses and signalling, immunosurveillance, apoptosis. These results help explain our prior finding of reduced tumoricidal activity of J774 cells after talc exposure [6]. While we did not observe increase in necrotic or apoptotic staining in prior experiments using this exposure protocol [6], we note that expression of relevant genes has been affected. We were intrigued to see that one of the pathways heavily involved was the epigenetic 'machinery'; we were interested especially in DNA methylation because the expression profiles of DNA methyltransferase 1 (DNMT1) have shown a particularly consistent and prominent inhibition by talc and, to a lesser extent, by TiO2, (Figure 9) hence we tested the overall DNA methylation levels using mC ELISA. The results indicated that both types of particles induced a substantial decline in overall mC levels (Figure 10) and prompted for a more detailed analysis of the affected loci via RRBS.

Epigenomic analysis revealed that both types of particles, with or without oestrogen, induced a substantial DNA methylation change. The epigenomic signatures of the exposures can be found in the supplementary files. At lower stringency ($p < 0.05$) talc induced a higher number of DMLs than titanium, however, the number of DMLs was approximately similar at higher stringency ($p < 0.02$) and when filtered ± 5000 bp of the nearest transcript (Figure 11). It is notable that these changes have occurred over a fairly short exposure time (24 hours). Others have reported that DNA methylation changes can occur over relatively short time [37–39] but not quite that short. Specifically, there has been more interest in the long-term, lifetime exposure effects when it comes to particulate matter [40]. We believe we are the first to show that a single short-term exposure of MΦs in vitro to particles can be linked to epigenome-wide DNA methylation changes. This is consistent with our in vivo studies showing that a single maternal exposure to particles can lead to increased inflammatory (asthma) risk in the neonates [8,9] that can be transgenerationally transmitted to 3 generations of progeny potentially via an epigenetic mechanism [41].

Our epigenomic data analysis aimed to identify loci that are more likely to be involved into transcriptional deregulation. For this we filtered the DMLs to only include those that are within 5000 bp of a known transcript. We then compared this list of DMLs to the lists of differentially expressed genes from the transcriptomic assay and found ~50 such loci which represents approximately 10% of all DMLs. For the TE vs. E analysis, these 50 genes have mostly directly interacted around two transcription factors (NF-kappa B and ESR) that were found on this list (Figure 14) indicating possible involvement of inflammatory/immune deregulation. As evident from the supplementary tables these loci were largely not the same comparing talc+oestrogen effect and talc alone effect. We conclude that the data do not suggest a strong potential for mechanistic involvement of the DMLs we identified with the transcriptional changes we observe at the moment. This is consistent with findings by others that in antigen-presenting cells gene activation precedes DNA demethylation and not the other way around [42]. In general, it is not uncommon in studies linking DNA methylation and gene expression changes to observe that only either phenomenon occurs to a subset of genes while another subset shares both types of alterations, e.g [41]. In part, this likely occurs because DNA methylation is not the only mechanism of gene transcription control. It is also possible that a longer incubation period could allow revealing more transcriptional changes in the loci with altered DNA methylation; however, this was beyond the scope of our study. As a result of our work, however, we postulate that the 'reshuffle' of epigenetic machinery induced by the particles may be responsible for downstream malfunctioning of the exposed MΦs we found: the reduced tumoricidal function induced by talc [6] and the enhanced pro-inflammatory responses induced by TiO_2 [8,9]. Overall, our study has led to this 'two-hit' hypothesis that merits further testing.

Disclosure statement

The authors declare no conflict of interest.

Funding

The research was supported in part by Rhode Island Hospital, Department of Surgery funds. This research was partially

supported by Institutional Development Award Number P20GM109035 from the National Institute of General Medical Sciences of the National Institutes of Health, which funds COBRE Center for Computational Biology of Human Disease. Dr. Fedulov receives support in part through grant ES030227 from NIEHS.

ORCID

V. C. Tripathi http://orcid.org/0000-0002-9589-0709
J. Wallace http://orcid.org/0000-0001-8842-4921

References

[1] Chen S, Yang J, Wei Y, et al. Epigenetic regulation of macrophages: from homeostasis maintenance to host defense. Cell Mol Immunol. 2020;17(1):36–49. PMC6952359.
[2] Marr AK, MacIsaac JL, Jiang R, et al. Leishmania donovani infection causes distinct epigenetic DNA methylation changes in host macrophages. PLoS Pathog. 2014;10(10):e1004419. PMC4192605.
[3] Kawasaki H. A mechanistic review of particle overload by titanium dioxide. Inhal Toxicol. 2017;29(12–-14):530–540. PMID: 29458306.
[4] Warheit DB, Overby LH, George G, et al. Pulmonary macrophages are attracted to inhaled particles through complement activation. Exp Lung Res. 1988;14 (1):51–66. PMID: 2830106.
[5] Gilberti RM, Knecht DA. Macrophages phagocytose nonopsonized silica particles using a unique microtubule-dependent pathway. Mol Biol Cell. 2015;26(3):518–529. PMC4310742.
[6] Mandarino A, Gregory DJ, McGuire CC, et al. The effect of talc particles on phagocytes in co-culture with ovarian cancer cells. Environ Res. 2020;180:108676. PMID: 31785414.
[7] Berge W, Mundt K, Luu H, et al. Genital use of talc and risk of ovarian cancer: a meta-analysis. Eur J Cancer Prev. 2018 May;27(3):248–257. PMID: 28079603.
[8] Fedulov AV, Leme A, Yang Z, et al. Pulmonary exposure to particles during pregnancy causes increased neonatal asthma susceptibility. Am J Respir Cell Mol Biol. 2008;38(1):57–67. PMC2176127.
[9] Zhang Y, Mikhaylova L, Kobzik L, et al. Estrogen-mediated impairment of macrophageal uptake of environmental TiO2 particles to explain inflammatory effect of TiO2 on airways during pregnancy. J Immunotoxicol. 2015;12(1):81–91. PMID: 24825546.
[10] Ralph P, Prichard J, Cohn M. Reticulum cell sarcoma: an effector cell in antibody-dependent cell- mediated immunity. J Immunol. 1975;114:898–905. PMID: 1089721.
[11] Ralph P, Nakoinz I. Phagocytosis and cytolysis by a macrophage tumour and its cloned cell line. Nature. 1975;257:393–394. PMID: 1101071.
[12] Józefowski S, Arredouani M, Sulahian T, et al. Disparate regulation and function of the class A scavenger receptors SR-AI/II and MARCO. J Immunol. 2005;175(12):8032–8041. PMID: 16339540.
[13] Hayashi T, Yamada K, Esaki T, et al. Physiological concentrations of 17beta-estradiol inhibit the synthesis of nitric oxide synthase in macrophages via a receptor-mediated system. J Cardiovasc Pharmacol. 1998;31(2):292–298. PMID: 9475272.
[14] Meer A, Gnirke A, Bell GW, et al. Reduced representation bisulfite sequencing for comparative high-resolution DNA methylation analysis. Nucleic Acids Res. 2005;33(18):5868–5877. PMC1258174.
[15] Gu H, Smith ZD, Bock C, et al. Preparation of reduced representation bisulfite sequencing libraries for genome-scale DNA methylation profiling. Nat Protoc. 2011;6(4):468–481. PMID: 21412275.
[16] Fouse SD, Nagarajan RO, Costello JF. Genome-scale DNA methylation analysis. Epigenomics. 2010;2 (1):105–117. PMC2907108.
[17] Garrett-Bakelman FE, Sheridan CK, Kacmarczyk TJ, et al. Enhanced reduced representation bisulfite sequencing for assessment of DNA methylation at base pair resolution. J Vis Exp. 2015;96:e52246. PMC4354670
[18] Mejías Rivera L, Fedulov AV The effect of talc on J774 cells. Gene expression omnibus (GEO) database entry. Record# GSE135238.
[19] Andrews S FastQC: a quality control tool for high throughput sequence data. Available from: http://www.bioinformatics.babraham.ac.uk/projects/fastqc
[20] Krueger F. Trim galore. Available from: http://www.bioinformatics.babraham.ac.uk/projects/trim_galore.
[21] Krueger F, Andrews SR. Bismark: a flexible aligner and methylation caller for Bisulfite-Seq applications. Bioinformatics. 2011;27(11):1571–1572. PMC3102221.
[22] Chen Y, Pal B, Visvader JE, et al. Differential methylation analysis of reduced representation bisulfite sequencing experiments using edgeR. F1000Res. 2017;6(2055):PMC5747346.
[23] Emi T, Mejias-Rivera L, Wallace J, et al. Epigenomic effect of talc particles on macrophages. Gene Expression Omnibus (GEO) database entry. Record# GSE150322.
[24] Gimenez JLG, Carbonell NE, Mateo CR, et al. Epigenetics as the driving force in long-term immunosuppression. J Clin Epigenet. 2016;2:2.
[25] Gordon S. Phagocytosis: an immunobiologic process. Immunity. 2016;44(3):463–475. PMID: 26982354.
[26] Baan R, Straif K, Grosse Y, et al.; WHO International Agency for Research on Cancer Monograph Working Group. Carcinogenicity of carbon black, titanium dioxide, and talc. Lancet Oncol. 2006 Apr;7(4):295–296.No abstract available. Erratum in: Lancet Oncol.

2006 May;7(5):365.PMID: 16598890. doi:10.1016/S1470-2045(06)70651-9.

[27] Cramer DW, Vitonis AF, Terry KL, et al. The association between talc use and ovarian cancer: a retrospective case-control study in two US states. Epidemiology. 2016 May;27(3):334–346. PMC4820665.

[28] Langseth H, Hankinson SE, Siemiatycki J, et al. Perineal use of talc and risk of ovarian cancer. J Epidemiol Community Health. 2008 Apr;62(4):358–360. PMID: 18339830.

[29] Cramer DW, Welch WR, Berkowitz RS, et al. Presence of talc in pelvic lymph nodes of a woman with ovarian cancer and long-term genital exposure to cosmetic talc. Obstet Gynecol. 2007;110(2 Pt 2):498–501.

[30] Titanium dioxide in food — should you be concerned? Available from: https://www.healthline.com/nutrition/titanium-dioxide-in-food#uses

[31] Titanium dioxide. Available from: https://www.chemicalsafetyfacts.org/titanium-dioxide/

[32] Nogueira CM, de Azevedo WM, Dagli ML, et al. Titanium dioxide induced inflammation in the small intestine. World J Gastroenterol. 2012;18(34):4729–4735. PMC3442211.

[33] IARC monographs on the evaluation of carcinogenic risks to humans. Vol. 93. Lyon, France: Carbon Black, Titanium Dioxide, and Talc; 2010. Available from: https://www.ncbi.nlm.nih.gov/books/NBK326521/

[34] Titanium Dioxide (TiO2). by Eileen D. Kuempel and Avima Ruder. Citation for most recent IARC review. IARC Monograph 93 (in press). TR42-4. Available from: https://monographs.iarc.fr/wp-content/uploads/2018/06/TR42-4.pdf.

[35] Kim BG, Lee PH, Lee SH, et al. Effect of TiO_2 nanoparticles on inflammasome-mediated airway inflammation and responsiveness. Allergy Asthma Immunol Res. 2017;9(3):257–264. PMC5352577.

[36] Refaat T, West D, El Achy S, et al. Distribution of iron oxide core-titanium dioxide shell nanoparticles in VX2 tumor bearing rabbits introduced by two different delivery modalities. Nanomaterials (Basel). 2016;6(8):143. PMC5224625.

[37] Sandoval-Sierra JV, Salgado García FI, Brooks JH, et al. Effect of short-term prescription opioids on DNA methylation of the OPRM1 promoter. Clin Epigenetics. 2020;12(1):76. PMC7268244.

[38] Byun HM, Nordio F, Coull BA, et al. Temporal stability of epigenetic markers: sequence characteristics and predictors of short-term DNA methylation variations. PLoS One. 2012;7(6):e39220. PMC3379987.

[39] Hartley I, Elkhoury FF, Heon Shin J, et al. Long-lasting changes in DNA methylation following short-term hypoxic exposure in primary hippocampal neuronal cultures. PLoS One. 2013;8(10):e77859. PMC3808424.

[40] Ferrari L, Carugno M, Bollati V. Particulate matter exposure shapes DNA methylation through the lifespan. Clin Epigenetics. 2019;11(1):129. PMC6717322.

[41] Gregory DJ, Kobzik L, Yang Z, et al. Transgenerational transmission of asthma risk after exposure to environmental particles during pregnancy. Am J Physiol Lung Cell Mol Physiol. 2017;313(2):L395–L405. PMC5582941.

[42] Pacis A, Mailhot-Léonard F, Tailleux L, et al. Gene activation precedes DNA demethylation in response to infection in human dendritic cells. Proc Natl Acad Sci U S A. 2019;116(14):6938–6943. PMC6452747.

Exhibit 107

Management of a malignant pleural effusion: British Thoracic Society pleural disease guideline 2010

Mark E Roberts,[1] Edmund Neville,[2] Richard G Berrisford,[3] George Antunes,[4] Nabeel J Ali[1], on behalf of the BTS Pleural Disease Guideline Group

[1]Sherwood Forest Hospitals NHS Foundation Trust, UK
[2]Portsmouth Hospitals NHS Trust, UK
[3]Royal Devon and Exeter NHS Trust, UK
[4]South Tees NHS Foundation Trust, UK

Correspondence to
Dr Nabeel J Ali, Sherwood Forest Hospitals NHS Foundation Trust, Kingsmill Hospital, Mansfield Road, Sutton in Ashfield NG17 4JL, UK;
nabeel.ali@sfh-tr.nhs.uk

Received 12 February 2010
Accepted 4 March 2010

INTRODUCTION

The discovery of malignant cells in pleural fluid and/or parietal pleura signifies disseminated or advanced disease and a reduced life expectancy in patients with cancer.[1] Median survival following diagnosis ranges from 3 to 12 months and is dependent on the stage and type of the underlying malignancy. The shortest survival time is observed in malignant effusions secondary to lung cancer and the longest in ovarian cancer, while malignant effusions due to an unknown primary have an intermediate survival time.[2–6] Historically, studies showed that median survival times in effusions due to carcinoma of the breast are 5–6 months. However, more recent studies have suggested longer survival times of up to 15 months.[7–10] A comparison of survival times in breast cancer effusions in published studies to 1994 calculated a median survival of 11 months.[9]

Currently, lung cancer is the most common metastatic tumour to the pleura in men and breast cancer in women.[4 11] Together, both malignancies account for 50–65% of all malignant effusions (table 1). Lymphomas, tumours of the genito-urinary tract and gastrointestinal tract account for a further 25%.[2 12–14] Pleural effusions from an unknown primary are responsible for 7–15% of all malignant pleural effusions.[3 13 14] Few studies have estimated the proportion of pleural effusions due to mesothelioma: studies from 1975, 1985 and 1987 identified mesothelioma in 1/271, 3/472 and 22/592 patients, respectively, but there are no more recent data to update this in light of the increasing incidence of mesothelioma.[4 13 14]

Attempts have been made to predict survival based on the clinical characteristics of pleural fluid. None has shown a definite correlation: a recent systematic review of studies including 433 patients assessing the predictive value of pH concluded that low pH does not reliably predict a survival of <3 months.[15 16] In malignant mesothelioma, one study has shown an association between increasing pH and increasing survival.[17] Burrows *et al* showed that only performance status was significantly associated with mortality: median survival was 1.1 months with a Karnofsky score <30 and 13.2 months with a score >70.[18]

An algorithm for the management of malignant pleural effusions is shown in figure 1.

CLINICAL PRESENTATION

- **The majority of malignant effusions are symptomatic. (C)**
- **Massive pleural effusions are most commonly due to malignancy. (C)**

The majority of patients who present with a malignant pleural effusion are symptomatic, although up to 25% are asymptomatic with an incidental finding of effusion on physical examination or by chest radiography.[1] Dyspnoea is the most common presenting symptom, reflecting reduced compliance of the chest wall, depression of the ipsilateral diaphragm, mediastinal shift and reduction in lung volume.[19] Chest pain is less common and is usually related to malignant involvement of the parietal pleura, ribs and other intercostal structures. Constitutional symptoms including weight loss, malaise and anorexia generally accompany respiratory symptoms.

A massive pleural effusion is defined as complete or almost complete opacification of a hemithorax on the chest x-ray. It is usually symptomatic and is commonly associated with a malignant cause.[20] The diagnosis of a malignant pleural effusion is discussed in the guideline on the investigation of a unilateral pleural effusion.

MANAGEMENT OPTIONS

Treatment options for malignant pleural effusions are determined by several factors: symptoms and performance status of the patient, the primary tumour type and its response to systemic therapy, and degree of lung re-expansion following pleural fluid evacuation. Although small cell lung cancer, lymphoma and breast cancer usually respond to chemotherapy, associated secondary pleural effusions may require intervention during the course of treatment (figure 1). Malignant pleural effusions are often most effectively managed by complete drainage of the effusion and instillation of a sclerosant to promote pleurodesis and prevent recurrence of the effusion. Options for management include observation, therapeutic pleural aspiration, intercostal tube drainage and instillation of sclerosant, thoracoscopy and pleurodesis or placement of an indwelling pleural catheter.

Observation

- **Observation is recommended if the patient is asymptomatic and the tumour type is known. (C)**
- **Advice should be sought from the respiratory team and/or respiratory multidisciplinary team for symptomatic malignant effusions. (✓)**

The majority of these patients will become symptomatic in due course and require further intervention. There is no evidence that initial thoracentesis carried out according to standard techniques will

Table 1 Primary tumour site in patients with malignant pleural effusion

Primary tumour site	Salyer[14] (n=95)	Chernow[1] (n=96)	Johnston[13] (n=472)	Sears[4] (n=592)	Hsu[12] (n=785)	Total (%)
Lung	42	32	168	112	410	764 (37.5)
Breast	11	20	70	141	101	343 (16.8)
Lymphoma	11	–	75	92	56	234 (11.5)
Gastrointestinal	–	13	28	32	68	141 (6.9)
Genitourinary	–	13	57	51	70	191 (9.4)
Other	14	5	26	88	15	148 (7.8)
Unknown primary	17	13	48	76	65	219 (10.7)

reduce the chances of subsequent effective pleurodesis after tube drainage. However, repeated thoracentesis may limit the scope for thoracoscopic intervention as it often leads to the formation of adhesions between the parietal and visceral pleura.

Therapeutic pleural aspiration

- **Pleural effusions treated by aspiration alone are associated with a high rate of recurrence of effusion at 1 month so aspiration is not recommended if life expectancy is >1 month. (A)**
- **Caution should be taken if removing >1.5 l on a single occasion. (C)**

Repeated therapeutic pleural aspiration provides transient relief of symptoms and avoids hospitalisation for patients with limited survival expectancy and poor performance status. It is appropriate for frail or terminally ill patients. However, as small-bore chest tubes are widely available, effective and may be inserted with minimal discomfort,[21–26] they may be preferable. The amount of fluid evacuated by pleural aspiration will be guided by patient symptoms (cough, chest discomfort)[27] and should be limited to 1.5 l on a single occasion. Pleural aspiration alone and intercostal tube drainage without instillation of a sclerosant are associated with a high recurrence rate and a small risk of iatrogenic pneumothorax and empyema.[28–36] Therapeutic pleural aspiration should take place under ultrasound guidance (see guideline on pleural procedures).

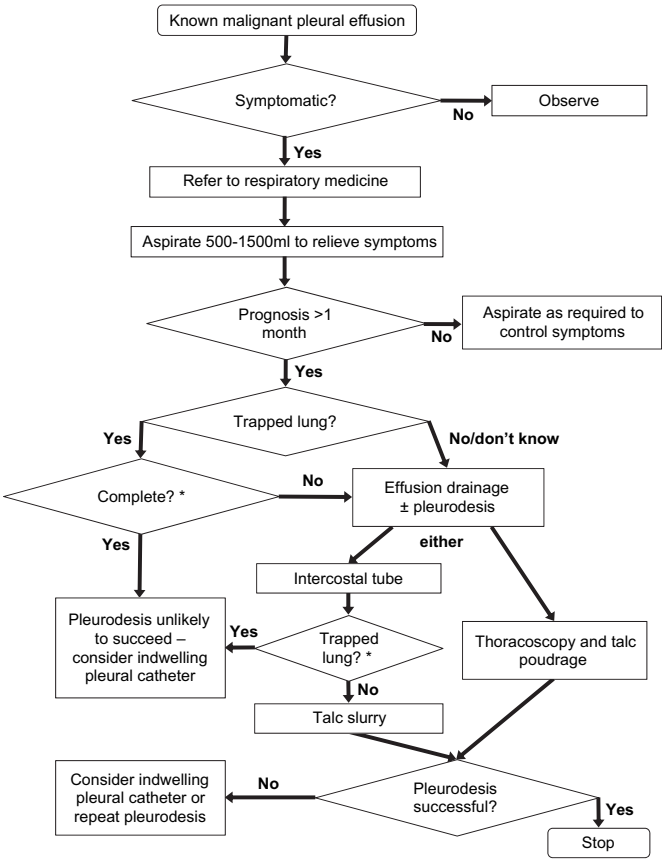

Figure 1 Management algorithm for malignant pleural effusion.

Intercostal tube drainage and intrapleural instillation of sclerosant

- **Other than in patients with a very short life expectancy, small-bore chest tubes followed by pleurodesis are preferable to recurrent aspiration. (✓)**
- **Intercostal drainage should be followed by pleurodesis to prevent recurrence unless lung is significantly trapped. (A)**

Pleurodesis is thought to occur through a diffuse inflammatory reaction and local activation of the coagulation system with fibrin deposition.[37 38] Increased pleural fibrinolytic activity is associated with failure of pleurodesis, as is extensive tumour involvement of the pleura.[39 40] Intercostal drainage without pleurodesis is associated with a high rate of effusion recurrence and should be avoided (see evidence table available on the BTS website at www.brit-thoracic.org.uk). A suggested method for undertaking pleurodesis is shown in box 1.

In animals the effectiveness of pleurodesis may be reduced by concomitant use of corticosteroids. Recent evidence in rabbits has shown reduced pleural inflammatory reaction and, in some cases, prevention of pleurodesis with administration of corticosteroids at the time of talc pleurodesis.[41] A subgroup analysis comparing the efficacy of pleurodesis in the presence and absence of non-randomised oral corticosteroid use also suggested a negative effect of corticosteroids on efficacy.[42] The administration of non-steroidal anti-inflammatory drugs (NSAIDs) at the time of pleurodesis is more contentious. Animal studies have suggested that the use of NSAIDs may impair the action of pleurodesis agents, but there is no evidence from human studies.[43]

Size of intercostal tube

- **Small-bore (10–14 F) intercostal catheters should be the initial choice for effusion drainage and pleurodesis. (A)**

Conventional large-bore intercostal tubes (24–32 F) have been employed in most studies involving sclerosing agents.[44] They have traditionally been used because they are thought to be less

Box 1 How to perform talc slurry chemical pleurodesis

- Insert small-bore intercostal tube (10–14 F).
- Controlled evacuation of pleural fluid.
- Confirm full lung re-expansion and position of intercostal tube with chest x-ray. In cases where incomplete expansion occurs, see text regarding trapped lung.
- Administer premedication prior to pleurodesis (see text).
- Instill lidocaine solution (3 mg/kg; maximum 250 mg) into pleural space followed by 4-5 g sterile graded talc in 50 ml 0.9% saline.
- Clamp tube for 1-2 h.
- Remove intercostal tube within 24-48 h.

prone to obstruction by fibrin plugs, but there is little published evidence to confirm this. The placement of large-bore tubes is perceived to be associated with significant discomfort[45] and this has led to the assessment of smaller bore tubes (10–14 F) for drainage and administration of sclerosing agents.[22 46 47] Three randomised trials investigating the difference in efficacy between small- and large-bore chest tubes all concluded that they were equivalent (see evidence table available on the BTS website at www.brit-thoracic.org.uk).[21–23] Studies using small-bore intercostal tubes with commonly used sclerosants have reported similar success rates to large-bore tubes and appear to cause less discomfort.[24–26 48] The small-bore tubes in these studies were inserted either at the patient's bedside by a physician or under radiological guidance.

Small-bore tubes have been used for ambulatory or outpatient pleurodesis. Patz and colleagues used a fluoroscopically-placed tube (10 F) connected to a closed gravity drainage bag system for this purpose.[49] Bleomycin was the preferred sclerosing agent and the pleurodesis success rate approached 80%. Ambulatory drainage is discussed further in the section on indwelling pleural catheters.

Fluid drainage, pleurodesis and trapped lung

- **Large pleural effusions should be drained in a controlled fashion to reduce the risk of re-expansion pulmonary oedema. (C)**
- **In patients where only partial pleural apposition can be achieved, chemical pleurodesis may still be attempted and may provide symptomatic relief. (B)**
- **In symptomatic cases where pleural apposition cannot be achieved ('trapped lung'), indwelling pleural catheters offer a more attractive therapeutic approach than recurrent aspiration. (✓)**
- **Once effusion drainage and lung re-expansion have been radiographically confirmed, pleurodesis should not be delayed. (B)**
- **Suction to aid pleural drainage before and after pleurodesis is usually unnecessary but, if applied, a high-volume low-pressure system is recommended. (C)**

Large pleural effusions should be drained incrementally, draining a maximum of 1.5 l on the first occasion. Any remaining fluid should be drained 1.5 l at a time at 2 h intervals, stopping if the patient develops chest discomfort, persistent cough or vasovagal symptoms. Re-expansion pulmonary oedema is a well-described serious but rare complication following rapid expansion of a collapsed lung through evacuation of large amounts of pleural fluid on a single occasion and the use of early and excessive pleural suction.[50 51] Putative pathophysiological mechanisms include reperfusion injury of the underlying hypoxic lung, increased capillary permeability and local production of neutrophil chemotactic factors such as interleukin-8.[52 53]

The most important requirement for successful pleurodesis is satisfactory apposition of the parietal and visceral pleura, confirmed radiologically.[44 54 55] Incomplete lung re-expansion may be due to a thick visceral peel ('trapped lung'), pleural loculations, proximal large airway obstruction or a persistent air leak. Most studies indicate that the lack of a response following instillation of a sclerosant is associated with incomplete lung expansion.[56] Where complete lung re-expansion or pleural apposition is not achieved, pleurodesis may still be attempted or an indwelling pleural catheter may be inserted. Robinson and colleagues reported a favourable response in 9 out of 10 patients with partial re-expansion of the lung in a study using doxycycline as a sclerosing agent.[57] The amount of trapped lung compatible with successful pleurodesis is unknown. Complete lack of pleural apposition will prevent pleurodesis: consideration of an indwelling pleural catheter is recommended in this situation. Where more than half the visceral pleura and parietal pleura are apposed, pleurodesis may be attempted although there are no studies to support this recommendation.

The amount of pleural fluid drained per day before the instillation of a sclerosant (<150 ml/day) is less relevant for successful pleurodesis than radiographic confirmation of fluid evacuation and lung re-expansion. In a randomised study, a shorter period of intercostal tube drainage and hospital stay was seen in the group in whom sclerotherapy was undertaken as soon as complete lung re-expansion was documented (majority <24 h) than in the group in whom pleurodesis was attempted only when the fluid drainage was <150 ml/day. The success rate in both groups approached 80%.[55] After sclerosant instillation, the duration of intercostal drainage appears not to affect the chances of successful pleurodesis, although the only randomised study to address this question was underpowered.[58]

Suction may rarely be required for incomplete lung expansion and a persistent air leak. When suction is applied, the use of high-volume low-pressure systems is recommended with a gradual increment in pressure to about −20 cm H_2O.

Analgesia and premedication

- **Lidocaine (3 mg/kg; maximum 250 mg) should be administered intrapleurally just prior to sclerosant administration. (B)**
- **Premedication should be considered to alleviate anxiety and pain associated with pleurodesis. (C)**

Intrapleural administration of sclerosing agents may be painful; significant pain is reported in 7% patients receiving talc to 60% with historical agents such as doxycycline.[57 59] Discomfort can be reduced by administering local anaesthetic via the drain prior to pleurodesis. Lidocaine is the most frequently studied local anaesthetic for intrapleural administration. The onset of action of lidocaine is almost immediate and it should therefore be administered just before the sclerosant. The maximum dose of lidocaine is 3 mg/kg (21 ml of a 1% lidocaine solution for a 70 kg male), with a ceiling of 250 mg. The issue of safety has been highlighted in two studies. Wooten *et al*[60] showed that the mean peak serum concentration of lidocaine following 150 mg of intrapleural lidocaine was 1.3 μg/ml, well below the serum concentration associated with central nervous system side effects (ie, >3 μg/ml). In an earlier study of 20 patients, larger doses of lidocaine were necessary to achieve acceptable levels of local anaesthesia. The patients receiving 250 mg lidocaine had more frequent pain-free episodes than those given 200 mg, while serum levels remained within the therapeutic range. Side effects were limited to transient paraesthesiae in a single patient.[61] The reason for the significant difference in analgesia between the two groups with only a small increment in the lidocaine dose was unclear.

There are no studies to inform a recommendation on the use of premedication and sedation in non-thoracoscopic pleurodesis. Pleurodesis is an uncomfortable procedure and is associated with anxiety for the patient. The use of sedation may be helpful to allay such fears and induce amnesia. The level of sedation should be appropriate to relieve anxiety but sufficient to maintain patient interaction. Sedation employed before pleurodesis should be conducted with continuous monitoring with pulse oximetry and in a setting where resuscitation equipment is available.[62] Further research is underway to address this issue.

Sclerosant and complications

- **Talc is the most effective sclerosant available for pleurodesis. (A)**
- **Graded talc should always be used in preference to ungraded talc as it reduces the risk of arterial hypoxaemia complicating talc pleurodesis. (B)**
- **Talc pleurodesis is equally effective when administered as a slurry or by insufflation. (B)**
- **Bleomycin is an alternative sclerosant with a modest efficacy rate. (B)**
- **Pleuritic chest pain and fever are the most common side effects of sclerosant administration. (B)**

An ideal sclerosing agent must possess several essential qualities: a high molecular weight and chemical polarity, low regional clearance, rapid systemic clearance, a steep dose-response curve and be well tolerated with minimal or no side effects. The choice of a sclerosing agent will be determined by the efficacy or success rate of the agent, accessibility, safety, ease of administration, number of administrations to achieve a complete response and cost. Despite the evaluation of a wide variety of agents, to date no ideal sclerosing agent exists.

Comparison of sclerosing agents is hampered by the lack of comparative randomised trials, different eligibility criteria and disparate criteria for measuring response and end points. A complete response is usually defined as no reaccumulation of pleural fluid after pleurodesis until death, and a partial response as partial reaccumulation of fluid radiographically but not requiring further pleural intervention such as aspiration. However, some studies use a 30-day cut-off. A recent Cochrane review concluded that thoracoscopic talc pleurodesis is probably the optimal method for pleurodesis.[63] This view is supported by a systematic review.[64] Studies are presently underway investigating other agents including the profibrotic cytokine transforming growth factor β.

Tetracycline

Until recently, tetracycline had been the most popular and widely used sclerosing agent in the UK. Unfortunately, parenteral tetracycline is no longer available for this indication in many countries as its production has ceased.[65]

Sterile talc

Talc ($Mg_3Si_4O_{10}(OH)_2$) is a trilayered magnesium silicate sheet that is inert and was first used as a sclerosing agent in 1935.[66] Talc used for intrapleural administration is asbestos-free and sterilised effectively by dry heat exposure, ethylene oxide and gamma radiation. It may be administered in two ways: at thoracoscopy using an atomiser termed 'talc poudrage' or via an intercostal tube in the form of a suspension termed 'talc slurry'.

Success rates (complete and partial response) for talc slurry range from 81% to 100%.[30 54 56 67–70] The majority of studies have used talc slurry alone and only a limited number of comparative studies have been published (see evidence table available on the BTS website at www.brit-thoracic.org.uk). A truncated randomised study by Lynch and colleagues[71] compared talc slurry (5 g) with bleomycin (60 000 units) and tetracycline (750 mg). Although the study was terminated early because of the removal of tetracycline from the US market, analysis of the data to that point revealed no differences between the three treatment groups 1 month after pleurodesis. In a randomised trial between talc slurry (5 g) and bleomycin (60 000 units), 90% of the talc group achieved a complete response at 2 weeks compared with 79% of the bleomycin group, which was statistically insignificant.[72] Three studies have directly compared talc slurry with talc poudrage (see evidence table available on the BTS website at www.brit-thoracic.org.uk).[73–75] For one randomised study the data are available only in abstract form.[73] It suggests superiority of poudrage over slurry, but limited data are available to validate this conclusion. Of the other two studies, Stefani *et al* compared medical thoracoscopy and talc poudrage with talc slurry in a non-randomised way.[75] Their results suggest superiority of poudrage over slurry, but the two groups were not equal with respect to performance status. In the largest study, Dresler *et al* compared a surgical approach to talc poudrage with talc slurry.[74] They concluded equivalence, but 44% of patients dropped out of the study before the 30-day end point due to deaths and a requirement of 90% lung re-expansion radiologically after intervention to be included in the analysis.

Three studies have compared talc poudrage with other agents administered via an intercostal tube. One compared bleomycin (see below) and the other two tetracyclines (see evidence table available on the BTS website at www.brit-thoracic.org.uk).[76–78] Diacon *et al* concluded that talc insufflation at medical thoracoscopy was superior to bleomycin instillation on efficacy and cost grounds.[76] Kuzdzal *et al* and Fentiman *et al* both showed an advantage of talc insufflation over tetracyclines.[77 78] Each of the three studies analysed fewer than 40 patients.

Talc slurry is usually well tolerated and pleuritic chest pain and mild fever are the most common side effects observed. A serious complication associated with the use of talc is adult respiratory distress syndrome or acute pneumonitis leading to acute respiratory failure. There have been many reports of pneumonitis associated with talc pleurodesis, although predominantly from the UK and the USA where historically non-graded talc has been used.[56 79–87] The mechanism of acute talc pneumonitis is unclear and has been reported with both talc poudrage and slurry.[56 80] This complication is related to the grade of talc used. Maskell and colleagues undertook two studies to determine this association. In the first study they randomised 20 patients to pleurodesis using either mixed talc or tetracycline and compared DTPA clearance in the contralateral lung with that undergoing pleurodesis at 48 h after pleurodesis.[88] DTPA clearance half time decreased by more in the talc group, which is a marker of increased lung inflammation. There was also a greater arterial desaturation in those patients exposed to talc. In the second part of the study, graded (particle size >15 μm) and non-graded (50% particle size <15 μm) talc were compared. There was a greater alveolar–arterial oxygen gradient in the group exposed to non-graded talc at 48 h after pleurodesis. In a subsequent cohort study of 558 patients who underwent thoracoscopic pleurodesis using graded talc, there were no episodes of pneumonitis.[89]

Two studies have investigated the systemic distribution of talc particles in rats after talc pleurodesis. The earlier study using uncalibrated talc found widespread organ deposition of talc particles in the lungs, heart, brain, spleen and kidneys at 48 h. The later study used calibrated talc and found liver and spleen deposition (but no lung deposition) at 72 h, but no evidence of pleurodesis in the treated lungs.[90 91] A further study in rabbits found greater systemic distribution of talc with 'normal' (small particle talc).[92] This supports the evidence from clinical studies that large particle talc is preferable to small particle talc.

Bleomycin

Bleomycin is the most widely used antineoplastic agent for the management of malignant pleural effusions. Its mechanism of action is predominantly as a chemical sclerosant similar to talc

and tetracycline. Although 45% of the administered bleomycin is absorbed systemically, it has been shown to cause minimal or no myelosuppression.[93] Bleomycin is an effective sclerosant with success rates after a single administration ranging from 58% to 85% with a mean of 61%. No studies have demonstrated superiority over talc.[42 71 72 94–102] It has an acceptable side effect profile with fever, chest pain and cough the most common adverse effects.[99 102] The recommended dose is 60 000 units mixed in normal saline. Bleomycin has also been used in studies evaluating small-bore intercostal tubes placed under radiological guidance with similar efficacy rates.[46 48 49 103] In the USA, bleomycin is a more expensive sclerosant than talc, but this is not the case in Europe where non-proprietary formulations are available.[42 72 104]

Rotation following pleurodesis

- **Patient rotation is not necessary after intrapleural instillation of sclerosant. (A)**

Rotation of the patient to achieve adequate distribution of the agent over the pleura has been described in many studies. However, rotating the patient is time consuming, inconvenient and uncomfortable. A study using radiolabelled tetracycline showed that tetracycline is dispersed throughout the pleural space within seconds and rotation of the patient did not influence distribution.[105] A subsequent randomised trial using tetracycline, minocycline and doxycycline revealed no significant difference in the success rate of the procedure or duration of fluid drainage between the rotation and non-rotation groups.[106] A similar study using talc showed no difference in distribution of talc after 1 min or 1 h and no difference in the success rate of pleurodesis at 1 month.[107]

Clamping and removal of intercostal tube

- **The intercostal tube should be clamped for 1 h after sclerosant administration. (C)**
- **In the absence of excessive fluid drainage (>250 ml/ day) the intercostal tube should be removed within 24–48 h of sclerosant administration. (C)**

Clamping of the intercostal tube following intrapleural administration of the sclerosant should be brief (1 h) to prevent the sclerosant from immediately draining back out of the pleural space, although there are no studies to prove that this is necessary.[105] Intercostal tube removal has been recommended when fluid drainage is <150 ml/day, but there is little evidence to support this action.[58 68 108 109] In the only randomised study that has addressed the issue, Goodman and Davies randomised patients to 24 h versus 72 h drainage following talc slurry pleurodesis regardless of volume of fluid drainage. They found no difference in pleurodesis success, although they did not reach the recruitment target based upon the power calculation. In the absence of any evidence that protracted drainage is beneficial, and given the discomfort associated with prolonged drainage, we recommend removal of the intercostal tube within 24–48 h after the instillation of the sclerosant, provided the lung remains fully re-expanded and there is satisfactory evacuation of pleural fluid on the chest x-ray.

Pleurodesis failure

The most likely cause of pleurodesis failure is the presence of trapped lung. There is no reliable way to predict pleurodesis failure: a recent systematic review found that an arbitrary cut-off of pH <7.20 did not predict pleurodesis failure.[15] Where pleurodesis fails, there is no evidence available as to the most effective secondary procedure. We recommend that further evacuation of pleural fluid should be attempted with either a repeat pleurodesis or insertion of indwelling pleural catheter, depending upon the presence of trapped lung. Surgical pleurectomy has been described as an alternative option for patients with mesothelioma (see later).

Malignant seeding at intercostal tube or port site

- **Patients with proven or suspected mesothelioma should receive prophylactic radiotherapy to the site of thoracoscopy, surgery or large-bore chest drain insertion, but there is little evidence to support this for pleural aspirations or pleural biopsy. (B)**

Local tumour recurrence or seeding following diagnostic and therapeutic pleural aspiration, pleural biopsy, intercostal tube insertion and thoracoscopy is uncommon in non-mesothelioma malignant effusions.[110–113] However, in mesothelioma up to 40% of patients may develop malignant seeding at the site of pleural procedures. Three randomised studies have addressed the efficacy of procedure site radiotherapy to prevent tract metastasis (see evidence table available on the BTS website at www.brit-thoracic.org.uk).[114–116] Boutin and colleagues[114] found that local metastases were prevented in patients who received radiotherapy (21 Gy in three fractions) to the site of thoracoscopy. All the patients received radiotherapy within 2 weeks of thoracoscopy. The incidence of tract metastases in the control group in this study was 40%. This study was followed by a longitudinal study that supported its conclusions.[117] In two later studies including sites from a wider range of procedures such as needle biopsy and chest drain, the incidence of tract metastases was not significantly different. Bydder and colleagues showed no benefit of a single 10 Gy radiotherapy fraction to the intervention site in preventing recurrence.[116] All the patients received radiotherapy within 15 days of the procedure, but 46% of procedures were fine needle aspirations. O'Rourke and colleagues used the same radiotherapy dose as Boutin but to smaller fields. They found no benefit of radiotherapy, but again included a range of procedures including needle biopsy. The study included 60 patients but only 16 thoracoscopies, 7 in the radiotherapy group and 9 in the best supportive care group. Tract metastases occurred in 4 patients in the best supportive care group (a rate of 44%) and none in the radiotherapy group.[115] This is very similar to the incidence of tract metastasis in the study by Boutin *et al* (40%). The other procedures were pleural biopsies (45%) and chest tubes (25%). A longitudinal study by Agarwal *et al* found the highest rate of pleural tract metastases in association with thoracoscopy (16%), thoracotomy (24%) and chest tube (9%), but a much lower rate in association with pleural aspiration (3.6%) and image-guided biopsy (4.5%).[118] Careful analysis of the available data therefore supports the use of radiotherapy to reduce tract metastasis after significant pleural instrumentation (thoracoscopy, surgery or large-bore chest drain), but not for less invasive procedures such as pleural biopsy or pleural aspiration. A larger study to specifically address this question would be of use.

A cohort of 38 patients described by West *et al* reported an incidence of pleural tract metastasis after radiotherapy of 5%, but in these cases the metastasis occurred at the edge of the radiotherapy field. Of six patients who received radiotherapy after an indwelling pleural catheter, one subsequently developed pleural tract metastasis.[119] There are, at present, insufficient data on which to make a recommendation about the use of radiotherapy in the presence of indwelling pleural catheters.

The role of prophylactic radiotherapy following pleural procedures in non-mesothelioma malignant effusions has not been established and therefore cannot be recommended.

Intrapleural fibrinolytics

- **Intrapleural instillation of fibrinolytic drugs is recommended for the relief of distressing dyspnoea due to multiloculated malignant effusion resistant to simple drainage. (C)**

The use of fibrinolytic agents to ameliorate symptoms related to complex pleural effusions has been described in several studies although there are no randomised controlled trials.

Davies *et al* found that intrapleural streptokinase increased pleural fluid drainage and led to radiographic improvement and amelioration of symptoms in 10 patients with multiloculated or septated malignant effusions. Intrapleural streptokinase was well tolerated and no allergic or haemorrhagic complications were reported.[120] Gilkeson *et al*[121] preferred urokinase in their prospective but non-randomised study. Twenty-two malignant pleural effusions were treated with urokinase resulting in a substantial increase in pleural fluid output in patients both with and without radiographic evidence of loculations. The majority then underwent pleurodesis with doxycycline resulting in a complete response rate of 56%. Similarly, no allergic or haemorrhagic complications were encountered. In the largest series, 48 patients unfit for surgical release of trapped lung after incomplete lung re-expansion following tube drainage were given intrapleural urokinase.[122] Breathlessness was improved in 29 patients, 27 of whom eventually successfully achieved pleurodesis. This study compared cases with historical controls treated solely with saline flushes and in whom breathlessness was not assessed.

None of these studies is large enough to accurately describe the safety profile of fibrinolytic drugs in this setting. Immune-mediated or haemorrhagic complications have rarely been described with the administration of intrapleural fibrinolytics in contrast to systemic administration of these agents.[123 124] A chest physician should be involved in the care of all patients receiving this treatment.

Thoracoscopy

- **In patients with good performance status, thoracoscopy is recommended for diagnosis of suspected malignant pleural effusion and for drainage and pleurodesis of a known malignant pleural effusion. (B)**
- **Thoracoscopic talc poudrage should be considered for the control of recurrent malignant pleural effusion. (B)**
- **Thoracoscopy is a safe procedure with low complication rates. (B)**

Thoracoscopy (under sedation or general anaesthesia) has grown in popularity as a diagnostic and therapeutic tool for malignant effusions. Under sedation, it is now widely used by respiratory physicians in the diagnosis and management of pleural effusions in patients with good performance status.[125–128] Patient selection for thoracoscopy and talc poudrage is important in view of the invasive nature of the procedure and cost.[129] A significant benefit of thoracoscopy is the ability to obtain a diagnosis, drain the effusion and perform a pleurodesis during the same procedure.

The diagnostic yield and accuracy of thoracoscopy for malignant effusions is >90%.[99 125 127 130 131] Talc poudrage performed during thoracoscopy is an effective method for controlling malignant effusions with a pleurodesis success rate of 77–100%.[6 68 97 132–138] Randomised studies have established the superiority of talc poudrage over both bleomycin and tetracyclines (see evidence table available on the BTS website at www.brit-thoracic.org.uk).[73 76–78] One large randomised study comparing talc poudrage with talc slurry failed to establish a difference in efficacy between the two techniques.[74] A further small non-randomised study comparing these two techniques also established equivalence.[133] A large study has established the safety of talc poudrage using large particle talc; no cases of respiratory failure were seen in this cohort of 558 patients.[89] Talc poudrage is known particularly to be effective in the presence of effusions due to carcinoma of the breast.[139]

Thoracoscopy has less to offer in patients with a known malignant pleural effusion and a clearly trapped lung on the chest x-ray. However, under general anaesthesia, reinflation of the lung under thoracoscopic vision will inform whether the lung is indeed trapped and therefore guide the decision to perform talc poudrage or insert a pleural catheter. The procedure can facilitate breaking up of loculations or blood clot in haemorrhagic malignant pleural effusion and can allow the release of adhesions and thereby aid lung re-expansion and apposition of the pleura for talc poudrage.[140 141]

Thoracoscopy is a safe and well-tolerated procedure with a low perioperative mortality rate (<0.5%).[6 126 129 142] The most common major complications are empyema and acute respiratory failure secondary to infection or re-expansion pulmonary oedema, although the latter may be avoided by staged evacuation of pleural fluid and allowing air to replace the fluid.[127 129 143]

Long-term ambulatory indwelling pleural catheter drainage

- **Ambulatory indwelling pleural catheters are effective in controlling recurrent and symptomatic malignant effusions in selected patents. (B)**

Insertion of a tunnelled pleural catheter is an alternative method for controlling recurrent and symptomatic malignant effusions including patients with trapped lung. Several catheters have been developed for this purpose and the published studies employing them have reported encouraging results.[140 144–147] The presence of foreign material (silastic catheter) within the pleural space stimulates an inflammatory reaction, and vacuum drainage bottles connected to the catheter every few days encourage re-expansion and obliteration of the pleural space. Most catheters can be removed after a relatively short period.

In the only randomised and controlled study to date, Putnam and colleagues[145] compared a long-term indwelling pleural catheter with doxycycline pleurodesis via a standard intercostal tube. The length of hospitalisation for the indwelling catheter group was significantly shorter (1 day) than that of the doxycycline pleurodesis group (6 days). Spontaneous pleurodesis was achieved in 42 of the 91 patients in the indwelling catheter group. A late failure rate (defined as reaccumulation of pleural fluid after initial successful control) of 13% was reported compared with 21% for the doxycycline pleurodesis group. There was a modest improvement in the quality of life and dyspnoea scores in both groups. The complication rate was higher (14%) in the indwelling catheter group and included local cellulitis (most common) and, rarely, tumour seeding of the catheter tract.

The largest series to date reported on 250 patients, with at least partial symptom control achieved in 88.8%. Spontaneous pleurodesis occurred in 42.9% while catheters remained until death in 45.8%.[148] A more recent series of 231 patients treated with an indwelling catheter to drain pleural effusion reported a removal rate of 58% after spontaneous cessation of drainage, with only 3.8% reaccumulation and 2.2% infection.[147] This group included those with trapped lung (12.5% of all patients) or who had failed other therapy. A further series of 48 patients reported a spontaneous pleurodesis rate of 48%.[149] Pien *et al* studied a group of 11 patients in whom an indwelling catheter

was placed specifically for a malignant effusion in the presence of trapped lung; 10 patients reported symptomatic improvement.[144]

A recent series of 45 patients reported by Janes *et al* described three cases of catheter tract metastasis associated with indwelling pleural catheters occurring between 3 weeks and 9 months after insertion. Metastases occurred in 2 of 15 patients with mesothelioma but in only 1 of 30 patients with other metastatic malignancy.[150]

An indwelling pleural catheter is therefore an effective option for controlling recurrent malignant effusions when length of hospitalisation is to be kept to a minimum (reduced life expectancy) or where patients are known or are suspected to have trapped lung and where expertise and facilities exist for outpatient management of these catheters. Although there is a significant cost associated with the disposable vacuum drainage bottles that connect to indwelling pleural catheters, there may be a cost reduction associated with reduced length of hospital stay or avoidance of hospital admission.

Pleurectomy

Pleurectomy has been described as a treatment for malignant pleural effusions. Open pleurectomy is an invasive procedure with significant morbidity. Complications may include empyema, haemorrhage and cardiorespiratory failure (operative mortality rates of 10–19% have been described).[151–153] Pleurectomy performed by video-assisted thoracic surgery has been described in a small series of patients with mesothelioma. There is not sufficient evidence to recommend this as an alternative to pleurodesis or indwelling pleural catheter in recurrent effusions or trapped lung.[154]

Competing interests No member of the Guideline Group is aware of any competing interests.

Provenance and peer review The draft guideline was available for online public consultation (July/August 2009) and presented to the BTS Winter Meeting (December 2009). Feedback was invited from a range of stakeholder institutions (see Introduction). The draft guideline was reviewed by the BTS Standards of Care Committee (September 2009).

REFERENCES

1. **Chernow B,** Sahn SA. Carcinomatous involvement of the pleura: an analysis of 96 patients. *Am J Med* 1977;**63**:695–702. (**3**).
2. **Abbruzzese JL,** Abbruzzese MC, Hess KR, *et al*. Unknown primary carcinoma: natural history and prognostic factors in 657 consecutive patients. *J Clin Oncol* 1994;**12**:1272–80. (**2+**).
3. **van de Molengraft FJ,** Vooijs GP. Survival of patients with malignancy-associated effusions. *Acta Cytol* 1989;**33**:911–16. (**2+**).
4. **Sears D,** Hajdu SI. The cytologic diagnosis of malignant neoplasms in pleural and peritoneal effusions. *Acta Cytol* 1987;**31**:85–97. (**2+**).
5. **Bonnefoi H,** Smith IE. How should cancer presenting as a malignant pleural effusion be managed? *Br J Cancer* 1996;**74**:832–5. (**2−**).
6. **Kolschmann S,** Ballin A, Gillissen A. Clinical efficacy and safety of thoracoscopic talc pleurodesis in malignant pleural effusions. *Chest* 2005;**128**:1431–5. (**2−**).
7. **Raju RN,** Kardinal CG. Pleural effusion in breast carcinoma: analysis of 122 cases. *Cancer* 1981;**48**:2524–7. (**3**).
8. **Fentiman IS,** Millis R, Sexton S, *et al*. Pleural effusion in breast cancer: a review of 105 cases. *Cancer* 1981;**47**:2087–92. (**3**).
9. **Banerjee AK,** Willetts I, Robertson JF, *et al*. Pleural effusion in breast cancer: a review of the Nottingham experience. *Eur J Surg Oncol* 1994;**20**:33–6. (**3**).
10. **Dieterich M,** Goodman SN, Rojas-Corona RR, *et al*. Multivariate analysis of prognostic features in malignant pleural effusions from breast cancer patients. *Acta Cytol* 1994;**38**:945–52. (**3**).
11. **DiBonito L,** Falconieri G, Colautti I, *et al*. The positive pleural effusion. A retrospective study of cytopathologic diagnoses with autopsy confirmation. *Acta Cytol* 1992;**36**:329–32. (**2+**).
12. **Hsu C.** Cytologic detection of malignancy in pleural effusion: a review of 5,255 samples from 3,811 patients. *Diagn Cytopathol* 1987;**3**:8–12. (**2−**).
13. **Johnston WW.** The malignant pleural effusion. A review of cytopathologic diagnoses of 584 specimens from 472 consecutive patients. *Cancer* 1985;**56**:905–9. (**3**).
14. **Salyer WR,** Eggleston JC, Erozan YS. Efficacy of pleural needle biopsy and pleural fluid cytopathology in the diagnosis of malignant neoplasm involving the pleura. *Chest* 1975;**67**:536–9. (**3**).
15. **Heffner JE,** Heffner JN, Brown LK. Multilevel and continuous pleural fluid pH likelihood ratios for evaluating malignant pleural effusions. *Chest* 2003;**123**:1887–94. (**1−**).
16. **Rodriguez-Panadero F,** Lopez Mejias J. Low glucose and pH levels in malignant pleural effusions. Diagnostic significance and prognostic value in respect to pleurodesis. *Am Rev Respir Dis* 1989;**139**:663–7. (**2+**).
17. **Gottehrer A,** Taryle DA, Reed CE, *et al*. Pleural fluid analysis in malignant mesothelioma. Prognostic implications. *Chest* 1991;**100**:1003–6. (**3**).
18. **Burrows CM,** Mathews WC, Colt HG. Predicting survival in patients with recurrent symptomatic malignant pleural effusions: an assessment of the prognostic values of physiologic, morphologic, and quality of life measures of extent of disease. *Chest* 2000;**117**:73–8. (**2+**).
19. **Judson M,** Sahn S. Pulmonary physiologic abnormalities caused by pleural disease. *Semin Respir Crit Care Med* 1995;**16**:346–53. (**4**).
20. **Maher GG,** Berger HW. Massive pleural effusion: malignant and nonmalignant causes in 46 patients. *Am Rev Respir Dis* 1972;**105**:458–60. (**3**).
21. **Parulekar W,** Di Primio G, Matzinger F, *et al*. Use of small-bore vs large-bore chest tubes for treatment of malignant pleural effusions. *Chest* 2001;**120**:19–25. (**2+**).
22. **Clementsen P,** Evald T, Grode G, *et al*. Treatment of malignant pleural effusion: pleurodesis using a small percutaneous catheter. A prospective randomized study. *Respir Med* 1998;**92**:593–6. (**1+**).
23. **Caglayan B,** Torun E, Turan D, *et al*. Efficacy of iodopovidone pleurodesis and comparison of small-bore catheter versus large-bore chest tube. *Ann Surg Oncol* 2008;**15**:2594–9. (**1+**).
24. **Seaton KG,** Patz EF Jr, Goodman PC. Palliative treatment of malignant pleural effusions: value of small-bore catheter thoracostomy and doxycycline sclerotherapy. *AJR* 1995;**164**:589–91. (**2+**).
25. **Morrison MC,** Mueller PR, Lee MJ, *et al*. Sclerotherapy of malignant pleural effusion through sonographically placed small-bore catheters. *AJR* 1992;**158**:41–3. (**2+**).
26. **Parker LA,** Charnock GC, Delany DJ. Small bore catheter drainage and sclerotherapy for malignant pleural effusions. *Cancer* 1989;**64**:1218–21. (**3**).
27. **Feller-Kopman D,** Walkey A, Berkowitz D, *et al*. The relationship of pleural pressure to symptom development during therapeutic thoracentesis. *Chest* 2006;**129**:1556–60. (**2−**).
28. **Sorensen PG,** Svendsen TL, Enk B. Treatment of malignant pleural effusion with drainage, with and without instillation of talc. *Eur J Respir Dis* 1984;**65**:131–5. (**1−**).
29. **Zaloznik AJ,** Oswald SG, Langin M. Intrapleural tetracycline in malignant pleural effusions. A randomized study. *Cancer* 1983;**51**:752–5. (**1−**).
30. **Leverenz A,** Heckmayr M, Tischer-Neuhauss R, *et al*. Intrapleural palliative treatment of malignant pleural effusions with talcum versus placebo (pleural tube alone) [abstract]. *Lung Cancer* 2000;**29A**274. (**1−**).
31. **Groth G,** Gatzemeier U, Haussingen K, *et al*. Intrapleural palliative treatment of malignant pleural effusions with mitoxantrone versus placebo (pleural tube alone). *Ann Oncol* 1991;**2**:213–15. (**1+**).
32. **O'Neill W,** Spurr C, Moss H, *et al*. A prospective study of chest tube drainage and tetracycline sclerosis versus chest tube drainage alone in the treatment of malignant pleural effusions [abstract]. *Proc Annu Meet Am Assoc Cancer Res* 1980;**21**:349. (**3**).
33. **Lambert CJ,** Shah HH, Urshel HC Jr, *et al*. The treatment of malignant pleural effusions by closed trocar tube drainage. *Ann Thorac Surg* 1967;**3**:1–5. (**2−**).
34. **Anderson CB,** Philpott GW, Ferguson TB. The treatment of malignant pleural effusions. *Cancer* 1974;**33**:916–22. (**3**).
35. **Izbicki R,** Weyhing BT 3rd, Baker L, *et al*. Pleural effusion in cancer patients. A prospective randomized study of pleural drainage with the addition of radioactive phosphorous to the pleural space vs. pleural drainage alone. *Cancer* 1975;**36**:1511–18. (**1−**).
36. **Boland GW,** Gazelle GS, Girard MJ, *et al*. Asymptomatic hydropneumothorax after therapeutic thoracentesis for malignant pleural effusions. *AJR* 1998;**170**:943–6. (**2−**).
37. **Antony VB.** Pathogenesis of malignant pleural effusions and talc pleurodesis. *Pneumologie* 1999;**53**:493–8. (**2+**).
38. **Antony VB,** Rothfuss KJ, Godbey SW, *et al*. Mechanism of tetracycline-hydrochloride-induced pleurodesis. Tetracycline-hydrochloride-stimulated mesothelial cells produce a growth-factor-like activity for fibroblasts. *Am Rev Respir Dis* 1992;**146**:1009–13. (**2−**).
39. **Antony VB,** Nasreen N, Mohammed KA, *et al*. Talc pleurodesis: basic fibroblast growth factor mediates pleural fibrosis. *Chest* 2004;**126**:1522–8. (**2−**).
40. **Rodriguez-Panadero F,** Segado A, Martin Juan J, *et al*. Failure of talc pleurodesis is associated with increased pleural fibrinolysis. *Am J Respir Crit Care Med* 1995;**151**(3 Pt 1):785–90. (**2+**).
41. **Xie C,** Teixeira LR, McGovern JP, *et al*. Systemic corticosteroids decrease the effectiveness of talc pleurodesis. *Am J Respir Crit Care Med* 1998; **157**(5 Pt 1):1441–4. (**2+**).
42. **Haddad FJ,** Younes RN, Gross JL, *et al*. Pleurodesis in patients with malignant pleural effusions: talc slurry or bleomycin? Results of a prospective randomized trial. *World J Surg* 2004;**28**:749–54. (**1−**).

43. **Hunt I,** Teh E, Southon R, *et al*. Using non-steroidal anti-inflammatory drugs (NSAIDs) following pleurodesis. *Interact Cardiovasc Thorac Surg* 2007;**6**:102—4. (**4**).
44. **Hausheer FH,** Yarbro JW. Diagnosis and treatment of malignant pleural effusion. *Semin Oncol* 1985;**12**:54—75. (**2—**).
45. **Owen S,** Gould D. Underwater seal chest drains: the patient's experience. *J Clin Nurs* 1997;**6**:215—25. (**2—**).
46. **Goff BA,** Mueller PR, Muntz HG, *et al*. Small chest-tube drainage followed by bleomycin sclerosis for malignant pleural effusions. *Obstet Gynecol* 1993;**81**:993—6. (**3**).
47. **Chen YM,** Shih JF, Yang KY, *et al*. Usefulness of pig-tail catheter for palliative drainage of malignant pleural effusions in cancer patients. *Support Care Cancer* 2000;**8**:423—6. (**2—**).
48. **Patz EF Jr,** McAdams HP, Erasmus JJ, *et al*. Sclerotherapy for malignant pleural effusions: a prospective randomized trial of bleomycin vs doxycycline with small-bore catheter drainage. *Chest* 1998;**113**:1305—11. (**1—**).
49. **Patz EF Jr,** McAdams HP, Goodman PC, *et al*. Ambulatory sclerotherapy for malignant pleural effusions. *Radiology* 1996;**199**:133—5. (**2—**).
50. **Tarver RD,** Broderick LS, Conces DJ Jr. Reexpansion pulmonary edema. *J Thorac Imaging* 1996;**11**:198—209. (**4**).
51. **Mahfood S,** Hix WR, Aaron BL, *et al*. Reexpansion pulmonary edema. *Ann Thorac Surg* 1988;**45**:340—5. (**3**).
52. **Nakamura H,** Ishizaka A, Sawafuji M, *et al*. Elevated levels of interleukin-8 and leukotriene B4 in pulmonary edema fluid of a patient with reexpansion pulmonary edema. *Am J Respir Crit Care Med* 1994;**149**(4 Pt 1):1037—40. (**3**).
53. **Trachiotis GD,** Vricella LA, Aaron BL, *et al*. As originally published in 1988: Reexpansion pulmonary edema. Updated in 1997. *Ann Thorac Surg* 1997;**63**:1206—7. (**4**).
54. **Adler RH,** Sayek I. Treatment of malignant pleural effusion: a method using tube thoracostomy and talc. *Ann Thorac Surg* 1976;**22**:8—15. (**3**).
55. **Villanueva AG,** Gray AW Jr, Shahian DM, *et al*. Efficacy of short term versus long term tube thoracostomy drainage before tetracycline pleurodesis in the treatment of malignant pleural effusions. *Thorax* 1994;**49**:23—5. (**1+**).
56. **Kennedy L,** Rusch VW, Strange C, *et al*. Pleurodesis using talc slurry. *Chest* 1994;**106**:342—6. (**2—**).
57. **Robinson LA,** Fleming WH, Galbraith TA. Intrapleural doxycycline control of malignant pleural effusions. *Ann Thorac Surg* 1993;**55**:1115—22. (**2—**).
58. **Goodman A,** Davies CWH. Efficacy of short-term versus long-term chest tube drainage following talc slurry pleurodesis in patients with malignant pleural effusions: a randomised trial. *Lung Cancer* 2006;**54**:51—5. (**1—**).
59. **Pulsiripunya C,** Youngchaiyud P, Pushpakom R, *et al*. The efficacy of doxycycline as a pleural sclerosing agent in malignant pleural effusion: a prospective study. *Respirology* 1996;**1**:69—72. (**2—**).
60. **Wooten SA,** Barbarash RA, Strange C, *et al*. Systemic absorption of tetracycline and lidocaine following intrapleural instillation. *Chest* 1988;**94**:960—3. (**2—**).
61. **Sherman S,** Grady KJ, Seidman JC. Clinical experience with tetracycline pleurodesis of malignant pleural effusions. *South Med J* 1987;**80**:716—19. (**2—**).
62. **Whitwam J,** C W. *Sedation and sedoanalgesia*. In: Whitwam J, editor. *Day-case anaesthesia and sedation*. London: Blackwell Scientific Publications; 1994:262—74. (**4**).
63. **Shaw P,** Agarwal R. Pleurodesis for malignant pleural effusions. *Cochrane Database Syst Rev* 2004;(1):002916. (**1++**).
64. **Tan C,** Sedrakyan A, Browne J, *et al*. The evidence on the effectiveness of management for malignant pleural effusion: a systematic review. *Eur J Cardiothorac Surg* 2006;**29**:829—38. (**1+**).
65. **Heffner JE,** Unruh LC. Tetracycline pleurodesis. Adios, farewell, adieu. *Chest* 1992;**101**:5—7. (**4**).
66. **Bethune N.** Pleural poudrage: new technique for deliberate production of pleural adhesions as preliminary to lobectomy. *J Thorac Cardiovasc Surg* 1935;**4**:251—61. (**3**).
67. **Webb WR,** Ozmen V, Moulder PV, *et al*. Iodized talc pleurodesis for the treatment of pleural effusions. *J Thorac Cardiovasc Surg* 1992;**103**:881—6. (**2—**).
68. **Yim AP,** Chan AT, Lee TW, *et al*. Thoracoscopic talc insufflation versus talc slurry for symptomatic malignant pleural effusion. *Ann Thorac Surg* 1996;**62**:1655—8. (**1—**).
69. **Marom EM,** Patz EF Jr, Erasmus JJ, *et al*. Malignant pleural effusions: treatment with small-bore-catheter thoracostomy and talc pleurodesis. *Radiology* 1999;**210**:277—81. (**2+**).
70. **Thompson RL,** Yau JC, Donnelly RF, *et al*. Pleurodesis with iodized talc for malignant effusions using pigtail catheters. *Ann Pharmacother* 1998;**32**:739—42. (**3**).
71. **Lynch TJ Jr.** Optimal therapy of malignant pleural effusions: Report of a randomized trial of bleomycin, tetracycline, and talc and a meta-analysis. *Int J Oncol* 1996;**8**:183—90. (**1—**).
72. **Zimmer PW,** Hill M, Casey K, *et al*. Prospective randomized trial of talc slurry vs bleomycin in pleurodesis for symptomatic malignant pleural effusions. *Chest* 1997;**112**:430—4. (**1+**).
73. **Manes N,** Rodriguez-Panadero F, Bravo J, *et al*. Talc pleurodesis. Prospective and randomized study clinical follow up [abstract]. *Chest* 2000;**118**:131S. (**1—**).
74. **Dresler CM,** Olak J, Herndon JE 2nd, *et al*. Phase 3 intergroup study of talc poudrage vs talc slurry sclerosis for malignant pleural effusion. *Chest* 2005;**127**:909—15. (**1—**).
75. **Stefani A,** Natali P, Casali C, *et al*. Talc poudrage versus talc slurry in the treatment of malignant pleural effusion. A prospective comparative study. *Eur J Cardiothorac Surg* 2006;**30**:827—32. (**2—**).
76. **Diacon AH,** Wyser C, Bolliger CT, *et al*. Prospective randomized comparison of thoracoscopic talc poudrage under local anesthesia versus bleomycin instillation for pleurodesis in malignant pleural effusions. *Am J Respir Crit Care Med* 2000;**162**(4 Pt 1):1445—9. (**1+**).
77. **Kuzdzal J,** Sladek K, Wasowski D, *et al*. Talc powder vs doxycycline in the control of malignant pleural effusion: a prospective, randomized trial. *Med Sci Monitor* 2003;**9**:PI54—9. (**1—**).
78. **Fentiman IS,** Rubens RD, Hayward JL. A comparison of intracavitary talc and tetracycline for the control of pleural effusions secondary to breast cancer. *Eur J Cancer Clin Oncol* 1986;**22**:1079—81. (**1—**)
79. **Brant A,** Eaton T. Serious complications with talc slurry pleurodesis. *Respirology* 2001;**6**:181—5. (**2—**).
80. **Rinaldo JE,** Owens GR, Rogers RM. Adult respiratory distress syndrome following intrapleural instillation of talc. *J Thorac Cardiovasc Surg* 1983;**85**:523—6. (**3**).
81. **Bouchama A,** Chastre J, Gaudichet A, *et al*. Acute pneumonitis with bilateral pleural effusion after talc pleurodesis. *Chest* 1984;**86**:795—7. (**3**).
82. **Rehse DH,** Aye RW, Florence MG. Respiratory failure following talc pleurodesis. *Am J Surg* 1999;**177**:437—40. (**2—**).
83. **Campos JRM,** Werebe EC, Vargas FS, *et al*. Respiratory failure due to insufflated talc. *Lancet* 1997;**349**:251—2. (**3**).
84. **Nandi P.** Recurrent spontaneous pneumothorax; an effective method of talc poudrage. *Chest* 1980;**77**:493—5. (**4**).
85. **Ferrer J,** Villarino MA, Tura JM, *et al*. Talc preparations used for pleurodesis vary markedly from one preparation to another. *Chest* 2001;**119**:1901—5. (**2++**).
86. **Kuzniar T,** Mutlu GM. Post-talc pleurodesis acute lung injury: case report and review of literature. *Adv Clin Exp Med* 2004;**13**:367—70. (**3**).
87. **Bondoc AY,** Bach PB, Sklarin NT, *et al*. Arterial desaturation syndrome following pleurodesis with talc slurry: incidence, clinical features, and outcome. *Cancer Invest* 2003;**21**:848—54. (**2—**).
88. **Maskell NA,** Lee YC, Gleeson FV, *et al*. Randomized trials describing lung inflammation after pleurodesis with talc of varying particle size. *Am J Respir Crit Care Med* 2004;**170**:377—82. (**1+**).
89. **Janssen JP,** Collier G, Astoul P, *et al*. Safety of pleurodesis with talc poudrage in malignant pleural effusion: a prospective cohort study. *Lancet* 2007;**369**:1535—9. (**2++**).
90. **Werebe EC,** Pazetti R, Milanez de Campos JR, *et al*. Systemic distribution of talc after intrapleural administration in rats. *Chest* 1999;**115**:190—3. (**2+**).
91. **Fraticelli A,** Robaglia-Schlupp A, Riera H, *et al*. Distribution of calibrated talc after intrapleural administration: an experimental study in rats. *Chest* 2002;**122**:1737—41. (**2+**).
92. **Ferrer J,** Montes JF, Villarino MA, *et al*. Influence of particle size on extrapleural talc dissemination after talc slurry pleurodesis. *Chest* 2002;**122**:1018—27. (**2+**).
93. **Alberts DS,** Chen HS, Mayersohn M, *et al*. Bleomycin pharmacokinetics in man. 2. Intracavitary administration. *Cancer Chemother Pharmacol* 1979;**2**:127—32. (**3**).
94. **Bitran JD,** Brown C, Desser RK, *et al*. Intracavitary bleomycin for the control of malignant effusions. *J Surg Oncol* 1981;**16**:273—7. (**3**).
95. **Emad A,** Rezaian GR. Treatment of malignant pleural effusions with a combination of bleomycin and tetracycline. A comparison of bleomycin or tetracycline alone versus a combination of bleomycin and tetracycline. *Cancer* 1996;**78**:2498—501. (**1—**).
96. **Hamed H,** Fentiman IS, Chaudary MA, *et al*. Comparison of intracavitary bleomycin and talc for control of pleural effusions secondary to carcinoma of the breast. *Br J Surg* 1989;**76**:1266—7. (**1+**).
97. **Hartman DL,** Gaither JM, Kesler KA, *et al*. Comparison of insufflated talc under thoracoscopic guidance with standard tetracycline and bleomycin pleurodesis for control of malignant pleural effusions. *J Thorac Cardiovasc Surg* 1993;**105**:743—8. (**2—**).
98. **Kessinger A,** Wigton RS. Intracavitary bleomycin and tetracycline in the management of malignant pleural effusions: a randomized study. *J Surg Oncol* 1987;**36**:81—3. (**1—**).
99. **Martinez-Moragon E,** Aparicio J, Rogado MC, *et al*. Pleurodesis in malignant pleural effusions: a randomized study of tetracycline versus bleomycin. *Eur Respir J* 1997;**10**:2380—3. (**1+**).
100. **Noppen M,** Degreve J, Mignolet M, *et al*. A prospective, randomised study comparing the efficacy of talc slurry and bleomycin in the treatment of malignant pleural effusions. *Acta Clin Belg* 1997;**52**:258—62. (**1+**).
101. **Ong KC,** Indumathi V, Raghuram J, *et al*. A comparative study of pleurodesis using talc slurry and bleomycin in the management of malignant pleural effusions. *Respirology* 2000;**5**:99—103. (**1—**).
102. **Ruckdeschel JC,** Moores D, Lee JY, *et al*. Intrapleural therapy for malignant pleural effusions. a randomized comparison of bleomycin and tetracycline [erratum appears in Chest 1993;103:1640]. *Chest* 1991;**100**:1528—35. (**1++**).
103. **Hsu WH,** Chiang CD, Chen CY, *et al*. Ultrasound-guided small-bore Elecath tube insertion for the rapid sclerotherapy of malignant pleural effusion. *Jpn J Clin Oncol* 1998;**28**:187—91. (**3**).
104. **Kilic D,** Akay H, Kavukcu S, *et al*. Management of recurrent malignant pleural effusion with chemical pleurodesis. *Surg Today* 2005;**35**:634—8. (**3**).
105. **Lorch DG,** Gordon L, Wooten S, *et al*. Effect of patient positioning on distribution of tetracycline in the pleural space during pleurodesis. *Chest* 1988;**93**:527—9. (**3**).
106. **Dryzer SR,** Allen ML, Strange C, *et al*. A comparison of rotation and nonrotation in tetracycline pleurodesis. *Chest* 1993;**104**:1763—6. (**1—**).

107. **Mager HJ,** Maesen B, Verzijlbergen F, *et al*. Distribution of talc suspension during treatment of malignant pleural effusion with talc pleurodesis. *Lung Cancer* 2002;**36**:77–81. (**1+**).
108. **Sahn SA.** Pleural diseases related to metastatic malignancies. *Eur Respir J* 1997;**10**:1907–13. (**4**).
109. **Lynch TJ Jr.** Management of malignant pleural effusions. *Chest* 1993; **103**(4 Suppl):385–9S. (**4**).
110. **Jones FL Jr.** Subcutaneous implantation of cancer: a rare complication of pleural biopsy. *Chest* 1970;**57**:189–90. (**3**).
111. **Berger RL,** Dargan EL, Huang BL. Dissemination of cancer cells by needle biopsy of the lung. *J Thorac Cardiovasc Surg* 1972;**63**:430–2. (**3**).
112. **Kumar UN,** Varkey B. Case report: subcutaneous metastasis. Rare complication of drainage of malignant pleural fluid. *Postgrad Med* 1976;**60**:253–5. (**3**).
113. **Chen TP,** Liu HP, Lu HI, *et al*. Incidence of incisional recurrence after thoracoscopy. *Surg Endosc* 2004;**18**:540–2. (**2–**).
114. **Boutin C,** Rey F, Viallat JR. Prevention of malignant seeding after invasive diagnostic procedures in patients with pleural mesothelioma. A randomized trial of local radiotherapy. *Chest* 1995;**108**:754–8. (**1+**).
115. **O'Rourke N,** Garcia JC, Paul J, *et al*. A randomised controlled trial of intervention site radiotherapy in malignant pleural mesothelioma. *Radiother Oncol* 2007;**84**:18–22. (**1+**).
116. **Bydder S,** Phillips M, Joseph DJ, *et al*. A randomised trial of single-dose radiotherapy to prevent procedure tract metastasis by malignant mesothelioma. *Br J Cancer* 2004;**91**:9–10. (**1+**).
117. **Low EM,** Khoury GG, Matthews AW, *et al*. Prevention of tumour seeding following thoracoscopy in mesothelioma by prophylactic radiotherapy. *Clin Oncol* 1995;**7**:317–18. (**3**).
118. **Agarwal PP,** Seely JM, Matzinger FR, *et al*. Pleural mesothelioma: sensitivity and incidence of needle track seeding after image-guided biopsy versus surgical biopsy. *Radiology* 2006;**241**:589–94. (**2–**).
119. **West SD,** Foord T, Davies RJ. Needle-track metastases and prophylactic radiotherapy for mesothelioma. *Respir Med* 2006;**100**:1037–40. (**2–**).
120. **Davies CW,** Traill ZC, Gleeson FV, *et al*. Intrapleural streptokinase in the management of malignant multiloculated pleural effusions. *Chest* 1999;**115**:729–33. (**3**).
121. **Gilkeson RC,** Silverman P, Haaga JR. Using urokinase to treat malignant pleural effusions. *AJR* 1999;**173**:781–3. (**3**).
122. **Hsu L-H,** Soong TC, Feng A-C, *et al*. Intrapleural urokinase for the treatment of loculated malignant pleural effusions and trapped lungs in medically inoperable cancer patients. *J Thorac Oncol* 2006;**1**:460–7. (**2–**).
123. **Tillett WS,** Sherry S. The effect in patients of streptococcal fibrinolysin and streptococcal desoxyribonuclease on fibrinous, purulent, and sanguinous pleural exudations. *J Clin Invest* 1949;**28**:173–90. (**3**).
124. **Godley PJ,** Bell RC. Major hemorrhage following administration of intrapleural streptokinase. *Chest* 1984;**86**:486–7. (**3**).
125. **Loddenkemper R.** Thoracoscopy: state of the art. *Eur Respir J* 1998;**11**:213–21. (**4**).
126. **Harris RJ,** Kavuru MS, Rice TW, *et al*. The diagnostic and therapeutic utility of thoracoscopy. A review. *Chest* 1995;**108**:828–41. (**4**).
127. **Menzies R,** Charbonneau M. Thoracoscopy for the diagnosis of pleural disease. *Ann Intern Med* 1991;**114**:271–6. (**3**).
128. **Danby CA,** Adebonojo SA, Moritz DM. Video-assisted talc pleurodesis for malignant pleural effusions utilizing local anesthesia and I.V. sedation. *Chest* 1998;**113**:739–42. (**3**).
129. **Arapis K,** Caliandro R, Stern JB, *et al*. Thoracoscopic palliative treatment of malignant pleural effusions: results in 273 patients. *Surg Endosc* 2006;**20**:919–23. (**2+**).
130. **Canto A,** Blasco E, Casillas M, *et al*. Thoracoscopy in the diagnosis of pleural effusion. *Thorax* 1977;**32**:550–4. (**3**).
131. **Ferrer J,** Roldan J, Teixidor J, *et al*. Predictors of pleural malignancy in patients with pleural effusion undergoing thoracoscopy. *Chest* 2005;**127**:1017–22. (**2+**).
132. **Aelony Y,** King RR, Boutin C. Thoracoscopic talc poudrage in malignant pleural effusions: effective pleurodesis despite low pleural pH. *Chest* 1998;**113**:1007–12. (**2–**).
133. **Debeljak A,** Kecelj P, Triller N, *et al*. Talc pleurodesis: comparison of talc slurry instillation with thoracoscopic talc insufflation for malignant pleural effusions. *J BUON* 2006;**11**:463–7. (**2–**).
134. **Foroulis CN,** Kotoulas C, Konstantinou M, *et al*. The management of malignant pleural effusions: talc pleurodesis versus bleomycin pleurodesis. *J BUON* 2001;**6**:397–400. (**3**).
135. **Harley HR.** Malignant pleural effusions and their treatment by intercostal talc pleurodesis. *Br J Dis Chest* 1979;**73**:173–7. (**3**).
136. **Jones GR.** Treatment of recurrent malignant pleural effusion by iodized talc pleurodesis. *Thorax* 1969;**24**:69–73. (**3**).
137. **Viallat JR,** Rey F, Astoul P, *et al*. Thoracoscopic talc poudrage pleurodesis for malignant effusions. A review of 360 cases. *Chest* 1996;**110**:1387–93. (**2–**).
138. **Weissberg D,** Ben-Zeev I. Talc pleurodesis. Experience with 360 patients. *J Thorac Cardiovasc Surg* 1993;**106**:689–95. (**2–**).
139. **Gasparri R,** Leo F, Veronesi G, *et al*. Video-assisted management of malignant pleural effusion in breast carcinoma. *Cancer* 2006;**106**:271–6. (**2–**).
140. **Qureshi RA,** Collinson SL, Powell RJ, *et al*. Management of malignant pleural effusion associated with trapped lung syndrome. *Asian Cardiovasc Thorac Ann* 2008;**16**:120–3. (**2–**).
141. **Colt HG.** Therapeutic thoracoscopy. *Clin Chest Med* 1998;**19**:383–94. (**4**).
142. **Cardillo G,** Facciolo F, Carbone L, *et al*. Long-term follow-up of video-assisted talc pleurodesis in malignant recurrent pleural effusions. *Eur J Cardiothorac Surg* 2002;**21**:302–6. (**2+**).
143. **de Campos JR,** Vargas FS, de Campos Werebe E, *et al*. Thoracoscopy talc poudrage: a 15-year experience. *Chest* 2001;**119**:801–6. (**2+**).
144. **Pien GW,** Gant MJ, Washam CL, *et al*. Use of an implantable pleural catheter for trapped lung syndrome in patients with malignant pleural effusion. *Chest* 2001;**119**:1641–6. (**3**).
145. **Putnam JB Jr,** Walsh GL, Swisher SG, *et al*. Outpatient management of malignant pleural effusion by a chronic indwelling pleural catheter. *Ann Thorac Surg* 2000;**69**:369–75. (**2+**).
146. **Warren W,** Faber L. Clinical experience with Pleurx catheters for malignant pleural effusions. *Chest* 2000;**118**(Suppl):130S. (**3**).
147. **Warren WH,** Kalimi R, Khodadadian LM, *et al*. Management of malignant pleural effusions using the Pleur(x) catheter. *Ann Thorac Surg* 2008;**85**:1049–55. (**2–**).
148. **Tremblay A,** Michaud G. Single-center experience with 250 tunnelled pleural catheter insertions for malignant pleural effusion. *Chest* 2006;**129**:362–8. (**2–**).
149. **Bertolaccini L,** Zamprogna C, Barberis L, *et al*. Malignant pleural effusions: review of treatment and our experience. *Rev Recent Clinical Trials* 2007;**2**:21–5. (**2–**).
150. **Janes SM,** Rahman NM, Davies RJO, *et al*. Catheter-tract metastases associated with chronic indwelling pleural catheters. *Chest* 2007;**131**:1232–4. (**3**).
151. **Martini N,** Bains MS, Beattie EJ Jr. Indications for pleurectomy in malignant effusion. *Cancer* 1975;**35**:734–8. (**3**).
152. **Fry WA,** Khandekar JD. Parietal pleurectomy for malignant pleural effusion. *Ann Surg Oncol* 1995;**2**:160–4. (**2–**).
153. **Bernard A,** de Dompsure RB, Hagry O, *et al*. Early and late mortality after pleurodesis for malignant pleural effusion. *Ann Thorac Surg* 2002;**74**:213–17. (**2–**).
154. **Waller DA,** Morritt GN, Forty J. Video-assisted thoracoscopic pleurectomy in the management of malignant pleural effusion. *Chest* 1995;**107**:1454–6. (**3**).

Exhibit 108

Respiratory Medicine (2009) **103**, 91–97

available at www.sciencedirect.com

ScienceDirect

journal homepage: www.elsevier.com/locate/rmed

Talc pleurodesis: Evidence of systemic Inflammatory response to small size talc particles☆

Eduardo H. Genofre*, Francisco S. Vargas, Milena M.P. Acencio, Leila Antonangelo, Lisete R. Teixeira, Evaldo Marchi

Laboratory of Pleura, Disciplina de Pneumologia, Heart Institute (InCor), Faculdade de Medicina da Universidade de Sao Paulo (FMUSP), Av. Dr. Eneas de Carvalho Aguiar, 4 — 5° andar, Bloco II, CEP 05403-000 Sao Paulo, Brazil

Received 21 January 2008; accepted 25 July 2008
Available online 11 September 2008

KEYWORDS
Inflammation mediators;
Magnesium silicates;
Pleura;
Pleural effusion;
Pleurodesis

Summary
The mechanisms of the systemic response associated with talc-induced pleurodesis are poorly understood. The aim of this study was to assess the acute inflammatory response and migration of talc of small size particles injected in the pleural space.

Rabbits were injected intrapleurally with talc solution containing small or mixed particles and blood and pleural fluid samples were collected after 6, 24 or 48 h and assayed for leukocytes, neutrophils, lactate dehydrogenase, IL-8, VEGF, and TGF-beta. The lungs, spleen, liver and kidneys were assessed to study deposit of talc particles.

Both types of talc produced an acute serum inflammatory response, more pronounced in the small particles group. Pleural fluid IL-8 and VEGF levels were higher in the small particle talc group. Correlation between pleural VEFG and TGF-beta levels was observed for both groups. Although talc particles were demonstrated in the organs of both groups, they were more pronounced in the small talc group.

In conclusion, intrapleural injection of talc of small size particles produced a more pronounced acute systemic response and a greater deposition in organs than talc of mixed particles.

Introduction

Talc is the most extensively used agent for pleurodesis because of its wide availability and high rate of therapeutic success.[1] However, side effects associated with the intrapleural instillation of talc have been reported, particularly dyspnea,[2–4] that may be severe and manifest as acute

☆ This study was supported by the State of São Paulo Research Foundation (FAPESP) and the National Board of Scientific and Technologic Development (CNPq), Brazil.
* Corresponding author. Tel.: +55 11 3069 5034; fax: +55 11 3069 5643.
E-mail address: ehgenofre@uol.com.br (E.H. Genofre).

0954-6111/$ - see front matter © 2008 Elsevier Ltd. All rights reserved.
doi:10.1016/j.rmed.2008.07.021

respiratory distress syndrome in up to 9% of patients.[1,2,5] The pathophysiology of the syndrome associated with talc pleurodesis is poorly understood and mainly involve diffuse pneumonitis, which is not observed with the use of other sclerosing agents.[5–14] Several mechanisms have been proposed to explain talc-associated pneumonitis, including extension of the pleural inflammation to the lung parenchyma,[15] the possible absorption of talc contaminants and the instillation of high doses of talc.[1,14,16–18]

Another potential side effect of talc pleurodesis is the migration of talc particles from the pleural cavity to the systemic circulation,[1,5,14,18–23] and it has been speculated that smaller talc particles (less than 10 μm) may more easily migrate to the bloodstream [22–24] and contribute to the talc-associated pneumonitis.[25] Since the talc used for pleurodesis in Brazil presents a wide variation in particle size (6.4–50.5 μm),[15,26] with 10% of the particles measuring less than 10 μm, we calculate that in pleurodesis induced with 5 g of talc about 500 mg of this agent consists of small particles, corresponding to a substantial amount instilled into the pleural cavity.

In the present study, we characterized the systemic and pleural inflammatory response of two types of talc, one with particles of variable size used traditionally for pleurodesis and one with particles of small size (less than 10 μm). Our hypothesis is that the smaller talc particles are responsible for the more intense acute systemic inflammatory response associated with talc pleurodesis.

Methods

The study was approved by the Ethics Committees for the analysis of research projects in humans and animals of Heart Institute (InCor), Hospital das Clínicas da Faculdade de Medicina da Universidade de São Paulo, São Paulo, Brazil.

Talc particles

Asbestos-free talc [$Mg_6(Si_8O_{20})(OH)_4$] of ''mixed size'' (Magnesita, Brumado, BA, Brazil), routinely used for pleurodesis, which contains particles of varied size (mean size: 25.4 μm, range:6.4–50.5 μm – only 10% of particles smaller than 6.66 μm), and small size talc, calibrated to 10 mm maximum diameter (Sigma-Aldrich Chemical Company, Milwaukee, WI, USA; mean size: 4.2 μm, range: 1.6–7.3 μm – with 50% of particles smaller than 6.41 μm) were used in this study.

The size of the talc particles was confirmed by granulometric analysis using laser diffraction (Malvern Instruments – Malvern, UK). The chemical composition of the talc particles was analyzed by X-Ray fluorescence spectrometry in the Laboratory of Environmental Pollution of the Medical College of the University of São Paulo. Both analyses showed no difference between both talc samples.

Intrapleural injections

Two groups of 15 New Zealand rabbits (2–2.5 kg) received 3-mL intrapleural injection of 400 mg/kg of either ''mixed'' or ''small'' talc diluted in sterile saline. One group of 10 rabbits received intrapleural saline as control. Blood samples were collected before and 6, 24 or 48 h after the instillation of the agents studied for the determination of biochemical, cytological and cytokine measurements.

Blood and pleural fluid samples were collected into tubes containing EDTA for cytological analysis and into dry tubes for the measurement of lactate dehydrogenase (LDH) and cytokines (IL-8, VEGF and TGF-β).

For the surgical procedure, the animals were anesthetized by intramuscular injection of 35 mg/kg ketamine (Cristália, São Paulo, SP, Brazil) plus 5 mg/kg xylazine (Bayer, São Paulo, SP, Brazil), followed by antisepsis with iodine solution (Rioquímica, São Paulo, SP, Brazil). Next, the different solutions were instilled with a 21-G needle (Becton–Dickinson, São Paulo, SP, Brazil) into the right pleural cavity as described in detail elsewhere.[15,27–29] After instillation, the entire injection system was immediately removed to prevent the inadvertent entry of air into the pleural space. After the procedure, the animals were monitored for clinical evidence of pain (vocalization, dyspnea or agitation), and no analgesics were necessary.

The animals were sacrificed after 6, 24 or 48 h by a lethal injection of pentobarbital (60 mg/kg) through the marginal ear vein. To avoid inadvertent contamination of the materials with talc particles, the experiments were performed by the same examiner (EHG) who used talc-free gloves and each group was operated upon on different days.

Cytological and biochemical analysis

Blood and pleural fluid samples were collected into tubes containing EDTA for cytological analysis and into dry tubes for the measurement of lactate dehydrogenase (LDH) and cytokines. The cytology samples were stained with Leishman's stain for the determination of total leukocyte count and neutrophil percentage. LDH was measured by a kinetic UV method (normal serum levels ranging from 120 to 240 IU/L).

For the determination of cytokines, the supernatant of the samples was separated, aliquoted and stored in a freezer at −80 °C for subsequent analysis. IL-8 (OptEIA, rabbit IL-8 set; Pharmingen, San Diego, CA, USA), VEGF and TGF-β (R&D Systems, Minneapolis, MN, USA) were measured by enzyme-linked immunosorbent assay (ELISA) using the protocol suggested by the manufacturer and adapted for this study. Cytokines were quantified by the measurement of optical density in an ELISA reader (Power Wave, Bio-Tek, Winooski, VT, USA).

Tissue analysis

The thorax of the animals was removed en bloc and 50 mL 10% formaldehyde was injected into the trachea to prevent lung collapse and to facilitate histological analysis. The other organs (liver, spleen and kidneys) were removed and separately immersed in formalin for 48 h. For histological analysis by light microscopy, fragments were removed from the organs, embedded in paraffin, cut into 3-μm sections, and stained with hematoxylin-eosin (HE). Collection of the fragments was standardized in order to guarantee homogenous

samples. In the case of the lungs, the fragments were obtained from the inferior lobe. The other organs were sectioned transversely and fragments including the hilum of the organs were chosen as the most representative.

The presence of talc particles in the organs was analyzed by polarized light microscopy. The Leica Qwin image analysis program (Leica Q500IV Image Analysis System — Leica Imaging Systems Ltd., Heerbrugg, Switzerland), was used for microscopic analysis of the lungs (×40 magnification). Talc particles were quantified in 10 fields and the results are reported as the ratio between the areas occupied by the particles (detected by a colorimetric method) and the total area of the lung parenchyma, spleen, liver and kidneys.

Statistical analysis

The data were analyzed statistically using the SigmaStat software (San Raphael, CA, USA). Variables showing a normal distribution are reported as mean and standard deviation, and those showing no normal distribution are expressed as median and confidence interval. Blood and pleural fluid values were compared by analysis of variance (ANOVA) followed by the Tukey or Dunn multiple comparisons test when the difference was significant. Values obtained for small and mixed particle talc in pleural fluid were compared by the Student *t*-test. Pearson's (normally distributed data) or Spearman's (not normally distributed data) correlation test was used to determine the correlation between the pleural and serum parameters studied. The ratio of the area occupied by talc to the total lung or organs area was compared between groups by the Student *t*-test. A p value <0.05 was considered to be significant in all tests.[30,31]

Results

Blood/serum

Leukocytes

Blood leukocytes were found to be significantly elevated early at 6 h after instillation of the two types of talc compared to the control group. After 24 h, leukocyte counts returned close to control values for the mixed talc, but remained significantly elevated in the small particle talc group. After 48 h, leukocyte counts returned to control values for both types of talc (Fig. 1).

Neutrophil percentage

As observed for leukocytes, the percentage of blood neutrophils was significantly elevated 6 h after instillation of the two types of talc compared to the control group. The neutrophil percentage returned close to control levels after 24 h and again increased after 48 h only in the small particle talc group (data not shown).

Lactate dehydrogenase

In the small talc group, LDH levels followed a similar pattern as that observed for neutrophil percentage, increasing over the first 6 h followed by a decrease after 24 h and then increasing again after 48 h. No difference compared to the control over time was observed for mixed particle talc (data not shown).

Interleukin-8

Serum IL-8 levels were significantly higher for the two types of talc when compared to control at all times. In addition, serum IL-8 tended to increase over time in the small particle talc group compared to the mixed talc group, with no statistical difference (Fig. 1).

Vascular endothelial growth factor

As observed for IL-8, serum VEGF levels increased during the first 6 h and remained elevated over time in the two groups when compared to the control group. No significant difference was observed for VEGF in the comparison of the two types of talc (Fig. 1).

Transforming growth factor-β

Higher serum TGF-β levels were observed for mixed talc at all time points, and for small particle talc group only after 48 h in comparison to control levels. When the two groups of talc were compared, the serum TGF-β levels were more pronounced in the mixed talc group at all time points (Fig. 1).

Pleural fluid (data not shown)

Leukocytes

Total leukocyte counts in pleural fluid were significantly higher in the mixed talc group compared to the small particle talc group at all time points, with these values tending to decrease over time. Leukocyte counts increased after 24 h in the small particle talc group and again decreased after 48 h.

Neutrophil percentage

Pleural fluid neutrophils showed an opposite behavior than that of leukocytes when comparing the two types of talc. The neutrophil percentage was significantly higher in the small particle talc group compared to the mixed talc group at all time points, showing an initial increase and a tendency to decrease over time.

Lactate dehydrogenase

LDH levels followed a trend similar to that observed for total leukocyte count in pleural fluid. Significantly higher levels were observed in the mixed talc group compared to the small particle talc group after 6 and 24 h, whereas after 48 h LDH levels were higher in the small particle talc group.

Interleukin-8

IL-8 levels in pleural fluid were significantly higher in the small particle talc group compared to the mixed talc group at all times.

Vascular endothelial growth factor

As observed for IL-8, VEGF levels in pleural fluid were higher in the small particle talc group than in the mixed talc group at all times.

Transforming growth factor-β

As previously stated for the serum levels, pleural TGF-β levels were higher in the mixed talc group than in the small particle talc group at all times.

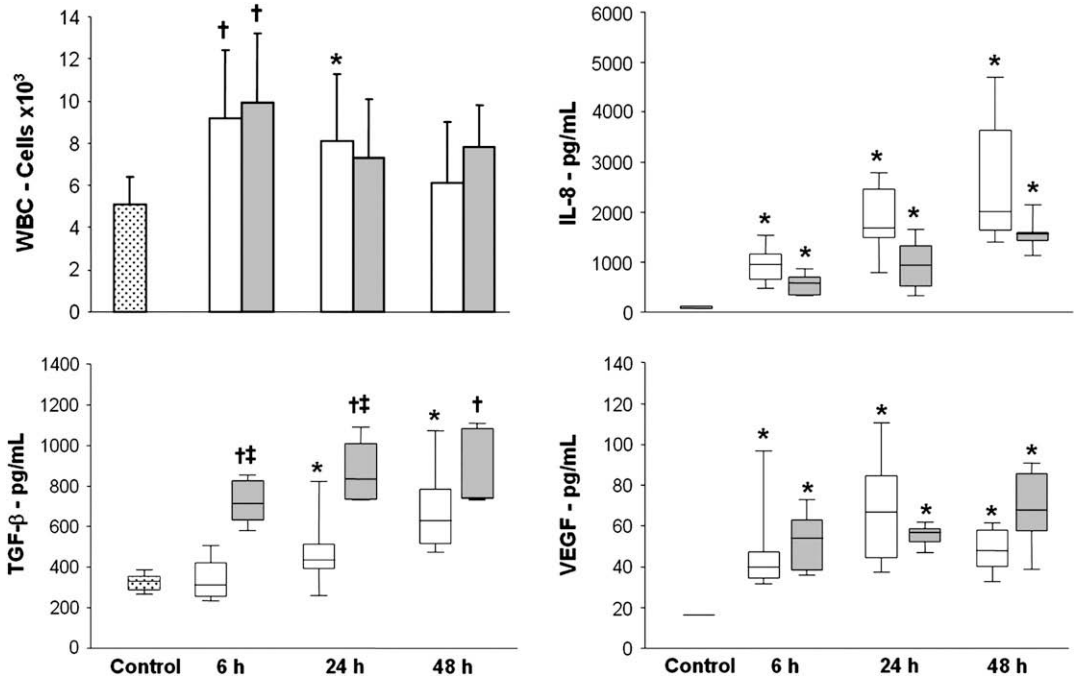

Figure 1 Serum inflammatory markers after intrapleural injection of talc. White blood cell count (WBC) and serum cytokines after intrapleural injection of small (ST- white bars) or mixed (MT- gray bars) particle talc. (1) WBC rise early at 6 h for both particles and remain elevated in the ST group until 24 h. After 48 h, WBC returns to normal for both groups. (2) IL-8 levels are higher than control at all times for both types of talc. (3) VEGF increases early at 6 h in both groups. (4) Higher TGF-b levels are seen in MT at all time points in comparison to ST ($^{\dagger}p < 0.001$ and $*p < 0.05$ vs. control; $^{\ddagger}p < 0.05$ MT vs. ST).

Correlations

Correlation between the pleural fluid and blood/serum parameters revealed a strong correlation only for TGF-β ($R = 0.80$; $p < 0.001$) in the small particle talc group, whereas in the mixed talc group a correlation was observed only for VEGF ($R = 0.74$; $p < 0.001$).

Comparison between the different parameters in each compartment (pleural fluid or blood) showed positive correlations only between VEGF and TGF-β in pleural fluid for both types of talc (small particle talc: $R = 0.94$; $p < 0.001$; mixed talc: $R = 0.72$; $p < 0.05$) (data not shown).

Tissue analysis

Lungs

In the small particle talc group, talc particles were observed adhered to the pleural surface and also in the lung parenchyma (alveolar spaces and septa) in the right lung (intrapleural injection side) (Fig. 2). In the left lung (contralateral to the injection side), talc particles were also detected in the alveolar septa but not in the lung parenchyma (Fig. 2).

In the mixed talc group, talc particles showed a heterogeneous distribution on the right pleural surface (side of injection), with particles rarely being observed in the lung parenchyma or alveolar septa (Fig. 2). In the left lung, talc particles were only visible in the alveolar septa (Fig. 2).

Quantification of talc particles in the parenchyma (ratio of the area occupied by talc to the total tissue area $\times 10^5$) revealed a significantly larger number of particles in both lungs in the small particle talc group compared to the mixed talc group (right lung: 71.1 ± 28.9 vs. 1.18 ± 0.69, $p < 0.001$; left lung: 68.7 ± 42.4 vs. 1.13 ± 1.14, $p < 0.001$). Of note, for both types of talc the particles deposition was similar in both lungs parenchyma (Fig. 3).

Spleen, liver and kidneys

Analysis of histological sections of the spleen parenchyma showed the presence of talc particles in the spleen pulp for both agents. Characteristically, the talc particles were found aggregated only in the red pulp, whereas the white pulp was preserved (Fig. 2).

A diffuse distribution of talc particles was also observed in sections of the liver parenchyma. As a particularity, the particles were characteristically located in perivascular regions and therefore more demonstrated close to the hila, centrolobular vessels and sinusoids (Fig. 2).

In the kidney, talc particles were predominantly detected in the medullary layer in both groups. Similar to the findings of other organs, talc particles were also detected in animals submitted to the intrapleural injection of mixed talc (Fig. 2).

Quantification of talc particles in the liver and kidneys showed a significantly larger number of particles in animals injected with small particle talc ($p < 0.05$). No significant difference was observed for the spleen (Fig. 3).

Correlation of the area ratio of talc in different organs

Analysis of the area ratio of talc in different organs revealed no positive correlations. In addition, no correlation between cytokine levels and the area ratio of talc was observed in any of the organs.

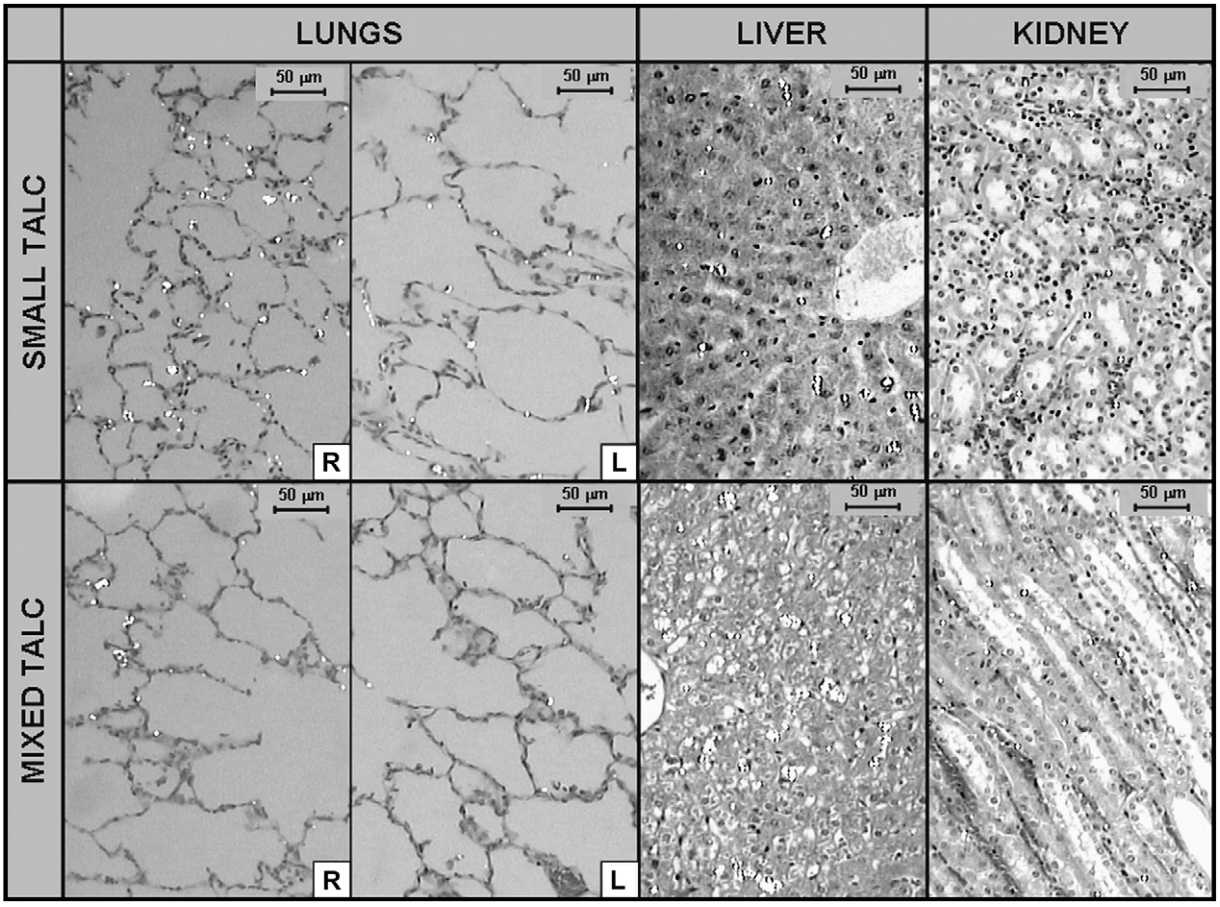

Figure 2 Photomicrographs of the lungs and organs — migration of talc particles. Photomicrographs of the lungs and organs. *Right lung*: talc particles are noted in the alveolar spaces and septa in both groups, with more particles in the ST (small talc) group than in the MT (mixed talc) group. *Left lung*: particles are seen only in alveolar septa with a greater number in the ST group. *Liver*: particles are characteristically located in the perivascular regions close to the hila, centrolobular vessels and sinusoids. *Kidneys*: particles are noted predominantly in the medullar layer (HE and polarized light, ×200).

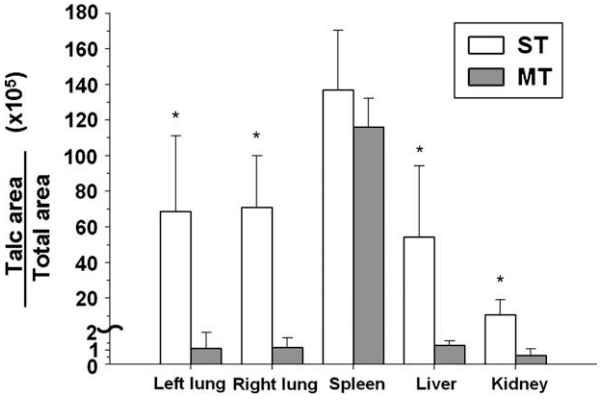

Figure 3 Particles deposition in the lungs and other organs. Ratio of talc area vs. total area ($\times 10^5$) in lungs, spleen, liver and kidney. Small talc (ST) has a higher ratio of deposition in the lungs, liver and kidney ($*p < 0.05$). No difference was observed in the spleen.

Discussion

Talc, the agent most used for pleurodesis, is known to produce systemic effects that can culminate in respiratory insufficiency and even death. The mechanisms underlying these systemic effects are not completely understood. Experimental and clinical reports comparing the systemic effects of talc containing mixed and large particles (larger than 12 μm[23] and 25 μm[25]) are available in the literature, but this is the first study that compares the systemic effects of talc containing mixed particles and talc containing particles smaller than 5 μm.

Our findings indicate that both small and mixed talc injected intrapleurally in rabbits produce an acute systemic inflammatory response. However, small particle talc produced a more pronounced pleural and systemic response and resulted in greater particle deposition in the organs than mixed talc. Both types of talc caused an early increase in serum leukocyte, IL-8 and VEGF levels compared to control, but this increase was more marked in the small talc group. On the other hand, serum and pleural fluid TGF-β levels showed a more marked increase in the mixed talc group. Similar to the serum findings, IL-8 and VEGF levels in pleural fluid were also higher in the small particle talc

group. Notably, IL-8 levels increased early and decreased over time, and a correlation between pleural VEGF and TGF-β levels was observed for both types of particles. Histological analysis of tissues showed dispersion of both types of talc particles to all organs studied. However, analysis of the size of the particles in the organs demonstrated a greater tissue deposition in animals receiving small particle talc. Curiously, large amounts of talc particles were observed in both lungs, with a more pronounced deposition in the small talc group.

Literature evidence points to a possible migration of talc particles from the pleural cavity to the systemic circulation.[1,5,14,18–23] In an experimental study, Ferrer et al.[23] demonstrated the presence of talc particles in different organs and suggested that small particles might be more easily absorbed by lymphatic stomata than larger particles. On the basis of the present observations, the question remains as to which mechanisms are involved in the systemic response to intrapleural talc instillation. One explanation for the systemic inflammatory response would be the direct passage of particles from the pleural space to the bloodstream, in agreement with the findings of previous studies.[14,23] In this respect, the same mechanism might explain the systemic effects observed for mixed talc, since about 10% of the particles of this type of talc were smaller than 10 μm.

Talc particles migration mechanisms are still unknown. One possible mechanism is the lymphatic absorption of talc particles from the pleural cavity. However, by this mechanism it would be difficult to explain the presence of talc particles in the liver, spleen and kidneys, since these particles migrate from the pleural cavity to the systemic venous circulation through the lymphatic route and return to the lung where they probably are being removed. In this respect, it is also possible that the presence of talc in the alveoli may produce an intense local inflammation and changes in the alveolar-capillary barrier, causing reflow of particles to the systemic circulation. In this situation, we would expect diffuse lung injury which might even be the cause of the respiratory insufficiency observed in talc pleurodesis. However, histological analysis of the lungs of the animals submitted to intrapleural talc injection showed no intense acute pulmonary lesions that would support this mechanism.

A second mechanism would be that of an intense pleural inflammatory process leading to rupture of the pleural barrier caused by diffuse mesothelial injury. An important observation of the present study was that the particles found in the organs studied were smaller than 5 μm, a finding strongly suggesting that the systemic effects can be explained by the presence of small particles.

The leakage of inflammatory mediators from the pleural space to the bloodstream is suggested by our findings, as showed that in the pleural cavity IL-8 levels increased early and decreased over time, whereas the opposite was observed in blood. In contrast, VEGF levels tended to increase progressively over time in both pleural fluid and blood, a finding reflecting an increase in capillary permeability that contributes to both the formation of pleural fluid and the passage of smaller molecules from the pleural cavity to the blood circulation.

Comparison of the levels of inflammatory mediators in pleural fluid and blood showed a strong pleural-serum correlation only for TGF-β levels in the small particle talc group and for VEGF in the mixed talc group, a finding suggesting a possible flow mechanism between the two compartments. However, these data alone do not allow us to infer that this is the only mechanism involved in the systemic response observed in talc pleurodesis. In addition to the increase in inflammatory mediators, we observed an acute increase in serum leukocytes and neutrophils in both talc groups coinciding with the acute pleural-serum inflammatory response, although no correlation was observed for these parameters.

A possible pro-inflammatory effect of TGF-β was demonstrated by the correlation that was observed between VEGF and TGF-β in pleural fluid. This fact was suggested in a previous study showing that TGF-β stimulates the production of VEGF by mesothelial cells and thus explains the increase in vascular permeability observed in pleurodesis inflammation.[32] However, our findings showed that pleural VEGF levels were higher in the small particle talc group than in the mixed talc group, whereas pleural TGF-β levels were higher in animals injected with mixed talc, suggesting a possible overlap of both distinct inflammatory mechanisms, the leakage of inflammatory mediators from the pleural space and the systemic effects of talc particles deposition in organs. In agreement with these findings, previous experimental study from our group showed an increase of serum IL-8 and VEGF levels in rabbits after intrapleural instillation of mixed talc,[28] suggesting that these mediators may reflow from the pleural cavity to the systemic circulation and are involved in the genesis of the systemic effects observed in pleurodesis. In addition, Maskell et al. showed in a clinical trial that talc containing particles standardized at 15 μm produced a local and systemic inflammation when compared to tetracycline and and talc particles larger than 25 μm.[25]

Our data do not permit any conclusion as to whether the systemic cellular response is due to the flow of cells from the pleural cavity to the bloodstream or to a direct systemic cellular response to the presence of talc particles in the organs. However, we may speculate that the intense pleural inflammation caused by talc promotes the loss of integrity of the pleural barrier, permitting the free flow of cytokines and talc particles between the two compartments. In a second step, the presence of talc particles in tissues would trigger a local cellular response that contributes to the maintenance and amplification of the systemic inflammatory response. These considerations indicate that the mechanism underlying the systemic inflammatory response observed in talc pleurodesis still needs further investigation. However, it seems reasonable to assume that the size of the talc particles influences the inflammatory response and, possibly, the side effects observed in clinical practice. In this respect, future studies correlating the cellular response with the number of particles deposited in tissues may contribute to clarify this question.

Conclusions

In conclusion, talc containing particles of small size injected into the pleural space of rabbits produced a more

intense systemic and pleural inflammatory response than mixed particle talc. Particles of both types of talc were detected in the lungs, spleen, liver and kidneys of the animals studied. These data, together with those obtained in previous studies, suggests the need for the commercial development of a type of talc for universal use in pleurodesis that preferentially contains particles larger than 20 μm to permit the clinical use with greater safety and a lower risk of adverse systemic effects.

Conflict of interest

The authors have no conflicts of interests.

Ethics statement

The study was approved by the Ethics Committees for the analysis of research projects in humans and animals of Heart Institute (InCor), Hospital das Clínicas da Faculdade de Medicina da Universidade de Sao Paulo, Sao Paulo, Brazil.

References

1. de Campos JR, Vargas FS, de Campos Werebe E, Cardoso P, Teixeira LR, Jatene FB, et al. Thoracoscopy talc poudrage: a 15-year experience. *Chest* 2001 Mar;**119**(3):801—6.
2. Sahn SA. Talc should be used for pleurodesis. *American Journal of Respiratory and Critical Care Medicine* 2000 Dec;**162**(6): 2023—4 [discussion].
3. Light RW. *Pleural diseases*. 4th ed. Philadelphia: Lippincott Williams & Wilkins; 2001.
4. Froudarakis ME, Klimathianaki M, Pougounias M. Systemic inflammatory reaction after thoracoscopic talc poudrage. *Chest* 2006 Feb;**129**(2):356—61.
5. Rehse DH, Aye RW, Florence MG. Respiratory failure following talc pleurodesis. *American Journal of Surgery* 1999 May; **177**(5):437—40.
6. Campos JR, Werebe EC, Vargas FS, Jatene FB, Light RW. Respiratory failure due to insufflated talc. *Lancet* 1997 Jan 25; **349**(9047):251—2.
7. Kennedy L, Sahn SA. Talc pleurodesis for the treatment of pneumothorax and pleural effusion. *Chest* 1994 Oct;**106**(4): 1215—22.
8. Kennedy L, Rusch VW, Strange C, Ginsberg RJ, Sahn SA. Pleurodesis using talc slurry. *Chest* 1994 Aug;**106**(2):342—6.
9. Stefani A, Natali P, Casali C, Morandi U. Talc poudrage versus talc slurry in the treatment of malignant pleural effusion. A prospective comparative study. *European Journal of Cardiothoracic Surgery* 2006 Dec;**30**(6):827—32.
10. Nandi P. Recurrent spontaneous pneumothorax; an effective method of talc poudrage. *Chest* 1980 Apr;**77**(4):493—5.
11. Migueres J, Jover A. Indications for intrapleural talc under pleuroscopic control in malignant recurrent pleural effusions. Based on 26 cases (author's transl). *Le Poumon et le coeur* 1981;**37**(5):295—7.
12. Rinaldo JE, Owens GR, Rogers RM. Adult respiratory distress syndrome following intrapleural instillation of talc. *The Journal of Thoracic and Cardiovascular Surgery* 1983 Apr;**85**(4): 523—6.
13. Bouchama A, Chastre J, Gaudichet A, Soler P, Gibert C. Acute pneumonitis with bilateral pleural effusion after talc pleurodesis. *Chest* 1984 Nov;**86**(5):795—7.
14. Ferrer J, Villarino MA, Tura JM, Traveria A, Light RW. Talc preparations used for pleurodesis vary markedly from one preparation to another. *Chest* 2001 Jun;**119**(6):1901—5.
15. Marchi E, Vargas FS, Acencio MM, Antonangelo L, Genofre EH, Teixeira LR. Evidence that mesothelial cells regulate the acute inflammatory response in talc pleurodesis. *The European Respiratory Journal* 2006 Nov;**28**(5):929—32.
16. van den Heuvel MM, Smit HJ, Barbierato SB, Havenith CE, Beelen RH, Postmus PE. Talc-induced inflammation in the pleural cavity. *The European Respiratory Journal* 1998 Dec; **12**(6):1419—23.
17. Genofre EH, Marchi E, Vargas FS. Inflammation and clinical repercussions of pleurodesis induced by intrapleural talc administration. *Clinics (Sao Paulo, Brazil)* 2007 Oct;**62**(5): 627—34.
18. Montes JF, Ferrer J, Villarino MA, Baeza B, Crespo M, Garcia-Valero J. Influence of talc dose on extrapleural talc dissemination after talc pleurodesis. *American Journal of Respiratory and Critical Care Medicine* 2003 Aug 1;**168**(3):348—55.
19. Marchi E, Teixeira LR, Vargas F. Talc for pleurodesis: hero or villain? *Chest* 2003 Jul;**124**(1):416 [author reply -7].
20. Nasreen N, Mohammed KA, Dowling PA, Ward MJ, Galffy G, Antony VB. Talc induces apoptosis in human malignant mesothelioma cells in vitro. *American Journal of Respiratory and Critical Care Medicine* 2000 Feb;**161**(2 Pt 1):595—600.
21. Li J. Ultrastructural study on the pleural stomata in human. *Functional and Developmental Morphology* 1993;**3**(4):277—80.
22. Werebe EC, Pazetti R, Milanez de Campos JR, Fernandez PP, Capelozzi VL, Jatene FB, et al. Systemic distribution of talc after intrapleural administration in rats. *Chest* 1999 Jan; **115**(1):190—3.
23. Ferrer J, Montes JF, Villarino MA, Light RW, Garcia-Valero J. Influence of particle size on extrapleural talc dissemination after talc slurry pleurodesis. *Chest* 2002 Sep;**122**(3):1018—27.
24. Fraticelli A, Robaglia-Schlupp A, Riera H, Monjanel-Mouterde S, Cau P, Astoul P. Distribution of calibrated talc after intrapleural administration: an experimental study in rats. *Chest* 2002 Nov;**122**(5):1737—41.
25. Maskell NA, Lee YC, Gleeson FV, Hedley EL, Pengelly G, Davies RJ. Randomized trials describing lung inflammation after pleurodesis with talc of varying particle size. *American Journal of Respiratory and Critical Care Medicine* 2004 Aug 15; **170**(4):377—82.
26. Marchi E, Vargas FS, Acencio MM, Teixeira LR, Antonangelo L, Lee YC, et al. Pleurodesis: a novel experimental model. *Respirology (Carlton, Vic)* 2007 Jul;**12**(4):500—4.
27. Vargas FS, Teixeira LR, Antonangelo L, Vaz MA, Carmo AO, Marchi E, et al. Experimental pleurodesis in rabbits induced by silver nitrate or talc: 1-year follow-up. *Chest* 2001 May;**119**(5): 1516—20.
28. Marchi E, Vargas FS, Acencio MM, Antonangelo L, Teixeira LR, Genofre EH, et al. Talc and silver nitrate induce systemic inflammatory effects during the acute phase of experimental pleurodesis in rabbits. *Chest* 2004 Jun;**125**(6):2268—77.
29. Teixeira LR, Vargas FS, Acencio MM, Bumlai RU, Antonangelo L, Marchi E. Experimental pleurodesis induced by antibiotics (macrolides or quinolones). *Clinics (Sao Paulo, Brazil)* 2006 Dec;**61**(6):559—64.
30. Cox DHD. *Theoretical statistics*. London: Chapman and Hall; 1974.
31. Schervish M. *Theory of statistics*. 2nd ed. New York: Springer-Verlag; 1997.
32. Gary Lee YC, Melkerneker D, Thompson PJ, Light RW, Lane KB. Transforming growth factor beta induces vascular endothelial growth factor elaboration from pleural mesothelial cells in vivo and in vitro. *American Journal of Respiratory and Critical Care Medicine* 2002 Jan 1;**165**(1):88—94.

Exhibit 109

SPANDIDOS PUBLICATIONS EXPERIMENTAL AND THERAPEUTIC MEDICINE 15: 733-738, 2018

Observational analysis on inflammatory reaction to talc pleurodesis: Small and large animal model series review

JACOPO VANNUCCI[1], GUIDO BELLEZZA[2], ALBERTO MATRICARDI[1], GIULIA MORETTI[3], ANTONELLO BUFALARI[3], LUCIO CAGINI[1], FRANCESCO PUMA[1] and NICCOLÒ DADDI[4]

[1]Department of Thoracic Surgery; [2]Institute of Pathological Anatomy and Histology, University of Perugia Medical School; [3]Department of Veterinary Medicine, University of Perugia, I-06134 Perugia; [4]Thoracic Surgery, Department of Medical and Surgical Sciences (DIMEC), Alma Mater Studiorum, University of Bologna, I-40126 Bologna, Italy

Received April 26, 2017; Accepted September 20, 2017

DOI: 10.3892/etm.2017.5454

Abstract. Talc pleurodesis has been associated with pleuropulmonary damage, particularly long-term damage due to its inert nature. The present model series review aimed to assess the safety of this procedure by examining inflammatory stimulus, biocompatibility and tissue reaction following talc pleurodesis. Talc slurry was performed in rabbits: 200 mg/kg checked at postoperative day 14 (five models), 200 mg/kg checked at postoperative day 28 (five models), 40 mg/kg, checked at postoperative day 14 (five models), 40 mg/kg checked at postoperative day 28 (five models). Talc poudrage was performed in pigs: 55 mg/kg checked at postoperative day 60 (18 models). Tissue inspection and data collection followed the surgical pathology approach currently used in clinical practice. As this was an observational study, no statistical analysis was performed. Regarding the rabbit model (*Oryctolagus cunicoli*), the extent of adhesions ranged between 0 and 30%, and between 0 and 10% following 14 and 28 days, respectively. No intraparenchymal granuloma was observed whereas, pleural granulomas were extensively encountered following both talc dosages, with more evidence of visceral pleura granulomas following 200 mg/kg compared with 40 mg/kg. Severe florid inflammation was observed in 2/10 cases following 40 mg/kg. Parathymic, pericardium granulomas and mediastinal lymphadenopathy were evidenced at 28 days. At 60 days, from rare adhesions to extended pleurodesis were observed in the pig model (*Sus Scrofa domesticus*). Pleural granulomas were ubiquitous on visceral and parietal pleurae. Severe spotted inflammation among the adhesions were recorded in 15/18 pigs. Intraparenchymal granulomas were observed in 9/18 lungs. Talc produced unpredictable pleurodesis in both animal models with enduring pleural inflammation whether it was performed via slurry or poudrage. Furthermore, talc appeared to have triggered extended pleural damage, intraparenchymal nodules (porcine poudrage) and mediastinal migration (rabbit slurry).

Correspondence to: Dr Jacopo Vannucci, Department of Thoracic Surgery, University of Perugia Medical School, Loc. Sant'Andrea delle Fratte, Pz.le Menghini 1, I-06134 Perugia, Italy
E-mail: jacopovannucci@tiscali.it

Key words: pleurodesis, talc, pleural disease, malignant effusion, pleuropulmonary, slurry, poudrage, pneumothorax, animal model, pleuritis

Introduction

Talc ($Mg_3(Si_2O_5)_2(OH)_2$) is the most commonly used pleurodesis agent worldwide due to its reported success rate especially for malignant pleural effusion (1). Prior to this, talc powder underwent an evolution over the decades in terms of depuration, particle size selection and production refining (2,3). Despite this, the safety of talc remains debatable in terms of local reactions and systemic syndromes such as ARDS. Being so, there is no consensus on whether it should be used for pleurodesis, especially in benign disease (4,5).

To date, most studies on humans have focused on assessing the clinical outcome exclusively, therein reporting only on short-term complications (often in severely symptomatic patients from a respiratory disease) while investigations on long-term complications have been few and mostly describing single cases (6-8). Limited available data on possible long term complications associated with talc pleurodesis are available in the Literature (2,3,5,6).

For the above, since experimental talc pleurodesis series were performed in rabbit and porcine models, belonging to independent experimental comparative studies, carried out by the same research group and using medical talc in different animal models, different dosages and distinctive surgical techniques, an observational model series review was performed to report the findings after this extended experience with talc. The aim of this analysis was to generate hypothesis regarding the functional profile of talc for pleurodesis. Therefore, talc biocompatibility, pleural reaction to talc deposition on the mesothelium, intrapulmonary and lymphatic spread are observed to highlight possible unknown events.

Materials and methods

This analysis of talc pleurodesis was performed as a secondary investigation (opportunistic study) analysing animal models series undergoing talc pleurodesis and belonging to already performed experimental research protocols (9-11). Talc slurry was performed in rabbits in different dosages with the aim to compare talc to antibiotic both at increasing concentration and administered via chest tube. The chosen dosages of talc were therefore arbitrary and sought to see differences in performance of talc at marked dose variation at different postoperative time. Besides, talc poudrage was performed at standard dosage in pigs for the impossibility to simulate an appropriate surgical surrogate for medical thoracoscopy in a smaller animal model. Moreover, some differences in the experimental techniques between the rabbit and the swine series depend on the study aims and designs.

Animal management was carried out following recommended practices pertaining to animal laboratory research (12,13). The protocol was approved by central and local authorities for animal care. Talc poudrage and slurry were tested using a commonly available depurated, calibrated preparation (Sterital, La Ciotat, France) in the following models/methodology.

Rabbit model-talc slurry: Twenty New Zealand White rabbits (*Oryctolagus cuniculi*), 7 weeks old, mean 2,450 g, (range: 2,100-2,450 g) were submitted to talc slurry and divided into 4 groups according to the following scheme: 200 mg/kg, checked at postoperative day 14 (5 models); 200 mg/kg, checked at postoperative day 28 (5 models); 40 mg/kg, checked at postoperative day 14 (5 models); 40 mg/kg, checked at postoperative day 28 (5 models).

The procedure was performed under general anaesthesia. A 10fr intrapleural catheter was placed time of surgery. Talc suspended in 2 ml saline was administered through the chest tube; pneumothorax was eliminated by syringe suction. The drain was locked for 24 h then left open until post-operative day 4, when it was removed.

Swine model-talc poudrage: Eighteen Landrance x Large White pigs *(Sus Scrofa domesticus)*, 4 months old, mean 42.7 kg, (range: 40-45 kg), were submitted to uniportal videothoracoscopy (VATS) using the same procedure for human care in each technical detail. Talc was sprayed and checked for homogenous deposit all over the pleural surface before ending the procedure. Complete resolution of pneumothorax was achieved under monitor view. No chest tube was left in place. Talc poudrage was performed according to the following design: 55 mg/kg, checked at postoperative day 60 (18 models).

All models were analyzed post-mortem after painless euthanasia. Autopsy was carried out according to the current medical technique with inspection of all anatomical spaces and cavities, systematically carried out following a standardized and repeatable procedure. Description of findings and pictures were performed by circulating members of the team. Autopsy operator followed a predetermined routine in dissection and samples collection, did not analyze the findings and was not involved in interpretation of data. Observation sought to estimate the extent of adhesions, pleural granulomas, intraprenchymal granulomas, and severe spotted inflammation without pleurodesis. After autoptic assessment, the pathologist and the surgeon evaluated the specimens with a teamwork approach. Macroscopic examination and microscopic assessment were systematically carried out according to the current clinical surgical pathology methodology. Considering the descriptive objective of the paper, no statistical analysis was applied to the numerical variables.

Results

The outcome of talc pleurodesis in rabbits (talc slurry) is reported in Tables I and II; the outcome of talc pleurodesis in pigs (talc poudrage) is summarized in Table III. The extent of the adhesions observed in rabbits after 14 days from 40 mg/kg talc slurry ranged from 0 to 30% of the pleural surface with no intraparenchymal granulomas, but frequent parietal pleura granulomas. Pleural granulomas were observed in all rabbits, whereas severe florid inflammation without pleurodesis was recorded in one case after 14 days. When this talc dosage was tested at 28 days, the range of pleurodesis extent resulted being between 0 and 10% of the pleural cavity with no intraperinchymal granuloma and only one case of florid inflammatory event of the pleura without pleurodesis. In the series of rabbits undergoing 200 mg/kg talc slurry, the extent of pleurodesis did not appear to increase dramatically (range from 0 to 10% at postoperative day 14, and 0 to 20% at postoperative day 28) with no intraparenchymal granuloma and no florid spotted pleural inflammation. For this series of rabbits, granulomas on the outer pericardium (seen on postoperative day 14), an isolated mediastinal lymphadenopathy below the main carina and an isolated parathymic granuloma (seen on postoperative day 28) were observed. Representative findings are shown in Fig. 1.

The series of pigs undergoing 55 mg/kg talc poudrage (uniportal VATS) had a wide range of outcomes regarding the extent of pleurodesis achieved after a post-operative period of 60 days. The outcome ranged from rare adhesions with no symphysis to a single case with a complete pleurodesis characterized by a fully extended pleural cavity obliteration. Pleural granulomas were observed in the entire series of the swine models, both visceral and parietal. Autopsies revealed severe spotted inflammation in sites of the pleural surface without pleurodesis in 15/18 pigs. Systematic sampling was performed at the bench and intraparenchymal granulomas were observed in 9/18 lungs. Patterns of disease post-talcing are shown in Fig. 2. Histologies of exemplifying findings are provided in Fig. 3.

Discussion

Talc is the most used sclerosing agent worldwide for achieving pleural space obliteration. Though its efficacy has been widely reported especially in neoplastic effusion, severe inflammatory reactions have been described both acute and long-term (14-16). For this, an analysis in animal models was carried out to investigate for the local reaction following the contact of talc powder on the pleura. The materials under investigation show interesting potentials considering that talc pleurodesis was performed in different animal models,

Table I. Talc slurry (40 mg/kg) in rabbits (10 Fr pleural catheter).

14 days postoperative observation					
No.	Adhesions	Pleural granuloma	Intraparenchymal granuloma	Severe spotted inflammation without pleurodesis	Note
1	YES <5%	YES parietal	NO	NO	None
2	YES <30%	YES parietal	NO	NO	None
3	YES <10%	YES parietal	NO	NO	Parasplenic Fibrosis
4	NO	YES parietal	NO	YES	None
5	NO	YES parietal	NO	NO	None
28 days postoperative observation					
No.	Adhesions	Pleural granuloma	Intraparenchymal granuloma	Severe spotted inflammation without pleurodesis	Note
1	NO	NO	NO	YES	None
2	YES <10%	NO	NO	NO	None
3	YES <10%	NO	NO	NO	None
4	YES <5%	YES visceral	NO	NO	None
5	YES <5%	YES parietal	NO	NO	None

Table II. Talc slurry (200 mg/kg) in rabbits (10 Fr pleural catheter).

14 days postoperative observation					
No.	Adhesions	Pleural granuloma	Intraparenchymal granuloma	Severe spotted inflammation without pleurodesis	Note
1	YES <5%	YES visceral/parietal	NO	NO	None
2	YES <10%	YES visceral	NO	NO	None
3	YES <5%	YES visceral/parietal	NO	NO	Pericardium granulomas
4	NO	YES visceral	NO	NO	None
5	NO	YES visceral	NO	NO	None
28 days postoperative observation					
No.	Adhesions	Pleural granuloma	Intraparenchymal granuloma	Severe spotted inflammation without pleurodesis	Note
1	NO	YES visceral/parietal	NO	NO	Lymphadenopathy (main carina)
2	YES <5%	YES visceral/parietal	NO	NO	None
3	YES <5%	YES visceral/parietal	NO	NO	None
4	YES <20%	YES visceral	NO	NO	None
5	YES <20%	YES parietal	NO	NO	Parathymic granuloma

alternative techniques and dosages. The available dataset represents a unique source of information for a single research group according to accessible Literature.

Talc pleurodesis is generally a technique supporting another procedure such as videothoracoscopy or chest drainage with several aspects of perfectibility (17). Any assessment of talc-related effects is complex in clinical research, so an experimental setting appears to be the only currently available way to evaluate biocompatibility, pleural reaction and any subsequent damage. For this animal series review, talc

Table III. Talc poudrage (55 mg/kg) in pigs (single-port videothoracoscopy).

	60 days postoperative observation				
No.	Adhesions (%)	Pleural granuloma	Intraparenchymal granuloma	Severe spotted inflammation without pleurodesis	Note
1	YES <5	Yes visceral/parietal	NO	YES	None
2	YES <15	Yes visceral/parietal	NO	NO	None
3	YES <5	Yes visceral/parietal	YES	YES	None
4	YES <50	Yes visceral/parietal	NO	YES	None
5	YES <50	Yes visceral/parietal	NO	YES	None
6	YES <5	Yes visceral/parietal	YES	YES	None
7	YES> 50	Yes visceral/parietal	YES	NO	None
8	YES <20	Yes visceral/parietal	YES	YES	None
9	YES <20	Yes visceral/parietal	NO	YES	None
10	YES <25	Yes visceral/parietal	YES	YES	None
11	YES <5	Yes visceral/parietal	YES	YES	None
12	YES <15	Yes visceral/parietal	NO	YES	None
13	YES <20	Yes visceral/parietal	NO	YES	None
14	YES <20	Yes visceral/parietal	YES	YES	None
15	YES <25	Yes visceral/parietal	NO	YES	None
16	YES <25	Yes visceral/parietal	NO	NO	None
17	YES <50	Yes visceral/parietal	YES	YES	None
18	YES <15	Yes visceral/parietal	YES	YES	None

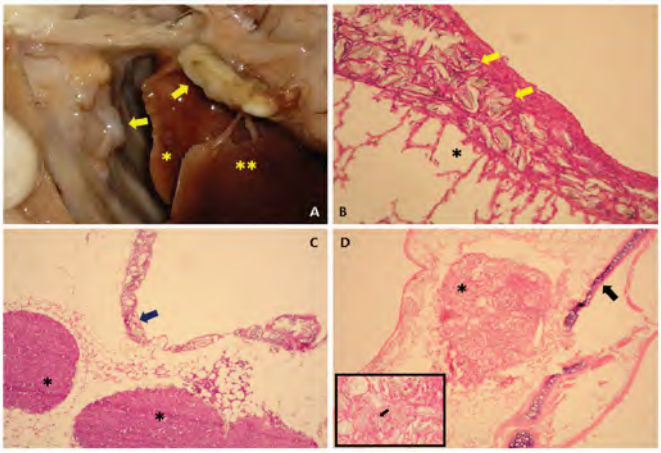

Figure 1. (A) Macroscopic appearance of the intrapleural rabbit space. The talc deposits (yellow arrows) were evident on the parietal and diaphragmatic pleura as well as few visceral granulomas (yellow asterisk) with pleural adhesions (double yellow asterisks) were identified. (B) Talc crystals (yellow arrows) were encased in the visceral pleura with mild intra-alveolar inflammatory response (x20 magnification, hematoxylin and eosin staining). (C) Talc crystals deposits (arrow) were identified in the mediastinal pleura with concomitant inflamed lymphnodes (asterisks) present in the surrounding fat pad (10X magnification, hematoxylin-eosin staining). (D) Subcarinal (arrow shows the cartilaginous part of the main airway, x10 magnification, hematoxylin-eosin staining) lymphnode (asterisk) with talc crystal deposits (framed figure, arrow, x20 magnification, hematoxylin and eosin staining).

was administered either poudrage or slurry in two different well-established animal models, pigs and rabbits, respectively.

When talc was administered slurry in rabbit pleural cavities, the obliteration of space never exceeded 30% of the entire pleural cavity surface. Whereas, poudrage outcome in the swine models varied from 0 to 100%, so that the effect of talc poudrage cannot have allowed for an accurate prediction of outcome after a videothoracoscopic administration of depurated, dry, sterilized talc. In rabbits, intrapulmonary granulomas were infrequent, while they were a common finding in the pig series. According to published case reports, the intraparenchymal deposit of talc could even provoke a high metabolic activity (18). The results from our model series analysis evidenced that talc-related events were common. Likewise, the exploration of the pleural cavities post-mortem evidenced that severe inflammation often afflicted the pleural layer without pleurodesis: noxa without effects.

The observation surprisingly evidenced some possible differences between models or surgical techniques. Specifically, there is no gross evidence of intraparenchymal granulomas after slurry in rabbits while it is a common finding in porcine poudrage. Besides, there is no particular mediastinal involvement after poudrage in pigs while high dose of talc slurry was associated with possible mediastinal migration and deposition of talc in extended granulomas. The study design is not able to explain these differences and does not allow for a fine comparison between techniques but supports some hypothesis regarding different outcome due to pleurodesis procedure as already suggested after clinical research (19). Many questions on what these differences are dependent on arise but they necessitate further specific studies with comparative design to experimentally test different dosages, slurry vs. poudrage, differences between the animal models and model-dependent variability for the procedure outcome. Nevertheless, the

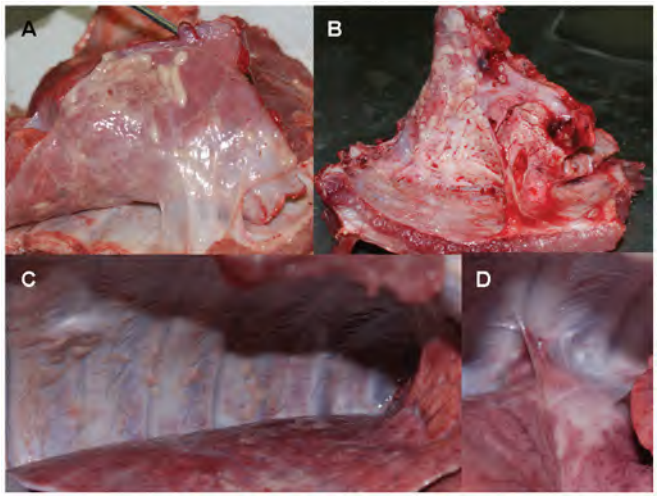

Figure 2. (A) A sparse adhesion with diffuse visceral pleura thickening and dullness. Lung parenchyma appears diffusely congested. Talc accumulation with pleural whitish soft reactive nodules are present (arrow). (B) Stronger pleurodesis reaction compared to A with much more evident pleural thickening and superficial talc accumulation (arrow). Significant blood supply of the area with consistent neoangiogenesis within the reactive tissue forming the adhesion. (C) Diffuse nodular pleuritis of both visceral and parietal pleurae (arrow) without any significant pleurodesis (damage without effect). (D) Isolated pleural adhesion with important lung parenchyma reaction: diffuse whitening of the parenchyma with palpable consolidation (arrow).

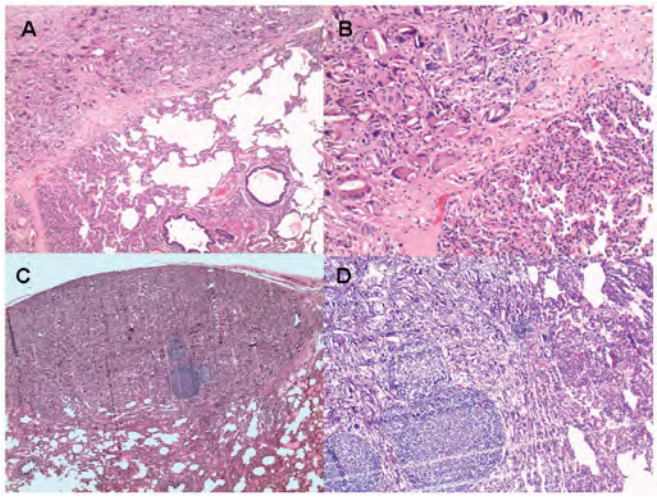

Figure 3. (A) Lung parenchyma shows area of atelectasis along with airspace enlargement in the lower part of the image and, in the upper part, a wide granulomatous reaction rich in foreign-body giant cells (arrow); haematoxylin and eosin staining, x100 magnification. (B) Foreign-body giant cells contain irregular pale-yellow talc particles that are strongly birefringent (arrow); haematoxylin and eosin staining, x400 magnification. (C) A subpleural intraparenchymal nodule consisting of a granulomatous reaction with many foreign-body giant cells admixed with early collagen tissue deposition (arrow); haematoxylin and eosin, x100 magnification. (D) In details, lymphatic reactive follicles with germinal centers are shown consisting with a strong host immune reaction (arrow); haematoxylin and eosin, x250 magnification.

pleurodesis outcome is associated with very variable results independently in all the animal series reviewed in this analysis.

Past controversies concerned the safety and severity of this procedure, specifically its possible reaction to dose, type of management and the particle size (20). The marked variations among these preparations were claimed to produce systemic inflammatory complications, molecule migration modalities and other effects such as acute lung injuries (21). Whereas, the most currently used talc preparations are standardized. In published studies to date on talc safety, especially those carried out over the 20th century, the preparation of talc was not usually well described and there was a lack of information regarding particles size, as well as degree of contamination (16).

As talc can cause damage when inhaled or after intravenous administration leading to granulomatosis, organ consolidation, deposition in parenchyma and diffuse pulmonary diseases (22,23), its use has been associated with acute lung injuries and its systemic absorption (24). Predictors of acute responses to talc pleurodesis have been hypothesised and different procedures for a safer administration have been developed (19,20). Acute events have been reported following pleurodesis including: fever, chest pain, hypoxemia, dyspnea, hypotension, lipothymia and less commonly hypercalcemia along with acute respiratory distress syndrome (25). As well, chronic events have also been reported including granulomas, pleural thickening, mesotheliod reaction and pulmonary nodules (6-8,26).

Despite concerns regarding the long-term consequences of talc in young patients, its use is on the rise, even for benign diseases as primary spontaneous pneumothorax (27). Nonetheless, recent experimental research in a mouse model, although reporting decreased effusion, concluded that there was an observed limited pleurodesis surface with marked pleural thickening following this procedure (28).

Our animal model series review had limitations. First, there was no comparative set up, unless for dosages in talc slurry, and it was based upon simple observation. Second, the animal series were extracted out of different protocols for a secondary scientific purpose; two different animal models and two different talc pleurodesis procedures were used and this might have led to a bias in the final results regarding the evaluation of effectiveness and reliability of talc action.

In conclusion, despite pleurodesis being one of the most requested procedures for the treatment of many systemic and thoracic diseases, there is still no consensus on which situation it is best suited for. Our study assessed for inflammatory stimulus, biocompatibility and tissue reaction in animal models and found that talc pleurodesis led to pleuropulmonary granulomas especially after poudrage in pigs, intrathoracic migration and diffuse pleural thickening. These findings suggest that talc was not an 'ideal' agent due to the observed chronic inflammatory patterns following the procedure, which could potentially have long term effects. In this regard, research must focus on biomedical properties of existing products to extend indications for use once they are tested for reliability, safety and risk/effectiveness while experimental research should aim at creating a new sclerosing agent with all those biochemical and functional traits to perform the ideal pleurodesis.

Acknowledgements

The study was reviewed for language editing by English language Service.

References

1. Janssen JP, Collier G, Astoul P, Tassi GF, Noppen M, Rodriguez-Panadero F, Loddenkemper R, Herth FJ, Gasparini S, Marquette CH, *et al*: Safety of pleurodesis with talc poudrage in malignant pleural effusion: A prospective cohort study. Lancet 369: 1535-1539, 2007.
2. Baron RD, Milton R and Thorpe JA: Pleurodesis using small talc particles results in an unacceptably high rate of acute lung injury and hypoxia. Ann Thorac Surg 84: 2136, 2007.
3. Genofre EH, Vargas FS, Acencio MM, Antonangelo L, Texweira LR and Marchi E: Talc pleurodesis: Evidence of sistemic inflammatory response to small size particles. Respir Med 103: 91-97, 2009.
4. Sahn SA: Talc should be used for pleurodesis. Am J Respir Crit Care Med 162: 2023-2049, 2000.
5. Light RW: Talc should not be used for pleurodesis. Am J Respir Crit Care Med 162: 2024-2026, 2000.
6. Vandemoortele T, Laroumagne S, Roca E, Bylicki O, Dales JP, Dutau H and Astoul P: Positive FDG-PET/CT of the pleura twenty years after talc pleurodesis: Three cases of benign talcoma. Respiration 87: 243-248, 2014.
7. Ergönül AG, Çakan A, Çağirici U and Nart D: Talc granulomatosis with multiple parenchymal and pleural nodules. Eur J Cardiothorac Surg 44: e308, 2013.
8. Tenconi S, Luzzi L, Paladini P, Voltolini L, Gallazzi MS, Granato F and Gotti G: Pleural granuloma mimicking malignancy 42 years after slurry talc injection for primary spontaneous pneumothorax. Eur Surg Res 44: 201-203, 2010.
9. Daddi N, Vannucci J, Maggio C, Giontella A, Bravi I, Marziani F, Capozzi R, Ragusa M, Bufalari A and Puma F: Efficacy of tigecycline pleurodesis: A comparative experimental study. J Surg Res 169: e109-e118, 2011.
10. Droghetti A, Vannucci J, Bufalari A, Bellezza G, De Monte V, Marulli G, Bottoli MC, Giovanardi M, Daddi N, De Angelis V, *et al*: Pleurodesis with Thulium Cyber Laser versus talc poudrage: A comparative experimental study. Lasers Med Sci 31: 1407-1413, 2016.
11. Vannucci J, Droghetti A, Bufalari A, De Monte V, Bellezza G, Bianconi F, Pecoriello R, Daddi N, Moriconi F and Puma F: Effectiveness and predictability of pleurodesis with the Tachosil® surgical patch compared with talc poudrage: An experimental study. Eur J Cardiothorac Surg 50: 668-9674, 2016.
12. Suckow MA, Schroeder V and Douglas FA: The Laboratory Rabbit. 2nd edition. CRC Press, Taylor, Francis Group, London, 2010.
13. Bufalari A, De Monte V, Pecoriello R, Donati L, Ceccarelli S, Cagini L, Ragusa M and Vannucci J: Experimental left pneumonectomy in pigs: Procedure and management. J Surg Res 198: 208-216, 2015.
14. Genofre HG, Marchi E and Vargas FS: Inflammation and clinical repercussions of pleurodesis induced by intrapleural talc administration. Clinics (Sao Paulo) 62: 627-634, 2007.
15. West SD, Davies RJ and Lee YC: Pleurodesis for malignant pleural effusions: Current controversies and variations in practices. Curr Opin Pulm Med 10: 305-310, 2004.
16. Aelony Y: Talc pleurodesis and acute respiratory distress syndrome. Lancet 369: 1494-1496, 2007.
17. Porcel JM, Lui MM, Lerner AD, Davies HE, Feller-Kopman D and Lee YC: Comparing approaches to the management of malignant pleural effusions. Expert Rev Respir Med 11: 273-284, 2017.
18. Kurian EM: Lung nodule with increasing fluorodeoxyglucose uptake in a patient with a history of lung carcinoma and talc pleurodesis evaluated by EBUS-TBNA on-site assessment. Acta Cytol 61: 84-86, 2017.
19. Stefani A, Natali P, Casali C and Morandi U: Talc poudrage versus talc slurry in the treatment of malignant pleural effusion. A prospective comparative study. Eur J Cardiothoracic Surg 30: 827-832, 2006.
20. Light RW: Talc for Pleurodesis? Chest 122: 1506-1508, 2002.
21. Baron RD, Milton R and Thorpe JAC: Pleurodesis using small talc particles results in an unacceptably high rate of acute lung injury and hypoxia. Ann Thorac Surg 84: 2136, 2007.
22. Iqbal A, Aggarwal B, Menon B and Kulshreshtha R: Talc granulomatosis mimicking sarcoidosis. Singapore Med J 49: e168-e170, 2008.
23. Fiorelli A, Accardo M, Rossi F and Santini M: Spontaneous pneumothorax associated with talc pulmonary granulomatosis after cocaine inhalation. Gen Thorac Cardiovasc Surg 64: 174-176, 2016.
24. Lee YC and Light RW: Management of malignant pleural effusions. Respirology 9: 148-156, 2004.
25. Aujila SJ, Michelson P, Langman CB, Shapiro R, Ellis D and Moritz ML: Refractory hypercalcemia in an infant secondary to talc pleurodesis resolving after renal transplantation. Am J Transplant 8: 1329-1333, 2008.
26. Faynberg T, Patel N, Nayar AP and Shienbaum AJ: Mesothelioid reaction following talc pleurodesis: A case report. Gen Thorac Cardiovasc Surg: Mar 7, 2017 (Epub ahead of print).
27. Cardillo G, Bintcliffe OJ, Carleo F, Carbone L, Di Martino M, Kahan BC and Maskell NA: Primary spontaneous pneumothorax: A cohort study of VATS with talc poudrage. Thorax 71: 847-853, 2016.
28. Iwasaki Y, Takamori S, Mitsuoka M, Kashihara M, Nishi T, Murakami D, Matsumoto R, Mifune H, Tajiri Y and Akagi Y: Experimental validation of talc pleurodesis for carcinomatous pleuritis in an animal model. Gen Thorac Cardiovasc Surg 64: 409-413, 2016.

Exhibit 110

Correspondence

ERRATUM: SMOOTH REFERENCE EQUATIONS FOR SLOW VITAL CAPACITY AND FLOW–VOLUME CURVE INDEXES

From the Authors:

Upon notification from a reader of our article (1), the authors have found three incorrect coefficients in Table 3, on page 901 entitled "Coefficients associated to the independent variables estimated for different regressions of eight lung function indices separately for the two sexes." The incorrect coefficients are those in the "Height-squared" row for "VC", "FEV_1", and "FVC" in males.

The published coefficients cause erroneous predicted values, as shown in the following example for a male 40 years of age whose height and weight are 180 cm and 75 kg, respectively:

	Published Incorrect Coefficient	Correct Coefficient
VC predicted, L	−8.32	5.60
FEV_1 predicted, L	−10.10	4.24
FVC predicted, L	−7.01	5.53

We had not previously discovered the errors because we kept applying the reference equations by using the values directly derived from the output of the datafile, instead of those published.

We apologize for the mistake, which was not due to the printing procedures of the *American Journal of Respiratory and Critical Care Medicine*, but to an error in the transcription of the coefficients from the output of the datafile to the original submitted manuscript.

We include below the relevant part of Table 3, after correction. We think that it may be more useful for the readers rather than publishing only the correct coefficients by themselves.

Francesco Pistelli

Institute of Clinical Physiology
Pisa, Italy

1. Pistelli F, Bottai M, Viegi G, DiPede F, Carrozzi L, Baldacci S, Pedreschi M, Giuntini C. Smooth reference equations for slow vital capacity and flow–volume curve indexes. *Am J Respir Crit Care Med* 2000;161:899–905.

TABLE 3. COEFFICIENTS ASSOCIATED TO THE INDEPENDENT VARIABLES ESTIMATED FOR DIFFERENT REGRESSIONS OF EIGHT LUNG FUNCTION INDICES SEPARATELY FOR THE TWO SEXES

	VC	FEV_1	FVC
Males			
Constant	12.11066	6.760398	11.70785
BMI	0.2394851	0.1879899	0.2819616
BMI-squared	−0.0043891	−0.0036597	−0.0054501
Height	−0.218829	−0.1368342	−0.2186871
Height-squared	0.000821	0.000548	0.0008324
Age	0.1927431	0.1459458	0.1659875
$Spline_1$ (Age)	0.0011271	0.0010309	0.0011508
$Spline_2$ (Age)	−0.0007911	−0.0007106	−0.0008498
(break-points)	(20, 25)	(19, 24)	(20, 24)
Normal 95th percentile, %	83	82	82
95% confidence interval	81–85	80–84	80–84

INCREASED MATRIX METALLOPROTEINASE (MMP)-9 IN THE AIRWAY AFTER ALLERGEN CHALLENGE

To the Editor:

In regard to the article by Kelly and colleagues (1) showing increased gelatinase B or matrix metalloproteinase (MMP)-9 levels and lack of its activation in airway after allergen challenge, we wish to point out the crucial role of timing in the collection of bronchoalveolar lavage fluid (BALF) when assessing the degree of MMP-9 activation following allergen challenge studies. Increased levels and degree of activation of neutrophil-derived MMPs (MMP-8 and MMP-9) in particular in BALF have been shown to be associated with human and equine inflammatory lung diseases (2–4), and pathologically elevated levels of MMP activation may reflect the active phase of lung inflammation as well as the severity of the ongoing inflammatory response.

Kelly and colleagues (1) demonstrated that increased levels of MMP-9, eventually originating from degranulating activated neutrophils, was present in allergen-challenged airways mainly in latent form, as determined from BALF collected 5 min and 48 h after challenge. In our recent study, applying different and more frequent timing of BALF sample collection (0 h, 5 h, 24 h, and 48 h) we have demonstrated a significantly elevated degree of activation of MMP-9 when horses with heaves (organic dust-induced asthma) in disease remission were challenged with inhaled organic dusts and inhaled endotoxin. The significant activation of MMP-9 was evident especially in BALF collected at 5 h after challenge, and was accompanied by elevation of proMMP-9, whereas elevation of proMMP-9, but not activation of MMP-9, was still evident 48 h after challenge. Additionally we have demonstrated pathologically elevated and activated levels of both MMP-9 in BALF from steroid-naive human asthmatic patients (median [range]; asthmatics: n = 10, pro-MMP-9 3.10 [1.04–9.18], active MMP-9 0.14 [0–3.73]; healthy controls: n = 10, pro-MMP-9 1.45 [0–2.52], active MMP-9 0 [0–0]) and MMP-8 in BALF collected from human bronchiectatic patients (2). In agreement with Kelly and coworkers (1) the functional significance of MMP-9 in BALF remains to be determined. Nonetheless, appropriate timing of BALF sampling in relation to allergen challenging evidences MMP-9 activation and permits investigation and identification of the potential pro-MMP-9 activators such as serine proteinases and/or reactive oxygen metabolites (5, 6). Furthermore, MMP-9 activation and its activators may prove to be useful tools to diagnose the active phase of inflammatory lung diseases.

Päivi Maisi

Timo Sorsa

Saara M. Raulo

Helsinki University
Helsinki, Finland

Kaiu Prikk

Ruth Sepper

Institute for Experimental and Clinical Medicine
Tallinn, Estonia

Bruce McGorum

Wellcome Trust Centre for Research in Comparative Respiratory Medicine
Edinburgh, United Kingdom

1. Kelly EAB, Busse WW, Jarjour NN. Increased matrix metalloproteinase-9 in the airway after allergen challenge. *Am J Respir Crit Care Med* 2000; 162:1157–1161.
2. Prikk K, Maisi P, Pirilä E, Sepper R, Salo T, Wahlgren J, Sorsa T. In vivo collagenase-2 (MMP-8) expression by human bronchial epithelial cells and monocytes/macrophages in bronchiectasis. *J Pathol* 2001;191:232–238.
3. Raulo SM, Sorsa T, Tervahartiala T, Pirilä E, Maisi P. MMP-9 as a marker of inflammation in tracheal epithelial lining fluid (TELF) and in bronchoalveolar fluid (BALF) of COPD horses. *Equine Vet J* 2001; 33:128–136.
4. Nevalainen M, Raulo SM, Brazil TJ, Pirie RS, Sorsa T, McGorum BC, Maisi P. Inhalation of organic dusts and lipopolysaccharide increases gelatinolytic matrix metalloproteinases (MMPs) in the lungs of heaves horses. *Equine Vet J* (in print).
5. Weiss SJ. Tissue destruction by neutrophils. *N Engl J Med* 1989;320:365–376.
6. Sorsa T, Salo T, Koivunen E, Tyynela J, Konttinen YT, Bergmann U, Tuuttila A, Niemi E, Teronen O, Heikkila P, *et al.* Activation of type IV procollagenases by human tumor-associated trypsin-2. *J Biol Chem* 1997;272:21067–21074.

From the Authors:

We thank Dr. Maisi and colleagues for their comments concerning the kinetics of the presence of activated MMP-9 in the airway following broncho-

provocation. In our recently published study (1), we demonstrated increased bronchoalveolar lavage (BAL) fluid levels of MMP-9 48 h after airway allergen challenge. Our intent was not to determine the activation status of MMP-9; however, zymographic analysis suggested a predominance of the latent form. Dr. Maisi has kindly provided us with preprints of his submitted manuscripts (2–4). In these studies, he and his colleagues have shown increased BAL fluid levels of MMP-9, but not MMP-2 or MMP-14 in horses with "chronic obstructive pulmonary disease" compared with normal healthy animals (2). In another study, horses with "COPD" were given an inhalation challenge with moldy straw/hay dust or lipopolysaccharide (LPS) and BAL was performed at 5 h, 24 h, 4 d, 7 d, and 14 d after challenge (3). At 5 h after challenge, dust or LPS-challenged horses showed increased BAL fluid levels of the activated form of MMP-9. They also conducted studies in patients with bronchiectasis. Both pro and latent MMP-8 were detectable in BAL fluid (Western blot analysis) and immunoreactive MMP-8 (immunohistochemistry) in bronchial biopsies from these patients. Studies of asthmatics were not included in this report. It should be emphasized that the studies by Maisi differ from ours in a number of key aspects. First, our study was conducted in atopic humans challenged with allergen, their study in bronchiectasis patients or in horses challenged with hay dust or LPS. Second, our protocol was designed to induce airway eosinophilia, their protocol was designed to induce airway neutrophilia. Finally, because of safety concerns for our human subjects, BAL was only performed at 5 min and 48 h (time of peak airway eosinophilia) after challenge, while BAL was performed at 5 time points, including 5 h post challenge in their study of horses.

Our study clearly demonstrated that MMP-9 is increased 48 h after allergen challenge of atopic individuals; however, we agree with Dr. Maisi, that we might have seen more active enzyme if BAL were performed 4–6 h after challenge, as this time point typically coincides with peak airway neutrophilia (5, 6). It is not clear whether the persistence of the latent form at 48 h is merely a marker of an earlier influx of airway neutrophils, or if it can be subsequently activated to contribute to tissue injury and repair.

Elizabeth A. Becky Kelly
University of Wisconsin-Madison
Madison, Wisconsin

1. Kelly EAB, Busse WW, Jarjour NN. Increased matrix metalloproteinase (MMP)-9 in the airway folowing allergen challenge. *Am J Respir Crit Care Med* 2000;162:1157–1161.
2. Raulo SM, Sorsa T, Tervahartiala T, Pirilä E, Maisi P. MMP-9 as a marker of inflammation in tracheal epithelial lining fluid and in bronchoalveolar fluid of COPD horses. *Equine Vet J* (In press).
3. Nevalainen M, Raulo SM, Brazil TJ, Pirie RS, Sorsa T, McGorum BC, Maisi P. *Equine Vet J* (submitted).
4. Prikk K, Maisi P, Pirilä E, Sepper R, Salo T, Wahlgren J, Sorsa T. In vivo collagenase-2 (MMP-8) expression by human epithelial cells and monocytes/macrophages in bronchiectasis. *J Pathol* (In press).
5. Nocker RE, Out TA, Weller FR, Mul EP, Jansen HM, van der Zee JS. Influx of neutrophils into the airway lumen at 4 h after segmental allergen challenge in asthma. *Int Arch Allergy Immunol* 1999;119:45–53.
6. Teran LM, Carroll M, Frew AJ, Montefort S, Lau LC, Davies DE, Lindley I, Howarth PH, Church MK, Holgate ST. Neutrophil influx and interleukin-8 release after segmental allergen or saline challenge in asthmatics. *Int Arch Allergy Immunol* 1995;107:374–375.

TALC SHOULD NOT BE USED FOR PLEURODESIS IN PATIENTS WITH NONMALIGNANT PLEURAL EFFUSIONS

To the Editor:

In the debate regarding the use of talc in pleurodesis, respiratory failure after intrapleural injection was cited as that complication potentially limiting employment of this agent (1, 2). We agree with this appraisal in the treatment of patients with malignant recurrent effusions. However, there should continue to be concern regarding the use of talc for pleurodesis in individuals with nonmalignant pleural effusions and spontaneous pneumothorax. This dilemma results from a possible increased risk of malignant mesothelioma in those patients treated with talc. Consequently, an alternative agent should be employed in any individual without malignancy requiring pleurodesis.

Talc is not a uniform substance, and varies significantly in size and chemical composition, with the latter depending on geologic origin. This sheet silicate can be contaminated by asbestos. An association between carcinogenesis and exposure to asbestos included in talc appears credible. Certainly, noncarcinogenic effects of asbestos (pleural plaque formation) have been reported in patients instilled with talc for pleurodesis. The paucity of evidence of malignant mesothelioma occurring after the use of talc for pleurodesis may reflect either an inadequate latency period or an insufficient number in the investigations conducted. Assuming a risk of the same magnitude as that seen in the cohort of asbestos-exposed insulation workers (3), less than one case of mesothelioma would have been expected in the two investigations of patients exposed to talc used in pleurodesis (4, 5). However, case reports of malignant mesothelioma after occupational exposure to talc suggest a potential association (6). Furthermore, epidemiologic studies demonstrate an excess mortality from lung and pleural carcinomas in talc miners and millers, while animal studies confirm an induction of mesothelioma after intrapleural injection of talc.

The assertion that contemporary purified preparations of talc do not contain asbestos, therefore eliminating a risk of mesothelioma, should be closely examined prior to its acceptance for clinical application. The methodology used to confirm the lack of asbestiform minerals in a finished product (i.e., X-ray diffraction, optical microscopy, and electron microscopy techniques) and its sensitivity must be provided. Even if the product is "asbestos-free," the mechanism of cancer induction by asbestos (i.e., metal-catalyzed radical generation) is similarly pertinent to talc and the occurrence of fibrous forms of the sheet silicate itself (Figures E1 and E2 in the online data supplement to this letter) raises issues about clearance and long-term safety. Simply stating that the talc is "asbestos-free" should not release us from a responsibility to the patient, especially when safe alternatives are available.

Andrew J. Ghio
United States Environmental Protection Agency
Chapel Hill, North Carolina

Victor Roggli
Duke University Medical Center
Durham, North Carolina

1. Sahn SA. Talc should be used for pleurodesis. *Am J Respir Crit Care Med* 2000;162:2023–2026.
2. Light RW. Talc should not be used for pleurodesis. *Am J Respir Crit Care Med* 2000;162:2024–2026.
3. Selikoff IJ. Cancer risk of asbestos exposure. In: Hiatt HH, Watson JD, Winsten JA, editors. Origin of human cancer. CSH Press; Cold Spring Harbor, New York: 1977. p. 1765–1784.
4. Research Committee of the British Thoracic Association and the Medical Research Council Pneumoconiosis Unit. A survey of the long-term effects of talc and kaolin pleurodesis. *Br J Dis Chest* 1979;73:285–288.
5. Lange P, Mortensen J, Viskum K. Long-term sequelae of talcum pleurodesis. *Ugeskr Laeger* 1987;149:2246–2248.
6. Barnes R, Rogers AJ. Unexpected occupational exposure to asbestos. *Med J Aust* 1984;140:488–490.

From the Authors:

I appreciate the comments of Drs. Ghio and Roggli concerning our article. I agree that talc should not be used to produce pleurodesis in patients with nonmalignant diseases such as spontaneous pneumothorax or recurrent nonmalignant pleural effusion. If talc should not be used to produce pleurodesis in patients with malignant disease because it might produce acute respiratory failure, it should not be used for pleurodesis in other situations for the same reasons.

Drs. Ghio and Roggli maintain that another reason talc should not be used in patients with nonmalignant disease is the possible increased risk of mesothelioma after the administration of talc intrapleurally. Talc can be contaminated with asbestos, which is known to be associated with the development of mesothelioma. Although previous studies have found no increased incidence of mesothelioma in patients who received talc intrapleurally, the authors rightly point out that the number of patients included in the studies was small. I believe that the risk of mesothelioma from talc pleurodesis is very small since, to my knowledge, there is not even a case report of such an occurrence. Nevertheless, the fact that the possibility exists provides another reason to not use talc for pleurodesis in nonmalignant conditions.

Richard W. Light
Vanderbilt University
Nashville, Tennessee

Dr. Sahn was given an opportunity to respond, but declined.